J. O. Jirsa
File Copy

THE SHEAR STRENGTH OF REINFORCED CONCRETE BEAM-COLUMN JOINTS

by

Donald F. Meinheit
and
James O. Jirsa

Final Report
on a
Research Project Sponsored by
THE NATIONAL SCIENCE FOUNDATION
Research Grant GK-40289

Department of Civil Engineering
Structures Research Laboratory
The University of Texas at Austin

January 1977

ACKNOWLEDGMENTS

The research reported herein is a study of the shear strength characteristics of beam-column connections subjected to large deformations. The specimens simulated full-size components of a reinforced concrete building frame. Experimental work was conducted in the Civil Engineering Structures Research Laboratory at Balcones Research Center, The University of Texas at Austin. The Laboratory is under the direction of Dr. J. E. Breen. The research was sponsored by the National Science Foundation under Grant Number GK-40289.

The authors wish to acknowledge the support of the project staff, including John W. Woollen and Marisol Abad de Aleman, former research assistants who supervised various phases of this project; Jerry D. Crane, Gary D. Iselt, Gorham W. Hinckley, and George E. Moden, technical staff personnel who assisted in the fabrication and testing of the specimens; and Maxine DeButts, Tina Robinson, and Charles D. Johnson, clerical staff personnel who assisted in the preparation of the report and carried out a wide variety of clerical duties.

This report was prepared as a doctoral dissertation by Donald F. Meinheit under the direction of James O. Jirsa, Professor of Civil Engineering.

A B S T R A C T

Beam-column joints were subjected to deformation to establish basic shear behavior. Fourteen interior type connections with reinforcing bars continuous through the joint were tested. The effects of column reinforcement, column load, joint hoop reinforcement, lateral beams, concrete strength, the ratio of the depth of the column to the depth of the main flexural member, and load reversals on the shearing strength of the beam-column joint were investigated. Specimens were designed using the recommendation of ACI-ASCE Committee 352 and were proportioned so that shear stress in the joint would determine the maximum loads rather than yielding of the flexural members. The failure mode of each specimen was observed. From a statistical analysis of the test data and the mode of failure, new design recommendations for basic shear strength are made that deemphasize column load, concrete shear cracking, and joint hoop reinforcement, and emphasize concrete strength. Based on the load reversal tests, a modification to the basic shear strength is proposed to account for shear strength degradation under cyclic load. The form of the proposed design equation is substantially different from the current ACI-ASCE Committee 352 recommended practice. The proposed design approach represents a significant advance in the understanding of the shear behavior of the beam-column joint.

C O N T E N T S

LIST OF TABLES

LIST OF FIGURES

NOTATION

a	depth of equivalent rectangular stress block for concrete, in.
A_{ch}	area of rectangular core measured to the outside of the joint hoop, in.^{2}
A_g	gross area of column section, in.^{2}
A_s	area of tension reinforcement, in.^{2}
A'_s	area of compressive reinforcement, in.^{2}
A_{sh}	total cross-sectional area of one rectangular joint hoop, in.^{2}
A_{sv}	area of reinforcement crossing a shear crack within a distance s, in.^{2}
b	width of the compression face of the column, in.
b_1	distance from face of column to point of load application, in.
$b_{column} = b_c$	width of the column at the beam-column joint, in.
c	distance from extreme compression fiber to neutral axis, in.
$C = C_c$	compressive force in the concrete
C_s	compressive force in reinforcement
d	distance from extreme compressive fiber to the centroid of the tensile force, in.
d'	distance from extreme compression fiber to centroid of compression reinforcement, in.
$d_{column} = d_c$	distance from extreme compressive fiber to the centroid of the tensile force in a column, in.
$E = E_c$	modulus of elasticity of concrete
E_s	modulus of elasticity of tensile reinforcement
E'_s	modulus of elasticity of compresssive reinforcement
f'_c	concrete compressive strength, psi
f_s	tensile stress in reinforcement
f'_s	compressive stress in reinforcement

f_{sp}	tensile splitting strength, psi
f_t	tensile strength of concrete
f_y	yield strength of reinforcement in tension
G	shearing modulus of concrete
$h_{beam} = h_b$	depth of main beam, in.
$h_{column} = h_c$	depth of column, in.
h_L	depth of lateral beam, in.
I	moment of inertia of section
I_{beam}	moment of inertia of beam
I_{column}	moment of inertia of column
I_g	moment of inertia of gross cross section
ℓ_h	maximum unsupported length of rectangular hoop, in.
L	length of main beam from face of column to free end, in.
L_c	length of column between supports, in.
$L_{\mathbb{C}_L}$	length from centerline of column to free end of main beam, in.
M	masking ratio of the joint
M_1 and M_2	beam moments
M_{c3} and M_{c4}	column moments
M_c	calculated bending moment
M_{j21}	measured maximum joint moment in cycle 2-1
M_{j22}	measured maximum joint moment in cycle 2-2
M_{j31}	measured maximum joint moment in cycle 3-1
M_{j32}	measured maximum joint moment in cycle 3-2
N_u	magnitude of design column load, compression positive
$P = P_u$	applied column load
P_1 and P_2	applied main beam load
P_{bal}	column load at balance point on load-moment interaction diagram
P_o	concentric column strength
r	correlation coefficient

s	spacing of reinforcing bars, in.
s_h	center-to-center spacing of hoops along vertical column bars, in.
T_1, T_2, T_3, T_4	tensile force in reinforcement
T'_1, T'_2, T'_3, T'_4	compressive force in reinforcement
T_s	tensile force in tensile reinforcement
T'_s	tensile force in compressive reinforcement
v	shear stress
v_c	nominal shear stress carried by concrete
v_{cr}	shear stress at diagonal crack of the concrete
v_j	nominal joint shear stress
v_{j21}	measured maximum joint shear stress in cycle 2-1, psi
v_{j22}	measured maximum joint shear stress in cycle 2-2, psi
v_{j31}	measured maximum joint shear stress in cycle 3-1, psi
v_{j32}	measured maximum joint shear stress in cycle 3-2, psi
v_s	shear stress in joint hoop reinforcement
v_u	ultimate joint shear stress, psi
V_{col}	column shear
V_{core}	volume of joint core enclosed by hoop reinforcement, $in.^3$
V_{cr}	joint shear at diagonal cracking
V_j	joint shear
V_{jf}	joint shear activated by friction and hoop reinforcement
V_{j21}	measured maximum joint shear in cycle 2-1
V_{j22}	measured maximum joint shear in cycle 2-2
V_{j31}	measured maximum joint shear in cycle 3-1
V_{j32}	measured maximum joint shear in cycle 3-2
V_s	volume of joint hoop enclosing concrete core, $in.^3$
$w_{lateral} = w_L$	width of lateral beam, in.
β	factor reflecting the amount of energy absorbing capacity or type of loading imposed on the joint

β_1	ratio of the depth of the equivalent rectangular stress block to the depth to the neutral axis measured from the extreme compressive fiber
γ	factor reflecting lateral members perpendicular to the plane in which shear is considered
γ_j	joint shear strain
Δ	deflection, in.
$\Delta_{cantilever}$	deflection of end of main beam assuming a cantilever support
Δ_{column}	deflection of end of main beam due to rotation of the column
Δ_γ	deflection of end of main beam due to joint shear deformation
Δ_{θ_B}	deflection of end of main beam due to inelastic main beam behavior
Δ_y	deflection of main beam at yield, in.
ϵ_c	strain in concrete
ϵ_s	strain in tensile reinforcement
ϵ'_s	strain in compressive reinforcement
ζ	factor reflecting the contribution of joint hoop
η	constant of proportionality
θ_B	rotation of the main beam at the face of the column
θ_c	rotation of the column at the joint
θ_{BT}	measured rotation in main beam 5 in. from column face
λ	constant of proportionality
ν	Poisson's Ratio of concrete
ρ_{bot}	reinforcement ratio on bottom of beam
ρ_g	column reinforcement ratio
ρ_s	ratio of volume of joint hoop reinforcement to enclosed concrete core
ρ_{top}	reinforcement ratio on top of beam
ρ_w	the joint steel ratio
σ_x	stress in the x-direction

σ_y	stress in the y-direction
σ_z	stress in the z-direction
φ	inclination of shear crack
φ_B	measured curvature at face of column
χ	internal friction angle

CHAPTER 1

INTRODUCTION

1.1 General Background

High strength concrete, high strength steel and high rise buildings of both steel and concrete have become popular for construction in central city areas where land is at a premium. The owner's capital outlay for land, structure, and furnishings requires a close examination of various structural schemes to achieve a suitable compromise on costs and at the same time to provide a structure that is safe, lasting, and serviceable. Economies can be realized by using higher strength materials and designs employing such materials have proven safe.[1]

The trend in current reinforced concrete design is toward higher strength materials, where appropriate for economy, checking both serviceability requirements at working loads and the capacities to sustain large deformations (ductility) in the event of overload. Proper application of appropriate specifications[2] is intended to ensure that behavior at service load is not objectionable and that ductility is present in the members to warn against impending failure. Much of the past research effort has concentrated on ensuring ductility for members in a structure; however, until recently, little attention has been given to service load and ductility performance of the connections between members of the structure. The general nature of the connection is such that its dimensions are usually larger than those of the flexural members framing into it, and therefore the connection was assumed to be a noncritical component.

For geographical areas within the United States where design is governed by gravity loads, shear design of the connections is not as critical as flexural design of beams or columns. Moments acting on the connection from the beams or column subtract algebraically, requiring the connection to transfer small unbalanced moments by means of shear in the joint. A joint located in the interior of a structural frame is often proportioned by a detailer who has the responsibility of lacing reinforcing bars through the interior connection. Joints located on the exterior of a building frame are engineered to a greater extent because the flexural beam reinforcement must be terminated and adequately anchored in the joint to prevent the reinforcing bars from being pulled out of the concrete. For the gravity load type structure, little if any service load distress has been observed when joint design was ignored except from a detailing viewpoint.

Proportioning connections in areas where lateral forces due to strong winds or earthquakes may be significant requires additional care at all stages of design, detailing, and construction. Code provisions for member design should guide the structural designer to proportion members to reach service and ultimate conditions before the connection reaches its ultimate load. The connections of such structures must, therefore, be proportioned to ensure that members can develop their strength and ductility. Premature failure of the joint could cause the entire structure to behave in a brittle rather than a ductile fashion. Code provisions have generally been governed by the objective of avoiding brittle failure to ensure the occupants' safety.

Numerous well-documented structural failures have pointed to connection inadequacies as a contributing factor in undesirable structural performance. Well-documented studies of structural performance have been carried out following the Alaskan 1964,[4] Caracas 1967,[5,6] Tokachi-Oki 1968,[7] and San Fernando 1971[8] earthquakes.

The studies indicate that connection design and detailing have not yet progressed to the same state of reliability as has member design.

Design Approaches. The design of the connection between the beam and column requires that the joint have enough shear strength to fully develop the moment capacities of the members at the joint. Hinging in the column is not considered desirable because it may produce greater damage to the frame than the damage produced by beam hinging. Therefore, the beams at a joint should be designed to permit plastic deformations while the column remains elastic. Figure 1.1(a) shows schematically a building frame subjected to a lateral loading. The member forces on a typical interior joint of a reinforced concrete structure are depicted in Fig. 1.1(b). If a planar action can be assumed, i.e., no biaxial bending of the column, for the interior joint of Fig. 1.1(b), the moments can be replaced with equivalent forces and lever arms, as shown in Fig. 1.2. The applied shear which the joint must carry is caused by forces developed in the reinforcement on either side of the joint. Cutting either a horizontal or vertical free body through the joint results in the same magnitude of joint shear. Following the design philosophy suggested above where the beam reaches ultimate while the column remains elastic, the maximum joint shear can be defined as follows:

$$V_j = T_1 + T_2' + C_2 - V_{col} \qquad (1\text{-}1)$$

where $T_1 = A_{s1} f_y$

$T_2' = A_{s1} f_s'$

$C_2 = \int_A f(f_c)\,dA$

A_{s1} = area of the reinforcing bars

f_y = yield of reinforcing bars in tension

f_s' = compressive stress in reinforcing bar

V_{col} = column shear

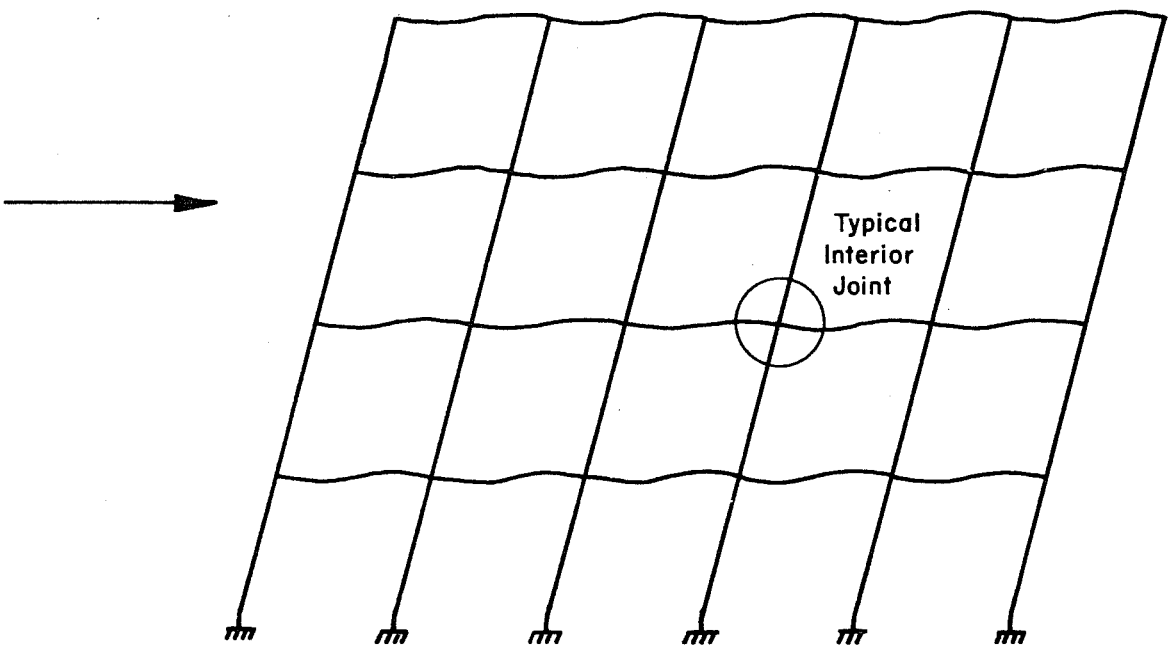

(a) Building frame subjected to lateral force

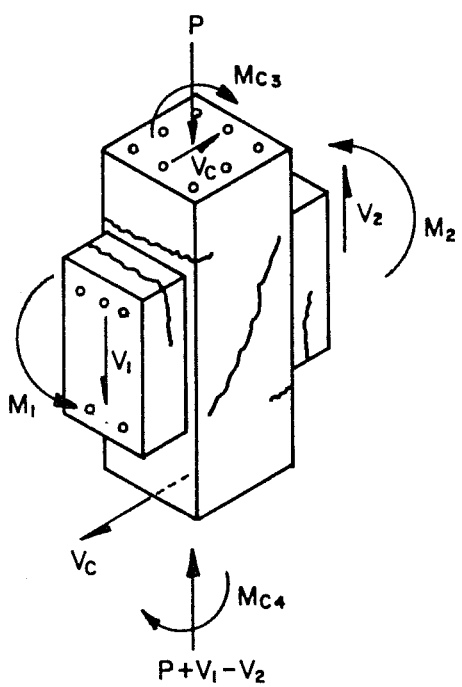

(b) Member forces on a typical interior joint

Fig. 1.1 Forces on joints in frames subjected to lateral loads

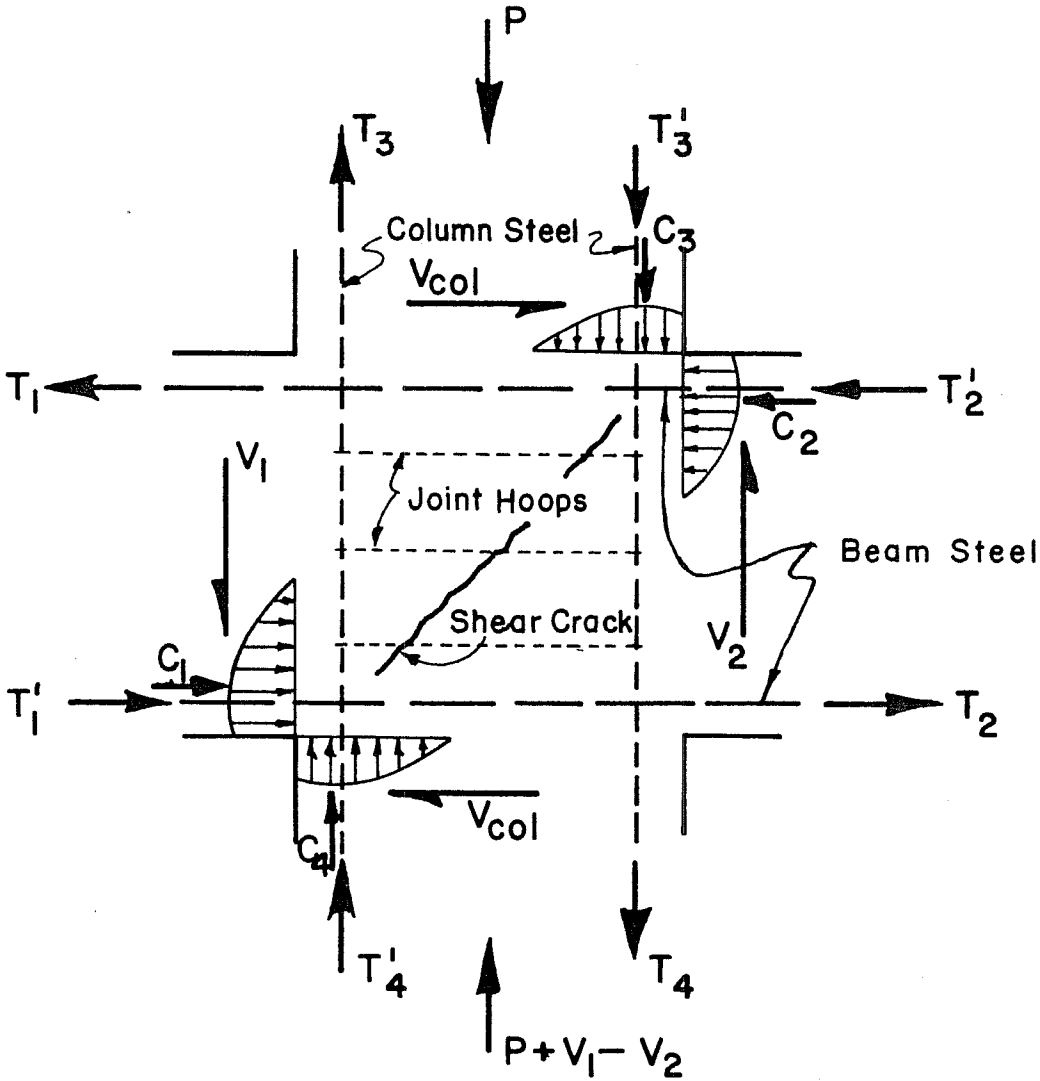

Fig. 1.2 Equivalent member forces on an interior joint

The forces T_2' and C_2 may be replaced with the magnitude of the tensile force, T_2, which is the equivalent by internal equilibrium, simplifying Eq. (1-1) to

$$V_j = T_1 + T_2 - V_{col} = A_{s1}f_y + A_{s2}f_y - V_{col} \qquad (1\text{-}2)$$

ACI-ASCE Committee 352 Design Recommendations. The design procedure, according to the current ACI-ASCE Committee 352,[9] involves separating the joint shear into two portions: one portion is assigned to the concrete, the other to reinforcing bars (joint hoops) crossing a potential diagonal shear crack, shown in Fig. 1.2 Calculations for proportioning the size of the joint or the joint reinforcing proceed in the same fashion as for a reinforced concrete beam designed for shear. This approach is frequently called the classical 45° truss analogy. Unit stresses are convenient when relating applied forces to material properties; therefore, the designer would first convert the joint shear (V_j) into a stress as follows:

$$v_j = V_j/bd \qquad (1\text{-}3)$$

where V_j = joint shear

b = width of the compression face of the column

d = distance from extreme compressive fiber to the centroid of the tension force

Concrete in the joint is allowed, by Code,[9] to carry a unit stress of:

$$v_c = 3.5\beta\gamma\sqrt{f_c'(1 + 0.002\ N_u/A_g)} \qquad (1\text{-}4)$$

where β = factor reflecting the amount of energy absorbing capacity or type of loading imposed on the structure

= 1.4 for joints which must have strength but no expected significant inelastic deformations (Type 1)

= 1.0 for joints which must have sustained strength under reversals in the inelastic range (Type 2)

γ = factor reflecting lateral confinement by members perpendicular to the plane in which the shear stress is calculated

= 1.4 if the confining members cover at least three-quarters of the width and three-quarters of the depth of the joint face

= 1.0 if the confining members do not meet the above requirements

f'_c = concrete compressive strength, psi

N_u = magnitude of column load (compression positive), lbs.

A_g = gross area of column, $in.^2$

The above equation represents the cracking strength of the concrete.

The unit stress carried by the transverse hoop reinforcement is:

$$v_s = A_{sv} f_y / bs \qquad (1\text{-}5)$$

where A_{sv} = area of reinforcement crossing a shear crack within a distance s, $in.^2$

f_y = yield strength of reinforcement, psi

b = width of the column in the joint, in.

s = spacing of reinforcement, in.

The two stresses are assumed to be additive, so that

$$v_j \leq v_c + v_s \qquad (1\text{-}6)$$

If the structural analysis indicates that the column is carrying a tension load rather than a compression load, the concrete shear strength is to be taken as zero.

Sugano and Koreishi (Japan). The Sugano and Koreishi[10] recommendation is similar to the ACI-ASCE Committee 352 recommendation. A portion of the total applied shear stress is assigned to each of the joint components, concrete and reinforcing steel. Reference 10 indicates that the concrete cracking stress and

ultimate capacity of the concrete in shear are two different values. The cracking shear stress of the concrete is computed by:

$$v_{cr} = \sqrt{f_t^2 + f_t(P_u/A_g)} \qquad (1\text{-}7)$$

where f_t = tensile strength of concrete
P_u = column load
A_g = gross area of the column

The tensile strength of the concrete is calculated from an empirical relationship (in metric units) given by Eq. (1-8).

$$f_t = 0.205f'_c - 0.0004f'^2_c (f'_c \leq 420 \text{ kg/cm}^2) \qquad (1\text{-}8) \text{ (metric)}$$

where f'_c = concrete compressive strength, kg/cm^2

Equation (1-8) is in fair agreement with concrete tensile strengths using Ref. 9 when the concrete strengths are less than about 4000 psi.

The Japanese test experience, however, indicates that the total shear stress, v_j, was not influenced by column load. Therefore, Sugano and Koreishi suggest that the concrete contribution to joint shear strength (in metric units), derived from test results, to be replaced with:

$$v_c = 0.51f'_c - 0.001f'^2_c (f'_c \leq 420 \text{ kg/cm}^2) \qquad (1\text{-}9) \text{ (metric)}$$

instead of the cracking strength of Eq. (1-7).

That portion of the applied shear stress that can be carried by transverse hoop reinforcement (in metric units) is calculated by an empirical equation:

$$v_s = 2.7\sqrt{\rho_w f_y} \qquad (1\text{-}10) \text{ (metric)}$$

where ρ_w = the steel ratio (A_s/bs)
A_s = total area of hoop reinforcement in the joint
f_y = yield strength of joint hoops, kg/cm^2
b = width of the column
s = spacing of hoops

The total shear is then calculated by adding the two components, as in Eq. (1-6). When comparing the Sugano-Koreishi and ACI-ASCE Committee 352 equations, one finds that the concrete shear strength for the Japanese equation is generally greater than that suggested by Committee 352 [see Fig. 1.3(a)]. The reinforcement contribution to the joint shear strength, shown in Fig. 1.3(b), indicates that reinforcement can be added to the joint but is not completely effective as it is assumed in the ACI-ASCE Committee 352 recommendation. The joint shear strengths for the two approaches considered are plotted in Fig. 1.3(c) and show that the Sugano-Koreishi recommendation assigns the majority of the shear stress to the concrete. Shear strength is also relatively unaffected by hoop reinforcement, as opposed to the ACI-ASCE Committee 352 recommendation.

Park and Paulay (New Zealand). Park and Paulay of the University of Canterbury, Christchurch, New Zealand, suggest that designers ignore the shear strength of the concrete and carry the total joint shear by joint reinforcement in accordance with Eq. (1-5) when seismic type of loads must be carried by the joint.[11] They feel that, under many reversals of an earthquake type load, the concrete will continuously degrade and have little or no shear strength remaining. However, when joint hoops are provided, the hoops can carry shear that the concrete will not carry. As a result, a large number of transverse hoops are required in the joint. A further suggestion is made that only two-thirds to three-quarters of the total joint reinforcement be considered as effective.[11] Tests conducted in New Zealand have indicated that hoops away from the center

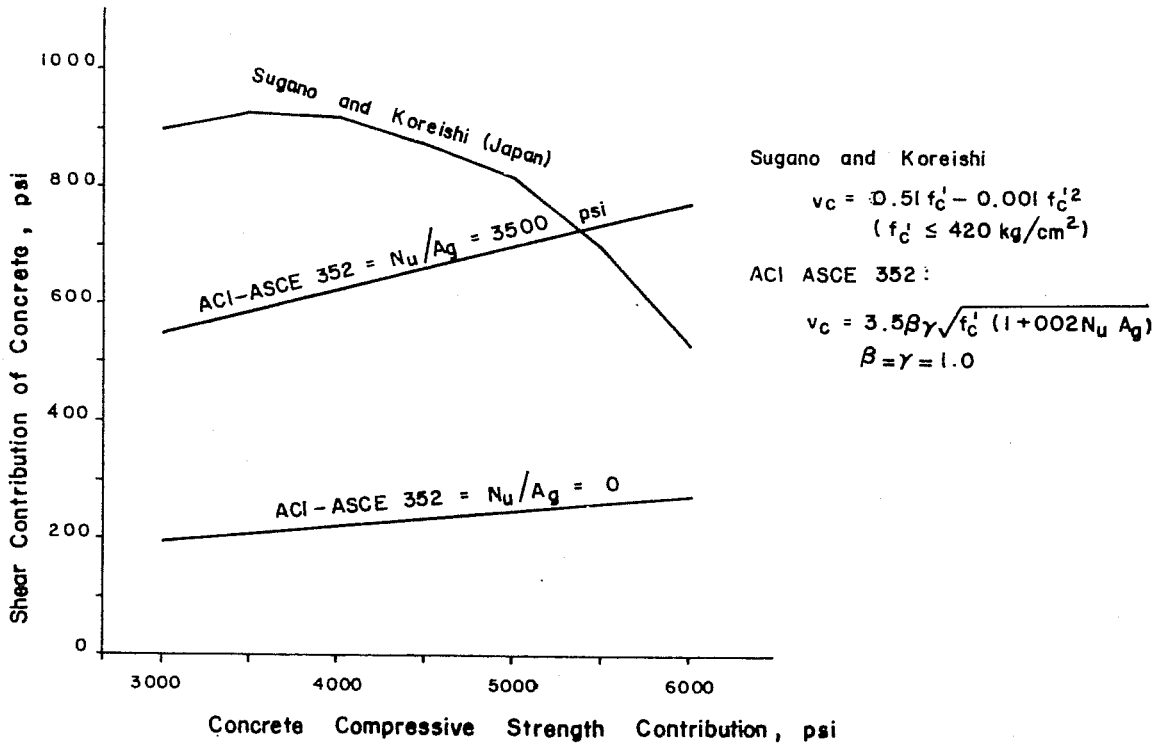

Fig. 1.3(a) Concrete contribution to joint shear strength

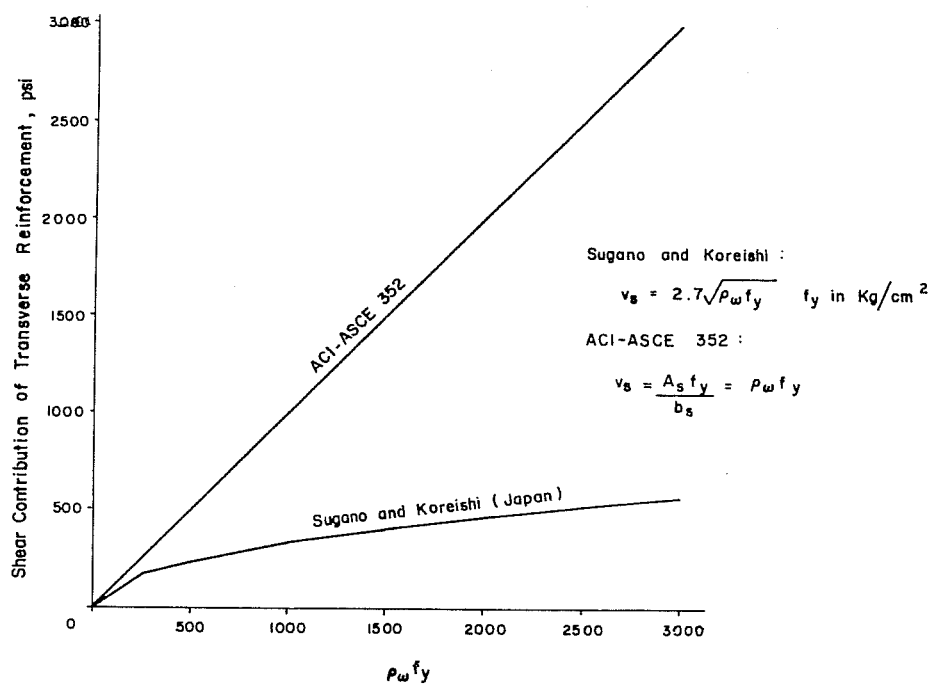

Fig. 1.3(b) Transverse hoop reinforcement contribution to joint shear strength

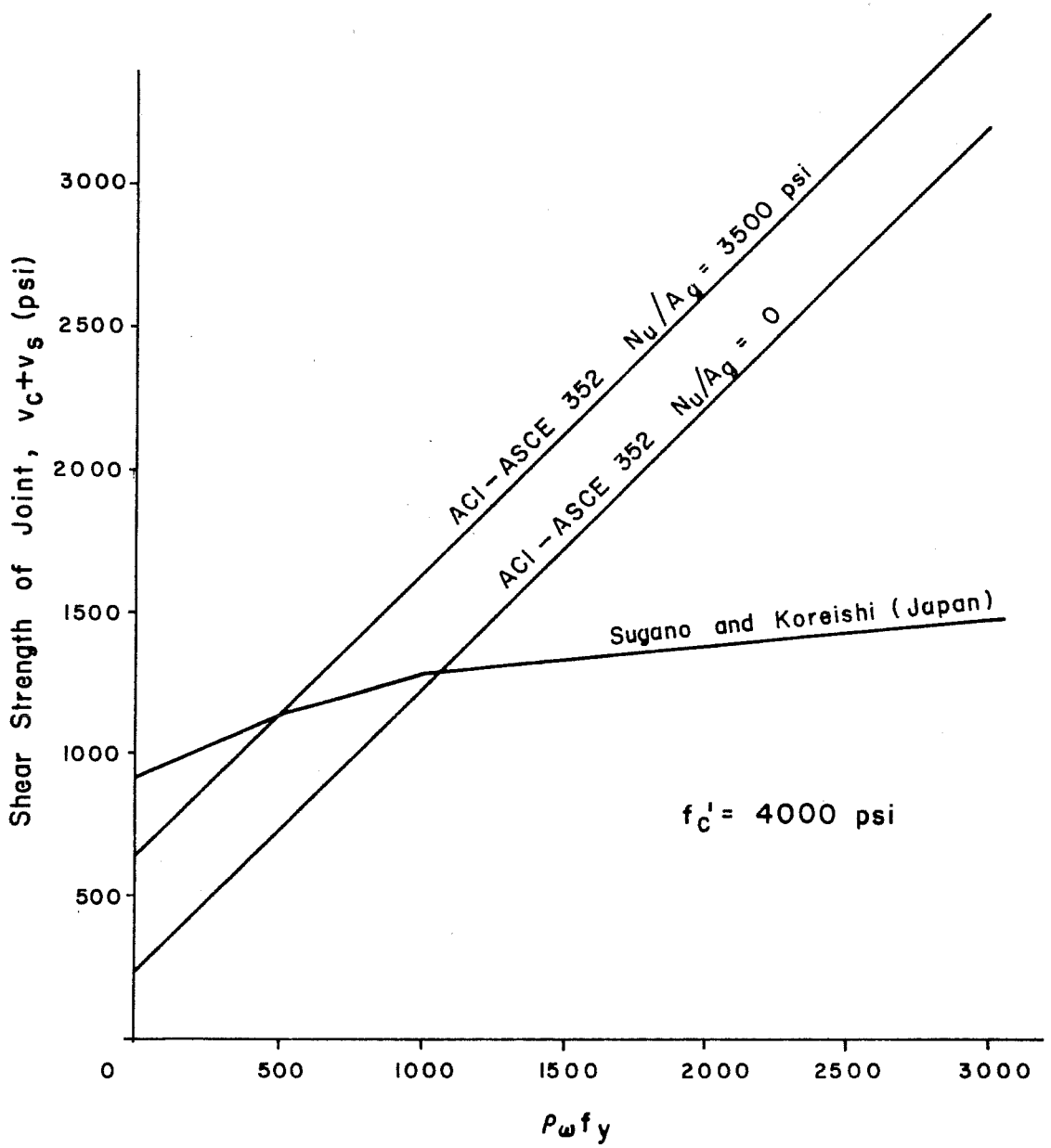

Fig. 1.3(c) Joint shear strength as affected by amount of reinforcement

of the joint are not as effective as those in the center. It is also suggested that hoop reinforcement be provided in both the horizontal and vertical directions in the joint because equilibrium should be satisfied in both directions.[11] No tests are reported in which this was done.

1.2 Implications of Other Current Research

Review of tests conducted at the Portland Cement Association,[12,13,14] the University of Toronto,[15] and in Japan[10,16] suggests that the joint strength is not significantly affected by the magnitude of the column load. However, in none of the test programs was column load systematically varied on specimens failing in shear. In most cases the applied normal load is less than the balance load of the column.

The studies at the University of Toronto and the University of Canterbury in New Zealand[11] also imply that the traditional 45^{o} truss analogy does not adequately predict the behavior of the joint. In the Toronto and New Zealand studies the test specimens were subjected to many cycles of repeated load near the yield moments of the beams. The concrete was seen to deteriorate and the shear reinforcement was assumed to be picking up a greater portion of the entire shear. To date, these experimental studies have found that the most reliable way of ensuring a failure away from the joint is to provide hoop reinforcement to carry the entire shear.

Several Japanese tests[16] and one PCA test[13] have shown that unloaded intersecting beams perpendicular to the applied shearing forces in the joint are effective in improving the shear strength and ductility of the reinforced concrete beam-column joint.

Shortcomings of Current Recommendations. At present, a number of different design approaches, as described above, are

available for designing a beam-column joint. Most approaches require inclusion of hoop reinforcement, making field fabrication of joints costly, especially since it is recommended that beam and column bars be spliced away from the joint. Congestion problems for the detailer as well as contractor are more severe when closely spaced hoop reinforcement is specified. The hoops must not interfere with the beam flexural or column longitudinal reinforcement or restrict the flow of concrete during casting.

The ACI-ASCE Committee 352 design recommendation is to use Eq. (1-4) as the contribution from the concrete to the joint shear strength. This equation originated from tests on members, not joints, subjected to compressive load in addition to shear and flexure.[17] One of the major incompatibilities between the specimen used for Eq. (1-4) and the beam-column joint is the difference in the shear span. The fact that Eq. (1-4) was derived from tests on members with large shear spans (greater than about 2) makes the application to beam-column joints with small shear spans (about 1) questionable.

1.3 Scope and Objective

Project Statement. Recent major earthquakes have pointed to connections as a major weakness in the structural design. Previous research on reinforced concrete beam-column joints has been directed toward the short-term goal of ensuring that joint failures do not precipitate major structural damage or a structural collapse. The short term goal has been satisfied by placing additional hoop reinforcement in the joint, which restricts easy placement of column and beam reinforcement as well as plastic concrete. The assumptions regarding joint behavior and the use of equations for joint shear strength which are based on beam tests cast reasonable doubt on the reliability of current joint designs. The underlying purpose of

this investigation is to examine the basic shear strength behavior of a beam-column joint.

Specific Objectives. The primary deficiency in evaluating the shear strength of beam-column joints is a lack of basic tests to appraise the shear strength of the concrete in the joint. It has been well-established that the compressive strength of concrete increases when lateral confinement is present.[18] The tests in this program provide a means of examining methods of confining the joint concrete anticipating that confinement will increase the joint shear strength.

A systematic variation of every possible parameter affecting beam-column joint strength is beyond the scope of any realistic testing program. However, by systematically varying selected parameters, valuable insight into the basic shear behavior of the beam-column joint can be obtained.

Variables anticipated as significant to provide confinement to the joint included the following:

(1) The percentage of vertical column reinforcement. With a greater number and more flexurally stiff column reinforcement, a "cage" effect of reinforcing steel could confine the internal deformations of the joint.

(2) Magnitude of column load. Axial compression has been shown to be important for beam shear strength.

(3) Amount of transverse reinforcement. Most previous investigations have shown transverse reinforcement significant in improving joint shear strength.

(4) Intersecting lateral beams. Limited tests have shown lateral beams to be beneficial to joint strength. Variations in the size and location of lateral beams have not been extensively investigated.

(5) The shear span or aspect ratio of the joint. The depth of the section carrying shear may be as important as the shear area of the joint.

Test Program. The testing program was established to investigate the basic shear strength of beam-column joints in reinforced concrete frame structures.

To systematically evaluate the effects of the variables listed above, the project was planned using full-size members. Full-scale models of beam-column joints were desired to eliminate scaling effects, especially relative to bond transfer along the reinforcing bars. Full-size members permitted the use of commercial reinforcing bars and concrete mixes typical of construction practice and allowed comparisons to be made with most of the existing data.

Deformation constraints between the actual structure and specimen will not be precisely modeled. In the actual structure, Fig. 1.1(a), moments introduced due to the lateral displacement of the column (P-Δ effect) were not duplicated. This should have no influence on the joint behavior because the joint must resist the applied actions regardless of the source. However, the total structural behavior may be greatly affected by the lateral displacements of the column which depends in part on the stiffness of the beam-column joint.

CHAPTER 2

EXPERIMENTAL STUDY

2.1 General

Fourteen test specimens were designed to meet the objectives of the research program. In each specimen only one of the five parameters discussed in Section 1.3 was varied. Table 2.1 outlines the fourteen tests and indicates which of the parameters was varied for each test. Specific details of the variables will be described in a following section.

All fourteen specimens were loaded slowly and cyclically to simulate the reverse load effects of an earthquake or the lateral loads from strong winds blowing from opposite directions. Loads were applied to each specimen so that clockwise moments at the beam-column joint caused a clockwise joint rotation. A counter-clockwise joint moment produced a counter-clockwise rotation of the joint. One complete load cycle included loadings that caused one clockwise and one counter-clockwise rotation of the joint. Figure 2.1 shows the directions and locations of applied loads. It should be pointed out that the applied loads did not simulate the actual moments occurring at a joint when a structure is subjected to combined gravity and lateral load effects. Gravity load moments reduce the lateral load moment on one side of the joint, while increasing it on the other side. Ignoring the gravity load moment would not change the moment differential at the joint in the test specimen. Therefore, if the gravity load is ignored, the severity of the loading on the joint is unchanged. In an actual case, lateral loads cause the column to deflect laterally and this lateral deflection causes a secondary

TABLE 2.1 EXPERIMENTAL TESTING PROGRAM

Specimen	Column Bending Axis		Percentage of Column Reinforcement			Nominal Compressive Stress on Column (psi)			Lateral Beams Perpendicular to Joint Deformations (Area of Lateral Beam/Area of Joint)				Reinforcement in Joint		
									None	Centered		Displaced			
	Strong	Weak	2.0	4.3	6.7	200	1500	2500	0%	70%	37%	37%	#4@6"	#4@2"	#5@2"
I	X		X				X		X				X		
II	X			X			X		X				X		
III	X				X		X		X				X		
IV		X		X			X		X				X		
V	X			X		X			X				X		
VI	X			X				X	X				X		
VII		X		X				X	X				X		
VIII	X			X			X			X			X		
IX	X			X			X				X		X		
X	X			X			X					X	X		
XI		X		X			X				X		X		
XII	X			X			X		X						X
XIII	X			X			X		X					X	
XIV		X		X			X		X					X	

Column Bending	W	H	B	w_L
Strong	11"	18"	13"	0",8",15"
Weak	16"	13"	18"	0",6"

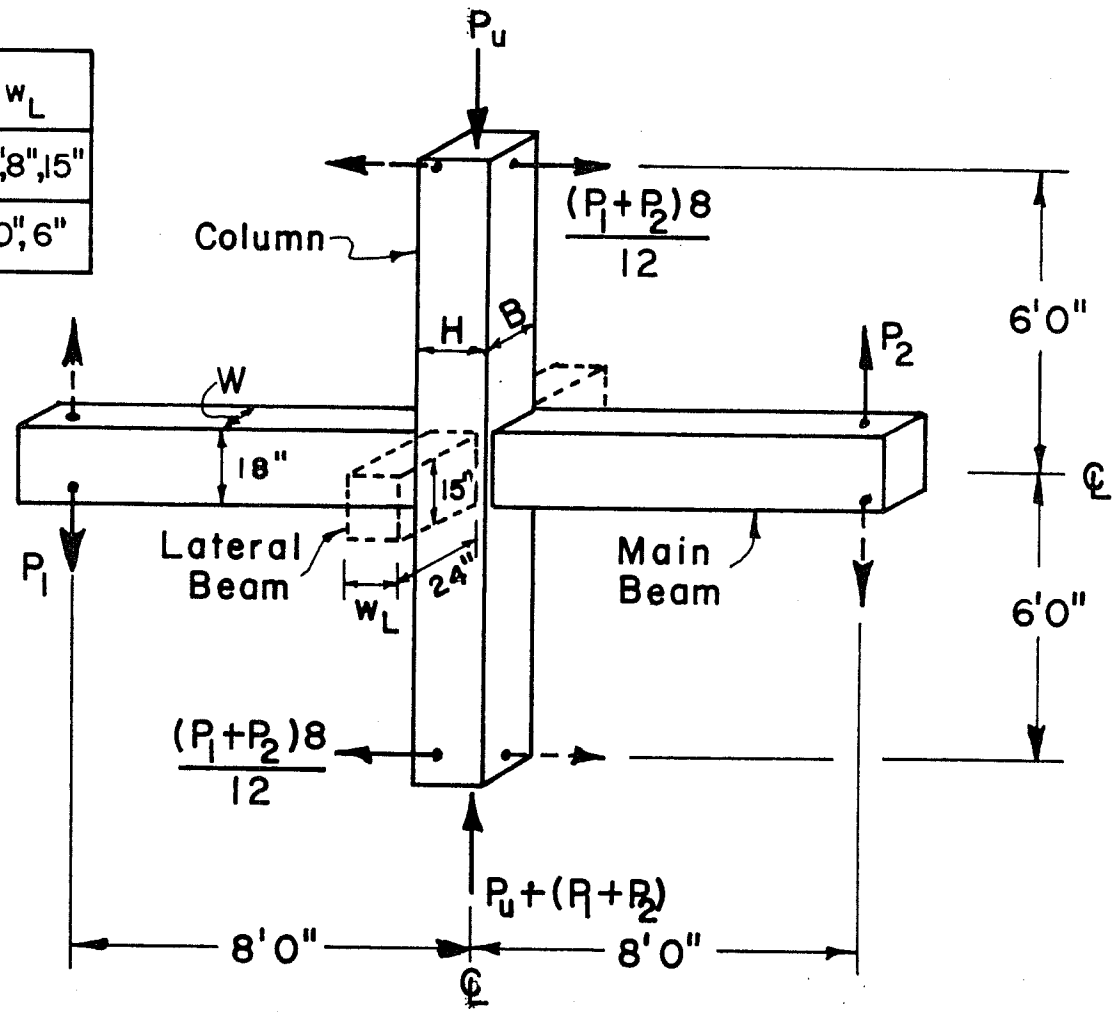

Fig. 2.1 Test specimen

moment on the joint due to the P-Δ effect. Whether the P-Δ effect in the column causes the column moments to be greater than or less than the beam moments is immaterial because the joint must resist shearing forces caused by the members that yield first. As stated earlier, the beams at a joint are the members that should exhibit yielding and ductility. For a specimen designed to measure the strength of a joint, testing it in a manner that neglects the P-Δ induced column moments and shears should have no influence on the joint strength as long as the beams are required to deform plastically. In these tests the column was held stationary while the beams were deflected. For reversal of load, the forces shown dashed in Fig. 2.1 were applied to the specimen.

2.2 Specimen Details

The overall specimen and member dimensions are indicated in Fig. 2.1. A more detailed drawing showing the location of beam stirrups and column ties can be found in Appendix A.

Main Beams. In each specimen, the depth of the main beam was 18 in. The width of the beam depended upon the width of the column face into which it framed. The width of the main beam was always 2 in. less than the corresponding width of the column. Beams that framed into a 13 in. wide column (strong axis bending of the column), see Fig. 2.1(a), were 11 in. wide and 18 in. deep, while beams framing into an 18 in. wide column (weak axis bending of the column) were 16 in. wide and 18 in. deep as shown in Fig. 2.2(b). Both of the beam cross sections were reinforced identically. By maintaining the size and number of bars constant in the main beams, even though the beam cross section changed, the maximum tension or compression force the beam could apply to the joint was eliminated as a variable. All main beams were reinforced with three #10 bars on top and three #8 bars on the bottom, Grade 60 reinforcement. All longitudinal beam reinforcement was continuous through the joint.

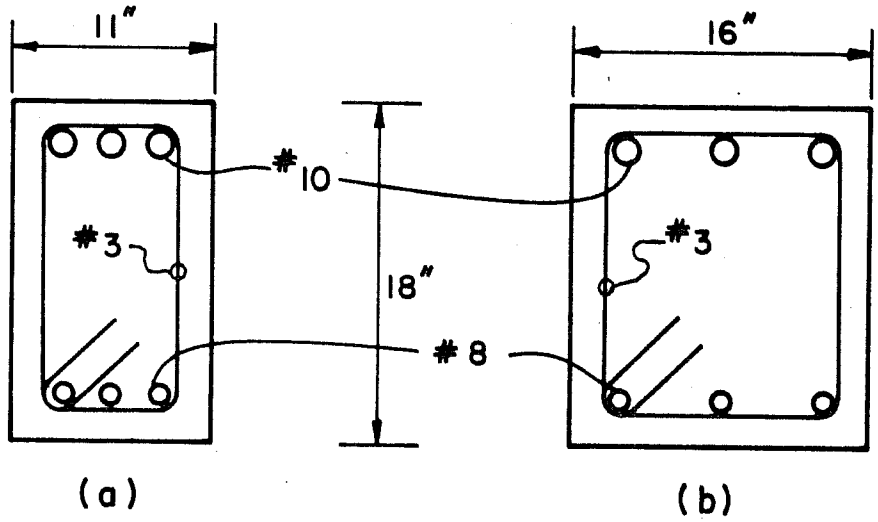

Clear Cover on #8 and #10 Bars = 2-in.
Side Cover on #3 Stirrups = 1½-in.

Fig. 2.2 Main beam cross sections

Stirrup reinforcement in the beams was proportioned for the total applied shear or for the minimum requirements for seismic design as specified by ACI 318-71.[2] A #3 closed stirrup with extra hook embedment length was used for all beam web reinforcement.

The distance from the point of load application to the face of the column was 87 in. for specimens in which the beams were 11 in. wide and 89-1/2 in. for specimens with the 16 in. wide beam. The distances were selected to fit the constraints of laboratory testing facilities.

Column. A 13 in. by 18 in. rectangular column cross section was used in all test specimens. To vary the shear span of the joint, the column cross section was rotated 90^{o} to allow the main beam to frame into either the wide or narrow column dimension. The column was designed assuming points of inflection at the midstory heights above and below the beam middepth. A column story height of 12 ft. was chosen as being typical of columns in reinforced concrete buildings and was also a compatible dimension for testing facilities.

Column reinforcing percentages were varied to determine the influence of the "cage" effect in providing confinement to joint concrete. Three different percentages of reinforcement were used in Specimens I, II, and III. The column cross sections are shown in Fig. 2.3.

Locations of column ties are detailed in Appendix A1 and A3 for two different design cases. For the specimen where the column load is greater than $0.4P_{bal}$, closely spaced #4 double hoops were used adjacent to the joint to confine the column core and to ensure ductility. Where column core confinement was no longer required, the bar size and spacing was dictated by shear in the column. The other design case results when the column is lightly loaded, $P < 0.4P_{bal}$ (Specimen V). Since the column behavior in this instance is like that of a beam, the reinforcement was sized and positioned as for a beam designed for shear.

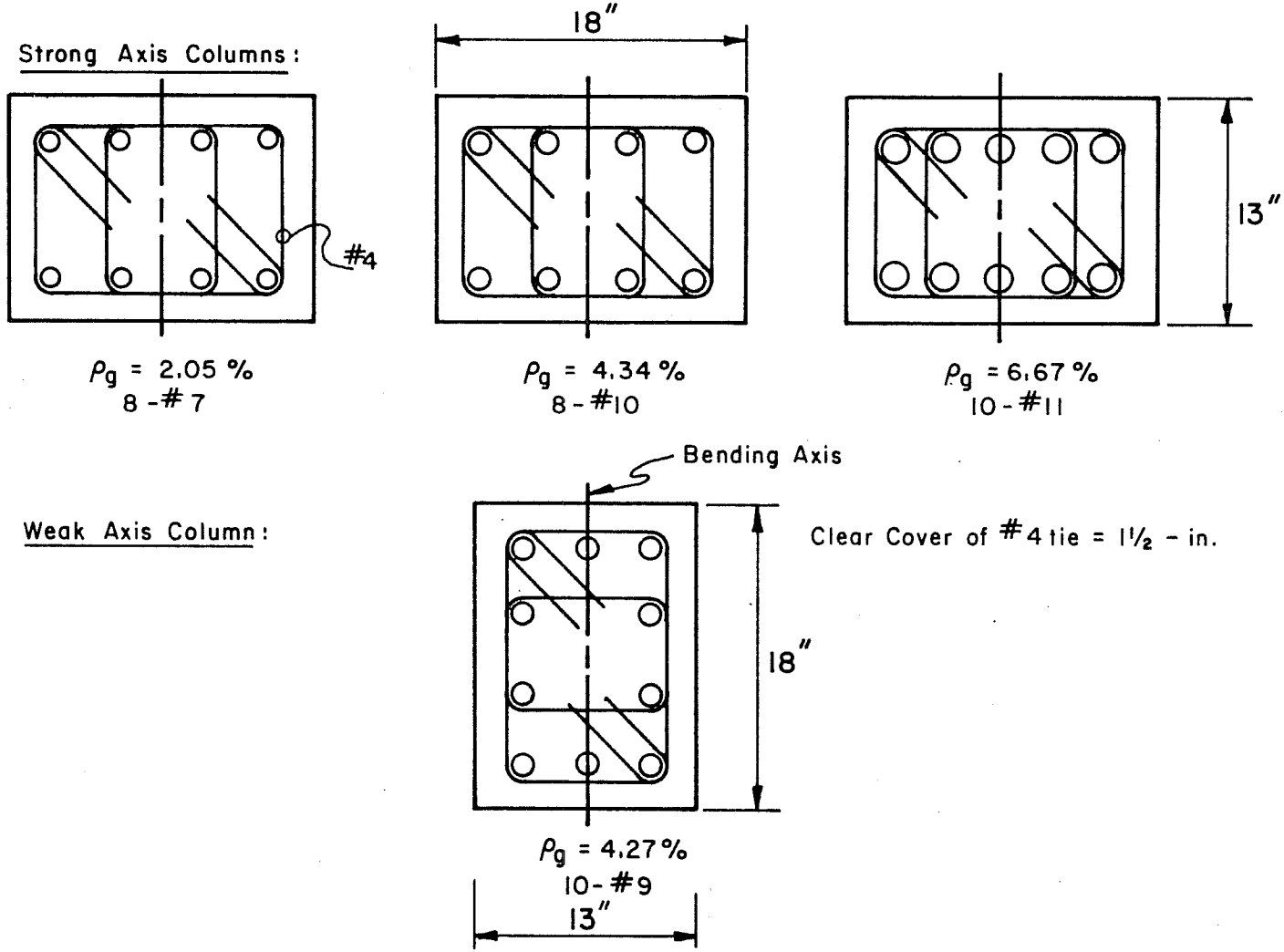

Fig. 2.3 Column cross sections

Lateral Beams. The main beams and column of the four specimens having lateral beams were designed identically to the main members of other specimens in the test series. Four specimens with lateral beams (Specimens VIII, IX, X, and XI) had two different ratios of the cross-sectional area of lateral beam to area of the joint, termed masking ratio (M). Lateral beams, masking either 70 or 37 percent of the joint area, framed into opposite sides of the joint and were perpendicular to the main beams (see Fig. 2.1). No loads were to be applied to these short lateral beams; consequently, there was no rigorous analysis to determine the size and number of reinforcing bars to be placed in the lateral beam cross section. Flexural reinforcement was selected as being typical for the lateral beam cross sections used. The percentage of reinforcement was constant for each lateral beam and the top and bottom beam bars were the same size and grade of steel. The top bars were located immediately beneath the negative moment reinforcement (#10 bars) in the main beam, while the bottom bars were positioned to have 2 in. of clear cover. Cross sections of the lateral beams and their location relative to the column centerline and main beam depth are shown in Fig. 2.4. Sufficient light stirrup reinforcement was provided to hold the lateral beam bars in position while casting. These stirrups were located near the free ends of each of the 2 ft. long lateral beams. The region adjacent to the column faces, therefore, was not confined by closed stirrups, requiring the concrete to carry any reflection of shear cracking propagating from the joint core.

Joint Reinforcing. A major objective of this testing program was to determine the ability of the concrete in the joint to carry shear stresses. Therefore, in a majority of the specimens the joint was underdesigned for shear. Numerous test results[12-16,19-22] on reinforced concrete beam-column joints with and without transverse reinforcement have indicated that some minimum joint reinforcement, in the form of hoops, improves the behavior of the joint. Table 2.2

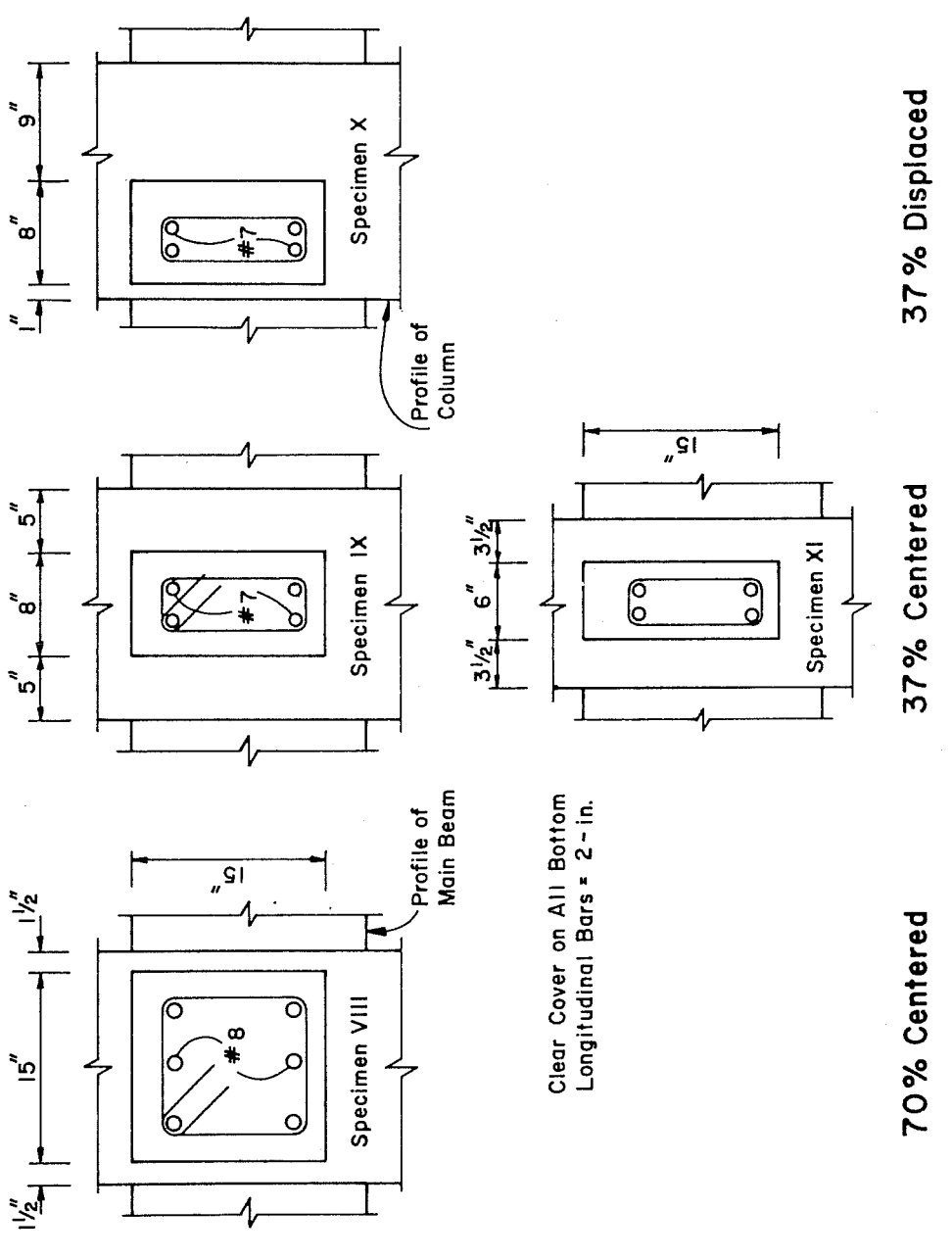

Fig. 2.4 Cross sections of lateral beams masking the joint

lists the minimum amount of transverse hoop reinforcement required by Ref. 9 and the amount provided in each type of test specimen.

In the report by the ACI-ASCE Joint Committee 352,[9] it is suggested that in any beam-column joint of a structure located in a seismic area (Type 2) a minimum amount of transverse hoop reinforcement be included. For these joints where ductility is required by the beams, the minimum area of joint reinforcement for the rectangular type hoop is computed by

$$A_{sh} \geq 0.3\, \ell_h s_h \left(\frac{A_g}{A_{ch}} - 1 \right) \frac{f'_c}{f_y} \qquad (2\text{-}1a)$$

but not less than

$$0.12\, \frac{f'_c}{f_y}\, \ell_h s_h \qquad (2.1b)$$

where A_{sh} = total cross-sectional area of a rectangular joint hoop, in.^{2}

ℓ_h = core dimension which joint hoop crosses, in.

s_h = center-to-center spacing of hoops along vertical column bars, in.

A_g = gross area of column, in.^{2}

A_{ch} = area of rectangular core measured to the outside of the joint hoop, in.^{2}

Using the column dimensions described earlier, the joint hoop area to spacing ratio required by Eq. (2-1) was 0.19 in. and 0.13 in. for specimens where the column bending was about the strong and weak bending axes, respectively. For other less severe loading conditions, where the joint must be designed for strength only (Type 1), it is recommended that, as a minimum, #3 bars spaced at 6 in. be included if all four faces on the joint are not confined by members. If member confinement is not present on opposite faces of the joint, the amount of reinforcement calculated by Eq. (2.1a) must be included in the joint as confinement reinforcement.

TABLE 2.2 COMPARISON OF TRANSVERSE REINFORCEMENT REQUIRED BY ACI-ASCE 352 WITH TRANSVERSE REINFORCEMENT PROVIDED IN TEST SPECIMENS

Column Bending Axis	ACI-ASCE 352 Requirements				Provided		
	Type 1		Type 2		Specimens		
	Confinement	Shear	Confinement	Shear	I, II, III, IV V, VI, VII, VIII IX, X, XI	XIII, XIV	XII
Strong	$\frac{A_{sh}}{s} \geq 0.19''$	0	$\frac{A_{sh}}{s} \geq 0.19''$	$\frac{A_{sv}}{s} \geq 0.31''$	#4@6" (0.07 in.)	#4@2" (0.20 in.)	#5@2" (0.31 in.)
Weak	$\frac{A_{sh}}{s} \geq 0.13''$	0	$\frac{A_{sh}}{s} \geq 0.13''$	$\frac{A_{sv}}{s} \geq 0.31''$	#4@6" (0.07 in.)	#4@2" (0.20 in.)	
			$\frac{V_u \text{ (provided)}}{V_u \text{ (required by shear)}}$		0.53	0.82	1.05

The confinement requirement can be satisfied for Type 1 or Type 2 joints by using #4 hoops at 2 in. through the joint. The hoop area to spacing ratio for shear in a Type 2 joint would be 0.31 in. for all specimens using the design procedure outlined in Chapter 1.

The bar size and spacing of the transverse joint reinforcement is shown in Table 2.2. The area to spacing ratio is shown in parentheses for comparison with ACI-ASCE Committee 352 requirements.

The joint reinforcement details are summarized in Fig. 2.5 for each of the joint types considered. If yielding of the beam tension reinforcement on opposite corners of the joint constitutes the ultimate shear on the joint, the ratios of the shear strength provided by the Committee 352 approach of Chapter 1 to the strength required to cause beam yielding are as shown in the last line in Table 2.2. These ratios were computed using a design concrete strength of 4500 psi, a reinforcement yield of 60000 psi, and Eq. (1-4) with N_u/A_g of 1500 psi, γ equal to 1.0, and β equal 1.4.

A summary of the geometric and reinforcement details is found in Table 2.3.

2.3 Material Properties

Concrete. The trend in reinforced concrete building design is to use a higher strength concrete in the column than in the flexural members.[1] Since concrete design strengths for the columns in medium rise buildings now range between 4000 and 5000 psi, 4500 psi concrete was selected and used in both the beams and column.

A concrete mix design using Type 1 portland cement, Colorado River sand and a graded gravel, 5/8 in. maximum, was delivered from a local ready-mix concrete producer for each specimen. All quantities were batched by weight at the dispatching plant. After casting the first specimen, the original concrete mix design was altered to maintain strength but use a higher slump to facilitate placement of

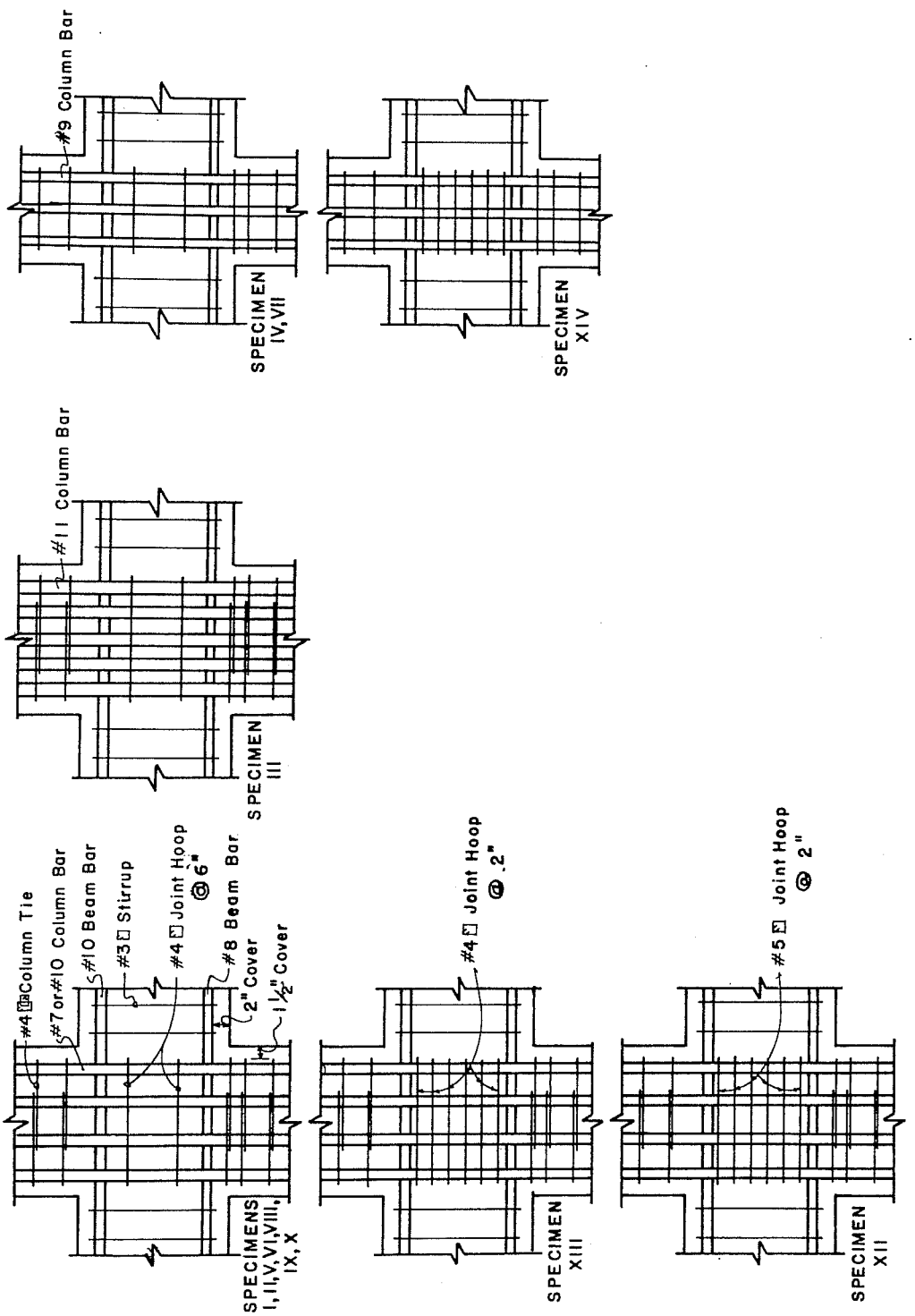

Fig. 2.5 Joint reinforcement details

TABLE 2.3 DETAILS OF TEST SPECIMENS

Specimen	Column Bending Axis	Column Reinforcement		Column Load (kips)	P_u/P_o Design	Main Beam			Lateral Beam				Joint Reinforcement
		Bars	ρ_g			Width (in.)	Depth (in.)	Reinf.	Width (in.)	Depth (in.)	Location	Reinf.* Top	
I	Strong	8 - #7	2.05	351	0.297	11	18	3 - #8 bottom; 2-in. clear cover on both	-	-	-	-	2 - #4 @ 6"
II	Strong	8 - #10	4.34	351	0.233	11	18		-	-	-	-	2 - #4 @ 6"
III	Strong	10 - #11	6.67	351	0.192	11	18		-	-	-	-	2 - #4 @ 6"
IV	Weak	10 - #9	4.27	351	0.235	16	18		-	-	-	-	2 - #4 @ 6"
V	Strong	8 - #10	4.34	47	0.031	11	18		-	-	-	-	2 - #4 @ 6"
VI	Strong	8 - #10	4.34	585	0.387	11	18		-	-	-	-	2 - #4 @ 6"
VII	Weak	10 - #9	4.27	585	0.391	16	18		-	-	-	-	2 - #4 @ 6"
VIII	Strong	8 - #10	4.34	351	0.233	11	18		15	15	Centered	3 - #8	2 - #4 @ 6"
IX	Strong	8 - #10	4.34	351	0.233	11	18		8	15	Centered	2 - #7	2 - #4 @ 6"
X	Strong	8 - #10	4.34	351	0.233	11	18		8	15	Displaced	2 - #7	2 - #4 @ 6"
XI	Weak	10 - #9	4.27	351	0.235	16	18		6	15	Centered	2 - #6	2 - #4 @ 6"
XII	Strong	8 - #10	4.34	351	0.233	11	18	3 - #10 top;	-	-	-	-	6 - #5 @ 2"
XIII	Strong	8 - #10	4.34	351	0.233	11	18		-	-	-	-	6 - #4 @ 2"
XIV	Weak	10 - #9	4.27	351	0.235	16	18		-	-	-	-	6 - #4 @ 2"

*Same reinforcing use on bottom--symmetrically reinforced.

concrete in the column. The mix proportions per cubic yard of the final mix design were 262 lbs. water, 564 lbs. Type 1 portland cement, 1830 lbs. of maximum size 5/8 in. aggregate, and 1500 lbs. of river sand. The water content was sufficient to maintain strength but keep the workability such that the slump[23] was 6 in. Properties of the concrete were determined from tests of standard 6 × 12 in. cylinders cured with the specimen. Cylinders were tested at the time the specimen was tested and the results are listed in Table 2.4.

Reinforcing Steel. All reinforcement used in this investigation conformed to ASTM Designation A615 Grade 60.[24] Bars of the same size were rolled by the same manufacturer and were from substantially the same lot. Measured yield stresses, an average of at least three test results, moduli of elasticity, ultimate stress, and percentage elongation in 8 in. for reinforcing bars used in specimen fabrication are listed in Table 2.5. Stress-strain curves for the beam reinforcement and joint hoop reinforcement are shown in Fig. 2.6. These curves are based on nominal bar areas and elongations measured in an 8 in. gage length.

2.4 Specimen Fabrication

Formwork. The form for casting the test specimens was constructed of 3/4 in. Grade B-B plywood which was stiffened with 2 × 4 in. lumber. The plywood surfaces on which concrete was placed were lightly oiled before each casting to aid in removal of the formwork from the specimen.

Specimens were cast vertically as they would be in an actual structure. Figure 2.7 shows an end view of the formwork before the simultaneous casting of two specimens. The form was designed so that two specimens, without lateral beams, could be cast together. Specimens with lateral beams were cast singly. Slight modifications in spacers at the joint were made when a specimen which had the

TABLE 2.4 CONCRETE PROPERTIES

Specimen	f'_c, psi	f_{sp},* psi	Age, days	Date Cast
I	3800	460	74	8-6-74
II	6060	610	57	11-8-74
III	3860	475	113	8-6-74
IV	5230	590	31	1-27-75
V	5200	560	56	12-17-74
VI	5330	585	65	12-17-74
VII	5400	555	38	1-27-75
VIII	4800	475	24	6-16-75
IX	4500	550	34	5-21-75
X	4290	550	24	7-2-75
XI	3720	440	33	5-5-75
XII	5100	575	52	3-24-75
XIII	5990	605	70	11-8-74
XIV	4810	550	30	3-24-75

*Tensile Splitting Strength

TABLE 2.5 REINFORCEMENT PROPERTIES

Bar Size	Yield Stress, ksi	Modulus of Elasticity, $\times 10^3$ ksi	Ultimate Stress, ksi	Percent Elongation in 8 in.
#3	70.3	27.4	106.3	14.2
#4	59.3	28.2	91.3	14.8
#5	61.3	28.0	106.6	15.0
#6	61.0*	26.5	99.4	15.8
#7	66.3	29.2	108.4	12.0
#8	58.8	27.8	96.5	15.4
#9	63.5	27.7	94.7	15.5
#10	65.1	27.3	101.7	13.7
#11	58.3	25.6	92.2	16.1

*Yield stress determined by 0.002 offset method.

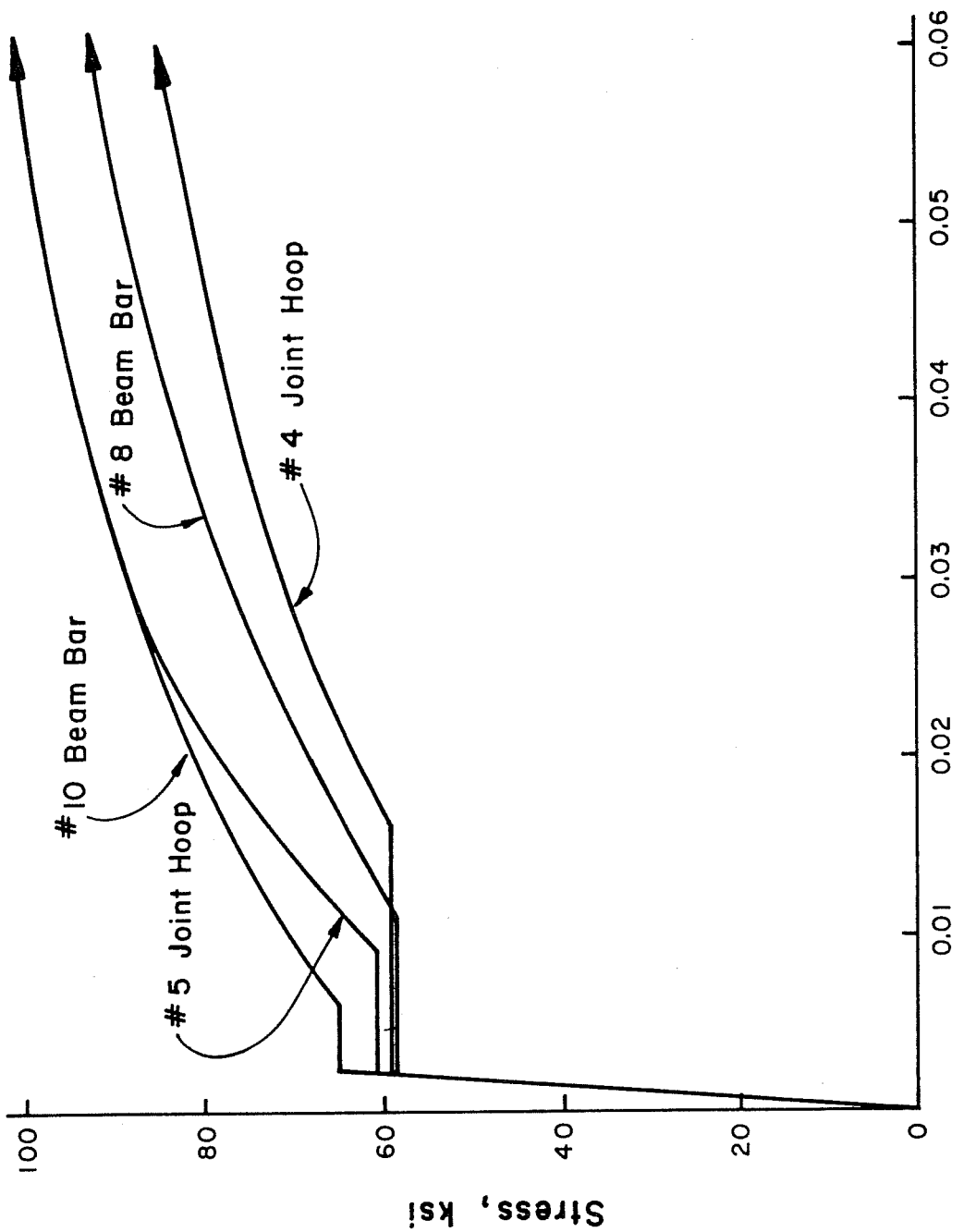

Fig. 2.6 Stress-strain relationships

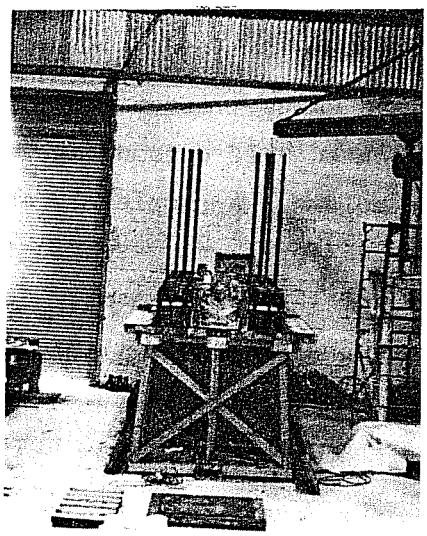

Fig. 2.7 Two test specimens before casting

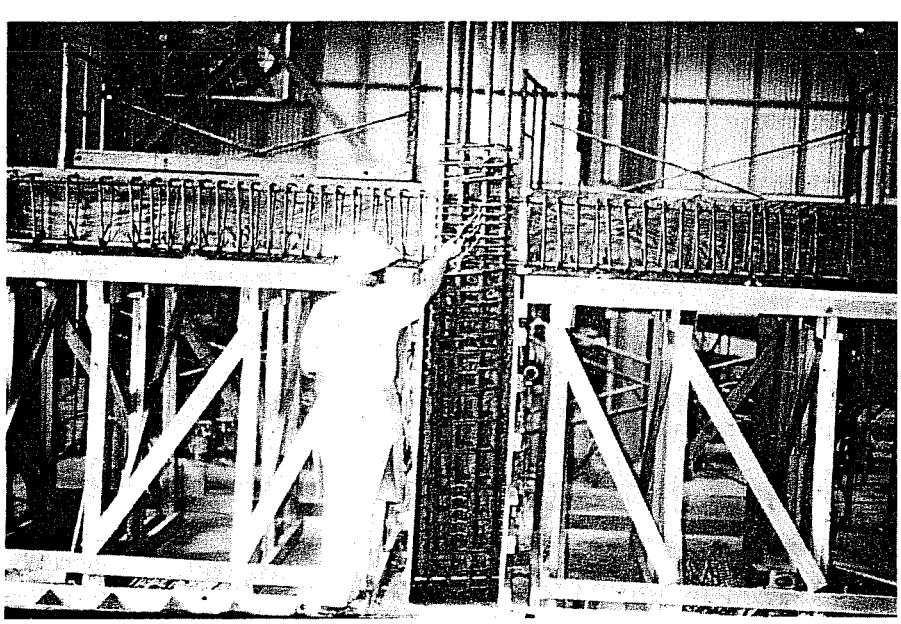

Fig. 2.8 Completed lower column and main beam cages with joint hoops in position

column bending about its weak axis was cast, but no new formwork was required.

Reinforcing Bar Cages. After the plywood form was aligned and oiled, a prefabricated half column cage was positioned in the lower portion of the column. A completely assembled main beam cage and loose joint hoop reinforcement was then threaded over the unassembled upper portion of the column bars. Subsequently, the joint hoop reinforcement was positioned in the joint and three column ties above the joint were placed, see Fig. 2.8. Column ties for the remainder of the unassembled column cage were positioned after casting the lower column and beams. Typical joint details are shown in Fig. 2.9.

Casting. The typical sequence for specimen casting was as follows: One-half of the joint formwork panel was left open to allow access to the lower column. When the lower column had been filled, either the lateral beam cage and its formwork were assembled or the open joint panel was closed. The main beams, lateral beams, joint, and a 6 in. portion of the upper column were then cast using concrete from the same batch as that used to cast the lower column.

Within three days following the casting of the lower column and beams, the remainder of the upper column ties were positioned, forms assembled and upper column cast. Specimens cast in this manner do not duplicate the location of cold construction joints found in actual construction. This casting procedure was used to eliminate any influence cold joints may have on the joint behavior.

Concrete consolidation in the column was aided by external form vibration as well as internal vibration. Reinforcing bar congestion and an open top of the beam form required the use of only internal vibration in the beams.

Sixteen standard 6 X 12 in. concrete cylinders were made for each specimen.[25] Six cylinders made from the concrete placed in

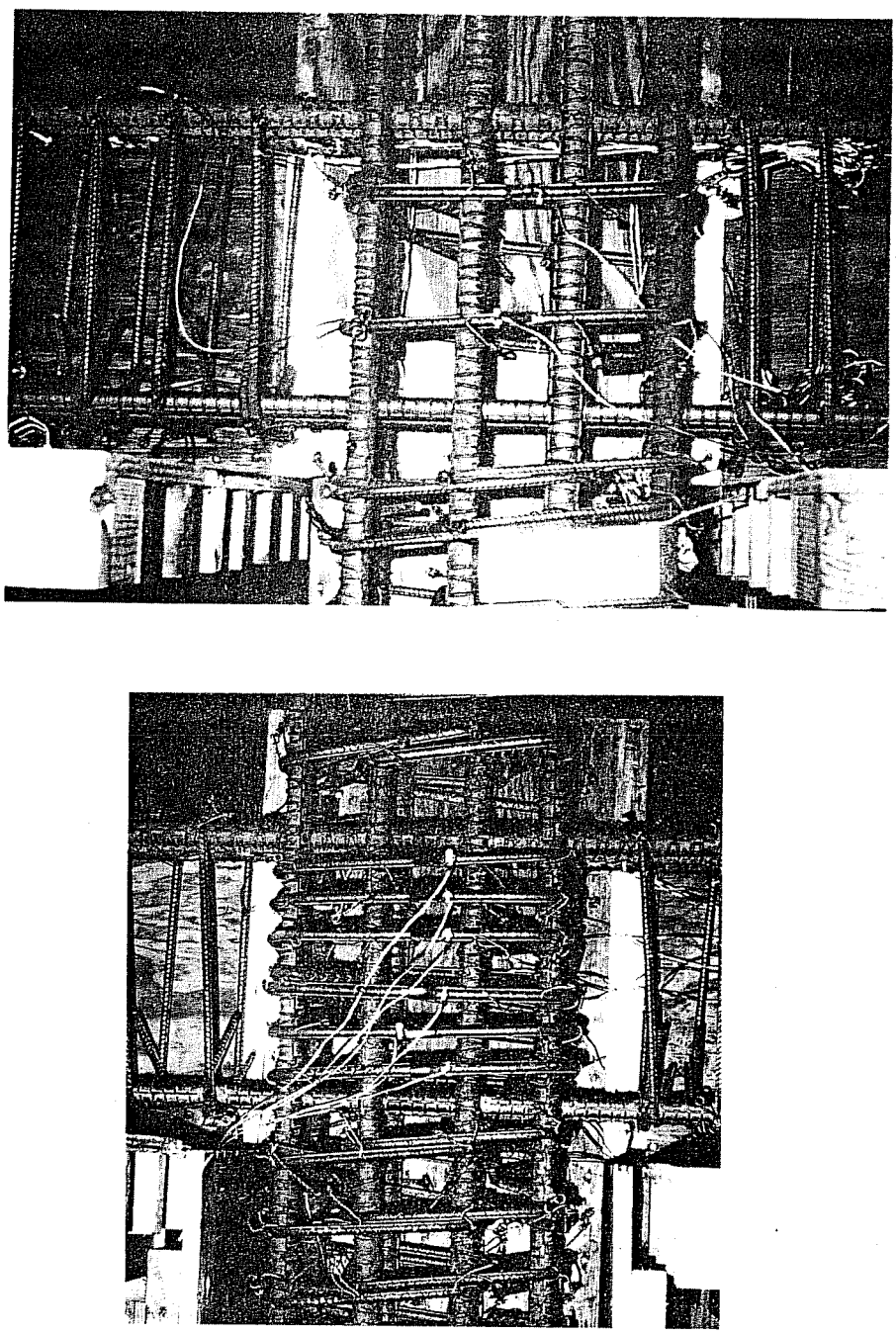

Fig. 2.9 Photographs of typical joint details

the lower column and beams were used to measure the compressive strength.[26] Six cylinders from the same concrete were tested to measure the tensile splitting strength.[27] Those results were reported in Table 2.4. The four remaining cylinders were from concrete used to cast the remainder of the column and all were tested in compression to check the concrete strength in the upper column. The average strength of concrete in the upper column was 100 psi less than the average strength of the lower column and beams.

Curing. After the top surface of the beams and upper column were screeded and troweled, they were covered with sheets of polyethylene plastic. The specimens were stored in the form and under polyethylene until the lower column and beams were at least seven days old. At seven days the polyethylene cover, column forms, and one side of the beam form were removed. Depending on the availability of storage space, the specimen was then moved from the form to a storage area or to the testing location. Concrete control cylinders were stripped and cured under the same atmospheric conditions as the specimen. There was no control of temperature or humidity during curing.

2.5 Specimen Instrumentation

Instrumentation for each test included the measurement of applied load, beam deflections, beam and column deformations near the joint, joint deformations, and reinforcing bar strains.

Strain Gages. Electrical resistance strain gages were bonded to the beam, column, and joint hoop reinforcement. The distribution of these strain gages is shown in Fig. 2.10. In the main beams and columns, gages outside the joint were located 9 in. from the joint-member boundary. Resistance wire type gages with resistance of 120 ohms and gage length of 0.64 in. were used on all reinforcing bar installations. Details of the installation procedure are reported elsewhere.[28]

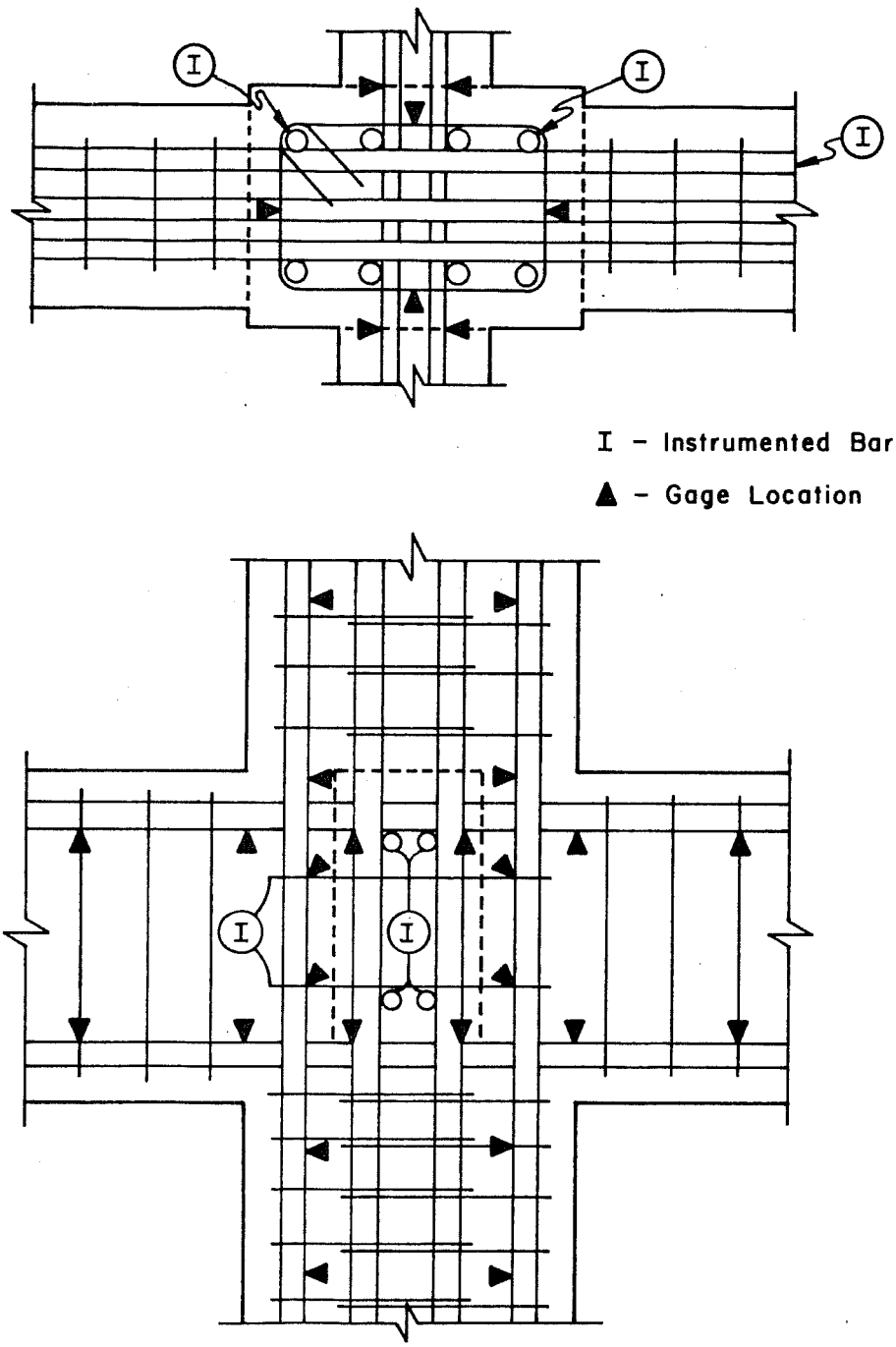

Fig. 2.10 Locations of electrical resistance strain gages on a typical specimen

Member and Joint Deformations. A schematic illustration of instrumentation, other than strain gages, is shown in Fig. 2.11. Two inch linear potentiometers were used to measure length changes. Beam curvatures were obtained from deformation measurements between the column face and a frame attached to the main beam 10 in. from the column face. For conversion of the beam deformations into beam curvatures, the deformation measurements were first converted to rotations by dividing by the distance between the deformation measurements (25 in.). To obtain curvature, the rotation was divided by the length (gage length) over which the deformations were measured (10 in.). The measurements used in computing main beam curvatures are marked ① in Fig. 2.11. Column curvatures were obtained using the same gage length but with the reference origin 3-1/2 in. above and below the top and bottom of the beam, respectively. Measurements used in computing column curvatures are marked ② in Fig. 2.11. The potentiometers and frames making the curvature measurement are shown in Fig. 2.12 for a typical installation.

Two types of joint deformation were measured in each test. Joint shear deformations were approximated by measuring length changes across opposite corners of the joint (on the top face) and using the law of cosines to obtain angular deformations. The shear deformation was taken as the average of the two measurements marked ③ in Fig. 2.11. The total angular rotation of the joint was measured by potentiometers attached to the ends of an arm rigidly fixed to either two steel studs embedded in the joint or to the lateral beam itself. Joint rotation was calculated knowing the total deflection of the ends of the arm and the distance between the deflection measurements. Deflections of the ends of the arm were measured by potentiometers marked ④ in Fig. 2.11. Figures 2.13(a) and (b) show the joint shear deformation apparatus and one end of the joint rotation arm with potentiometer when the specimen had a lateral beam.

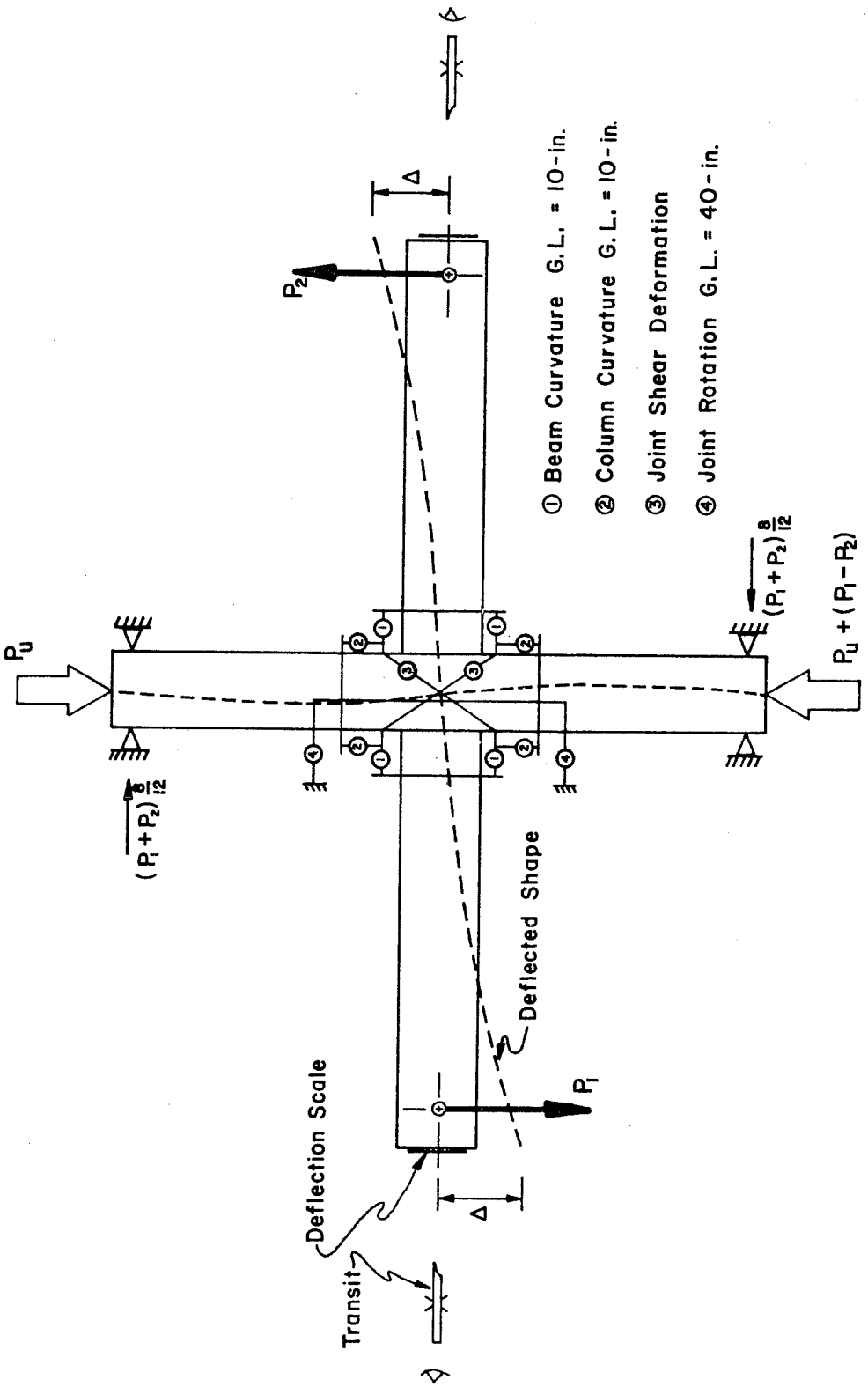

Fig. 2.11 Specimen statics and deformation instrumentation

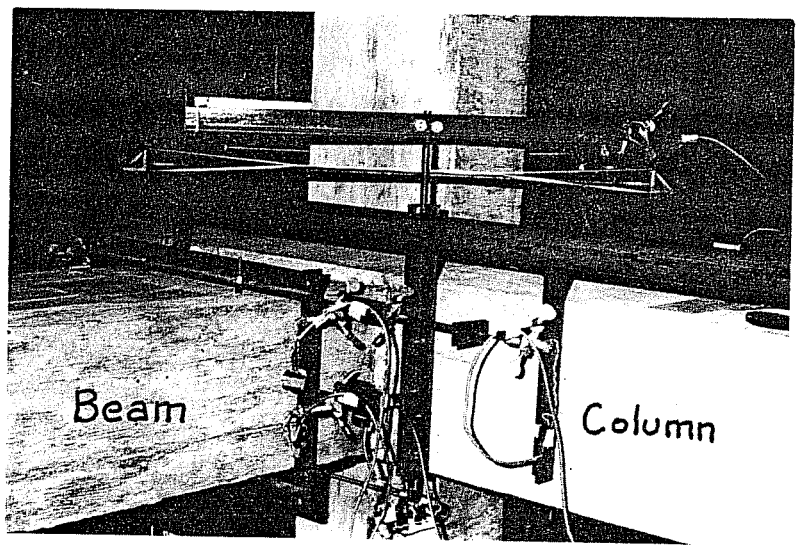

Fig. 2.12 Beam and column curvature instrumentation

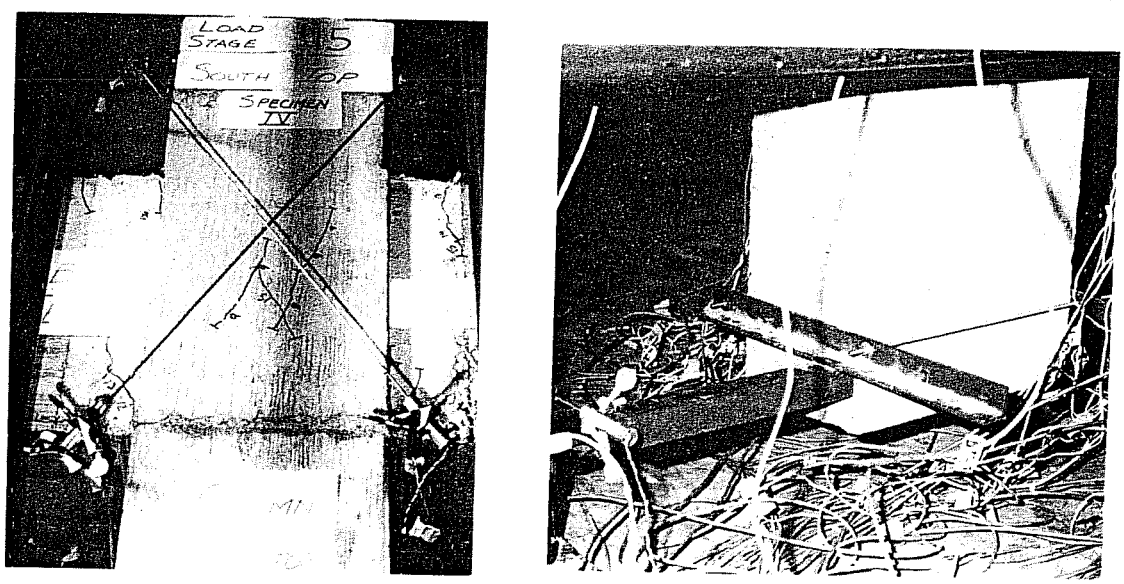

(a) Joint shear deformations (b) Joint rotation attachment

Fig. 2.13 Joint deformation instrumentation

Load Cells. Nine calibrated load cells measured the forces applied to the specimen. Two of these cells monitored the column load, and three cells measured the applied main beam loads, P_1 and P_2 shown in Fig. 2.11. The remainder of the cells were used to measure lateral or shear forces in the column.

Deflections. Deflections of the main beams were measured by sighting through a transit onto a 1/100 in. scale attached on the end of each main beam.

2.6 Testing Equipment

Limitations in existing testing equipment resulted in a test arrangement shown in Fig. 2.14. After the specimen was cast and cured in a vertical position, the column was rotated to a horizontal plane for transportation and placement in the test frame. The specimen was held off the test floor by four support blocks, shown in Fig. 2.14 as A. Rollers were placed between the deflecting beams and the support pedestal whereas a neoprene pad was placed between the nondeflecting column and support pedestal. The column load was applied by a self-contained loading system built from tension rods, hydraulic rams, and massive loading heads, shown as B. Spherical pivots were placed between the massive loading heads and the column (see C in Fig. 2.14). Main beam loads were applied by means of frames labeled D in Fig. 2.14. Moment equilibrium forces induced in the column were resisted by frames titled E. The main beam loads, P_1 and P_2, were not equal even though opposite in direction. Equilibrium was achieved by removing the unbalanced force from the column with diagonal tension ties shown as F in Fig. 2.14. All main beam frames (D) and column shear frames (E) were post-tensioned to the test floor. A post-tension of approximately 120 kips facilitated the transfer of all lateral load to the floor by friction. Exploratory tests indicated that the coefficient of friction between the steel base plate of the frame and the test floor,

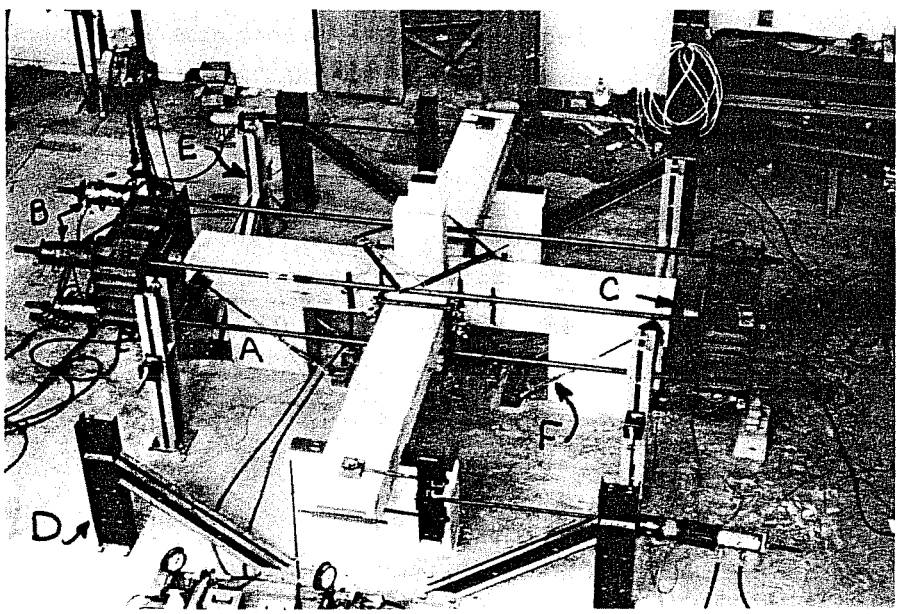

A: Supporting pedestals
B: Column load
C: Spherical pivot
D: Main beam frame
E: Column shear frame
F: Tension tie for unbalanced beam load

Fig. 2.14 Test setup

with a mortar grout in between, was in excess of 0.75. These frames worked satisfactorily during the testing program with no slippage being observed.

Three independent hydraulic systems were used to supply pressure to the hydraulic rams. One system supplied the four 200 kip rams for the column load, and one system each activated the pressure to the 60 kip rams applying the main beam loads. Pressures in each of the hydraulic systems were monitored with a pressure gage, and for the main beam hydraulic systems the pressures were also recorded with an electrically instrumented pressure transducer.

2.7 Testing Procedure

After aligning holes formed in the specimen with slots in the reaction frames, a column load of predetermined magnitude was applied and held constant for the duration of the test.

Loads were then applied to the free ends of the main beams as required to cause both beams to deflect equal amounts in opposite directions. In each test the forces on the joint were reversed by alternating the direction of load on the main beams. Three complete cycles of load reversal were applied according to the following procedure.

Cycle 1: The first cycle consisted of loading the main beams sufficiently to cause a visible diagonal shear crack to form in the joint or to reach 50 percent of the main beam yield moment at the face of the column.

Cycle 2: The main beams were deformed equal amounts from their respective residual deflections of Cycle 1 to cause the moment at the joint to be a maximum. The maximum moment was limited by either yielding of the tension reinforcement in both main beams or by the maximum shear the joint could resist.

Cycle 3: Cycle 3 repeated the loading scheme used in Cycle 2 except deflection increments were measured from the residual deflections of Cycle 2. Again, conditions producing a maximum joint shear were desired.

No maximum plastic deformation requirements were imposed on the beams after the beams produced a maximum joint shear. Testing was terminated with removal of the column load at the end of at least three complete cycles.

2.8 Data Acquisition and Reduction

Plots of load versus deflection were made for each beam during the test. In addition, a continuous trace of main beam load versus main beam curvature was automatically plotted on an x-y recorder. The curves were used to determine the magnitude of moment on the joint and as a check on the progress of the test.

All the electrical instrumentation, load cells, potentiometers, and strain gages were read with a VIDAR digital data acquisition system. Data in the form of voltages were recorded in two forms. The first was an immediate hardcopy printout of voltage for a particular instrument. This record aided in determining if a potentiometer required resetting and if the other instrumentation was functioning properly. Voltage data were also recorded on magnetic tape for processing with a computer program. The computer program converted changes in voltage to strain, load, or deflection.

A typical test lasted 12 to 16 hours and was usually completed in two days. When testing was terminated at the end of the day, the specimen was unloaded. This included removal of the column load. During each test and at the end of the test, a log describing the behavior, cracking, spalling, etc., was maintained for later reference.

CHAPTER 3

TEST RESULTS

3.1 General

In this chapter, relationships between applied loads and measured deformations will be presented for the specimens tested. Measured relationships for one specimen, Specimen II, will be discussed in detail because it is representative of the information collected for other specimens in this series and because it serves as a standard of comparison for other test program variables. A complete set of measured test data for each specimen can be found in Appendix B under the appropriate specimen number.

3.2 Column Load

One of three magnitudes of column load was applied and maintained on the column during testing. The column loads produced nominal stresses of 200, 1500, or 2500 psi on the gross cross section of the column. These nominal stresses represent levels of column compressive load below, near, or above the balance point on the compressive load-moment interaction diagram. Depending upon the percentage of vertical column steel, axis of column bending, and concrete strength, the balance point on the compressive load-moment interaction diagram can vary between nominal stresses of 1200 and 1600 psi. Actual column load used during testing was either 46.8, 351, or 585 kips. Representative plots of the compressive column load versus test duration are shown in Fig. 3.1. The specimen was completely unloaded, including removal of the column load, when testing stopped at the end of the day. The average applied column

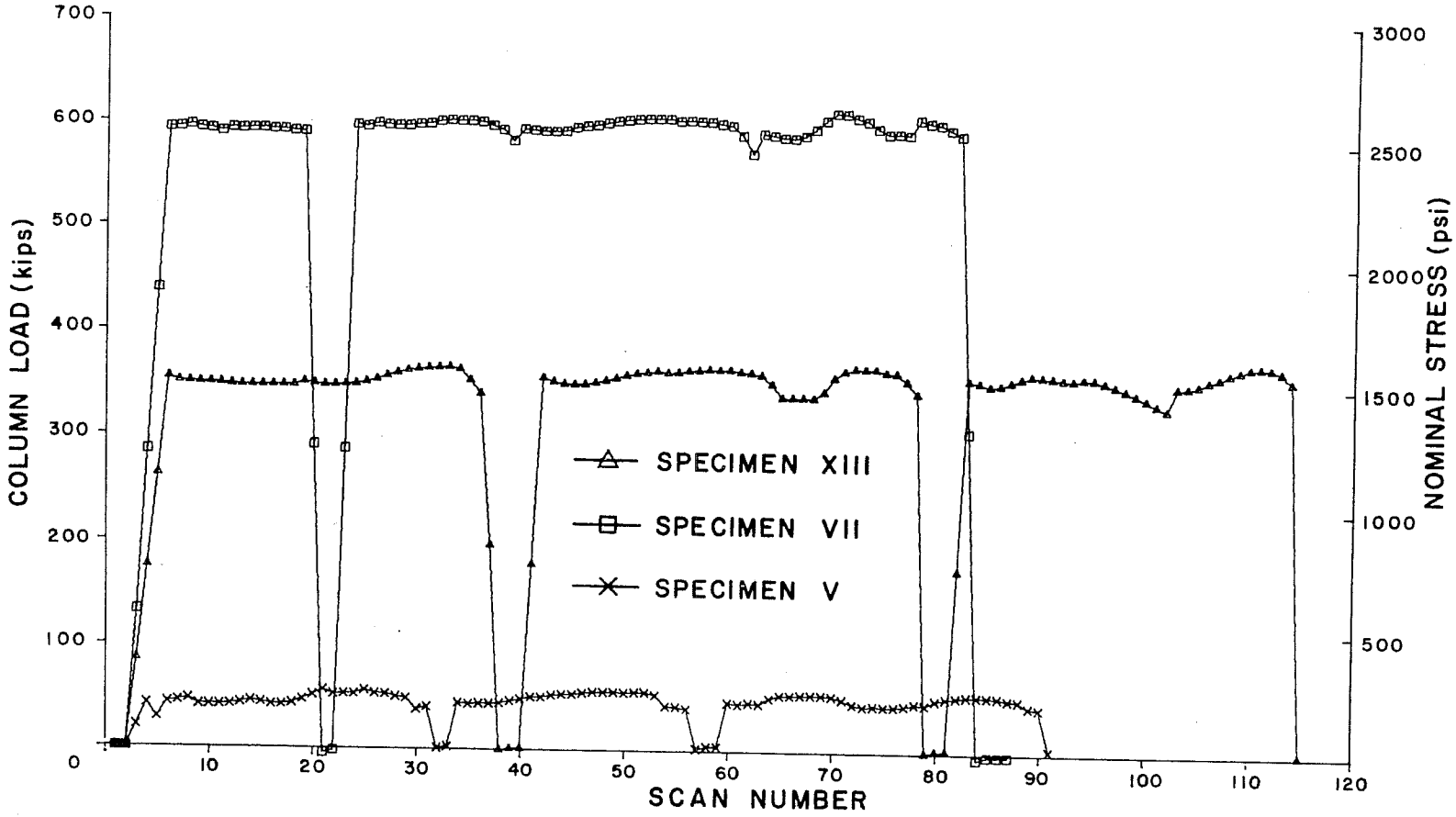

Fig. 3.1 Column load magnitudes

load and the percentage of the column concentric strength the applied load represents are given in Columns 1 and 2, respectively, of Table 3.1. The concentric strength was computed using the measured material properties for each specimen.

3.3 Typical Load-Deformation Relationships

Load-Deflection Curves. Two load-deflection curves, one for each main beam framing into the joint, were plotted for each specimen. A typical pair of load-deflection curves is shown in Fig. 3.2 for Specimen II. Note that one main beam is loaded in the up direction while the other beam is simultaneously loaded in the down direction. Deformation was controlled with both main beams subjected to equal deflection increments in opposite directions at any load stage. Under these conditions an unbalanced beam moment occurs at the joint applying shear forces to the joint. Points representing the same instant in the loading history lie in opposite quadrants of Figs. 3.2(a) and (b) of the curve. Note, for example, the points marked (load stage) 27.

Moment-Curvature of Main Beams. The instrumentation for deformations and the computation of main beam curvature were discussed previously in Section 2.5, Member and Joint Deformations. The main beam moment was computed by multiplying the applied load at the end of the main beam by the distance from the point of load application to the face of the column. Plots of the moment-curvature behavior for the east and west main beams are shown in Fig. 3.3.

Moment-Rotation of the Joint. Joint moment at any load stage is defined as the sum of the main beam moments at the face of the column. The measurement and computation of the joint angular rotation has been described in Section 2.5. Figure 3.4 is a plot of the joint moment-joint rotation behavior. Numbers adjacent to the curve represent load stages and correspond to those described in Fig. 3.2.

TABLE 3.1 TEST RESULTS

Specimen Number	Average Column Load (kips) P_u (1)	Percentage of Concentric Strength P_u/P_o (2)	Joint Shear Stiffness x 10^6 psi G (3)	Joint Shear at Diagonal Cracking V_{cr}, kips		Maximum Joint Shear V_j, kips				Maximum Joint Moment M_j, k-in				Failure Mode Limiting Maximum Load on Joint			
				1-1* (4)	1-2** (5)	2-1* (6)	2-2** (7)	3-1* (8)	3-2** (9)	2-1* (10)	2-2** (11)	3-1* (12)	3-2** (13)	2* (14)	2** (15)	3* (16)	3** (17)
I	357	0.34	1.15	-89	92	-245	234	-234	191	-3500	3340	-3330	2700	0	0	0	0
II	360	0.20	1.21	-108	124	-359	304	-269	224	-5120	4340	-3840	3170	0	0	0	0
III	356	0.22	1.00	-98	108	-276	244	-254	213	-3920	3470	-3620	3030	0	0	0	0
IV	363	0.22	1.04	-139	118	-327	294	-310	255	-4670	4170	-4440	3610	0	0	0	0
V	48	0.03	0.78	-54	43	-344	316	-265	241	-4920	4520	-3800	3440	0	0	0	0
VI	603	0.36	1.78	-168	150	-370	328	-281	225	-5300	4670	-4000	3210	X	0	0	0
VII	597	0.36	1.48	-180	180	-330	302	-272	240	-4700	4310	-3860	3410	0	0	0	0
VIII	355	0.23	1.25	-195	200	-381	378	-387	365	-5430	5440	-5500	5220	X	X	X	0
IX	367	0.24	1.15	-102	120	-359	350	-336	279	-5120	5000	-4780	3980	0	0	0	0
X	359	0.24	1.16	-103	146	-332	299	-288	244	-4730	4270	-4100	3480	0	0	0	0
XI	365	0.27	0.72	-90	124	-289	275	-264	250	-4100	3910	-3750	3550	0	0	0	0
XII	363	0.20	1.06	-136	110	-438	393	-328	313	-6230	5610	-4680	4460	X	X	0	0
XIII	353	0.20	1.52	-163	116	-350	333	-259	253	-4980	4760	-3690	3590	0	0	0	0
XIV	363	0.23	0.98	-123	132	-346	325	-284	238	-4910	4640	-4020	3400	0	0	0	0

*  ** 

0 Joint Failure

X Main Beam Reaches Yield Moment

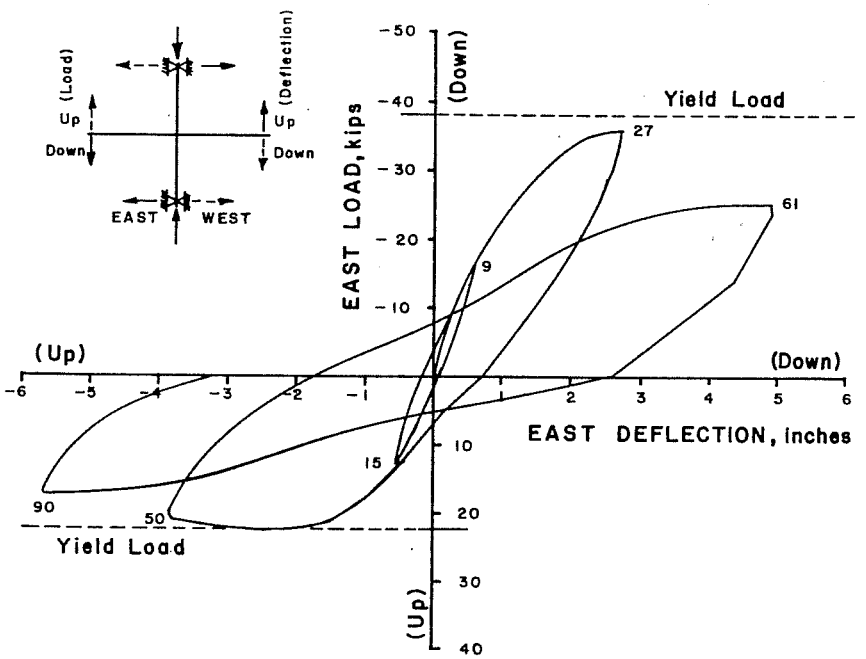

(a) East main beam load-deflection

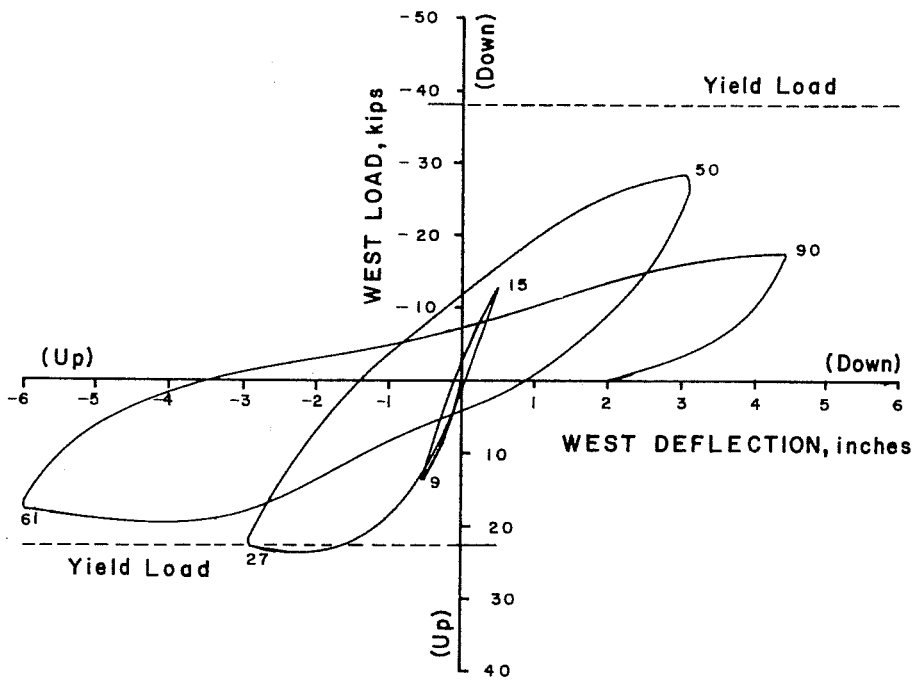

(b) West main beam load-deflection

Fig. 3.2 Load-deflection curves east and west main beams (Specimen II)

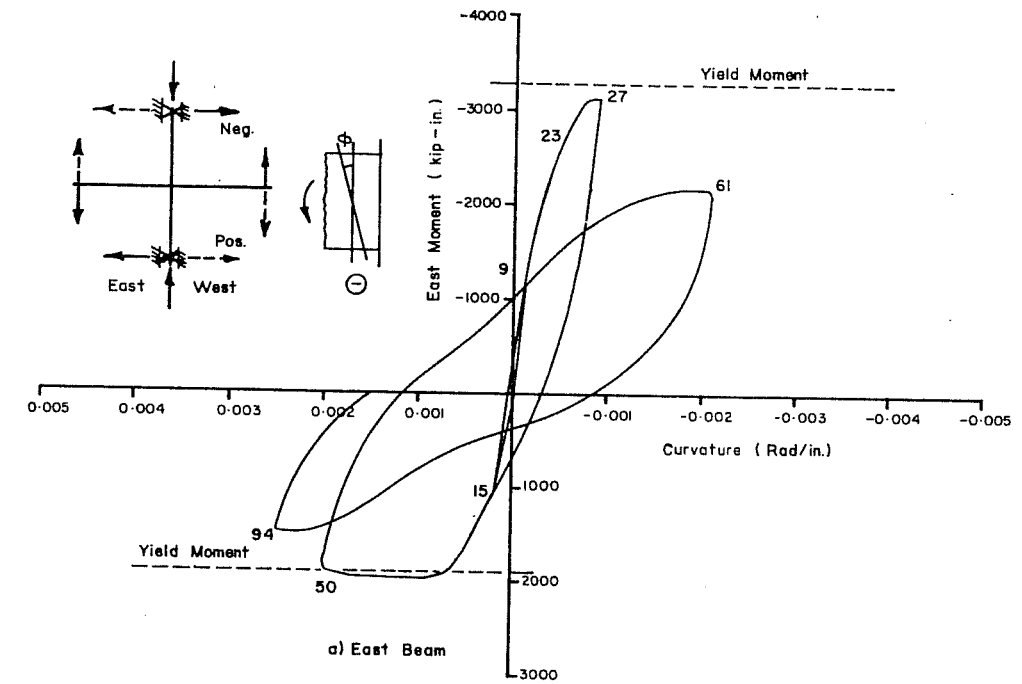

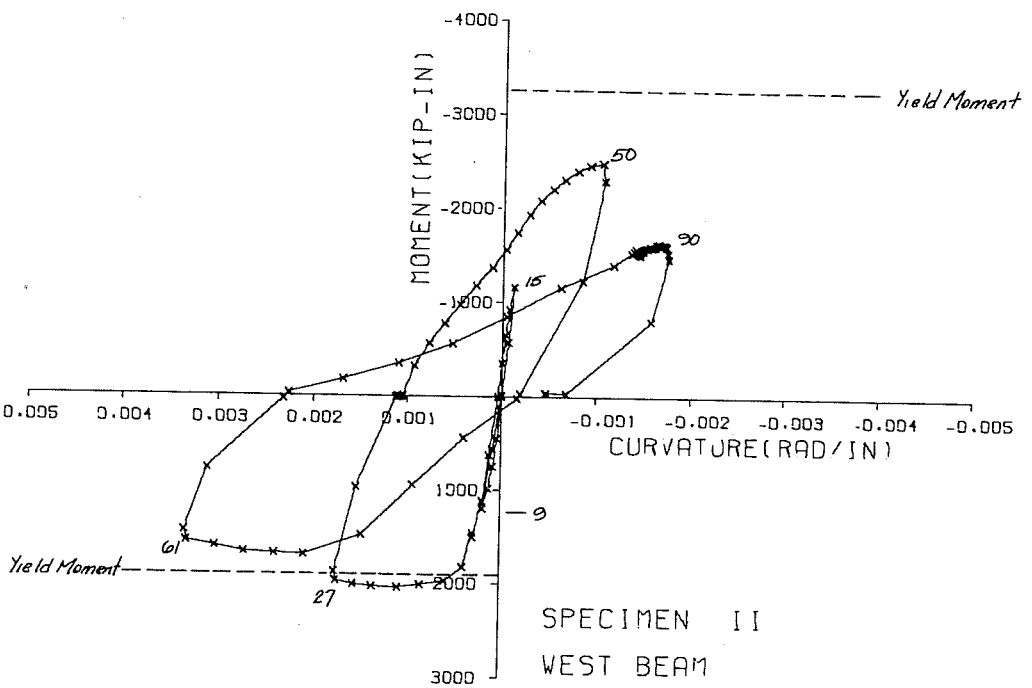

Fig. 3.3 Moment-curvature curves (Specimen II)

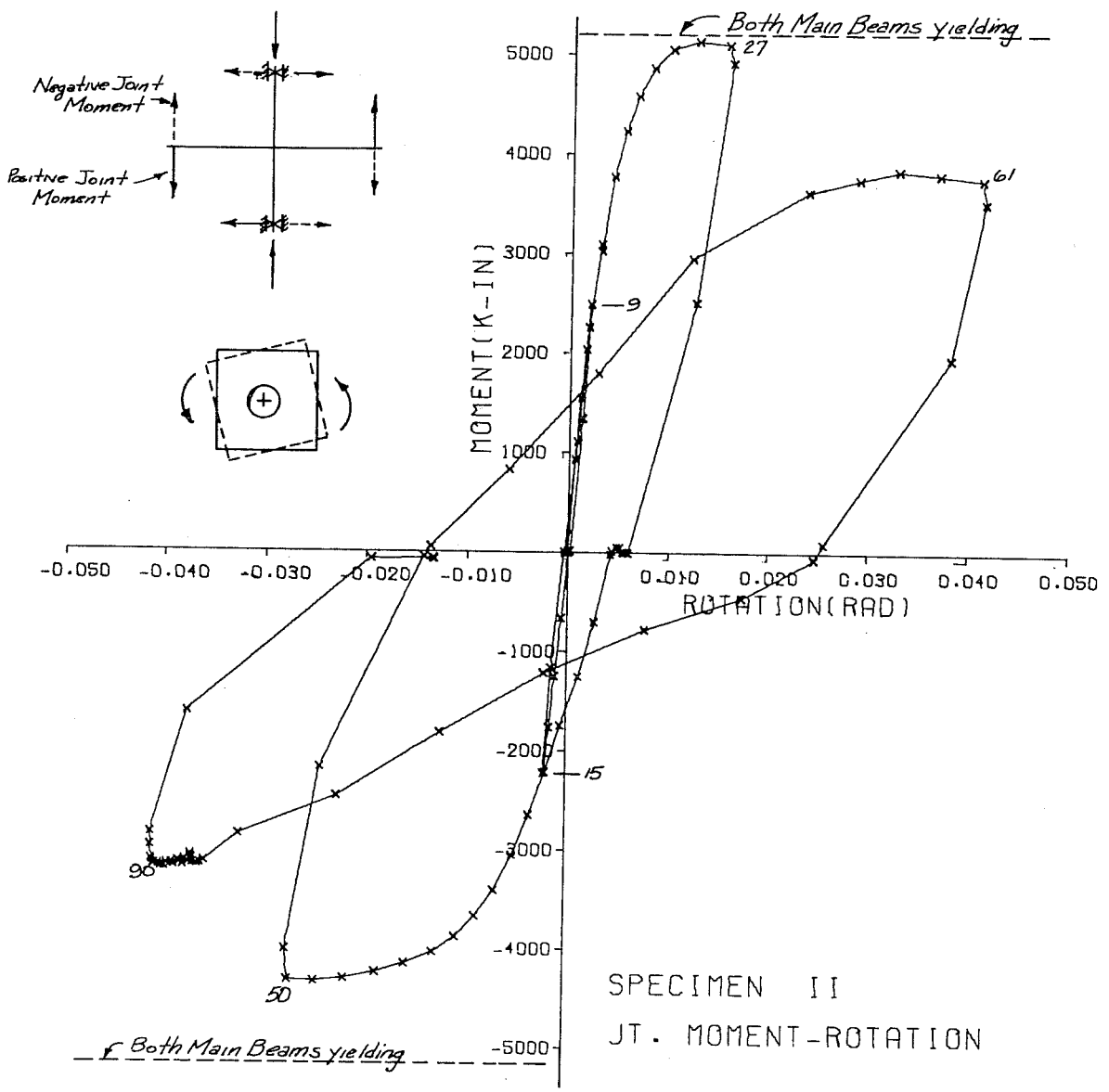

Fig. 3.4 Joint moment-joint rotation curve (Specimen II)

The value of the maximum joint moment for each half cycle of loading, is listed in Columns 10 through 13 of Table 3.1. The number in the column heading indicates the load cycle number and direction of applied shear on the joint. (Example: 2-1 represents the first half of the second load cycle.)

Applied Joint Shear-Shear Strain. When the main beam loads are applied in opposite directions, an unbalanced moment occurs at the joint. The main beam moments are transmitted to the column, which equilibrates the unbalance, through shear in the joint. The magnitude and direction of joint shear were computed from loads applied to the ends of the main beam. Figure 3.5 shows a diagrammatic representation of the real forces on the members and the substitute forces as they are applied to the joint. The external east and west main beam moments at the face of the column are resolved into internal forces by dividing the main beam moments by an assumed internal lever arm of (d-d'), the distance between the top and bottom layers of steel. For the specimen free body shown in Fig. 2.11 using the dimensions indicated on Fig. 2.1, the column shears must equilibrate the action of the applied beam loads. Column shears above and below the joint are equal in magnitude and opposite in direction. On a free body diagram of the joint, the joint shear (V_j) is the resultant of the algebraic summation of forces T_1, T_2, and V_{col}. All forces are calculated for the same instant in the load history. This procedure for calculating the joint shear was checked by examining the measured forces in the main beam longitudinal reinforcement and found to adequately predict the joint shear.

The angular distortion of the joint, the shear strain, was determined from measurements marked (3) in Fig. 2.11 and computed as described in Section 2.5. These shear strains are plotted in Fig. 3.6 with corresponding values of the applied joint shears. The applied joint shear has a direction opposite the internal resisting

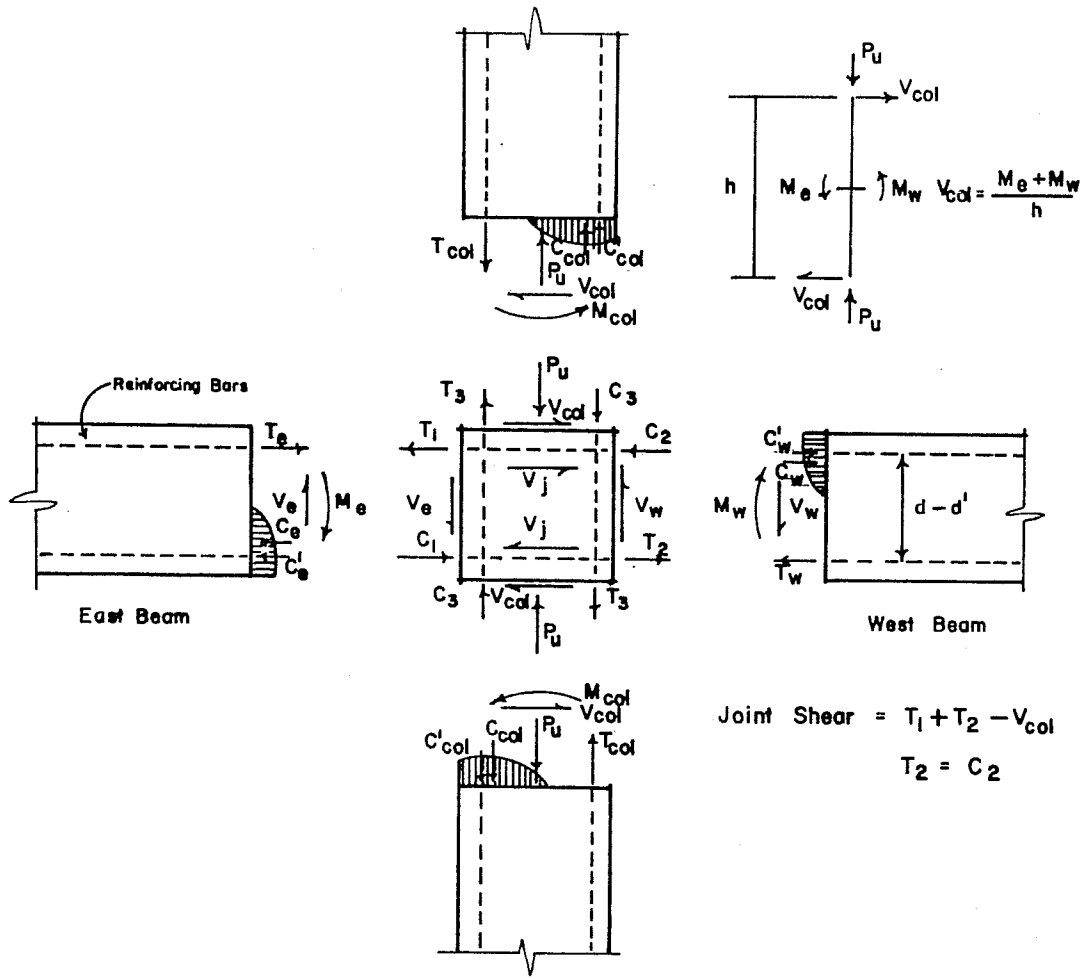

Fig. 3.5 Resolving internal member forces into applied shear

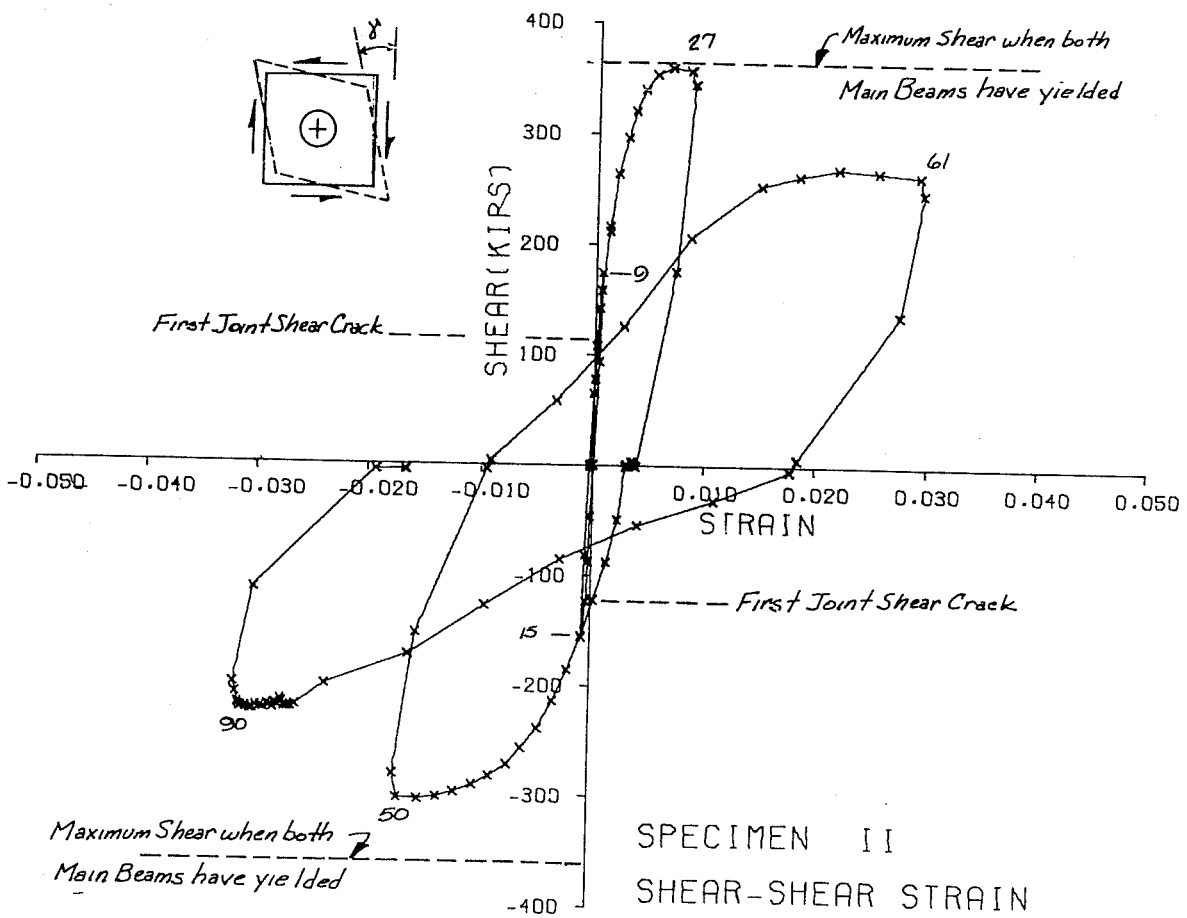

Fig. 3.6 Applied joint shear-shear strain curve (Specimen II)

shear shown in Fig. 3.5. Note the magnitude of the applied joint shear at the formation of the first diagonal shear crack as marked in Fig. 3.6. Using curves of applied joint shear and strain in the joint hoop reinforcement shown in Fig. 3.7, the joint cracking shear was easily determined as the point when the strain in the joint hoop first began to increase. As expected, applied joint shears at shear cracking determined using measured strains in the joint hoops are generally lower than the values obtained from visual inspection of cracking in the joint.

Figure 3.6 also illustrates the criterion used to terminate application of additional deflection. In Cycles 2 and 3 of the loading history, identical end deflection increments were applied to both beams until the value of applied joint shear was a maximum. When the applied joint shear was maximum, either the main beams had reached their respective yield moments or the joint had failed in shear and bond. The value of the maximum applied joint shear for each half cycle of loading is listed in Columns 6 through 9 of Table 3.1.

Joint Shear Cracking. A series of photographs showing a progression of the shear cracking in the joint is shown in Fig. 3.8. Load stages 9 and 15 [Fig. 3.8(a) and (b)] are at the terminations of one-half and one complete elastic load cycle and show that the shear cracks formed in the elastic range of the structural response were visible and did not necessarily propagate the entire diagonal distance between opposite corners of the joint. At load stages 32 and 50, Fig. 3.8(c) and (d) show the joint cracking patterns for the specimen as it reached a maximum applied joint shear in each direction of loading during the second cycle, which was the first cycle of large inelastic deformation.

The final load cycle, as discussed in Section 2.7, was applied to determine the repeated load strength of the joint. Few new shear cracks formed in this third cycle, as seen from the crack

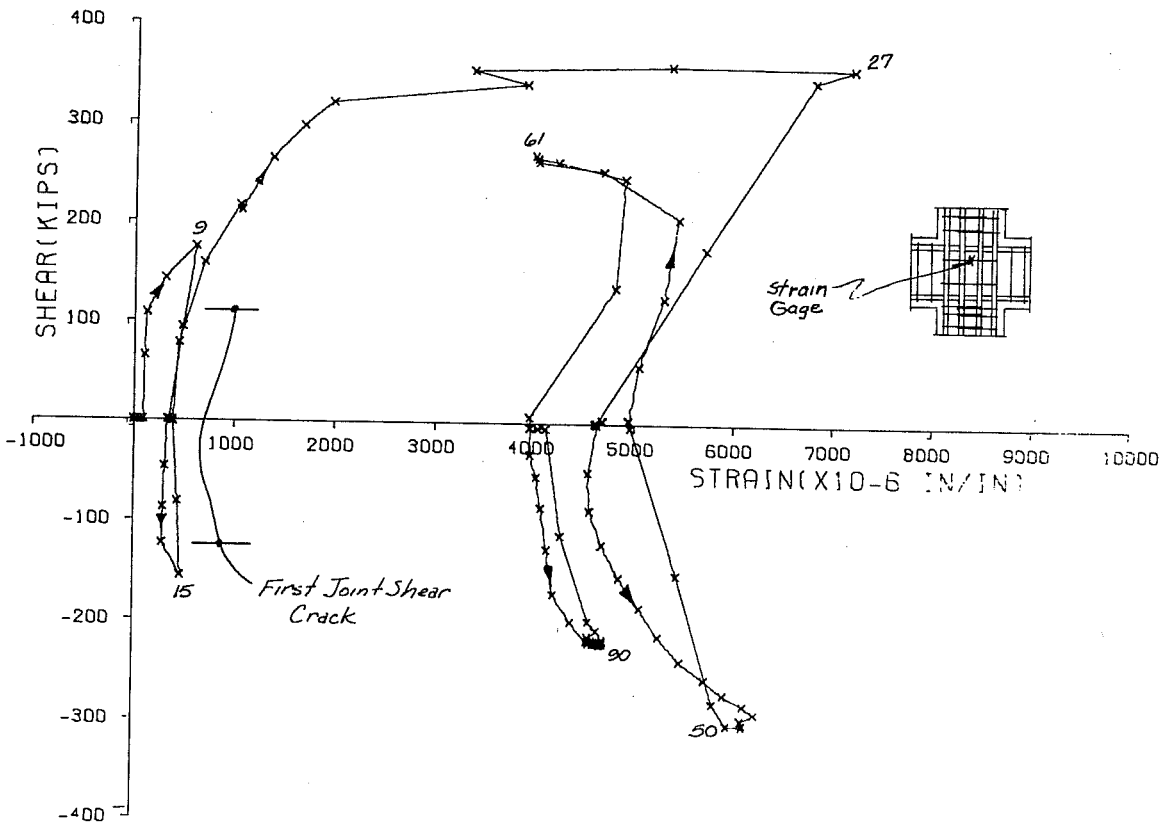

Fig. 3.7 Applied joint shear-strain in joint hoop (Specimen II)

First Cycle

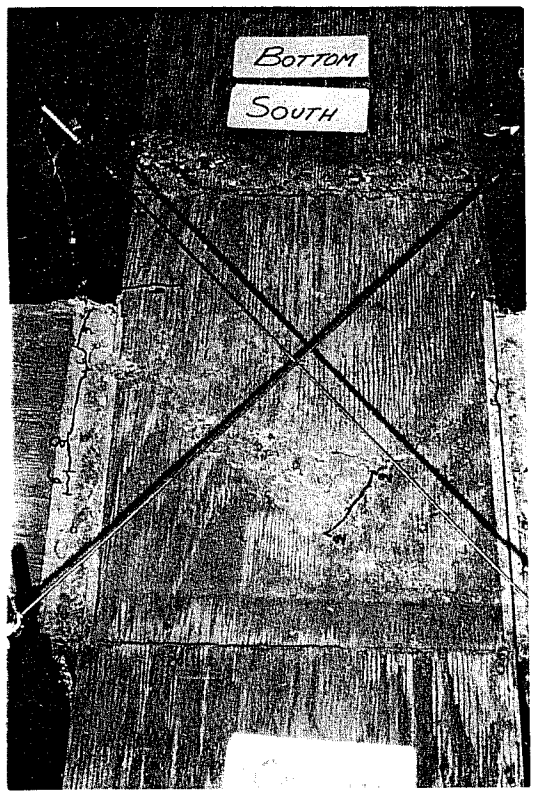

(a) Load Stage 9

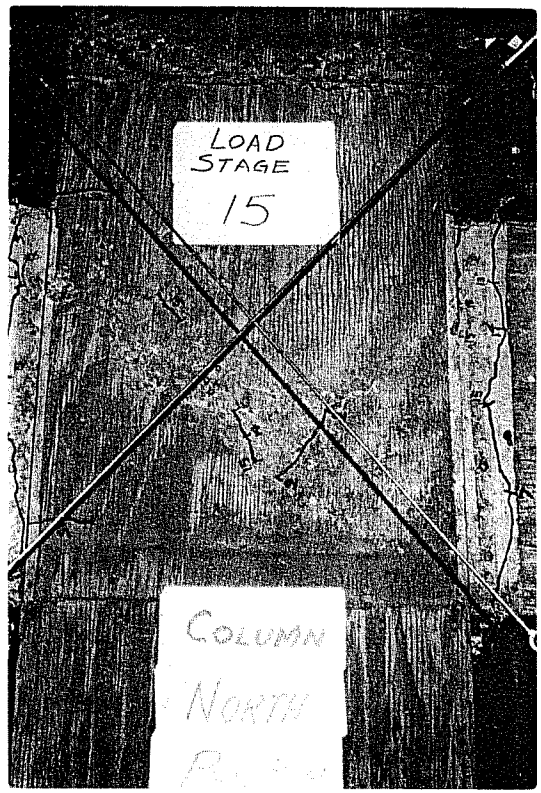

(b) Load Stage 15

Fig. 3.8 Joint cracking patterns (Specimen II)

Second Cycle

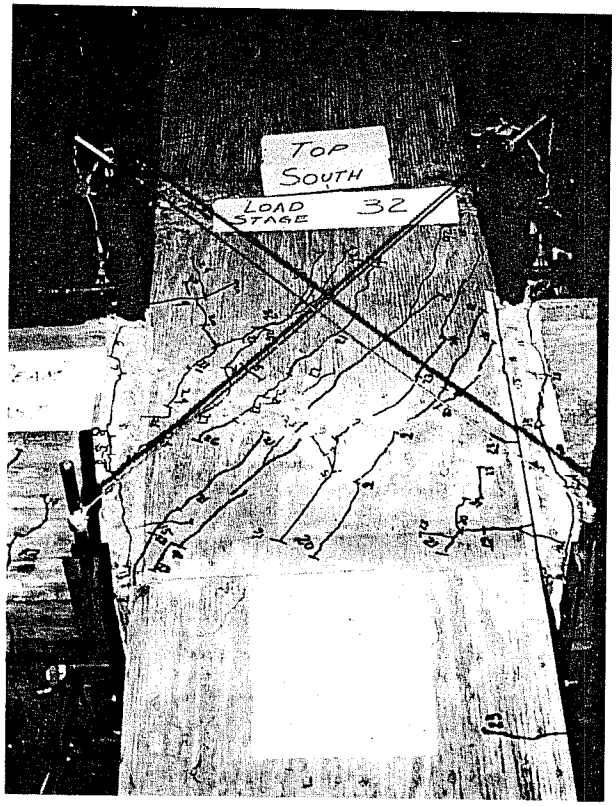

(c) Load Stage 32

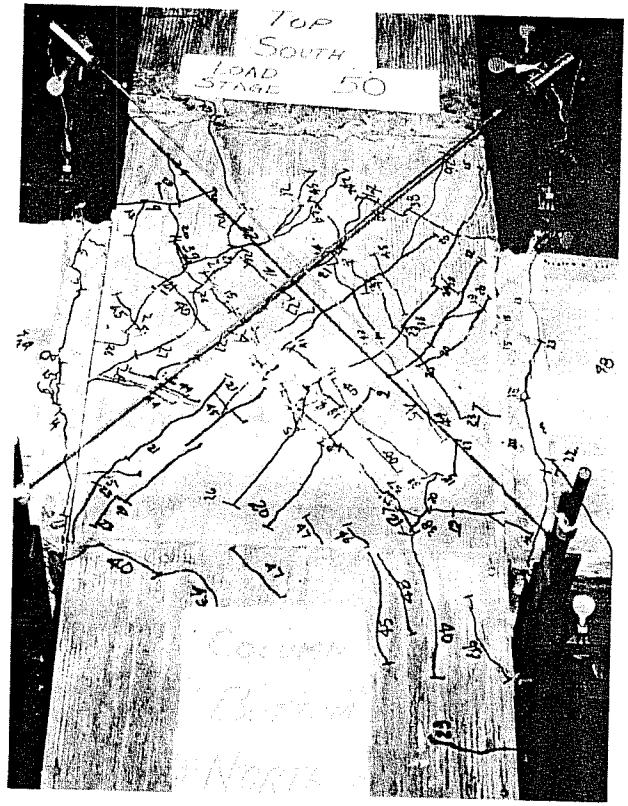

(d) Load Stage 50

Fig. 3.8 (Continued)

Third Cycle

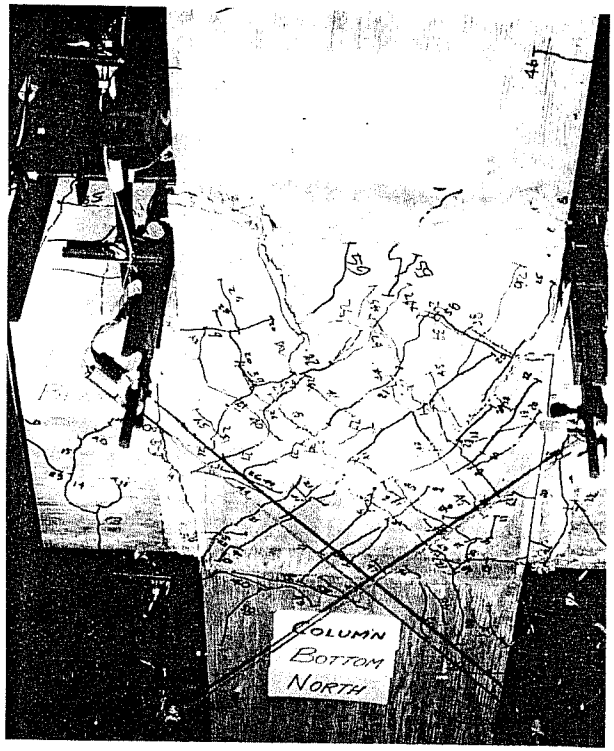

(e) Load Stage 60

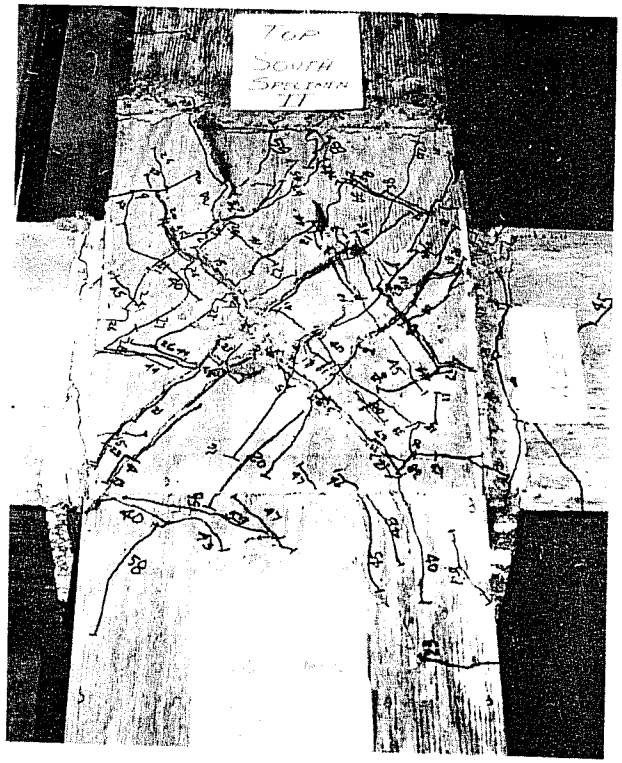

(f) Load Stage 95
(End of test)

Fig. 3.8 (Continued)

patterns for load stages 60 and 95, shown in Fig. 3.8(e) and (f). However, the large deformations applied in the third cycle caused the concrete cover over the joint hoop reinforcement to spall away from the joint core. The joint core is that volume enclosed by the joint hoops and column reinforcement. Figure 3.9 shows the exposed joint core after the loose concrete has been removed.

Failure Criterion. The maximum loads applied to the main beams were dictated by one of two failure modes. In the first and more desirable failure mode, the main beam bars yield and hinges form at points of maximum moment near the column face. An example of hinge formation is shown in the third quadrant of Fig. 3.3(b) at load stage 27, where the moment remains constant while the member deformations increase. Moments computed when the main beam tension reinforcement just reaches yield stress are 3270 and 1900 k-in. when the top and bottom reinforcement are in tension. These yield moments were computed using a concrete compressive strength of 4500 psi. Variations in the actual specimen concrete compressive strength have very little influence on the magnitude of the yield moment. The above yield moments were used to plot the yield loads shown in Fig. 3.2, and the yield moments in Fig. 3.3.

As an aid in determining the failure mode and the behavior of the individual main beams, strains in the #10 top and #8 bottom reinforcing bars at the face of the column were plotted against the moment at the face of the column. Figures 3.10 and 3.11 show the strain history for the east and west main beams at the column face, respectively, for both the top and bottom bars. Routine analysis of a section for negative moment indicates that the top bar is in tension and the bottom bar is in compression. A positive beam moment at the column has the reverse effect. Tension in a top bar is indicated by a slope up and to the right while tension in a bottom bar would have a slope down and to the right of the origin in Figs. 3.10 and 3.11. Horizontal lines at -3270 k-in. and +1900 k-in. are the

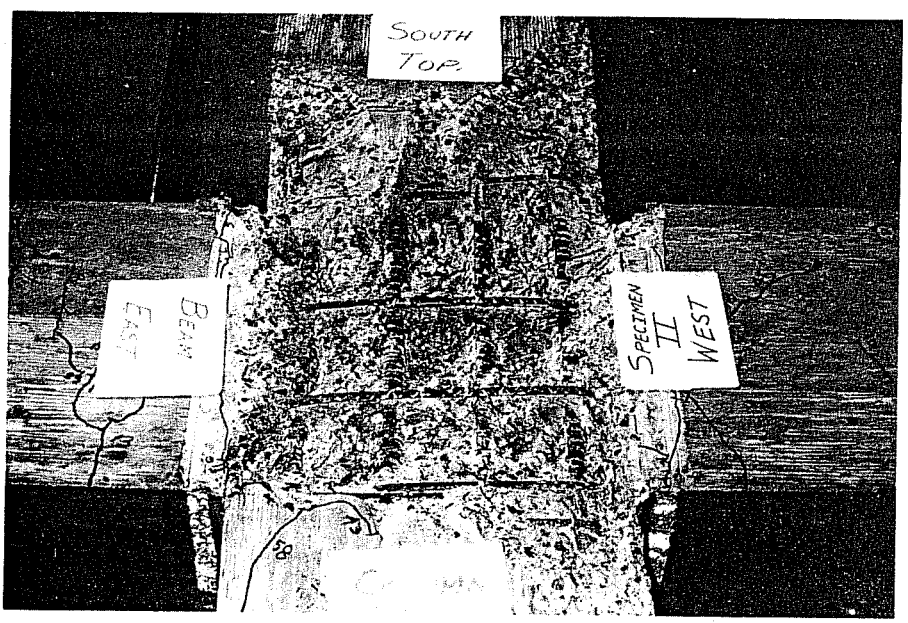

Fig. 3.9 Exposed joint core (Specimen II)

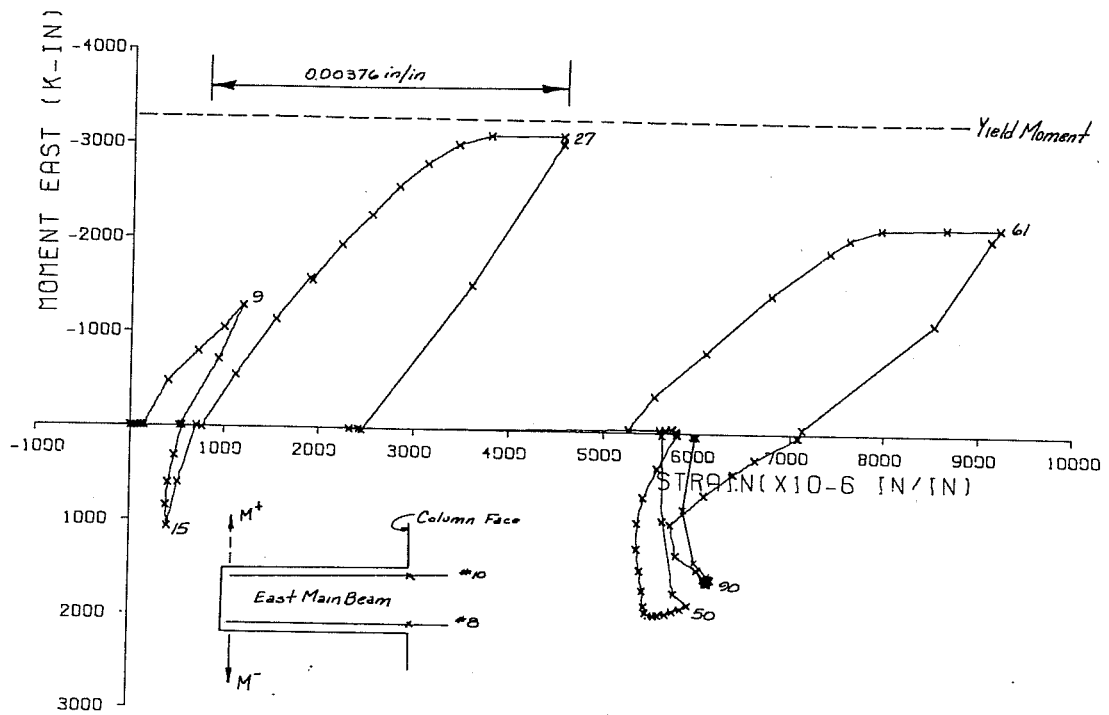

(a) #10 top bar--east beam

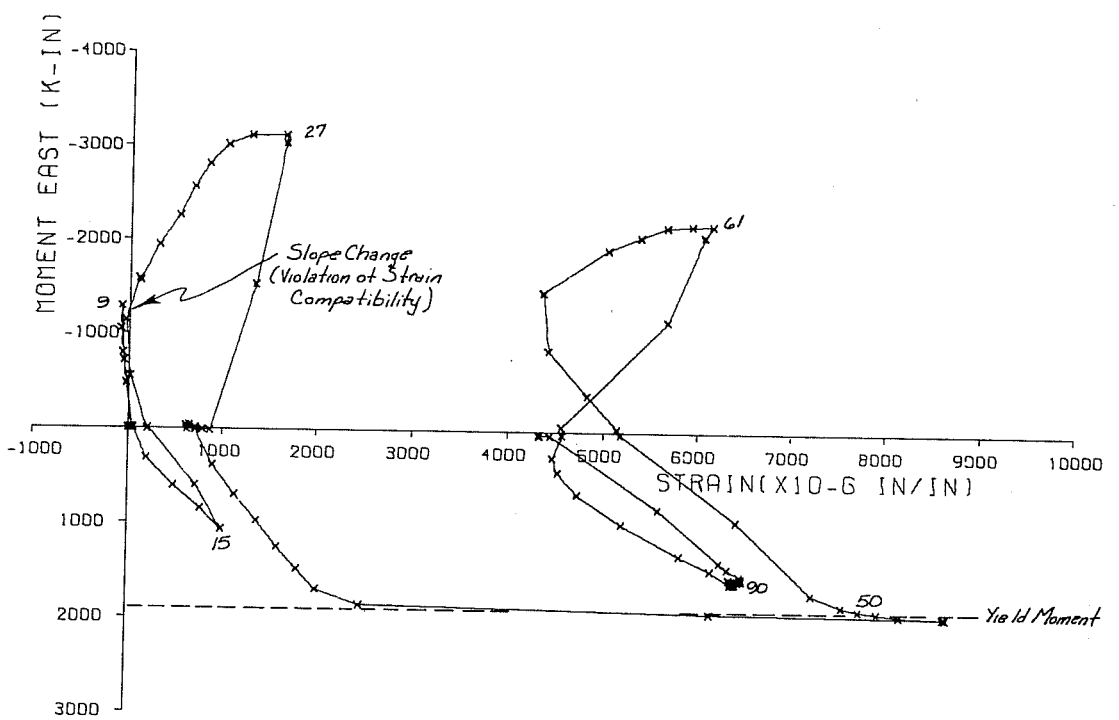

(b) #8 bottom bar--east beam

Fig. 3.10 Strain history in top and bottom reinforcing bar of the east main beam at the face of the column (Specimen II)

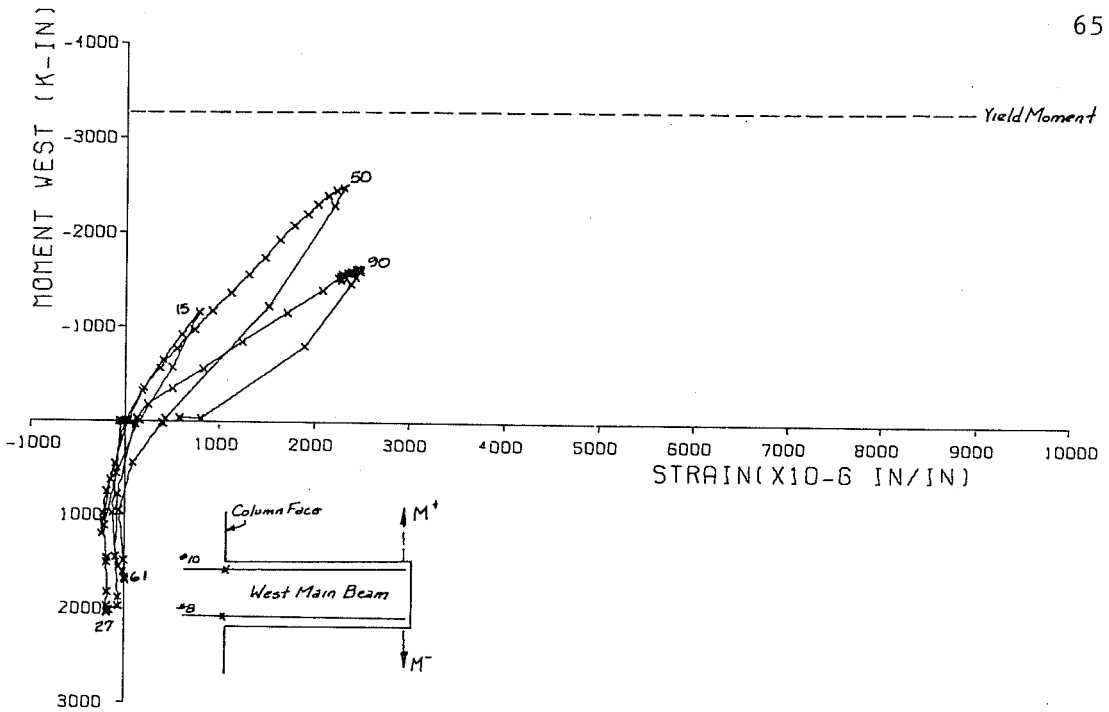

(a) #10 top bar--west beam

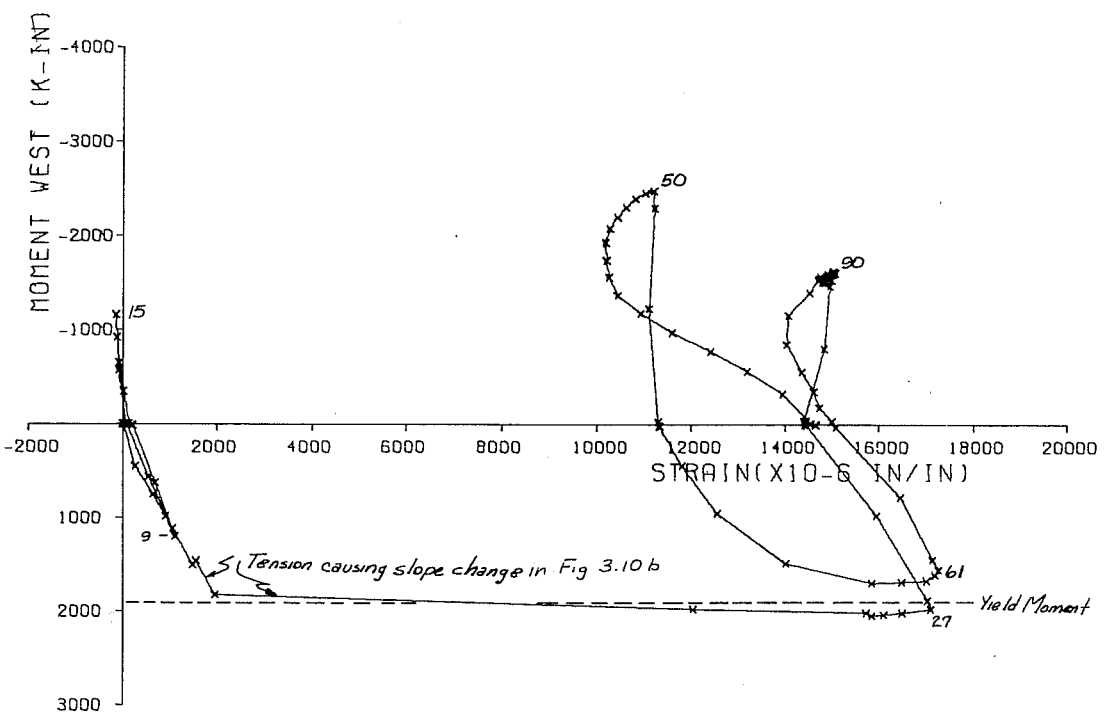

(b) #8 bottom bar--west beam

Fig. 3.11 Strain history in top and bottom reinforcing bar of the west main beam at the face of the column (Specimen II)

yield moments for the main beams when the top and bottom reinforcement, respectively, is in tension.

In Fig. 3.10(a), note that at load stage 27 the strain in the #10 top bar exceeds yield strain but the moment has not reached the yield moment. It is not clear whether the specimen has ceased to carry increased load due to flexural yielding of the reinforcing bars or has failed due to other causes.

An explanation of why the reinforcing bar strains indicate yield stress but the bending moment in the main beam is not at the yield moment can be discussed in the context of the second and less desirable mode of failure, one in which the joint fails by a combination of shear and bond. Figures 3.10 and 3.11 are representative of the type of main beam behavior observed when the joint was incapable of fully developing the main beam yield moment. An explanation of a shear-bond failure follows.

As the #10 top bars of the east main beam are strained in tension to load stage 27, the #8 bottom bars in that beam should be in compression, as shown by the sketch in Fig. 3.12(a), if strain compatibility is to be satisfied. Initially, the #8 bars are in compression with a slope up and to the left, but then the slope is reversed and tensile strains are recorded [see Fig. 3.10(b)]. The change in the sense of the strain is a result of the tension force in the bottom #8 bars of the west main beam, as indicated in Fig. 3.11(b). An explanation of this phenomenon is aided by the pictorial representation of the force equilibrium on the joint shown in Fig. 3.12(b). The measured tensile strains at the column face in the bottom bars of the east main beam can be attributed to loss of bond along the bar through the joint and joint shear deformations which are seen by the presence of shear cracks. Joint shear deformations force the members to rotate through greater angles than required had the joint remained rigid. It is these shear deformations that

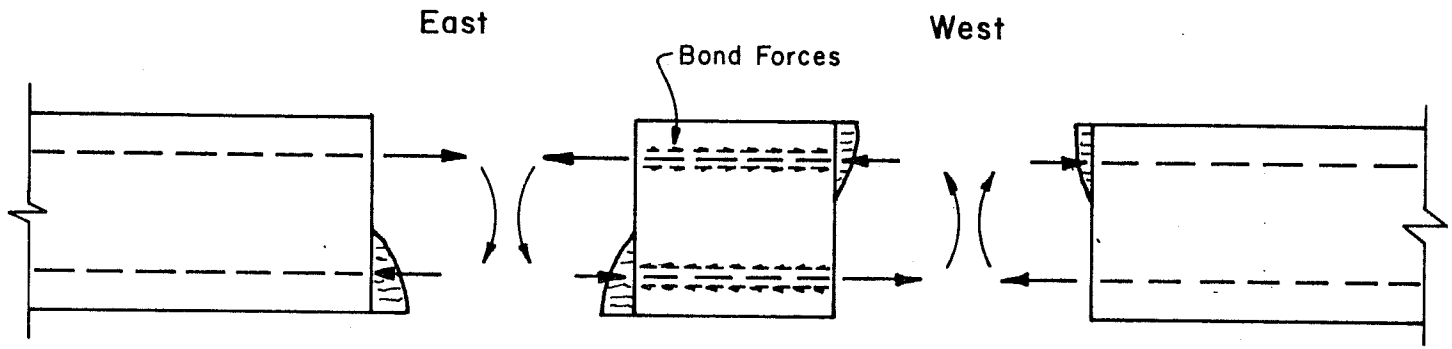

a) Force Equilibrium Required by Strain Compatibility

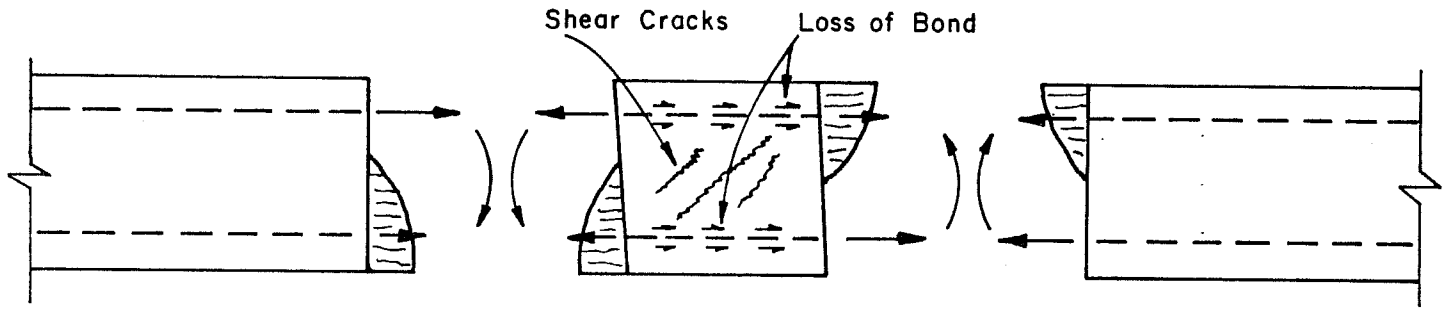

b) Force Equilibrium Because of Shear and Bond Failure

Fig. 3.12 Force equilibrium of joint failing by shear and bond

contribute significantly to the straight line deviations of the curves of Figs. 3.2 and 3.3.

At the column face of the east main beam, strain compatibility has been violated, as is obvious in Fig. 3.10(b). The result is that what was previously compressive steel is now in tension and must be balanced by a larger compressive force which can only be developed by a shift in location of the neutral axis. When the compression area increases, the location of the resultant concrete compression force changes to make the internal moment arm less than that required if strain compatibility had not been violated. The following two examples show numerically the trend of the behavior illustrated in Fig. 3.12 for a specific load stage and considering the east beam.

Example 1: Strain compatibility not violated

Strain in #10 top bars @ load stage 27 from Fig. 3.10(a)

$= 0.00376$ in./in.

Stress in #10 top bars

$= (3760 \times 10^{-6}\text{in./in.})(27.3 \times 10^{3}\text{ksi})$

$= 102.6$ ksi

This computed stress is greater than the yield stress for the #10 bar shown in the stress-strain curve of Fig. 2.6. Therefore, the maximum stress for the measured strain is $f_s = f_y = 61.5$ ksi.

To compute the moment on the cross section the procedure is one of trial and error with the maximum strain being assumed. Actual specimen material properties are used as defined in Tables 2.4 and 2.6, and Fig. 2.6.

By trial and error, try maximum compressive strain in the concrete = -0.00160 in./in.

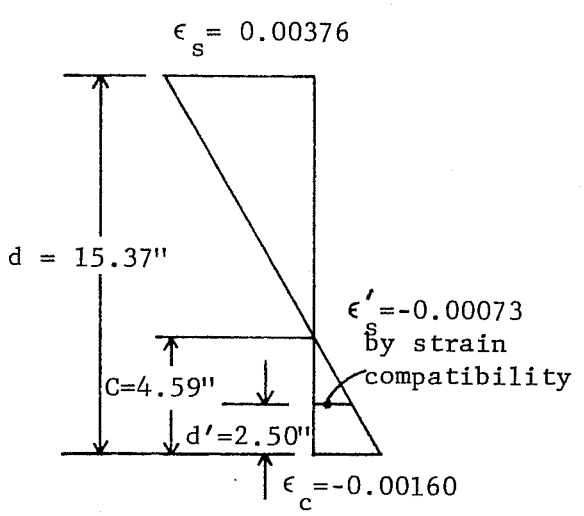

Strain Diagram

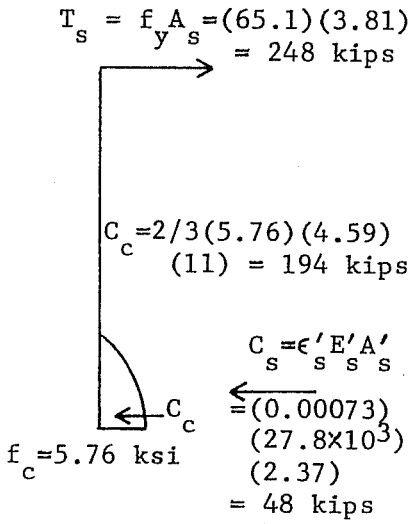

Force Diagram

Force Equilibrium: $\Sigma F_H = 0$

←	→
C_c = 194 k	T_s = 248 k
C_s = 48 k	
242 kips $\overset{?}{=}$	248 kips OK

Moment Equilibrium: ΣM @ tension steel = 0

$$M_c = C_s(d - d') + C_c(d - 3/8c)$$

$$= 48(15.37 - 2.5) + 194(15.37 - 1.72)$$

$$= 618 + 2648 = 3265 \text{ k-in.}$$

Example 2: Violate strain compatibility

Stress in #10 top bars @ L.S. 27 = 65.1 ksi, from previous example.

Stress in #8 bottom bars @ L.S. 27, measured from Fig. 3.10(b), is $\epsilon'_s = 0.00141$ in./in., $f'_s = (1410 \times 10^6)(27.8 \times 10^3)$

$= 39.2$ ksi

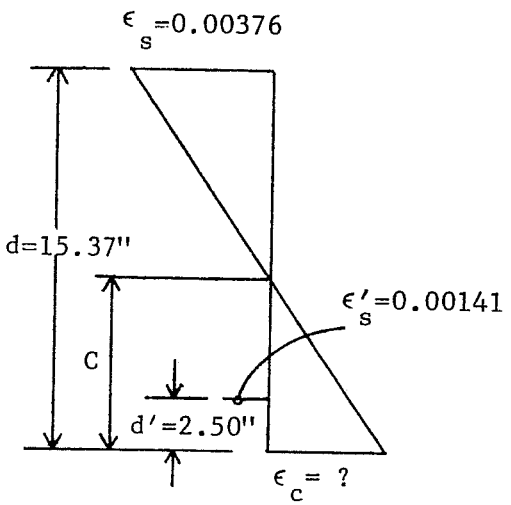

Strain Diagram

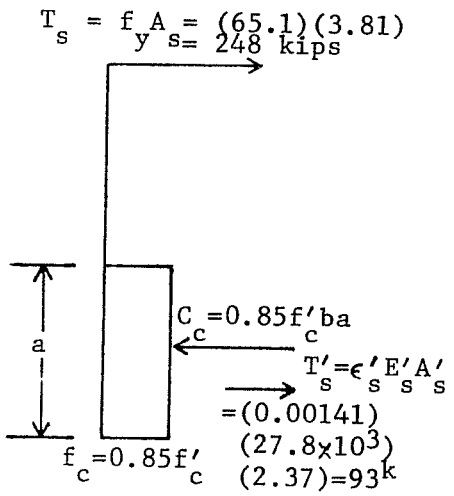

Force Diagram

Force Equilibrium: $\Sigma F_H = 0$

$\leftarrow$ $\qquad$ $\rightarrow$

$C_c = 0.85 f'_c$ ba $\qquad$ $T'_s = 93$ k

$T_s = 248$ k

$C_c = 341$ kips

$$a = \frac{C_c}{0.85 f'_c b} = \frac{341}{0.85(6.06)(11)} = 6.08 \text{ in.}$$

$$C = a/\beta_1 = 6.08/0.75 = 8.10 \text{ in.}$$

Moment Equilibrium = ΣM @ tension steel = 0

$M_c = C_c(d - a/2) - T'_s(d - d') = 41[15.37 - 6.08/2 - 93(15.37 - 2.5)]$

$M_c = 4204 - 1197 = 3008$ k-in.

Measured main beam moment = 3120 k-in.

Although the measured east main beam moment at load stage 27 is greater than predicted in Example 2, the measured moment is less than the moment computed assuming strain compatibility. Therefore, even though reinforcing bars have been strained beyond the yield strain, the main beam bending moments can be less than the yield moment because of a shear and bond failure in the joint.

Visual evidence of joint shear distress can be seen from the photographs of Fig. 3.8, particularly (d), (e), and (f). Evidence of bond distress through the joint is shown by the presence of longitudinal splitting cracks in the concrete cover over the main beam bars, as shown in Fig. 3.13. These longitudinal splitting cracks are typical of behavior observed in tests to determine the development length of high strength deformed bars.[29] In these tests the splitting cracks indicate that the tensile and compression forces in the bar on the opposite sides of the joint have destroyed the anchorage in the joint and have caused the tensile forces to be anchored in the compression zone of the beam on the opposite side of the joint. Hence, measured tensile strains are observed in reinforcing bars normally considered as compression reinforcement.

Definitions of Failure. Flexural failure will be defined in subsequent discussion as the ability to achieve both yield moment and yield strain in the reinforcement of both main beams at the joint.

Failure in the joint will be defined as the inability of the beams to develop yielding moments even if strains in the tension reinforcement exceed yield.

The flexural failure criteria are plotted as horizontal lines in Figs. 3.4 and 3.6.

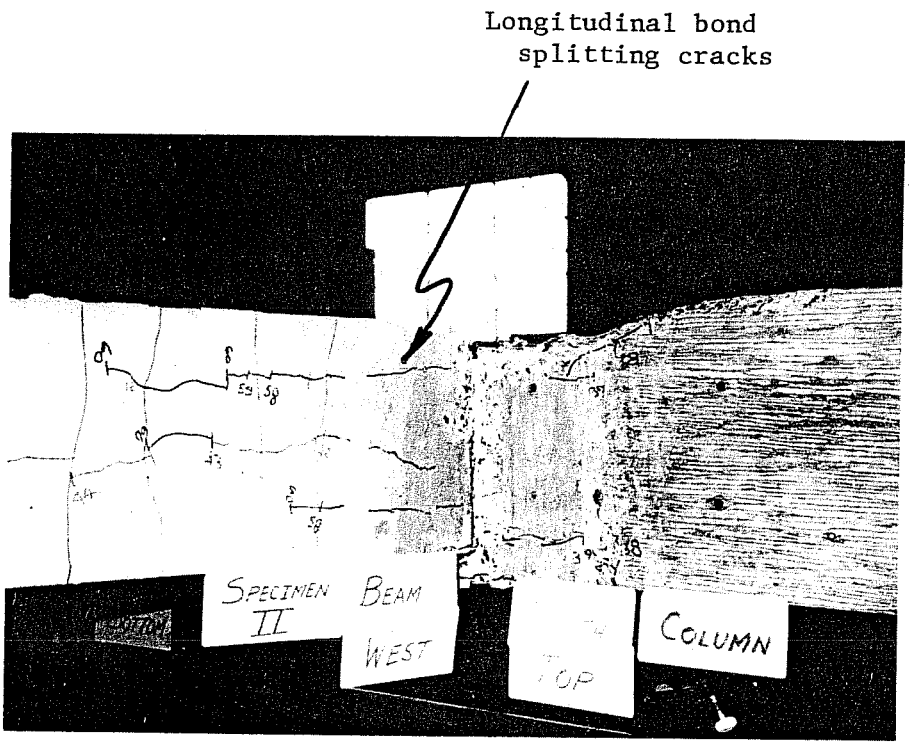

Fig. 3.13 Longitudinal bond splitting cracks above embedded deformed bars (Specimen II)

3.4 Elastic Behavior

Behavior prior to application of deflections greater than yield deflection is considered as a measure of the elastic response to load. For each specimen, one cycle of load at load levels less than those producing yield in the reinforcement was applied. In this cycle, the main beams cracked in flexure and the joint had diagonal cracking, as shown in Fig. 3.8(a) and (b). Elastic properties of the specimen were determined from the first elastic cycle of loading.

Elastic Joint Shear Behavior. As noted in Fig. 3.7, the applied joint shear was initially carried by the concrete alone, since the joint hoop reinforcement strains did not increase until joint shear cracking occurred. Approximate values of the concrete shearing modulus of elasticity were obtained by using the applied joint shear-shear strain curve of Fig. 3.6 and converting the joint shear to shear stress by dividing by the shear area of the joint. Reinforced concrete beam design uses the 45^{o} truss analogy for shear calculations. The shear area for a beam is computed as the product of the width (b) and the effective depth (d) of the member. The same 45^{o} truss analogy is assumed for determining the shear stresses in the joint, except that in accordance with Ref. 2 the width (b) is the wider of the two members and the effective depth is the distance from the extreme compression fiber to the centroid of the tension steel for the column. To calculate shear stress from applied joint shears, the shear area (bd) was calculated using the column cross section geometry.

Values of the shearing modulus, G, were found in this manner for the test specimens and are listed in Column 3 of Table 3.1. The average shearing modulus from the experimental data is about 25 percent less than the theoretical value computed by

$$G = E/2(1 + \nu)$$

where E = modulus of elasticity of concrete, psi
$= 57000 \sqrt{f'_c}$
ν = Poisson's Ratio of concrete
$= 1/6$

Applied joint shears at diagonal shear cracking in the joint are given in Columns 4 and 5 of Table 3.1. These values represent the shear necessary to cause cracking on each of the diagonals in the joint and were determined for each specimen using the relationship between applied joint shear and strain in the joint reinforcement such as that shown in Fig. 3.7.

Elastic Beam Behavior. The magnitude of elastic deflection is dependent upon the value of flexural stiffness (EI) used in the deflection calculation. If no other information is available, EI can be computed from a cracked transformed moment of inertia of the section and the modulus of elasticity of concrete. However, when moment-curvature diagrams are available, the slope of the moment-curvature relationship is the flexural stiffness of the cross section.

Flexural stiffnesses of the members were determined two ways: one using the transformed inertia and modulus of elasticity, and two from the slope of the measured moment-curvature relationship. The measured stiffnesses for the main beams were consistently less than the cracked transformed stiffness. For the beam cross section with #10 bars in tension, the measured stiffness was two-thirds the cracked transformed stiffness. Measured stiffnesses are not listed in Table 3.1, since each beam has two stiffnesses; however, an example using a stiffness obtained from Fig. 3.3(a) follows for a deflection calculation using data from Specimen II.

For a concrete member loaded in the elastic range, the unloading curve gives a better estimate of stiffness than does the loading curve. During the loading, the section is in the process

of cracking and the neutral axis constantly changes; but, during unloading, the neutral axis remains stationary. Loading and unloading curves would be identical if numerous prior elastic cycles to the same maximum load had been applied. For Specimen II, the unloading slope of the moment curvature plot of Fig. 3.3(a) for the first excursion in the elastic range (from L.S. 9 to zero load) was 1.03×10^{10} lb-in.^{2} The cracked transformed stiffness of Specimen II using a concrete strength of 6060 psi was 1.57×10^{10} lb-in.^{2} It should be pointed out that the curvatures of Fig. 3.3 represent an average curvature over the length on which the deformations were measured. This may account for some of the discrepancy between the measured and calculated stiffnesses.

3.5 Load-Deflection Behavior

Deflection at the end of the main beam is composed of several parts. There are both elastic and inelastic contributions to the total deflection, as summarized in Fig. 3.14. The cantilever deflection of the main beam ($\Delta_{cantilever}$) and deflection due to rotation of the column caused by application of a concentrated moment (Δ_{column}) can be considered elastic contributions to the total deflection. Inelastic deformations, namely the joint shear deformations (γ_j) and inelastic rotations at the face of the column in the main beam (θ_B) due to reinforcing bar slippage through the joint and crushing of the concrete, also contribute to the total deflection of the main beam.

To assess the accuracy of the deformation instrumentation placed in the joint area, total deflections were computed at the free end of the main beam assuming the column and main beam behaved elastically with stiffnesses measured from moment-curvature relationships as discussed in Section 3.4. The deformations due to inelastic action of the main beam (θ_B) and joint shear (γ_j) were determined from Figs. 3.3 and 3.6, respectively. The four deflection components

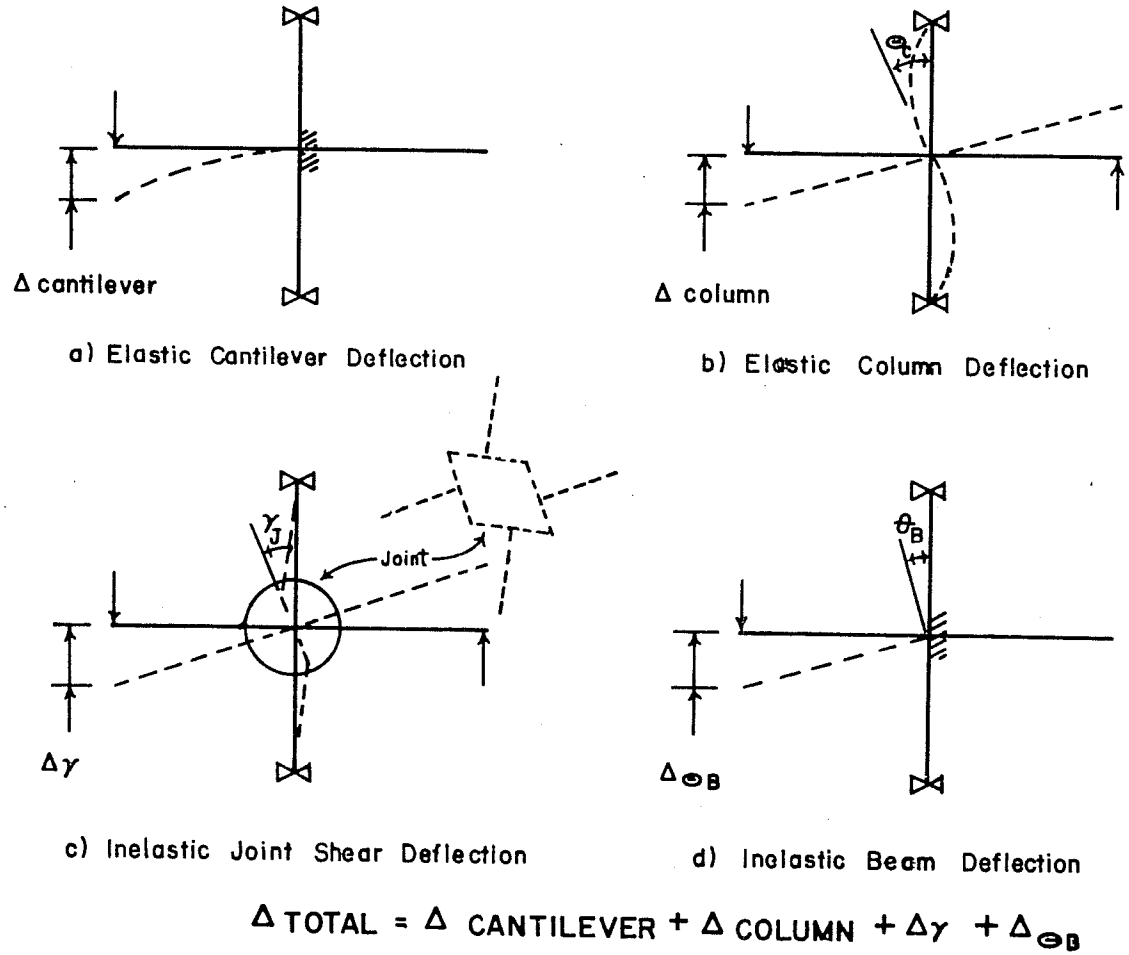

$$\Delta_{TOTAL} = \Delta_{CANTILEVER} + \Delta_{COLUMN} + \Delta\gamma + \Delta_{\ominus B}$$

Fig. 3.14 Components of total main beam deflection

were summed and compared with the measured end deflection, as shown in Fig. 3.15.

A typical component deflection calculation using the data from Specimen II follows for load stage 23.

$\underline{\Delta_{cantilever}}$

$$\Delta_{cantilever} = \frac{Pb_1^2(3L - b_1)}{6EI_{beam}}$$

$EI_{beam} = 1.03 \times 10^{10}$ lb-in.^{2}, from Fig. 3.3(a)

P @ L.S. 23 = 29.47 kips

L = 97.8 in. = length of main beam from face of column to free end

b_1 = 87 in. = distance from face of column to point of load application

$$\Delta_{cantilever} = \frac{29.47(1000)(87)^2}{6(1.03 \times 10^{10})}[3(97.8) - 87] = \underline{\underline{0.75 \text{ in.}}}$$

$\underline{\Delta_{column}}$

$$\Delta_{column} = \frac{M_j L_c L_{\mathbb{L}}^{\mathbb{C}}}{12\, EI_{column}}$$

$EI_{column} = 2.84 \times 10^{10}$ lb-in.^{2} from M-φ relationship for columns, not shown, can also be calculated from $E_c I_g$ of column

I_g = gross moment of inertia of column

M_j @ L.S. 23 = (29.47 + 23.15)87 = 4577 k-in. = moment at column face caused by loads at the free ends of the main beam

L_c = 144 in. = length of column between supports

$L_{\mathbb{L}}^{\mathbb{C}}$ = 106.8 in. = length from centerline of column to free end of main beam

$$\Delta_{column} = \frac{4577(144)(106.8)}{12(2.84 \times 10^{10})} = \underline{\underline{0.21 \text{ in.}}}$$

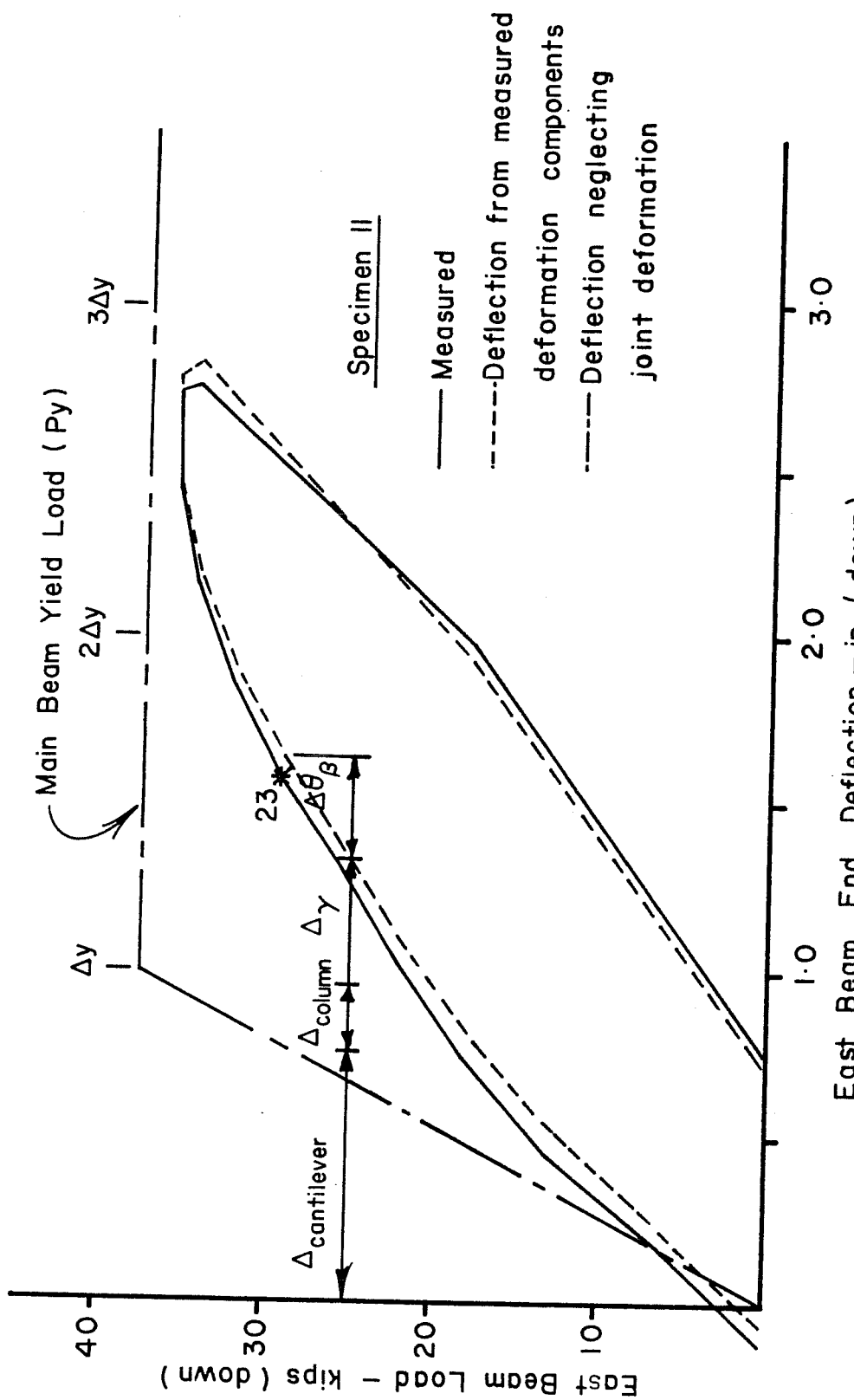

Fig. 3.15 Component and measured total deflection of east main beam (Specimen II)

Δ_γ (deflection from joint shear deformations)

$$\Delta_\gamma = \gamma_j (L_{\text{℄}})$$

γ_j = 0.00346 in./in. = shear strain of joint from Fig. 3.6

$L_{\text{℄}}$ = 106.8 in. (previously defined)

$$\Delta_\gamma = 0.00346(106.8) = \underline{0.37 \text{ in.}}$$

$\Delta_{\theta B}$ (deflection from inelastic main beam action)

$$\Delta_{\theta B} = [\theta_{BT} - \theta_{elastic}]L$$

θ_{BT} = 0.00043 rad/in.(10 in.) = 0.0043 rad. measured total average rotation 5 in. from face of column. Curvature from Fig. 3.3(a).

$$\theta_{elastic} = \int \frac{Mdx}{EI_{beam}} = \text{elastic rotation 5 in. from face of column}$$

$$= \frac{29.47(1000)(87.83)(5)}{1.03 \times 10^{10}(2)} = 0.00122 \text{ rad.}$$

L = 97.8 in. (previously defined)

$$\Delta_{\theta B} = [0.0043 - 0.0012]97.8 = \underline{0.30 \text{ in.}}$$

$$\Delta_{\text{total component}} = \Delta_{\text{cantilever}} + \Delta_{\text{column}} + \Delta_\gamma + \Delta_{\theta B}$$

$$= 0.75 + 0.21 + 0.37 + 0.30 = 1.63 \text{ in.}$$

Δ_{measured} = 1.57 in.

The total component deflection and the measured deflection are in very good agreement. The comparison between measured end deflection and the deflection from measured components is shown in Fig. 3.15. This indicates that deformation measurements made in the joint area are adequate indicators of joint behavior. Since deformation measurements are representative of joint behavior, the relationship between applied joint shear or shear stress and shear strain will be used in discussing comparisons between test specimens.

Figure 3.15 also shows the load-deflection relationship assuming the joint to be rigid. In such an analysis, joint shear distortions and slip of the anchored bars would be neglected. The beam flexural stiffness would be computed using the modulus of elasticity of concrete and a cracked transformed moment of inertia. A routine elastic deflection analysis results in prediction of a linear load-deflection curve until the member yields and then the load is constant with increasing deflection as plastic hinging takes place. For the material properties and cross sections of Specimen II the deflection predicted using these assumptions are shown in Fig. 3.15.

3.6 Strength and Repeated Load Behavior

A detailed discussion of the structural behavior of Specimen II has been furnished in Section 3.5. Specimen II is a representative sample of the information collected and also will serve as a standard of comparison for the other specimens. The other thirteen specimens will not be presented in the same detail; however, in the following paragraphs a brief description highlighting each test will be given. Load-deflection curves, moment-curvature relationships, joint moment-joint rotation relationships, and applied joint shear versus shear strain relationships for the remainder of the thirteen specimens can be found in Appendix B.

Magnitudes of maximum applied joint shear and maximum joint moment for the second and third loading cycles are tabulated in Table 3.1 for each specimen.

The failure mode of the joint was determined with the criterion previously defined. For failure to be flexural, the maximum moment applied to the joint was compared to the moment when the main beams yielded. The joint moment for a failure by flexure is the summation of the yield moments for each of the main beams, one beam having the top bars in tension while the other beam has the

bottom bars in tension (3270 k-in. + 1900 k-in. = 5170 k-in.). Values of maximum joint moment and mode of failure for each half cycle are given in Columns 10 through 17 of Table 3.1.

Specimen I. This specimen represents a joint with a rectangular tied column having a low percentage (2 percent) of column reinforcement, and is typical of a column in a low-rise building or a column near the top of a high-rise building.

The main beams were unable to achieve yield moments for either direction of loading. Maximum beam loads were limited by a joint failure. A photograph of the cracking pattern in the joint is shown in Fig. 3.16.

Specimen II. A more detailed description of Specimen II has been included in previous sections because Specimen II serves as a standard of comparison for other test variables. Additional highlights of the test are included below. The column cross section was reinforced with 4.3 percent steel. It represents typical proportions used in normal building construction. The joint of this specimen, as in other specimens except as noted, was reinforced with two #4 closed hoops. The column load was 351 kips for the duration of the test.

All main beam reinforcing bars reached yield strains during the second load cycle. Yield moment was reached and was maintained for the beam with the bottom steel in tension. Because of a joint shear-bond failure, the beam with top bars in tension did not reach its yield moment.

The main beams were found to have wide cracks on the tension surface at the column face and the concrete cover in the compression zones of the main beam spalled at each corner where beam and column intersected.

Once the strength of the joint had been reached in a monotonic test, the load was reversed and the joint strength was found

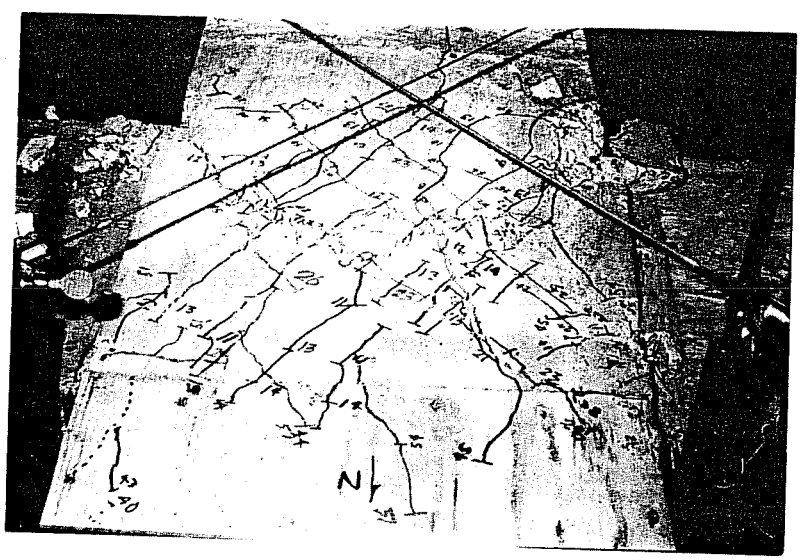

Fig. 3.16 Joint cracking pattern of Specimen I

to decrease with each load reversal. It should be remembered, however, that this specimen was not designed to have the beams reach yield or develop ductility, but was designed to fail in shear in the joint at a shear estimated to be about 60 percent of the maximum joint shear applied during the second cycle.

Specimen III. Columns in the lower stories of a building will frequently have the same cross section as those above, but contain larger percentages of reinforcement. Specimen III represents such a case with the column reinforced with 6-2/3 percent steel. That percentage of reinforcement exceeds the allowable percentage for columns[2] in seismic areas.

Neither of the main beams reached yield moment before the joint failed in the shear and bond mode. Tensile strains in the main beam bars remained in the elastic range. At the end of the second cycle, the concrete cover began to spall on the exposed joint surface. The spalling was a result of the principal compressive stress developed in the joint due to the applied shear stress.

As a joint fails in shear and bond, the concrete expands in a direction perpendicular to the plane of the main beams or perpendicular to the direction of the applied joint shear forces. This volumetric change can be resisted by the confining effects of the column and joint hoop reinforcement. Expansions of this type were observed as the concrete cover over the joint hoop reinforcement spalled away from the column core. The intersection of the column and main beam centerlines, because of load reversal, appears to experience the largest amount of lateral expansion. Once spalling of the cover in the joint is initiated, in this case the first half of the second cycle, spalling continued in each subsequent half cycle until the end of the test when the cover on the joint appears as in Fig. 3.17. At the end of this test, the joint cracking pattern had an appearance as shown in Fig. 3.18.

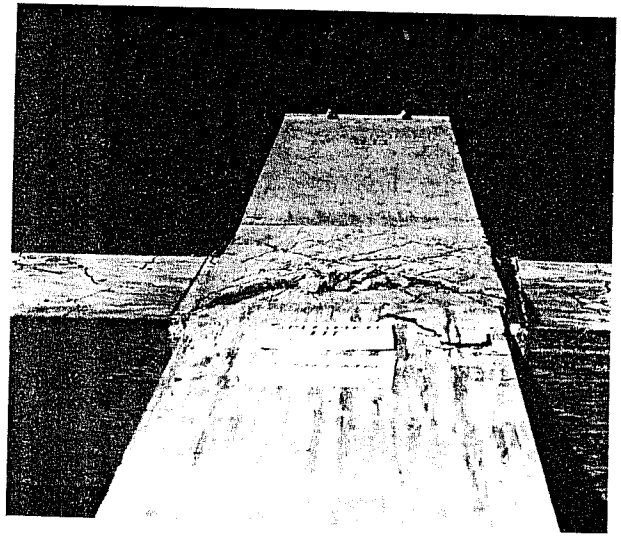

Fig. 3.17 Spalling of joint cover concrete (Specimen III)

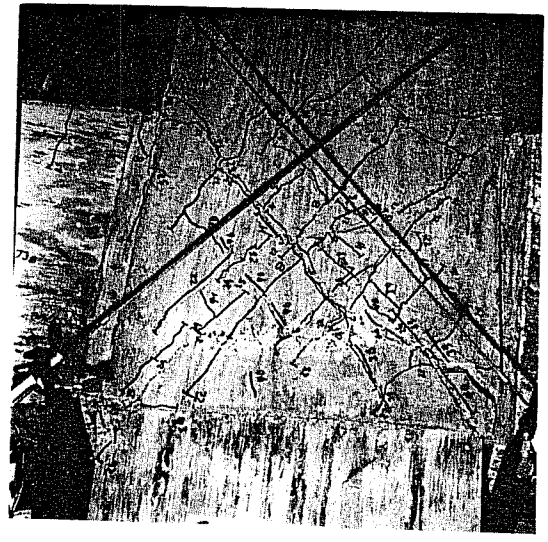

Fig. 3.18 Joint cracking pattern of Specimen III

Specimen IV. For a rectangular column, bending about its weak axis would cause deflections to increase in proportion to the reduction in stiffness of the column. Likewise, tension and compression forces in the beam reinforcement must be transferred to the concrete over a shorter distance in comparison to the joint panel that had the same beam and had bending about the stronger column axis (wider column dimension). Current ACI-ASCE Committee 352 recommended practice[9] assumes the diagonal shear crack forms at a 45^{o} angle with respect to member depth. Specimen IV is one of four specimens where the column dimension at the joint is only 72 percent of the beam depth. The diagonal between opposite corners of the joint is inclined 54^{o} relative to the axis of the main beam rather than 45^{o} for specimens that have column bending about their strong axis.

Major joint shear cracking was observed to propagate parallel to the line connecting the opposite corners of the rectangular joint panel. Figure 3.19 shows the cracking pattern after completing half of the second cycle. At the end of the test, the axis of the column had also been distorted by the large shear deformations of the joint. Figures 3.20 and 3.21 show the column axis distortions and the joint cracking pattern, respectively, at the end of the test.

When the loose cover in the joint region was removed, an interesting observation was made of the flexural cracks at the face of the column in the main beams. Since this specimen had a substantial residual deflection, the flexural cracks in the tension corners of the joint did not close. In fact, these cracks were not in the main beam cross section. Rather, the flexural crack had opened and followed a joint shear crack until it reached the column reinforcement. With reversed loading the main beam flexural cracks opened and closed inside the column cross section rather than at the face of the column. This distinctive feature occurred only if the joint

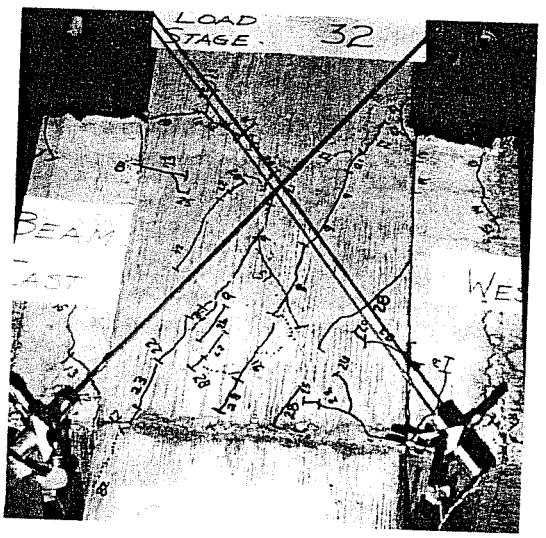

Fig. 3.19 Joint cracking pattern in second cycle of Specimen IV

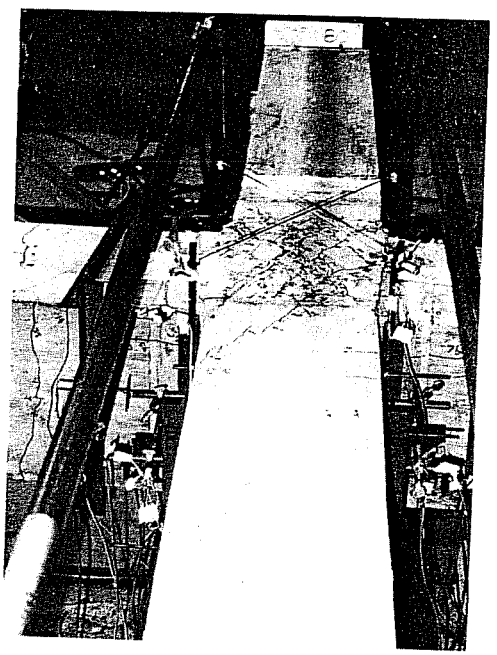

Fig. 3.20 Column distortion due to shear in the joint (Specimen IV)

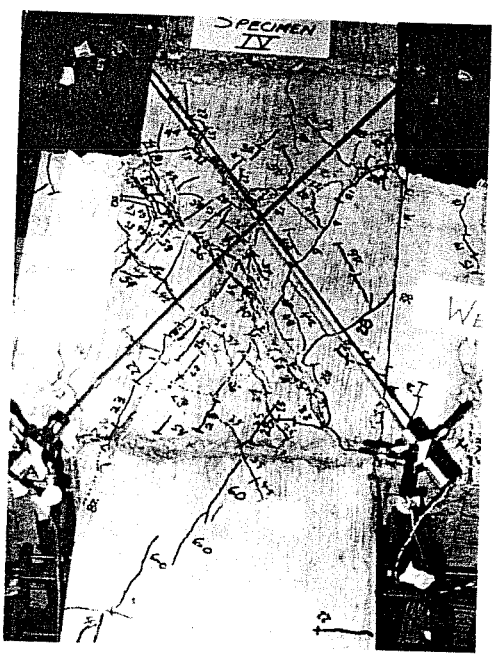

Fig. 3.21 Joint cracking pattern of Specimen IV

shear cracking had propagated to the joint corners. Figure 3.22 shows the joint region with the cover removed and the location of the main beam flexural crack open along the outermost column bars.

Specimen V. The overturning action resulting from large lateral forces presents the real possibility that the lower story columns in a building could carry either very low compressive loads or compressive loads greater than those of a normal gravity design. Specimen V represents the situation where the column carries a low sustained load while the shear on the joint is reversed.

An elastic analysis of the stresses in the joint for low column load would suggest that the concrete, a brittle material, would crack in tension at a lower applied joint shear than would the joint with a larger sustained compression load. Formation of the first diagonal cracks in the joint of Specimen V did occur at a very low applied joint shear, as seen from Columns 4 and 5 in Table 3.1.

The absence of a substantial compressive force on a column will also cause a column to behave more like a beam. Considerably more flexural cracking was evident in the column. There was little difference in the inclination of the joint crack when compared to the orientation observed for Specimen II which had a higher column compressive load. The joint cracking pattern at the end of the test for Specimen V is shown in Fig. 3.23. For comparison see Fig. 3.8(f).

A shear-bond failure in the joint prevented the formation of simultaneous yield moments on both sides of the column.

Specimen VI. Specimen VI represents the other possibility in column load magnitude. The column geometry and percentage of reinforcement are identical to those of Specimens II and V. A Mohr Circle analysis for this case of increased column load would suggest that the joint shear strength increase. In the first elastic cycle, very few diagonal shear cracks appeared on the joint surface. When

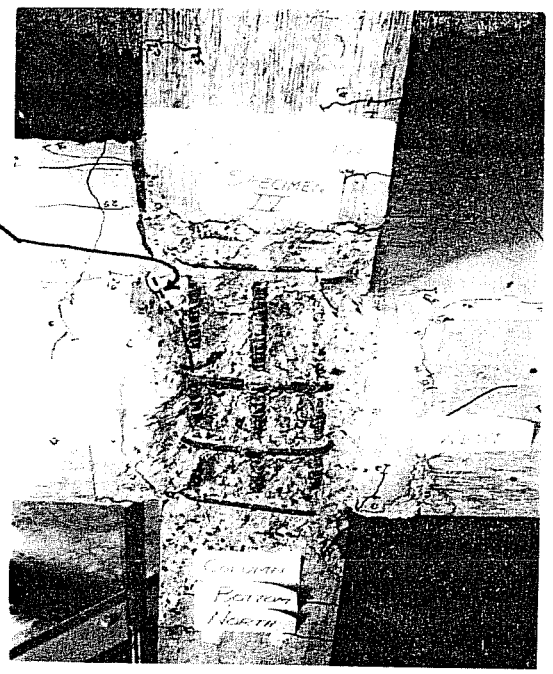

Fig. 3.22 Main beam flexural cracks opening within the column cross section (Specimen IV)

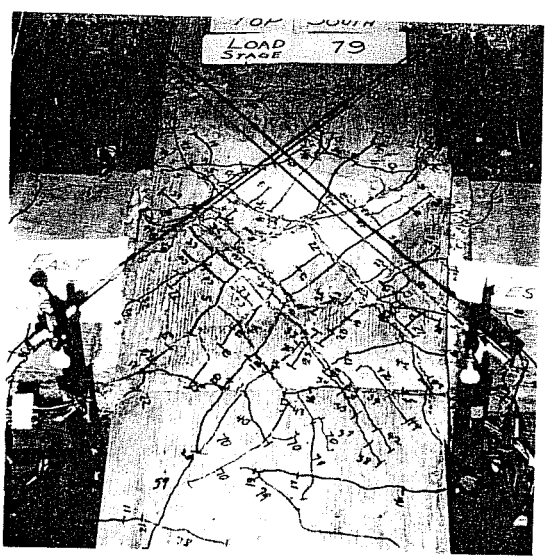

Fig. 3.23 Joint cracking pattern of Specimen V

the concrete tensile strength was exceeded, the orientation of cracking was not parallel to the opposite corner diagonal as in Specimens II and V, but was rotated toward the longitudinal axis of the column. A picture showing the crack orientation at the end of the test is shown in Fig. 3.24.

In the first half of the second cycle, both main beams successfully developed yield stresses and moments at the faces of the column. However, this was the only instance in which both beams were able to do so. Maximum beam moments for other half cycles were dictated by the capacity of the joint in shear and bond.

Specimen VII. Bending of a rectangular column about its weak axis with a higher column load (585 kips as used in Specimen VI) is represented by Specimen VII. Joint cracking load characteristics were similar to those observed for Specimen VI. The cracking pattern is shown in Fig. 3.25 and similar to that shown in Fig. 3.21 for Specimen IV.

The main beam top reinforcement did reach yield strain, but not yield moment. Only when the main beam bottom reinforcement was in tension could the steel yield and carry the yield moment.

Specimen VIII. Previous descriptions have concentrated on the behavior of a joint in a plane frame or, more realistically, joints found in the frame on the exterior of a building. Interior building frame connections will most likely have beams framing into all four faces of the column. Specimens VIII, IX, X, and XI represent interior connections in a frame structure. All four specimens have unloaded lateral beams framing into both sides of the joint perpendicular to the main beams. The cross section of the lateral beam for Specimen VIII covers 70 percent of the joint panel area, the area common to both beam and column. The top of the lateral beam is at the same elevation as the top of the main beam. The lateral beam depth was constant and 3 in. less than the main beam depth. See details in Fig. 2.4.

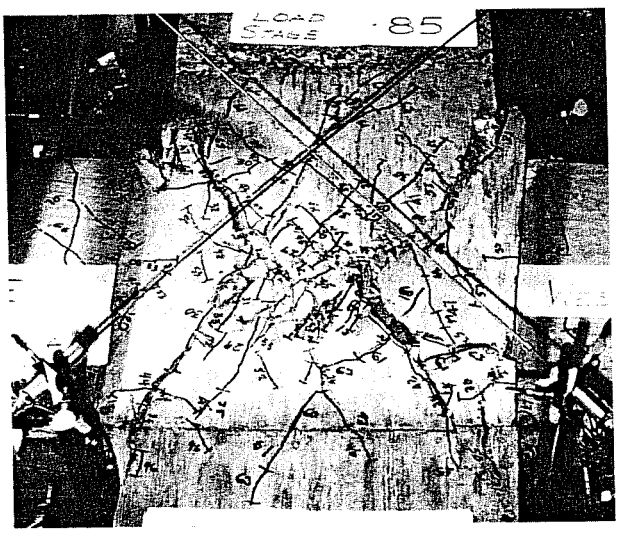

Fig. 3.24 Joint cracking pattern of Specimen VI

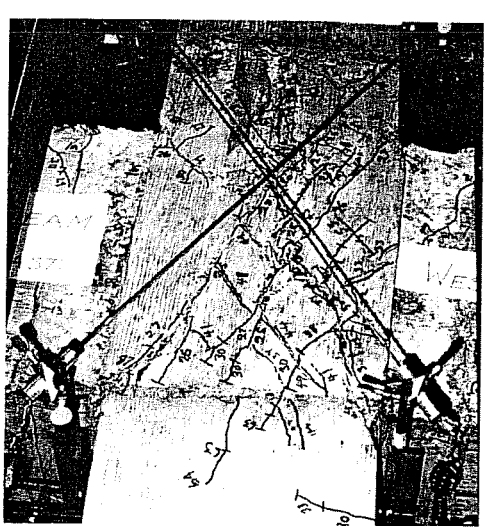

Fig. 3.25 Joint cracking pattern of Specimen VII

The lateral beams of Specimen VIII had a favorable influence on the specimen behavior. The main function of a lateral beam is thought to be that of a confining member. Confinement provided by these lateral beams perpendicular to the applied shear in the joint increased the joint shear cracking strength to 1.70 times that measured in Specimen II.

The effect of a large lateral beam also confined the deformations normal to the applied shear and was beneficial for strength. These lateral beam cross sections allowed the main beams to yield in every large deformation cycle except the second half of the third cycle.

Shear cracking that originated in the joint core eventually was reflected on the sides of the lateral beam. The cracking pattern reflected on the lateral beam gave the impression that it had been loaded in torsion. Figures 3.26(a) and (b) show the bottom and one side of the lateral beam, respectively, at the end of the test. Notice that the cracking is inclined at the lateral beam joint interface and then turns toward the longitudinal axis of this short unloaded beam. Removal of the loose concrete (see Fig. 3.27) on the lateral beam revealed that the cracking pattern observed on the surfaces had originated as diagonal shear cracks in the joint core. The joint crack orientation was typical of what had been observed in previous specimens.

As seen in Fig. 3.27, the lateral beam was reinforced. To avoid introducing an additional variable, all lateral beams were reinforced symmetrically and each had the same percentage reinforcement.

Specimen IX. The effectivensss of masking the joint perpendicular to the applied shear had been observed by other researchers.[13,14,16] However, the effectiveness of the lateral beams that cover (mask) less than 55 percent of the joint panel has

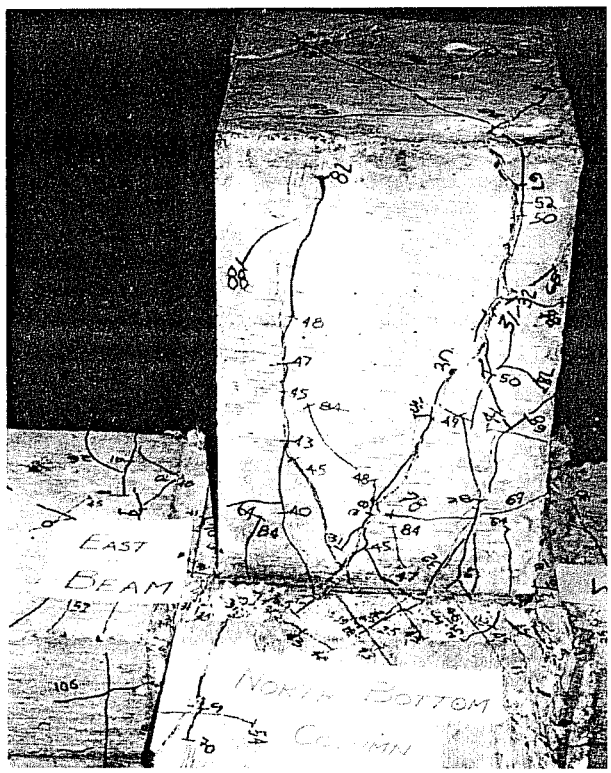

(a) Bottom surface

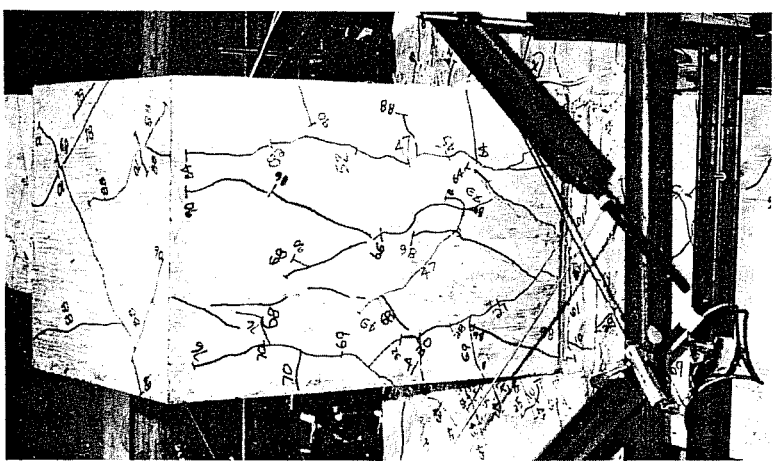

(b) Side surface

Fig. 3.26 Joint and lateral beam cracking pattern of Specimen VIII

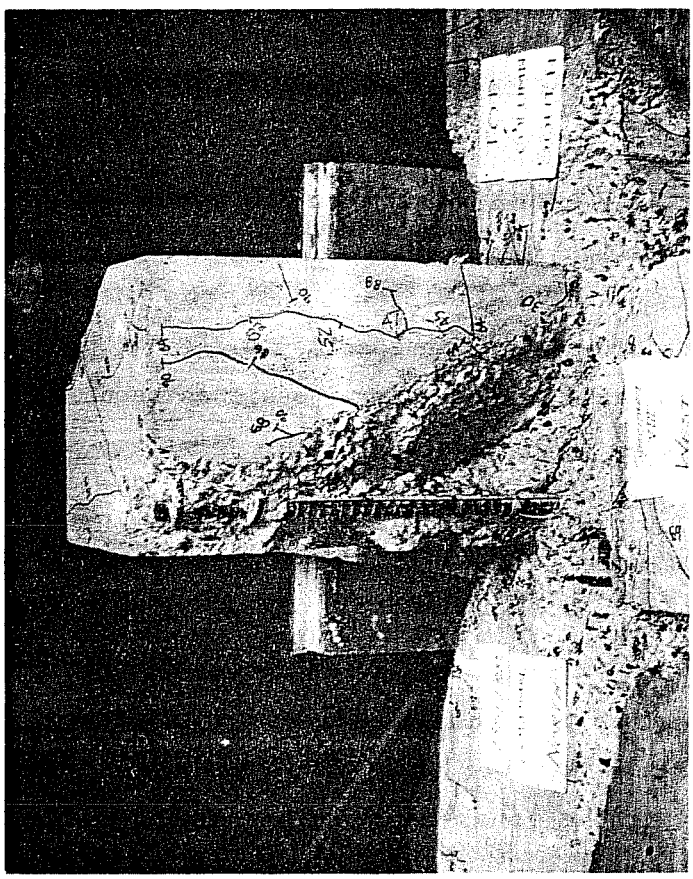

Fig. 3.27 Origin of cracks reflected on sides of lateral beam of Specimen VIII

not been extensively investigated. Specimen IX represents a masking ratio about half way between zero for Specimen II and 0.7 for Specimen VIII. The lateral beam was centered in the joint region along the centerline of the column and covers 37 percent of the joint panel.

Joint shear cracking in Specimen IX initiated in nearly the same fashion as shown for Specimen II (Fig. 3.8). Once the joint shear cracks intersected the lateral beam, they did not continue parallel to the diagonal as in Specimen VIII, but propagated along the longitudinal axis of the lateral beam, as seen in Fig. 3.28. The orientation of shear cracking in the joint was not altered, as shown in the closeup of Fig. 3.29.

Although the main beam top bars reached yield stress, the joint moment was less than the yield moment.

Specimen X. Specimen X is identical to Specimen IX, except that the lateral beam is displaced with respect to the longitudinal axis of the column, see Fig. 2.4. The specimen was designed to ascertain whether the beam must be centered on the column axis to provide confinement.

Failure of the joint in shear occurred before either of the main beams reached yield moment. Joint cracking was much like that of Specimen X. Initially, the lateral beam appeared to provide some confinement, but soon lost effectiveness as the cover spalled in the center of the joint. One of the lateral beam faces and the joint cracking pattern are shown in Fig. 3.30.

Specimen XI. Specimen XI has lateral beams that mask 38 percent of the joint panel, nearly the same masking ratio as Specimen IX (37 percent). In both specimens the lateral beam was centered on the centerline of the column. The only exception was that the orientation of the column was different for Specimen XI. Both Specimens IX

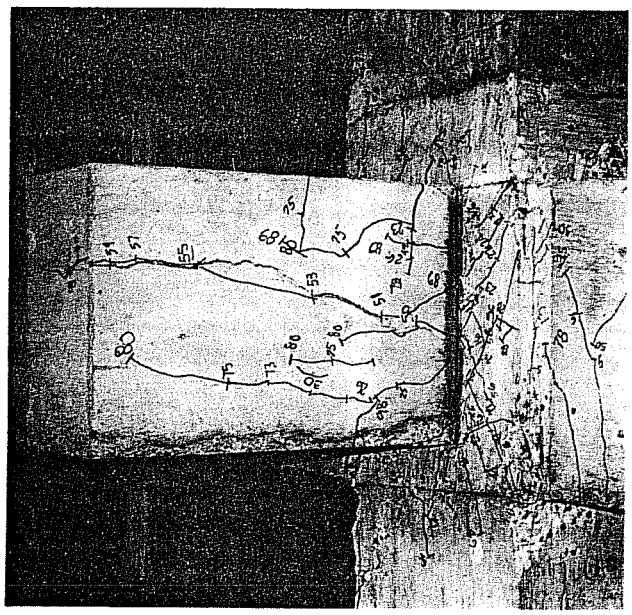

Fig. 3.28 Crack propagation on lateral beam of Specimen IX

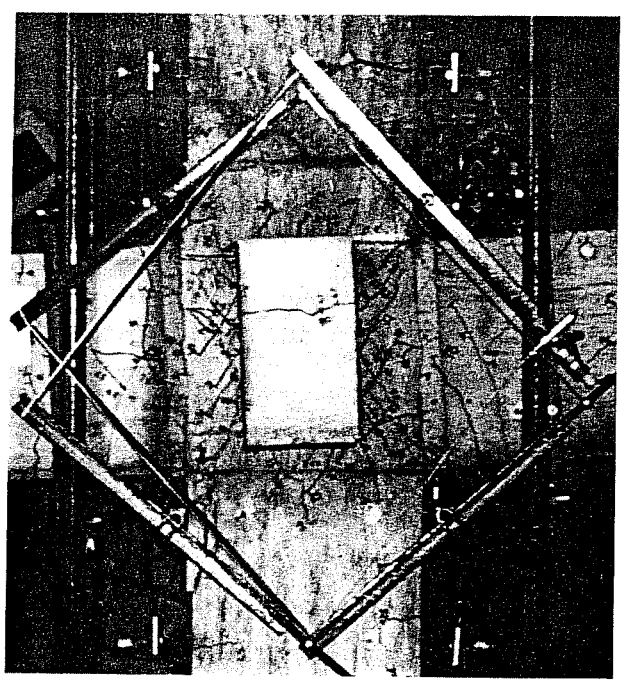

Fig. 3.29 Orientation of joint shear cracks in Specimen IX

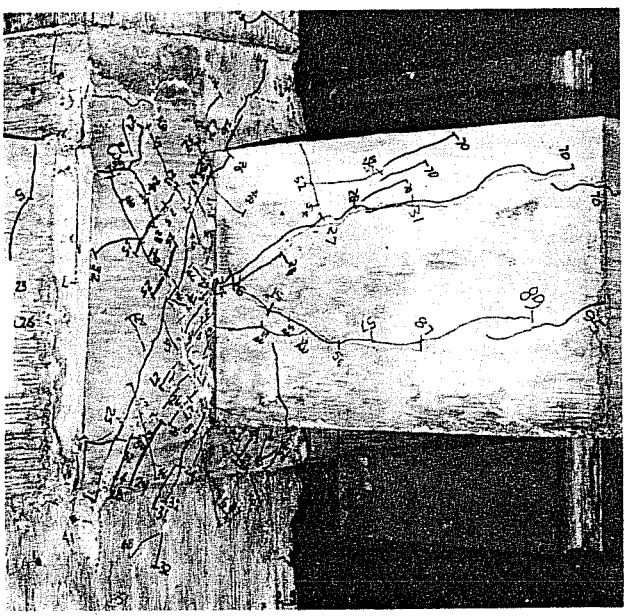

Fig. 3.30 Cracking pattern in joint area of Specimen X

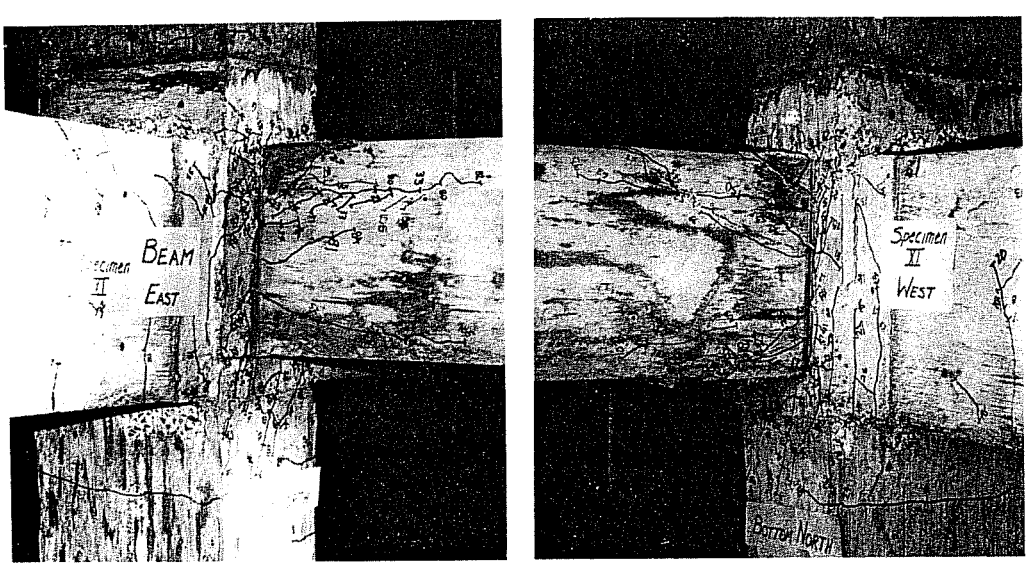

Fig. 3.31 Cracking pattern in joint area of Specimen XI

and XI were incapable of developing the main beam yield moment. The joint cracking followed the same pattern as other specimens having lateral beams. Photographs of the lateral beam sides are shown in Fig. 3.31.

In all the specimens with lateral beams, the lateral beam did not arrest the joint shear cracking; nor did it cause the diagonal crack to deviate from a basic propagation pattern between opposite corners of the joint. The lateral beam did have some influence in confining the joint perpendicular to the main beam. (See Appendix C and Ref. 30 for further details on lateral beam cracking and behavior for Specimens VIII, IX, X, and XI.)

Specimen XII. Joints designed to withstand large deformations and cyclic loads are called Type 2 joints by the ACI-ASCE Committee 352 on Joints and Connections.[9] Specimen XII was proportioned as a Type 2 joint according to the procedures recommended by Committee 352. For the main beams to fail by flexure, the joint required six #5 closed hoops spaced 2 in. on center according to the Committee recommendations.

At the end of three complete cycles of load (see Fig. 3.32), two of which imposed large deformations, the orientation of shear cracks in the joint were similar to those of previous specimens; however, the number of diagonal shear cracks was greater with the crack widths smaller and with no single diagonal crack dominating as the plane on which the shear deformation could concentrate. In previous specimens without lateral beams and with fewer joint hoops, the joint shear deformations parallel to opposite corners tended to concentrate along one diagonal crack.

Hoops in the joint of this specimen were effective in allowing the main beams to reach yield moment and above for both directions of loading in the second cycle. Strains in the top main beam reinforcing bars reached strain hardening.

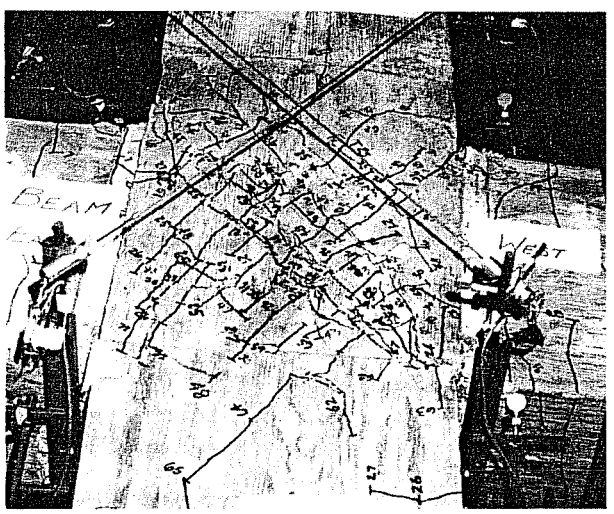

Fig. 3.32 Joint cracking pattern of Specimen XII

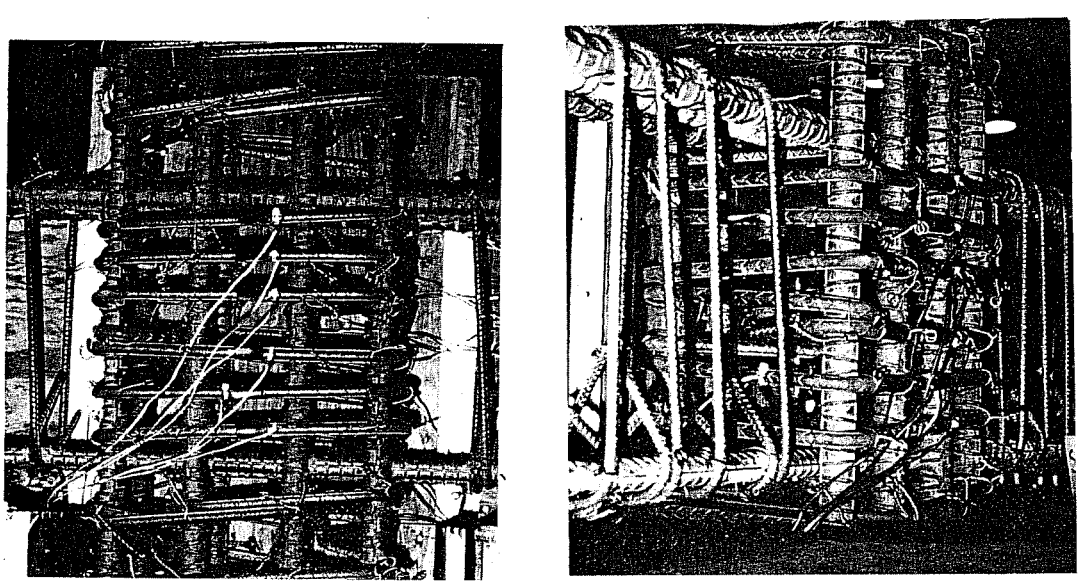

Fig. 3.33 Hoops in the joint of Specimen XIII

In the third cycle of loading, shear and bond strength deterioration dominated the behavior and caused the joint to fail by shear rather than in flexure in the main beams.

The behavior of this specimen in the second cycle was superior to that of any other specimen. However, a weakness still existed. Once diagonal cracking and shear planes were fully developed through the joint, for this specimen at the end of the second cycle, the joint began to weaken from the strength measured in the second cycle.

Specimen XIII. The transverse joint reinforcement in Specimen XIII was between that of Specimen II, two #4 at 6 in., and Specimen XII, six #5 at 2 in. The number of hoops in the joint was three times that of Specimen II, but only about two-thirds the area of steel provided in Specimen XII. Figure 3.33 shows the joint hoops in place before casting and the resulting congestion of reinforcing bars. Similar congestion occurred in Specimen XII.

The loss of the cover and the shear cracking pattern in the joint follows closely what was reported for Specimen XII. However, on each half cycle of this test, the maximum joint moment was dictated by the shear and bond strength of the joint. The main beams were unable to develop yield moments, although during the second cycle the stronger of the main beams was very close to the yield moment.

A photograph of the joint cracking pattern before the concrete cover had been removed is shown in Fig. 3.34. Upon removal of the loose concrete cover, the joint hoops were exposed and found to be bowed outward from the core of the joint (see Fig. 3.35). These hoops probably provided some confinement against lateral expansion of the joint, but were less effective than the flexurally stiffer hoops of Specimen XII. It would appear that supplementary cross-ties might be effective in this case.

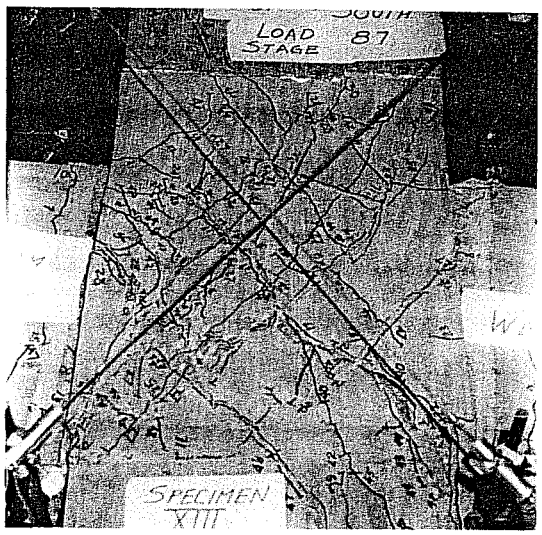

Fig. 3.34 Joint cracking pattern of Specimen XIII

Fig. 3.35 Residual deformations of joint hoops (Specimen XIII)

Specimen XIV. Specimen XIV and the previous specimen, Specimen XIII, are identically reinforced in the joint, beam, and column. The variable of this test is again the axis of bending of the column.

Maximum main beam loads were dictated by the shear and bond strength of the joint. Shear cracking in the joint was oriented parallel to lines connecting opposite corners. The cracking pattern at the end of the test is shown in Fig. 3.36. As in other specimens with the rectangular column bent about its weaker axis, the third cycle caused large visible shear deformations in the column. A photograph of the shear distortion in the column is shown in Fig. 3.37.

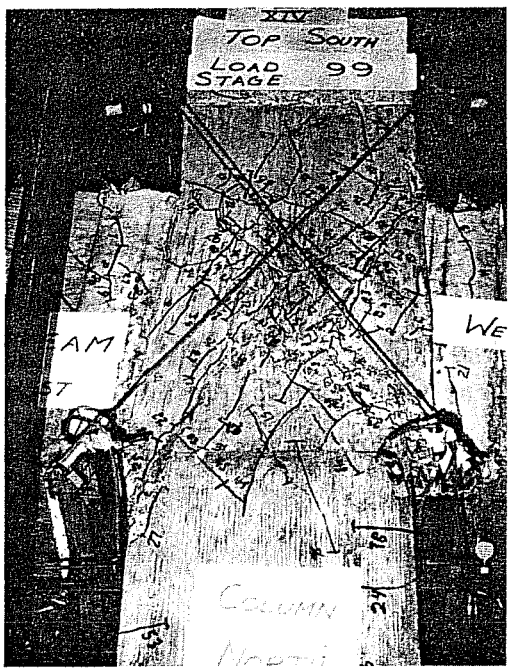

Fig. 3.36 Joint cracking pattern of Specimen XIV

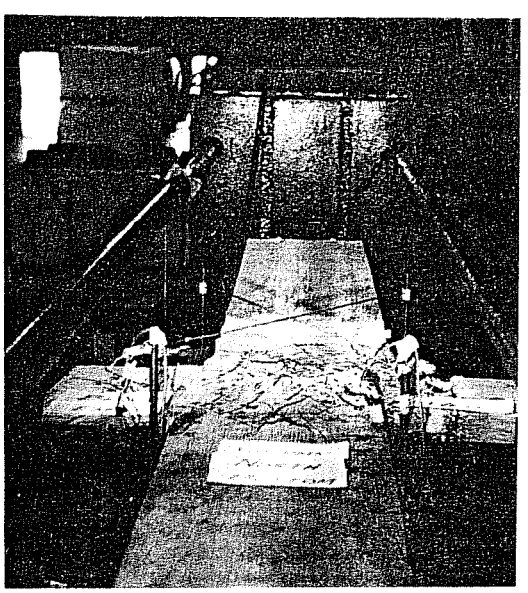

Fig. 3.37 Shear distortion in column of Specimen XIV

CHAPTER 4

DISCUSSION OF BEHAVIOR

4.1 General

The discussion of test results concentrates on a comparison of the behavior between selected specimens. If possible, only one of the variables is changed for each comparison. The comparisons are made with curves of the applied joint shear or joint shear stress versus the shearing deformations on the joint. In most cases the shear or shear stress is normalized to account for variations in concrete strength by dividing by $\sqrt{f'_c}$.

Joint shear stresses are calculated assuming that inclined shear cracks form at 45^o angles to the direction of applied shear. The form of this calculation is identical to the procedure used for reinforced concrete beams. To calculate the average shear stress in the joint, the recommendations of ACI 318-71[2] were followed. The applied shear force is divided by the area bd, where b is the full width of the member and d the effective depth from the extreme compression fiber to the centroid of the tension steel. The dimension b is that of the large member, beam or column, and d is the effective depth of the column.

The loading sequence of each specimen is shown diagrammatically in Fig. 4.1. Each specimen was first subjected to elastic loads of sufficient magnitude to cause inclined shear cracks to form in the joint region. As seen in Fig. 4.1, the load is reversed to cause cracking along both diagonal lines of the joint. Upon completion of the first (elastic) cycle, a second load cycle was applied to measure the strength of the joint in each direction of loading,

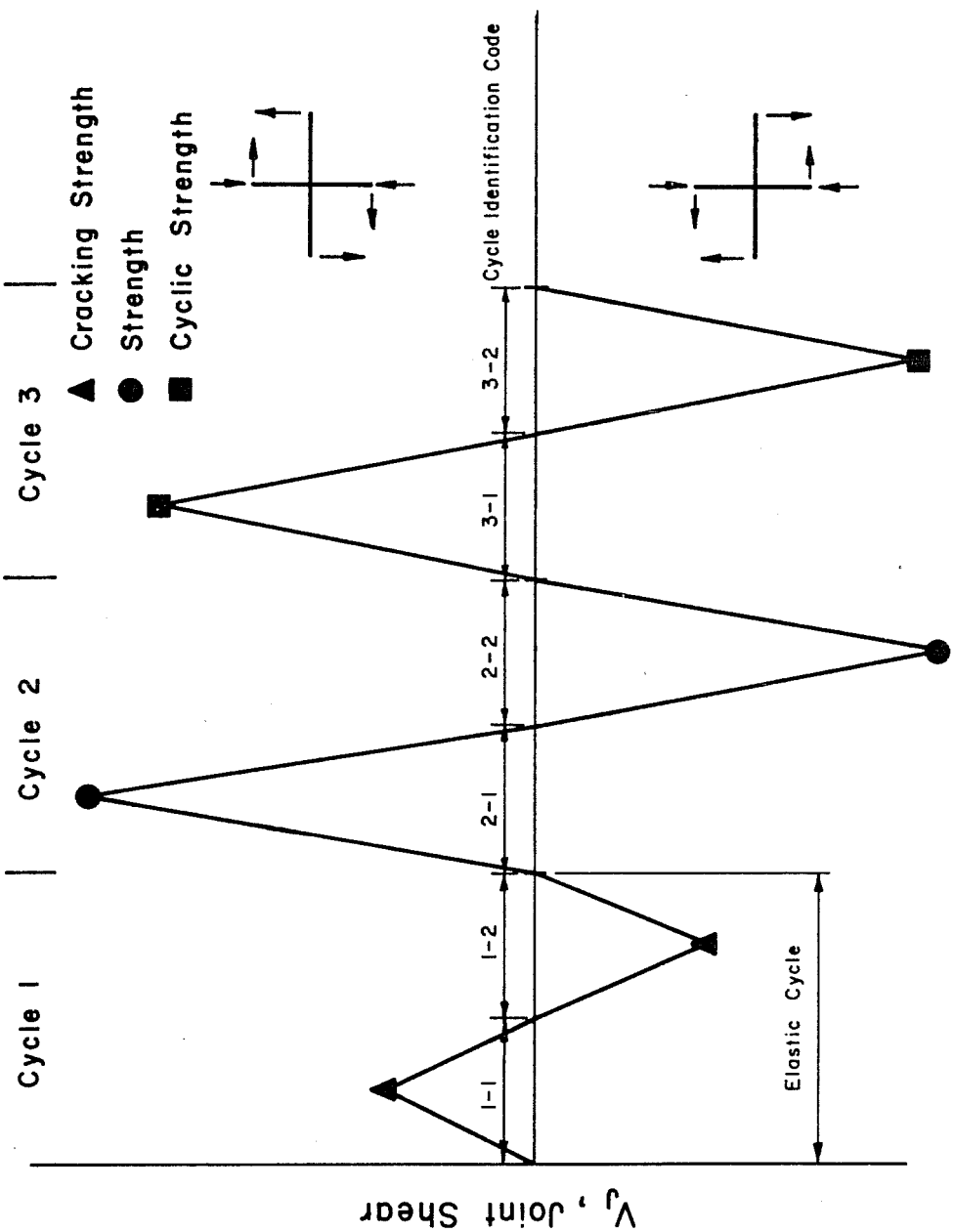

Fig. 4.1 Loading sequence

as seen in Fig. 4.1. As mentioned earlier, peak shear was established by summing the loads on both beams and determining if they had reached a maximum. It is likely that damage accrued in the first half of the second cycle lowered the strength in the second half of that same cycle. Therefore, strength is defined as it would be in a monotonic test to failure. Prior to the monotonic test, load excursions were never beyond the elastic range. The maximum joint shear applied during the first half of the second cycle of loading is defined as the strength of the beam-column joint regardless of the mode of failure. Other maximum joint shears on subsequent loadings are defined as cyclic strength values.

The influence of various parameters on strength will be examined using curves of shear or shear stress versus shear strain during the second cycle of loading. For each parameter the performance is discussed in terms of the elastic behavior, strength, and repeated load behavior. Overall observations made on both the strength and repeated load strengths of all specimens tested conclude the chapter.

4.2 Effect of Column Reinforcement

The effect of column reinforcement on joint shear strength was measured by comparing Specimens I, II, and III. Each specimen had identical geometry except for the percentage of column reinforcement, which varied from a minimum of 2.0 percent of the gross cross-sectional area in Specimen I to a maximum of 6.7 percent for Specimen III, as seen in Table 4.1. For Specimen II, the percentage of column steel selected was midway between the two extremes at 4.3 percent. In order to maintain the same column cross-sectional dimensions, the percentage of column reinforcement was varied by changing both the number and size of the reinforcing bars.

The purpose of these tests was to examine the premise that as the amount of column longitudinal steel passing through the

TABLE 4.1 SPECIMENS WITH DIFFERENT COLUMN REINFORCEMENT PERCENTAGES

Mark	Column Size		Column Reinforcement	Reinforcement Percentage
	Width in.	Depth in.	A_s, in.^{2}	
Specimen I	13	18	8 - #7 = 4.80	2.05
Specimen II	13	18	8 - #10 = 6.32	4.34
Specimen III	13	18	10 - #11 = 15.60	6.67

joint increases, the confinement around the joint increases and improves the performance of the joint. A comparison of the shear stress-strain curves for the three specimens is shown in Fig. 4.2. The curves indicate that as the column reinforcement is increased, there is minimal influence of the column bars in providing lateral confinement to improve joint shear strength. The most notable difference is seen in the comparison between Specimen I, ρ_g = 2.0 percent, and Specimen III, ρ_g = 6.7 percent. Specimens I and III were cast from the same concrete and eliminate the influence of quality of concrete on the results.

A summary of the strength at cracking, at ultimate and under load reversal is plotted in Fig. 4.3, with respect to the percentage of column reinforcement. The designations 2-1, 2-2, 3-1, and 3-2 represent the first half of Cycle 2, second half of Cycle 2, first half of Cycle 3, and second half of Cycle 3, respectively.

As is obvious in Fig. 4.3, the cracking shear strength of the joint is unchanged by the percentage of column reinforcement. Note, however, that the cracking shear strength of the beam-column joint is about 40 percent of the ultimate shear strength in Cycle 2-1. It is apparent from Fig. 4.3 that the cracking shear strength does not represent the useful capacity of the joint.

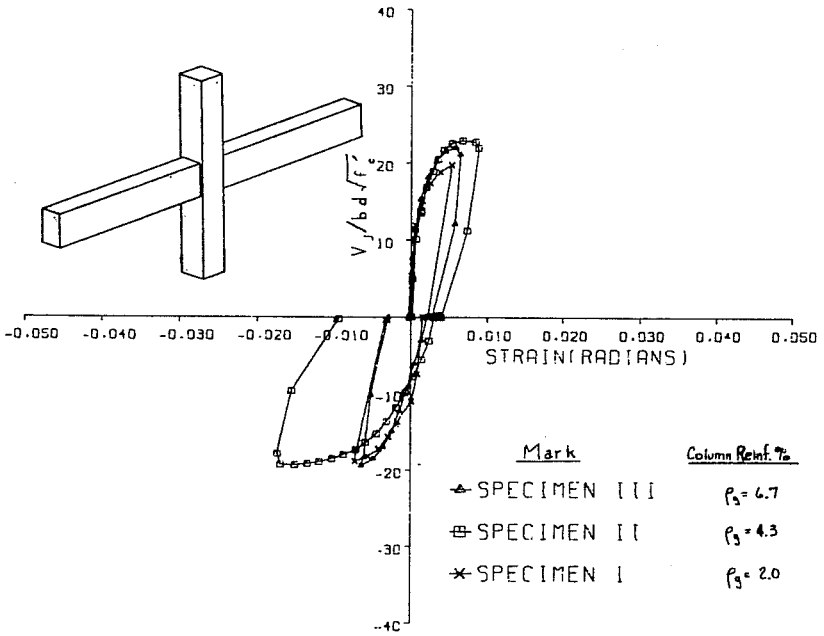

Fig. 4.2 Shear strength comparisons with column reinforcement percentage as the variable

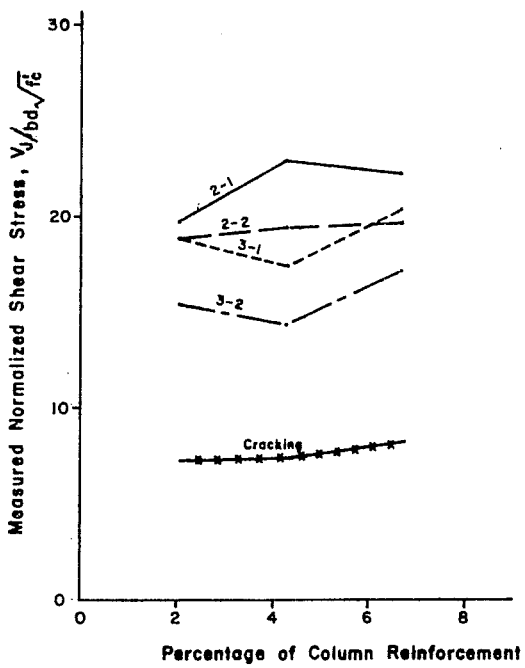

Fig. 4.3 Effect of column reinforcement on joint shear strength

The shear strength of the joints decreased with each reversal of load, as indicated by comparing the normalized stresses in Cycle 2-1 and 3-2, the first and last cycles in which large deformations were imposed. Figure 4.3 indicates that at the end of the third cycle any effects column reinforcement had on strength diminished, and the shear strength of the joint is independent of the column reinforcement percentage. However, the measured shear strength in Cycle 3-2 is still greater than the measured cracking resistance in all cases.

4.3 Effect of Column Orientation

Four pairs of specimens will be compared to investigate the influence orientation of the column has on joint shear strength. In each pair the column cross section is the same, but one specimen has bending about the strong axis of the column and the other is bent about its weak axis. The orientation of the column can be conveniently described by the aspect ratio of the joint perpendicular to the applied joint shear forces. The aspect ratio of the joint is defined as the ratio of the overall depth of the column to the overall depth of the main beam (h_c/h_b). Specimen details pertinent to the discussion are given in Table 4.2. For specimens with bending about the strong axis, the aspect ratio is 1.00 (18/18) and for specimens with bending about the weak axis, the aspect ratio is 0.72 (13/18). The curves for each pair of specimens are plotted separately because the column orientation was not the only variable changed in these four pairs of tests.

Comparison plots of normalized shear force versus shear strain are given in Fig. 4.4 rather than normalized shear stress versus shear strain curves, as shown in Fig. 4.3, because of the potential difference in shear area of joint depending on the assumptions made. The plots of Fig. 4.4 use shear force instead of stress

TABLE 4.2 SPECIMENS WITH DIFFERENT JOINT ASPECT RATIOS

Specimen	Column Width b_c, in.	Column Depth h_c, in.	Axis of Bending	Beam Depth h_b, in.	Aspect Ratio h_c/h_b	Remarks
II	13	18	Strong	18	1.00	Column load ≐ 358 kips
IV	18	13	Weak	18	0.72	2 joint hoops
VI	13	18	Strong	18	1.00	Column load ≐ 585 kips
VII	18	13	Weak	18	0.72	2 joint hoops
IX	13	18	Strong	18	1.00	Column load ≐ 358 kips 2 joint hoops
XI	18	13	Weak	18	0.72	Lateral beams cover 37 percent of joint
XIII	13	18	Strong	18	1.00	Column load ≐ 358 kips
XIV	18	13	Weak	18	0.72	6 joint hoops

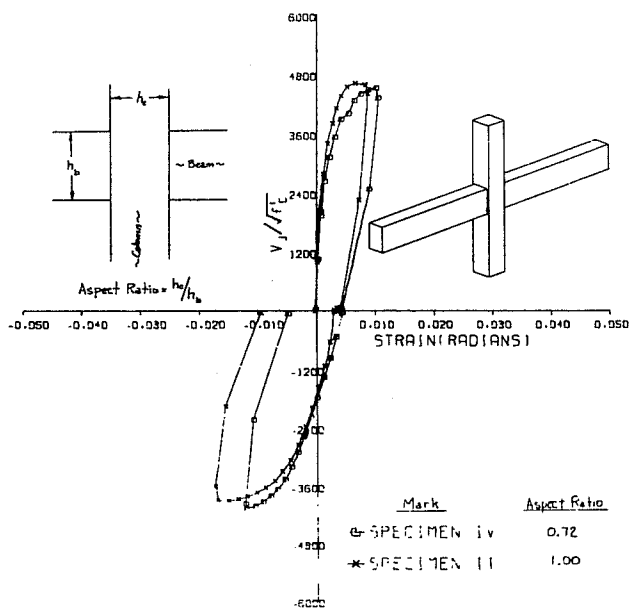

(a)

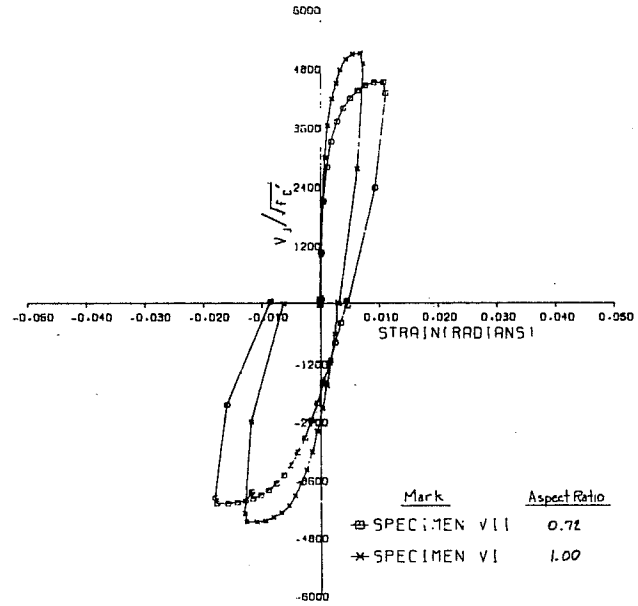

(b)

Fig. 4.4 Joint shear force comparisons with joint aspect ratio as the variable

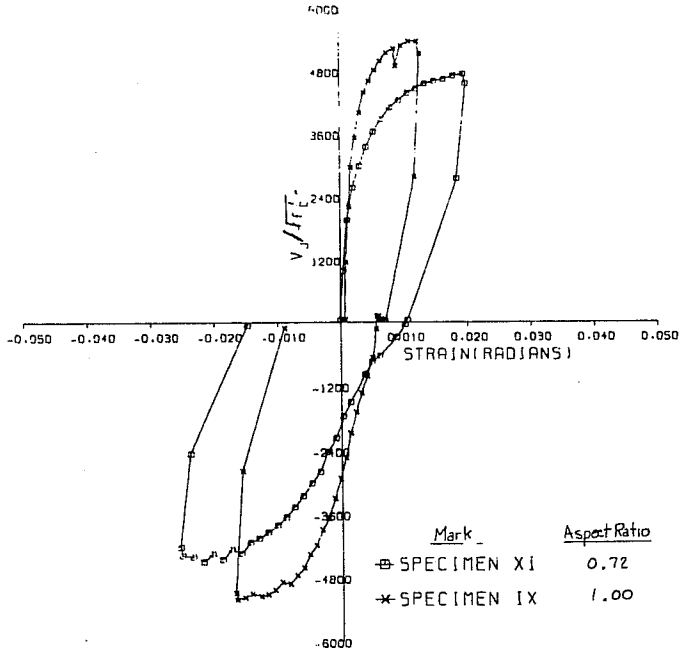

(c)

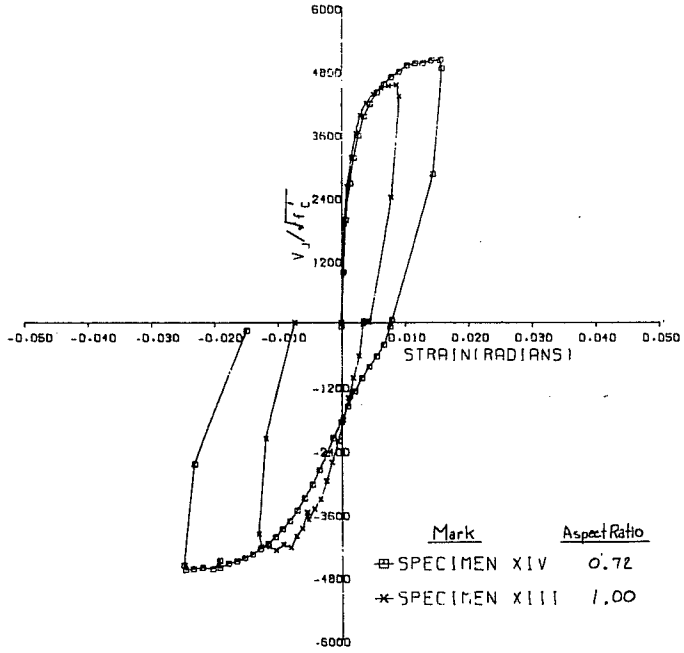

(d)

Fig. 4.4 (Continued)

and hence eliminate area as a variable and allow a more representative comparison of joint aspect ratio.

A trend, although not very strong, shown in Figs. 4.4(a), (b), and (c) is that specimens with aspect ratio (h_c/h_b) of 1.0 have greater shear capacity than those with aspect ratio of 0.72. Tests of deep beams, reported in Ref. 31, indicate that as the span-to-depth ratio becomes smaller the shear strength of the reinforced concrete beam increases. The aspect ratio of the joint is defined in the same manner as the span-to-depth ratio of the deep reinforced concrete beam. However, instead of the shear strength of the joint increasing when the aspect ratio decreases, as for the deep beam, the opposite was observed in Figs. 4.4(a), (b), and (c). Since shear area is not accounted for in Fig. 4.4, the differences in the size of the shear area may explain the above observations.

More meaningful comparisons of these tests may be possible if normalized shear stress instead of normalized shear force were used as the ordinate in Fig. 4.4. Recalling that the shear crack inclination changed when the aspect ratio changed, it is likely that the inclination of the shear crack should be considered when choosing the dimensions of the shear area. In the current recommendations,[9] the inclination of the shear crack or the aspect ratio of the joint is independent of the shear area. A description of the recommended calculation procedure was given in Sec. 4.1. Figure 4.5 reviews the orientation of shear cracks in joints with aspect ratios of 1.00, Fig. 4.5(a), and 0.72, Fig. 4.5(b). These pictures clearly show that cracks propagate along lines nearly parallel to opposite corners of the beam-column joint and that as the aspect ratio becomes smaller the crack inclination is steeper relative to the longitudinal axis of the main beam. This same behavior has been observed in deep beams loaded on the compression flange and supported on the tension flange so that a compression strut can develop. Increasing the column load also had the effect of increasing the crack inclination.

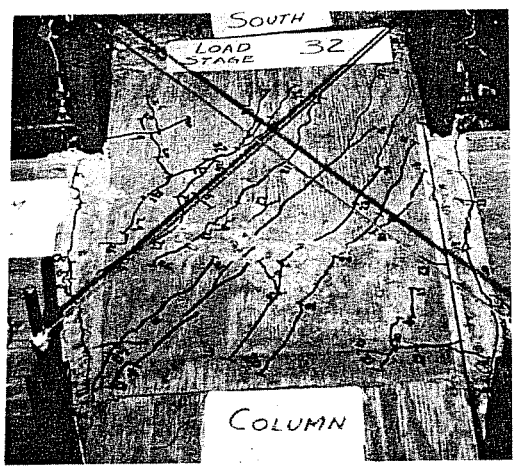

(a) Aspect ratio h_c/h_b = 1.00

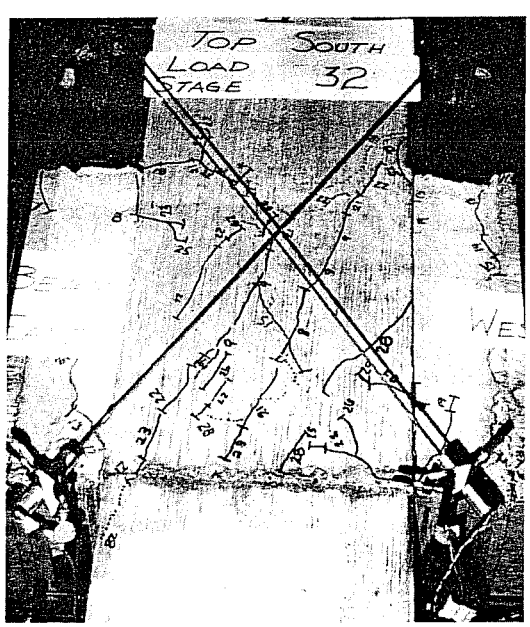

(b) Aspect ratio h_c/h_b = 0.72

Fig. 4.5 Orientation of joint shear cracks

Lacking more sophisticated theories for variable angle inclined cracking, and recognizing the success and acceptance of a shear area (bd) calculated using conventional techniques, the shear areas of the test specimens are shown in Table 4.3.

TABLE 4.3 SHEAR AREAS OF BEAM-COLUMN JOINT TEST SPECIMENS

Aspect Ratio	Width of widest member b_{column}, in.	Effective depth of column d_{column}, in.	Shear area bd, $in.^2$
1.00	13.0	15.4	200.2
0.72	18.0	10.5	189.0

The shear areas given in Table 4.3 were used with appropriate specimens to develop the comparison plots of Figs. 4.6(a) through (d). These plots show no consistent trend that the orientation of the rectangular column or joint aspect ratio has any effect on joint shear strength when the shear areas are approximately the same magnitude. When the aspect ratio is less than 1.00, the tests show that the shear strength is almost equal to the shear strength when the aspect ratio is 1.00.

If the horizontal area (bd) resisting shear is constant, joints with smaller aspect ratios, for these tests $h_c/h_b < 1.0$, may be stronger because of a built-in confining mechanism. It was observed in Figs. 4.2 and 4.3 that column reinforcement percentage had a very slight effect in confining the joint deformations perpendicular to the applied shear. A three-dimensional drawing of two beam-column joints having different aspect ratios is shown in Fig. 4.7. The restraint to the triaxial deformation at the center of the beam-column joint is increased as the dimension of the joint normal to the free surface increases.

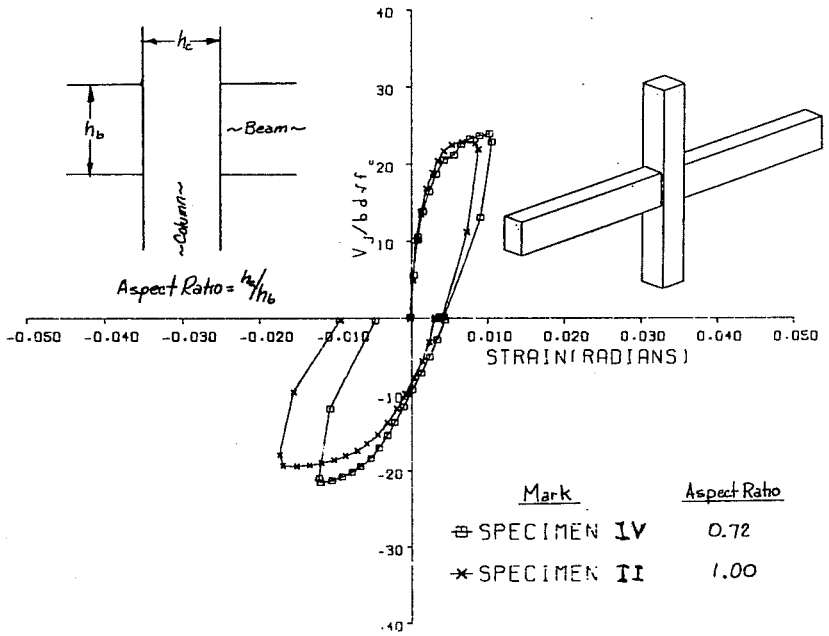

(a)

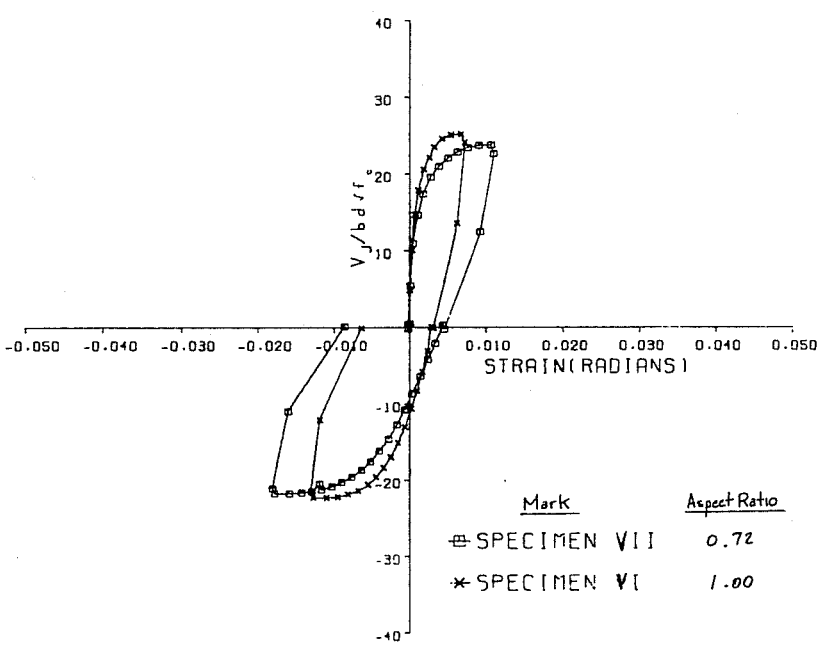

(b)

Fig. 4.6 Shear strength comparisons with joint aspect ratio as the variable

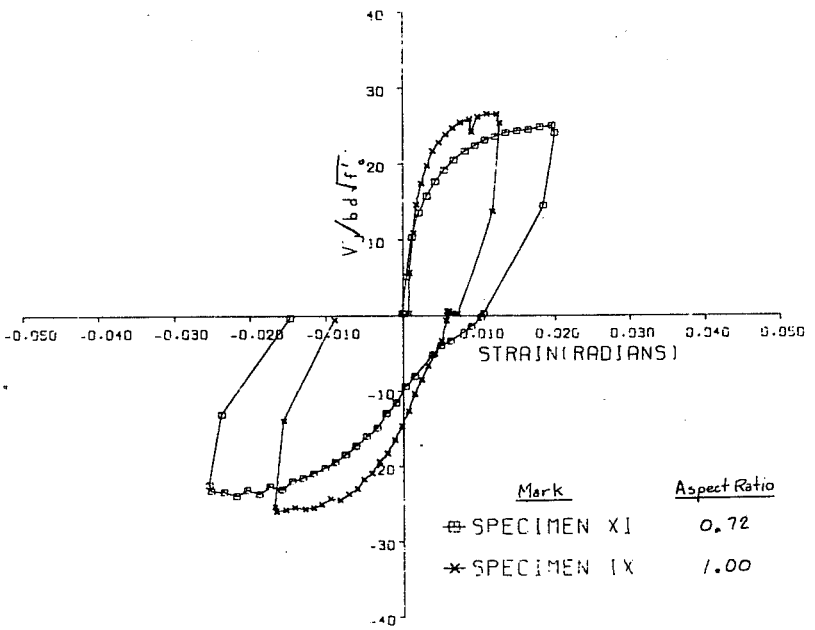

(c)

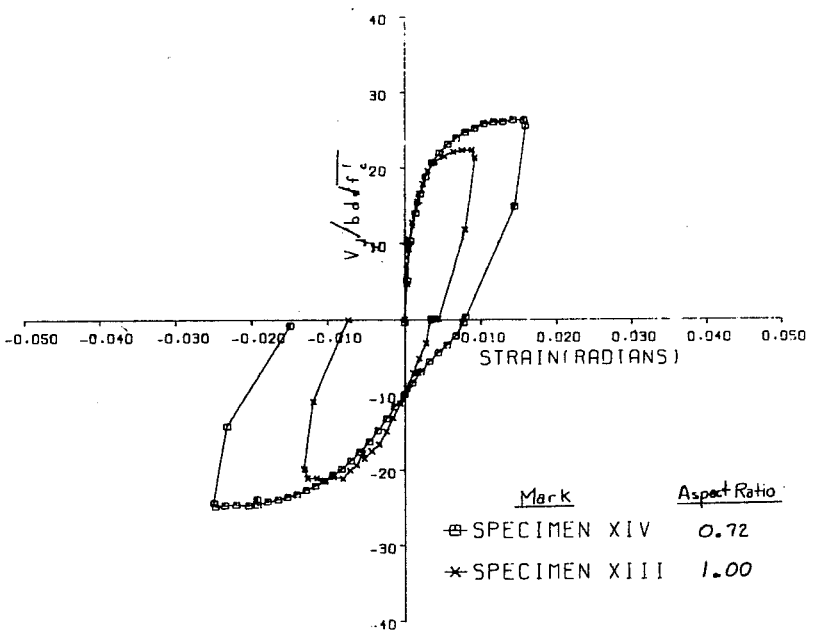

(d)

Fig. 4.6 (Continued)

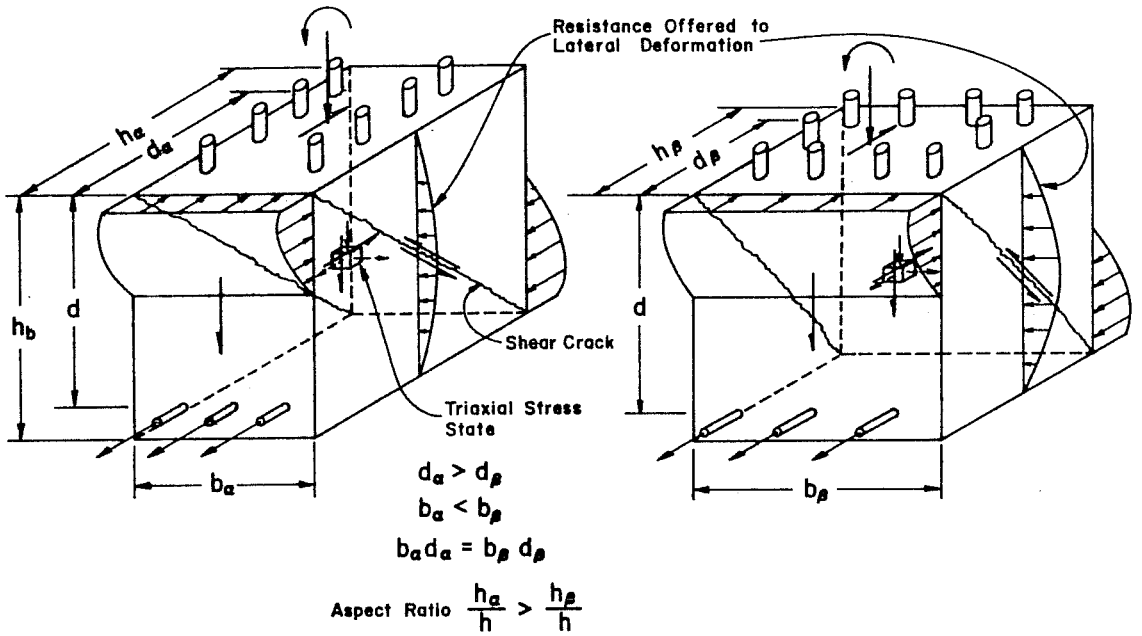

Fig. 4.7 Beam-column joints with different aspect ratios but the same shear area

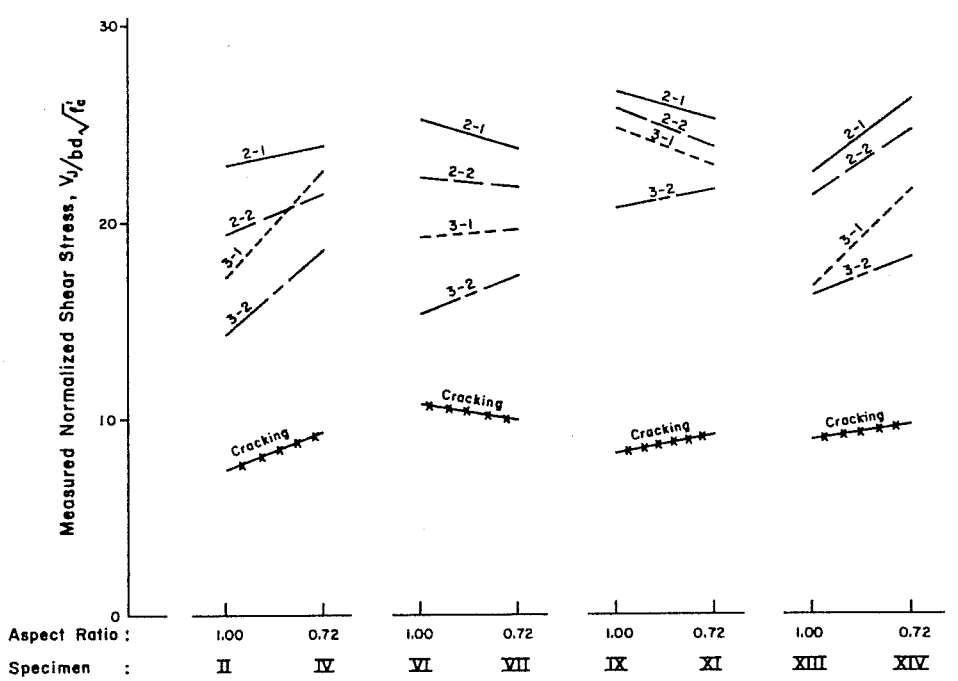

Fig. 4.8 Effect of column orientation on joint shear strength

A summary of the shear strength results for specimens in which the aspect ratio of the joint (or axis of column bending) changed is shown in Fig. 4.8. Those curves show that the joint strength is generally unaffected by geometry when the shear areas are approximately equal.

Figure 4.8 also points out that with each reversal of load the joint with the wider column, smaller aspect ratio, generally has a better cyclic capacity. This may be due to the triaxial confining effects of a wider column.

As indicated earlier in Section 3.6 and Fig. 4.5, the shear crack in the joint forms parallel to a line opposite diagonal corners. Cracking shear strengths as plotted in Fig. 4.8 show that there is no substantial difference in cracking shear strength when the orientation of a rectangular column is varied.

4.4 Effect of Column Load

There are five specimens of this test series in which column load was the primary variable, as listed below in Table 4.4.

TABLE 4.4 SPECIMENS WITH DIFFERENT COLUMN LOADS

Specimen No.	Column Width b_c, in.	Column Depth h_c, in.	Joint Aspect Ratio	Column Load kips
V	13	18	1.00	48
II	13	18	1.00	360
VI	13	18	1.00	603
IV	18	13	0.72	363
VII	18	13	0.72	597

Three of these specimens, Specimens II, V, and VI, had a joint aspect ratio equal to 1.00. Two of the specimens, Specimens IV and VII, had an aspect ratio of 0.72. The nominal column loads were 48 kips (Specimen V), 360 kips (Specimens II and IV), and 600 kips (Specimens VI and VII), and were applied concentrically and maintained constant for the duration of the test.

An elementary Mohr Circle two-dimensional elastic stress analysis for a material with limiting tensile strength, such as concrete, is shown in Fig. 4.9. As the figure indicates, with increase in the compressive stress on one face of the element the shear strength of the material will also increase, provided uniaxial compressive failure of the material is not reached.

Comparison of specimens in which column load is the variable is shown in Figs. 4.10(a) and (b). These plots indicate very little change in the joint shear strength as the column load changes drastically. This is contrary to the elastic Mohr Circle analysis presented in Fig. 4.9. However, it is important to point out that with high column load Specimen VI developed yield moments in both main beams framing into the joint for the loading sequence shown in the first quadrant of Fig. 4.10(a). In the other specimens of this subseries, the maximum loads were controlled by failure of the joint.

Although the strength of the beam-column joint was unaffected by the magnitude of the column load, both the cracking pattern in the joint and the shear at the formation of first cracking was found to change with column load. Figure 4.11 shows the orientation of joint shear cracks with the corresponding column load for each specimen considered. Comparing Figs. 4.11(a), (b), and (c) shows that as the column load increases from 48 to 600 kips, the inclination of the shear crack tends to rotate toward the longitudinal axis of the column. For the low and intermediate magnitudes of column load, there is essentially no difference in the orientation of the crack

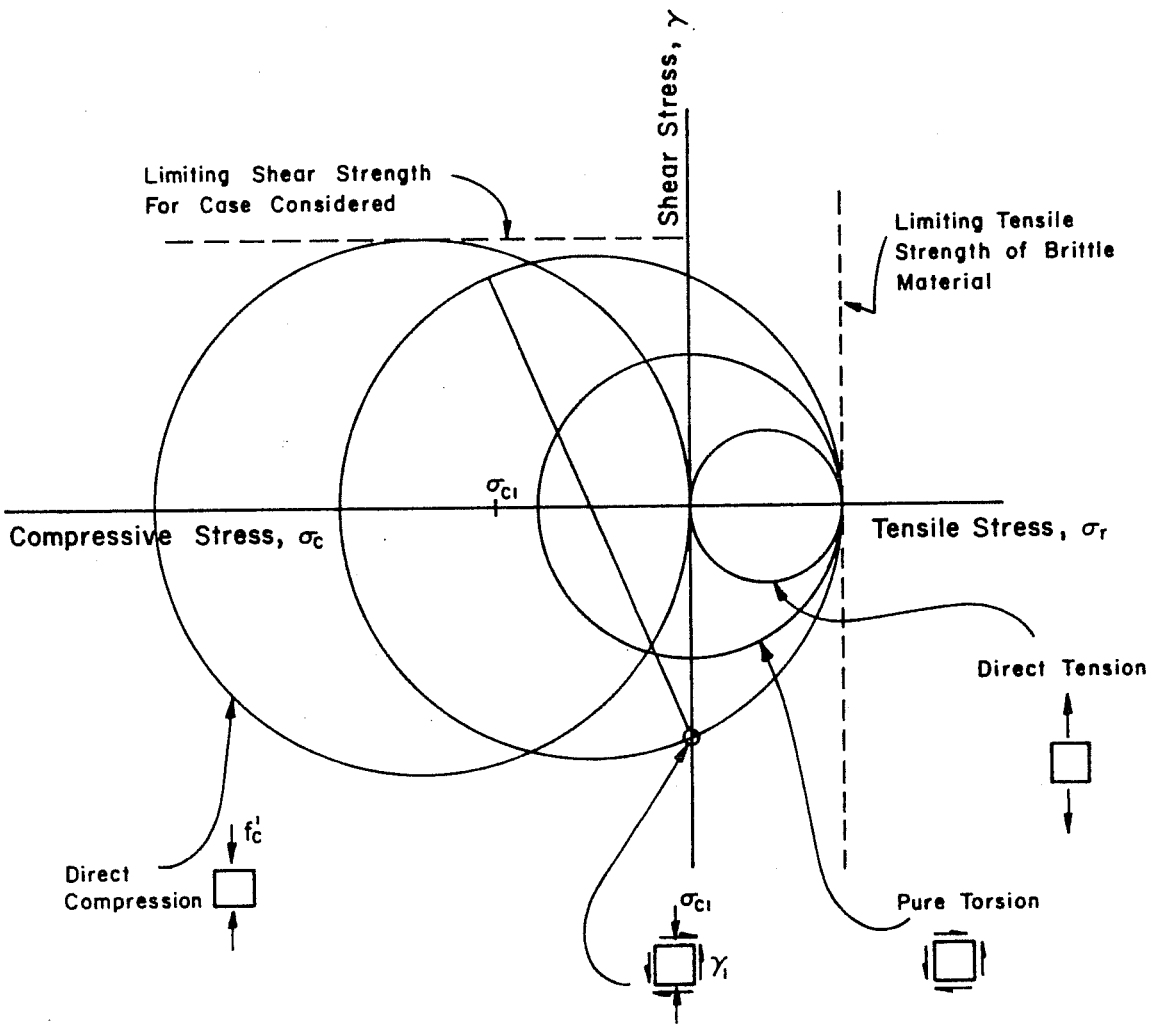

Fig. 4.9 Increase in shear strength as compressive stress on one side of element increases

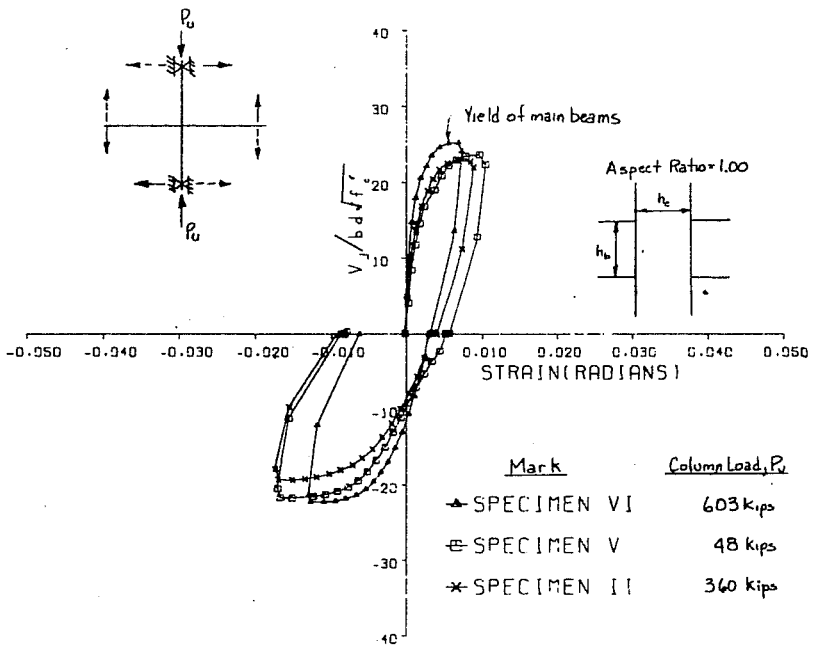

(a)

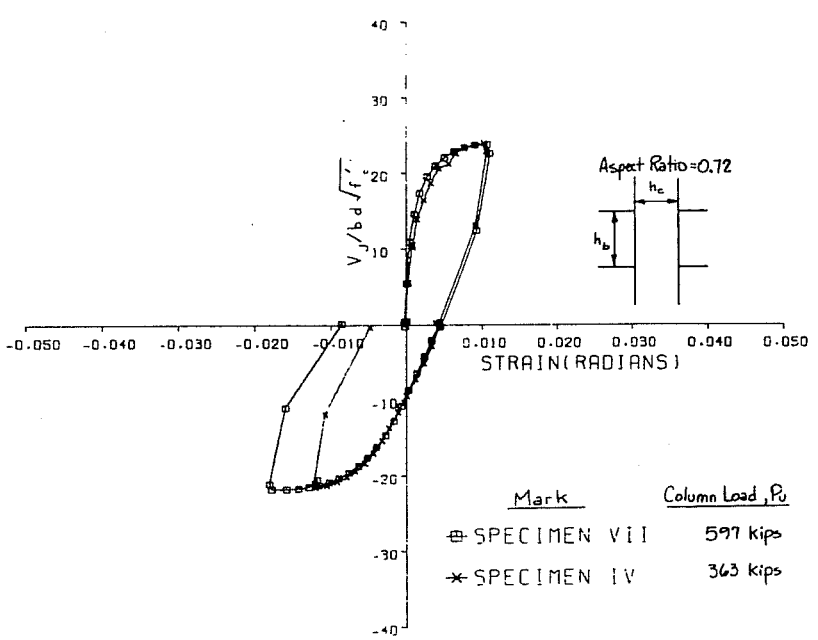

(b)

Fig. 4.10 Shear strength comparisons with column load as the variable

Aspect Ratio

$h_c/h_b \approx 1.00$

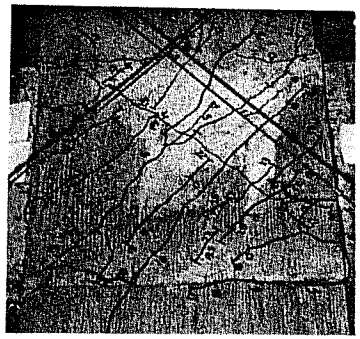

(a) Specimen V
P_u = 48 kips

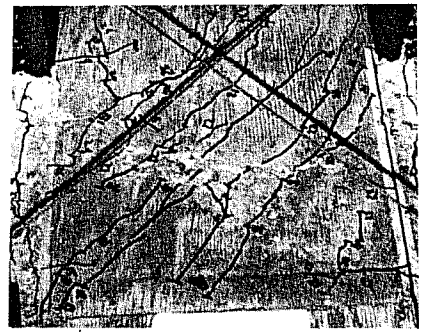

(b) Specimen II
P_u = 360 kips

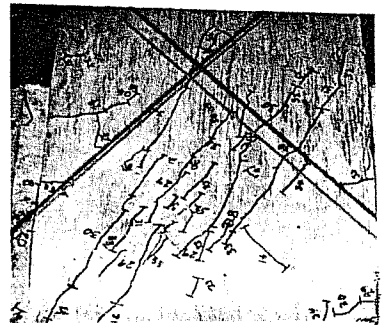

(c) Specimen VI
P_u = 603 kips

$h_c/h_b \approx 0.72$

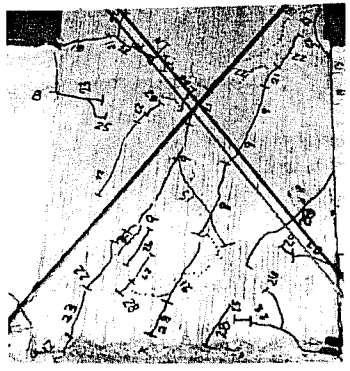

(d) Specimen IV
P_u = 363 kips

(e) Specimen VII
P_u = 597 kips

Fig. 4.11 Orientation of joint shear cracks with various column loads

and the inclination is typical of the 45^{o} angle found in beam shear cracking.

For Specimens IV and VII, the inclination of the shear cracks shown in Figs. 4.11(d) and (e) do not change as the column load increases. However, inclination of the cracks is greater than 45^{o} when the joint aspect ratio was less than 1.0.

The shear strength of the beam-column joint was found to be inconsistent with the failure theory presented in Fig. 4.9. However, this failure theory is based on a material failure in the concrete upon reaching a limiting tensile stress. The principal tensile stress exceeds the tensile capacity of the concrete when a diagonal shear crack forms. The cracking shear strength when plotted with respect to the magnitude of the column load in Fig. 4.12 supports the limiting tensile stress failure criteria, but failure is not reached at tensile cracking. As observed in Fig. 4.12, the cracking shear strength is dramatically increased, whereas the ultimate shear strength of the joint is relatively unaffected by the magnitude of the column load. Although the mechanism is not obvious, the concrete retains shear strength because the cracks do not separate sufficiently to negate beneficial aspects of friction and aggregate interlocking.

Upon being subjected to load reversals, each of these specimens showed a similar behavior. The load reversal strengths, shown in Fig. 4.12, were independent of column load, as were the ultimate strengths measured in the monotonic test (Cycle 2-1). Each specimen lost strength at about the same rate.

In summary, the column load only influences the magnitude of the shear cracking stress and perhaps the inclination of the shear cracks in the beam-column joint; however, the shear strength of the joint is unaffected by the magnitude of the column load.

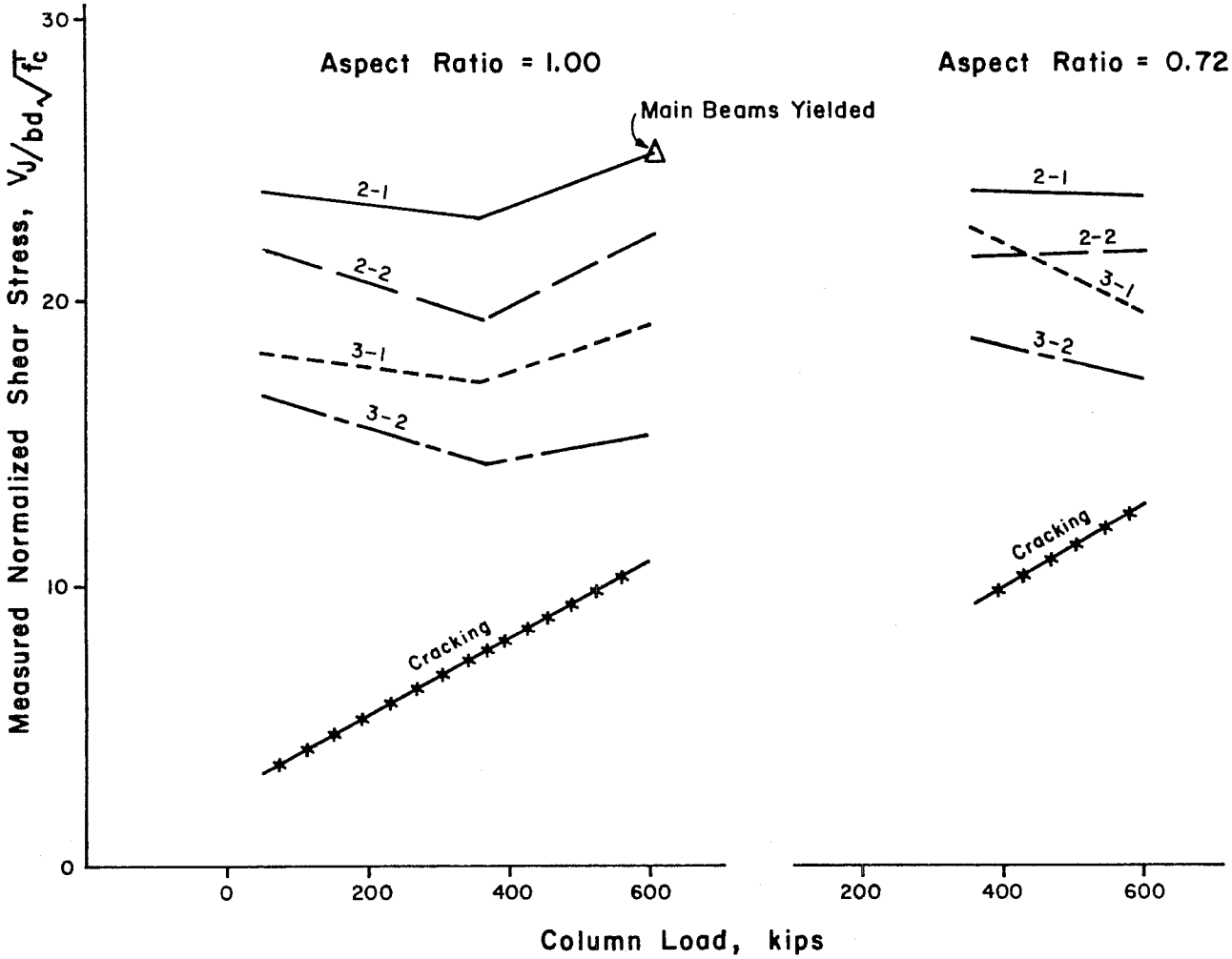

Fig. 4.12 Effect of column load on joint shear strength

4.5 Effect of Transverse Joint Reinforcement

Specimens in which the prime variable is the amount of lateral hoop reinforcement in the beam-column joint are shown in Table 4.5.

TABLE 4.5 SPECIMENS WITH DIFFERENT JOINT REINFORCEMENT

Specimen No.	Joint Aspect Ratio	Joint Hoop Reinforcing	Volume of enclosed core V_{core}, in.^{3}	Volumetric steel percentage $\rho_s = V_s/V_{core}$
II	1.00	2 #4 @ 6"	900	0.0111
XIII	1.00	6 #4 @ 2"	300	0.0333
XII	1.00	6 #5 @ 2"	300	0.0517
IV	0.72	2 #4 @ 6"	900	0.0111
XIV	0.72	6 #4 @ 2"	300	0.0333

Specimens II, XII, and XIII have aspect ratios of 1.00, and Specimens IV and XIV have aspect ratios of 0.72. The amount of transverse hoop reinforcement parallel to the main beam flexural bars is defined by the volumetric steel ratio, which is the volume of the transverse reinforcement divided by the volume of the enclosed core (outside dimensions of the joint hoops). The volumetric steel ratio is 0.0111 for Specimens II and IV, 0.0333 for Specimens XIII and XIV, and 0.0517 for Specimen XII. The ratio 0.0517 represents the amount of steel required to cause yielding in the main beams using the ACI-ASCE 352 design method outlined in Chapter 1.

If the cover in a reinforced concrete column is lost, the remaining unconfined concrete core does not have the same capacity as the original column unless the core can be confined to increase

the concrete strength. The intermediate ratio, 0.0333, represents the amount of steel required to provide confinement to the concrete core and increase the column axial capacity back to its original strength. Several photographs in Chapter 3 showed the loss of the cover in the joint region. The rectangular hoops used were considered as being only half as effective as confinement provided by an equivalent circular spiral.[9]

The minimum ratio, 0.0111, was based on use of a nominal column tie bar diameter and a maximum spacing of 6 in., as recommended by ACI-ASCE Committee 352.[9]

It is possible to include the transverse hoop reinforcement in shear strength calculations in a number of different ways. Three approaches to beam-column joint shear strength will be discussed.

The first approach is to consider the joint region behaving in shear as a reinforced concrete beam. In this approach, as seen in Fig. 4.13, the joint hoop reinforcement, i.e., shear reinforcement, is assigned a certain amount of the total shear on the joint. The magnitude of the shear assigned to the reinforcement is the difference between the total joint shear and the shear the concrete can carry. The shearing strength of the concrete in this case is primarily a function of concrete strength. This is the current approach to designing beam-column joints and was the approach used in proportioning these specimens.[2] A design approach of this type, especially when applied to beam-column joint design, may assign a large fraction of the load-carrying capacity in the joint to the transverse hoop reinforcement.

As a second approach, one can consider the reinforcing bars as tying forces holding the two blocks together. The existence of the tying forces allows the development of internal friction along the inclined path. Such an approach is represented in Fig. 4.14. A simple equilibrium analysis of the forces on an inclined surface

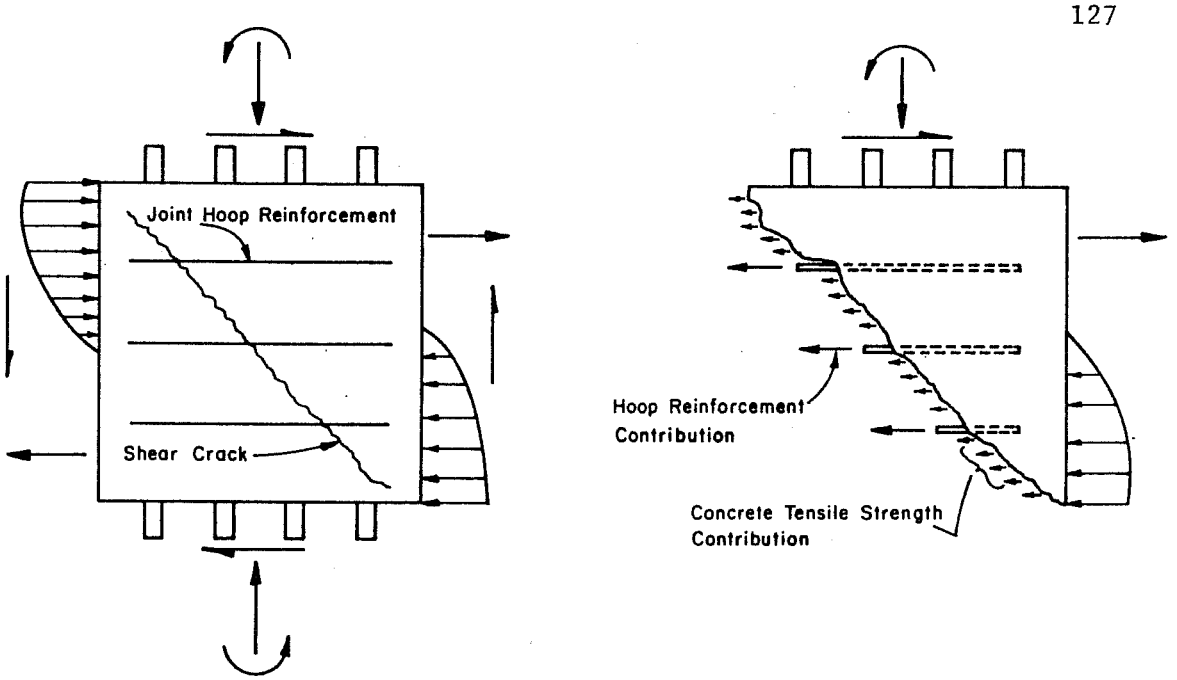

Fig. 4.13 Joint hoop reinforcement considered the same as beam stirrup reinforcement

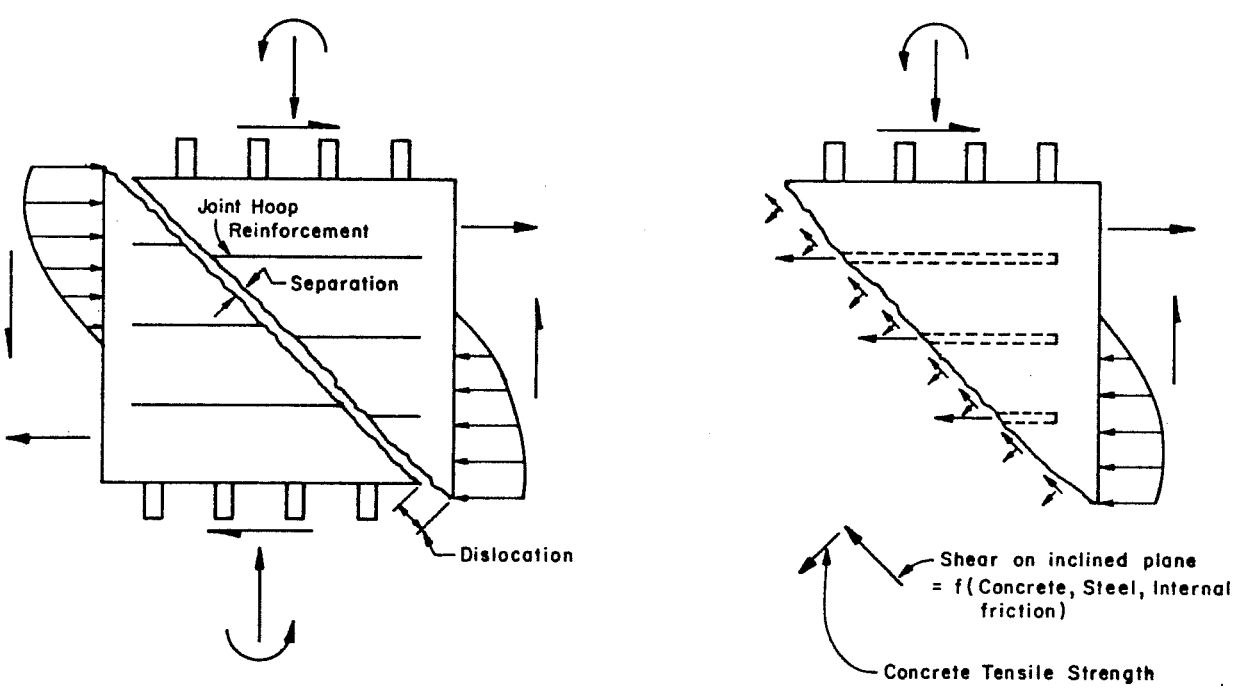

Fig. 4.14 Joint hoop reinforcement considered as tying reinforcement for shear friction

shown on the free body in Fig. 4.14 results in a strength equation which is again dependent upon the amount of transverse joint hoop reinforcement. By making the assumption that the frictional strength of the concrete is equal to the concrete cracking strength (tensile capacity) the joint shear strength equation is the same as that considering the joint analyzed as a beam, discussed above.

A third approach to strength is to consider the joint reinforcement providing confinement to restrain the lateral deformation of the joint core. Transverse hoop reinforcement confining effects can then be considered in the same way as the column width effect shown in Fig. 4.7. A three-dimensional view of the beam-column joint and possible distributions of confinement of joint reinforcement is shown in Fig. 4.15. As the number and size of hoops increases, the restraint to lateral deformations also increases. The confinement provided depends on a complex interaction of hoop spacing and stiffness (or bar diameter relative to unsupported "span"). Of the specimens tested in this subseries, the number of joint hoops as well as the hoop diameter were varied.

The shear stress-strain curves of the second load cycle for the five specimens have been plotted and are shown in Figs. 4.16(a) and (b). Figures 4.16(a) and 4.16(b) represent joints with aspect ratios of 1.00 and 0.72, respectively.

It is important to observe that while the volumetric steel ratios of Specimens XIII and XIV are three times the ratio of Specimens II and IV, very little improvement, if any, is seen in the joint shear strength. The joint, with the amount of the shear reinforcement increased 300 percent, did not perform proportionately better. The equations derived from force equilibrium on an inclined failure plane, as represented by Figs. 4.13 and 4.14, do not appear to be representative of the test data shown in Fig. 4.16. Comparing Specimen XII, which has a volumetric steel ratio 55 percent greater than

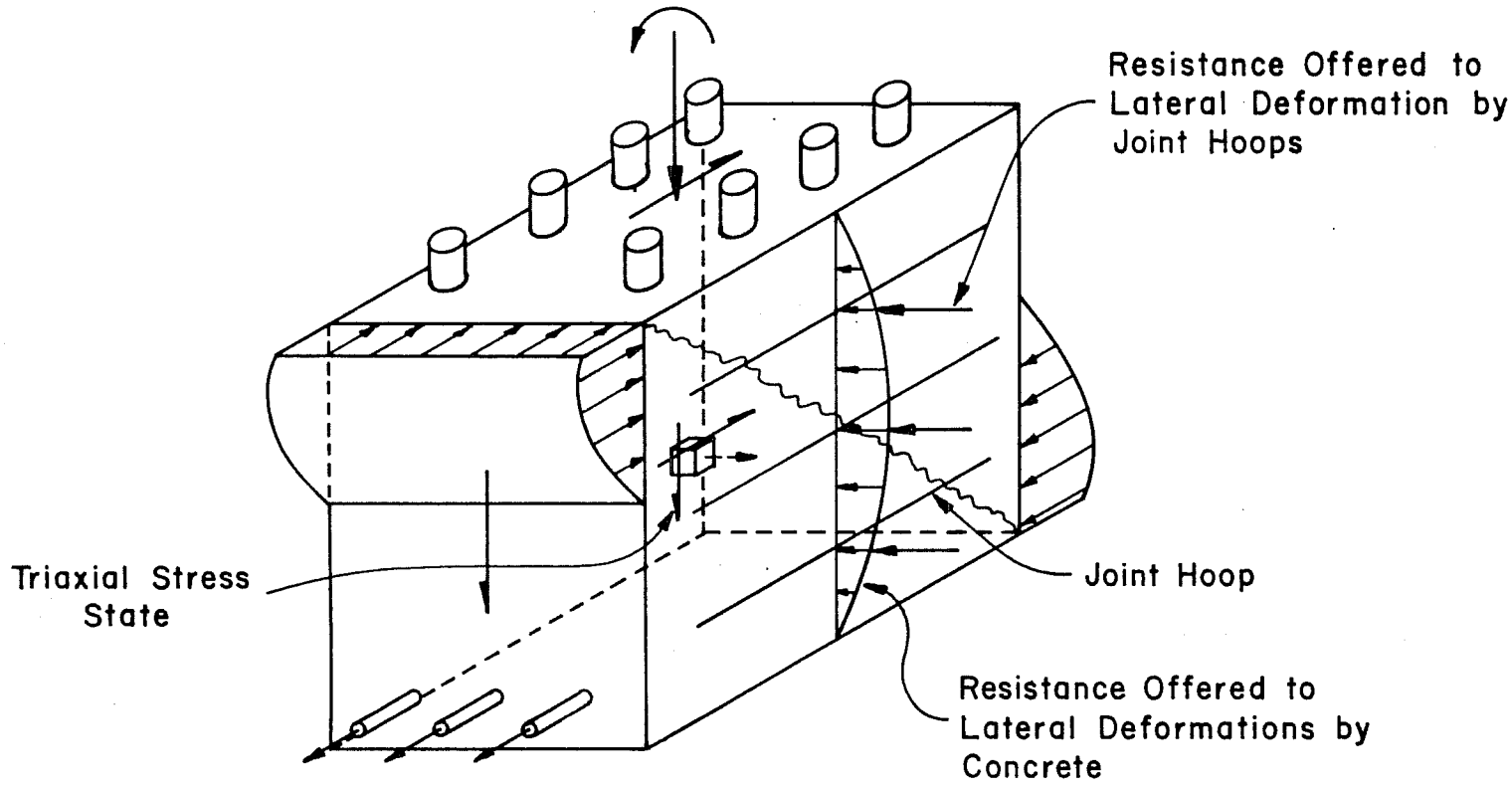

Fig. 4.15 Joint hoop reinforcement considered as providing confinement

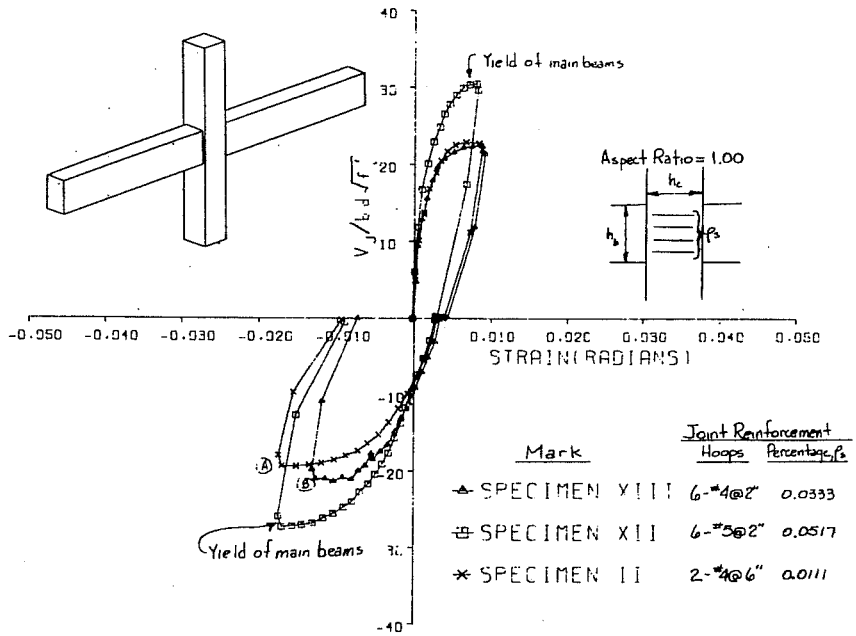

(a)

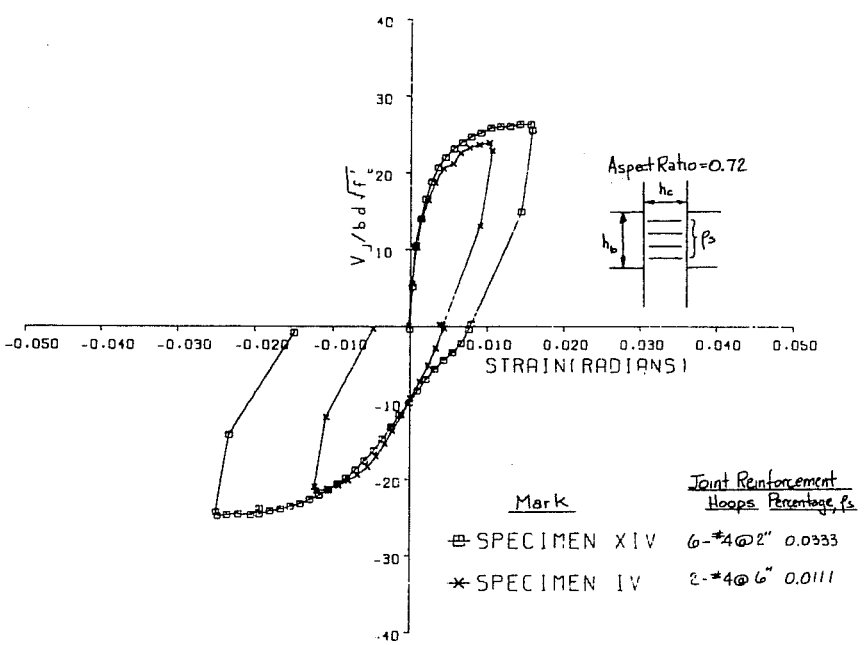

(b)

Fig. 4.16 Shear strength comparisons with volume of joint reinforcement as the variable

that of Specimen XIII, to the others shows the joint behavior as much superior. The improvement in behavior of Specimen XII was such that the joint was capable of allowing the main beams to develop yield moments and form hinges. These tests seem to indicate that there is a threshold of reinforcement both in numbers of hoops and in flexural stiffness of the hoop necessary to force a failure in the main beams rather than in the joint.

The strengths of these specimens when subjected to cyclic load reversals are shown in Fig. 4.17. It is quite apparent from Fig. 4.17 that when the volumetric steel ratio was 0.0517 the specimen failed in a more desirable mode. Note that in the second cycle for $\rho_s = 0.0517$ the joint allowed yield moments to form in both halves of the second cycle. However, none of the specimens were immune to strength deterioration, including the specimen with a 0.0517 volumetric joint steel ratio. Comparing specimens with volumetric steel ratios of 0.0111 and 0.0333, the joint shear strength in any particular half cycle appears to be only marginally influenced by the presence of a greater number of joint ties. Although one would expect that the larger number of hoops would improve the joint behavior after Cycle 2, i.e., maintain the ductility of the joint, such was not the case in these tests.

In comparison with low and intermediate values of volumetric steel ratio, the joint designed using current design philosophy,[9] $\rho_s = 0.0517$, exhibited improved shear strength and cyclic behavior. Although testing was terminated at the end of two large deformation cycles, the shear strength of all joints would probably continue to deteriorate with additional load reversals.

A final observation from Fig. 4.17 is that the cracking shear strength of the concrete was completely unaffected by the presence of joint hoop reinforcement.

To summarize, the major conclusion drawn from these test data is that shear strength does not appear to be a linear function

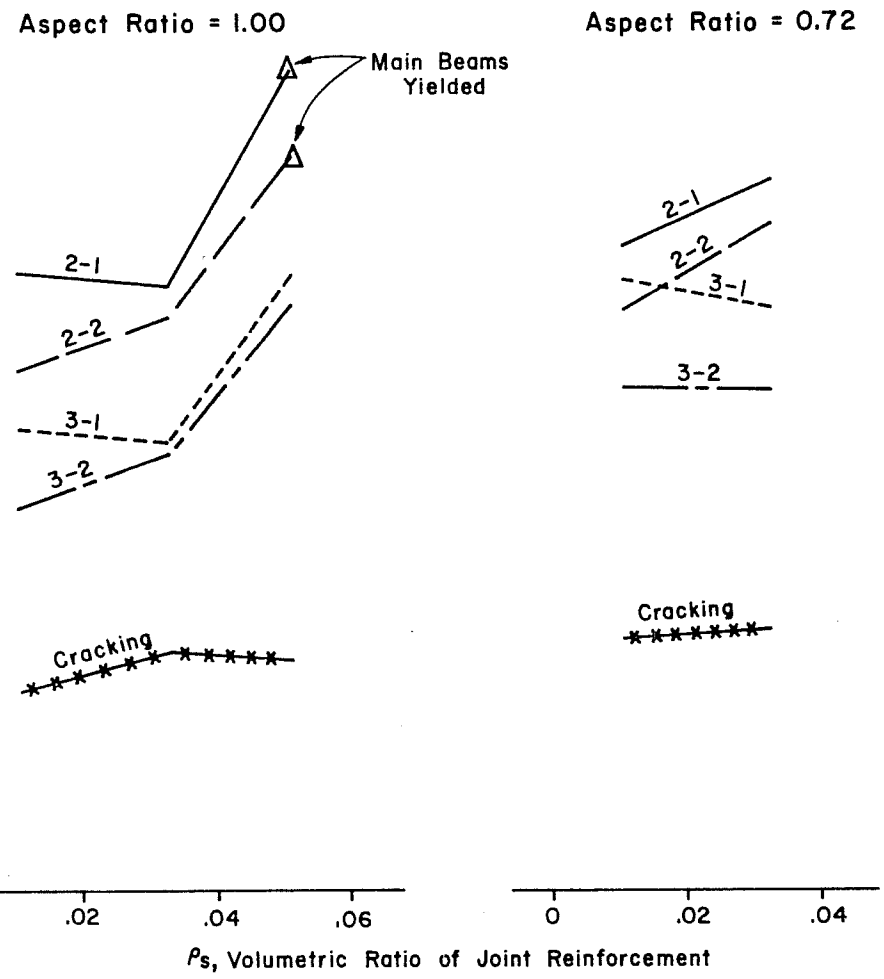

Fig. 4.17 Effect of joint hoop reinforcement on joint shear strength

of the joint hoop reinforcement as assumed in current ACI-ASCE Committee 352 design philosophy.[9]

4.6 Effect of Lateral Beams

Six specimens are available to evaluate the effects of lateral beams. Each of these specimens will be designated by a ratio indicating the percentage of joint area covered by the lateral beam. The joint area is defined as the total depth of the column times the total depth of the beam. The ratio of the cross-sectional area of the lateral beam to the entire joint area is designated a masking ratio (M) and varies from zero to 70 percent. Table 4.6 lists the specimens and geometric variables. Four specimens (II, IV, VIII, and X) have joint aspect ratios of 1.00 with masking ratios (M) of 0, 37 percent located eccentric to the centerline of the column, 37 percent located concentric to the centerline of the column, and 69 percent located concentric to the centerline of the column, respectively. Two specimens with aspect ratios of 0.72 (IV and XI) have masking ratios (M) of 0 and 38 percent. The lateral beam is concentric with the column centerline for Specimen XI.

Lateral beams exist on both sides of the joint and are not loaded either flexurally or axially. However, each lateral beam was symmetrically reinforced with the same percentage of flexural reinforcement based upon the gross cross-sectional area of the lateral beam.

Conceptually, the lateral beams can be visualized as a mechanism providing lateral confining forces to the joint. The lateral confinement or contribution to joint strength is idealized in the same form as shown in Fig. 4.7, where it was noted that as the width of the column increases the resistance to lateral deformations in the joint core is increased. One could think of the lateral resistance as being represented by an effectively wider column in only the joint region.

TABLE 4.6 SPECIMENS WITH DIFFERENT JOINT MASKING RATIOS

Specimen No.	Joint Dimensions: Depth of column h_c, in.	Joint Dimensions: Depth of main beam h_b, in.	Joint Aspect Ratio h_c/h_b	Lateral Beam Dimensions: Width w_L, in.	Lateral Beam Dimensions: Depth h_L, in.	Masking Ratio (M) $\frac{w_L h_L}{h_c h_b}$	Remarks
II	18	18	1.00	0	0	0.00	
X	18	18	1.00	8	15	0.37	Lateral beam eccentric with column ℄
IX	18	18	1.00	8	15	0.37	Lateral beam concentric with column ℄
VIII	18	18	1.00	15	15	0.69	Lateral beam concentric with column ℄
IV	13	18	0.72	0	0	0.00	
XI	13	18	0.72	6	15	0.38	Lateral beam concentric with column ℄

Shear stress-strain curves for Cycle 2 are presented in Fig. 4.18 showing the influence of lateral beams on joint strength. Relative to specimens that did not have lateral beams, Specimens II and IV, the presence of a lateral beam does influence the shear strength. It is important to note that even a lateral beam covering only 37 percent of the area, Specimen IX, improved the joint shear strength. The curve plotted for Specimen X is even more significant because the lateral beam masks 37 percent of the area and is shifted completely to one side of the joint. Figure 4.18 shows that even this displaced lateral beam improves shear strength; however, not as much as if the lateral beam were centered on the joint.

Comparisons plotted in Fig. 4.18(a) show a gradual increase in joint shear strength as the effective width of the lateral beam increases. Figure 4.18(b) also shows that the shear strength increases as the beam size increases, but the rate at which the strength increases when the aspect ratio is 0.72 is much less than the rate shown for joints with aspect ratios of 1.00. This fact is a good indication that the column width is just as influential in improving joint shear strength as is the existence of a lateral beam.

Load reversal shear strengths have been plotted in Fig. 4.19 with respect to the masking ratio (M) of the lateral beam. The values for Cycle 2-1 clearly indicate that the lateral beams improved the joint shear strength. Note that in Cycle 2-1 there is a gradual increase in the shear strength with increase in masking ratio. Specimen VIII, with masking ratio (M) of 0.69, had only a slightly greater joint shear strength than the specimen having a masking ratio of 0.37. However, when the masking ratio was 0.69, the main beams were capable of reaching yield moment, whereas with a smaller lateral beam the joint failed before the main beam flexural reinforcement yielded.

Following Cycle 2-1, the shear strength deteriorated with each additional load reversal, except for the specimen having the

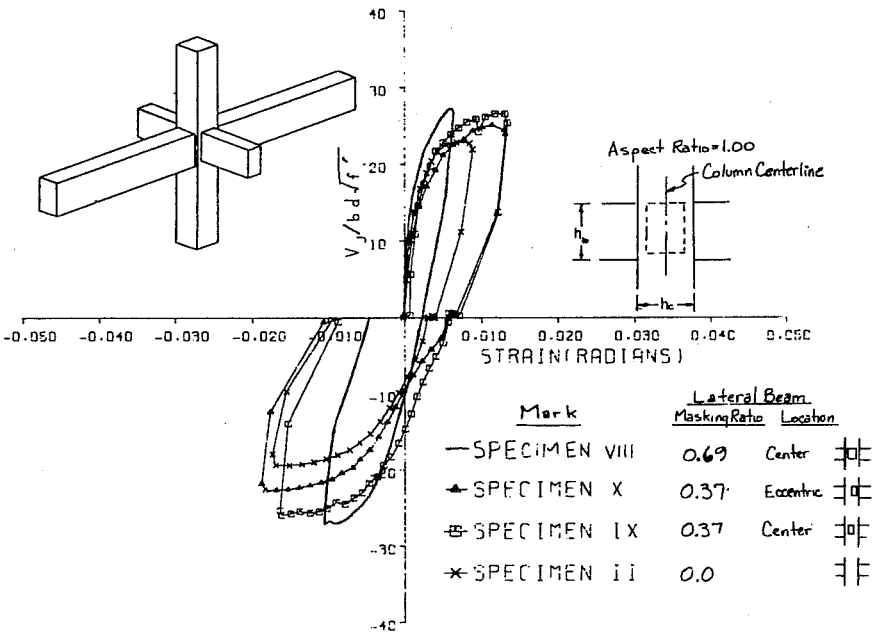

(a)

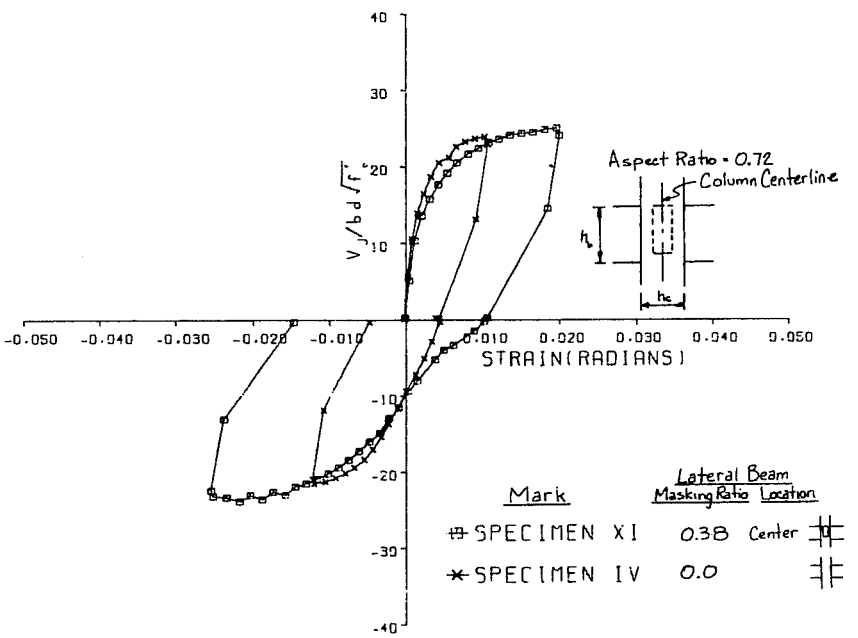

(b)

Fig. 4.18 Shear strength comparisons with size of lateral beam as the variable

largest lateral beam (Specimen VIII, M = 0.69). As indicated in Fig. 4.19, this specimen was capable of maintaining the integrity of the joint region so that yield moments could form in the main beams for one and one-half inelastic cycles.

During the load reversal tests, Specimen X, with the lateral beam displaced with respect to the centerline of the column, was definitely not as effective as the lateral beam whose centroid was coincident with the centerline of the column. As indicated in Fig. 4.19, however, the behavior of the specimen with the shifted lateral beam was consistently better than one with no beam.

As stated earlier, the joint shear strength is specifically related to the width of the lateral beam in these tests because the total depth of each lateral beam was a constant. From Fig. 4.19, there appears to be a reasonably linear relationship between joint shear strength and lateral beam size. This conclusion would generally apply for both aspect ratios investigated. Since the specimen with masking ratio of 0.69 performed in a desirable fashion for one and one-half large deformation cycles, it is likely there is a smaller masking ratio, between 0.38 and 0.69, that would allow the formation of yield moment in the beams and fail in joint shear simultaneously.

The cracking shear strength showed little change with variation in percentage of column reinforcement (Fig. 4.3), joint aspect ratio (Fig. 4.8), and joint hoop reinforcement (Fig. 4.17). In each case the geometry of the specimen was varied rather than applied force, such as column load. Since the lateral beams were unloaded both flexurally and axially, values of the cracking shear strength plotted in Fig. 4.19 suggest that the width of the column carrying the shear is larger than the column dimensions. For Specimen VIII with a masking ratio (M) of 0.69, the increase in cracking shear strength can be attributed to an increase in the shear area, since no forces were applied to the lateral beam.

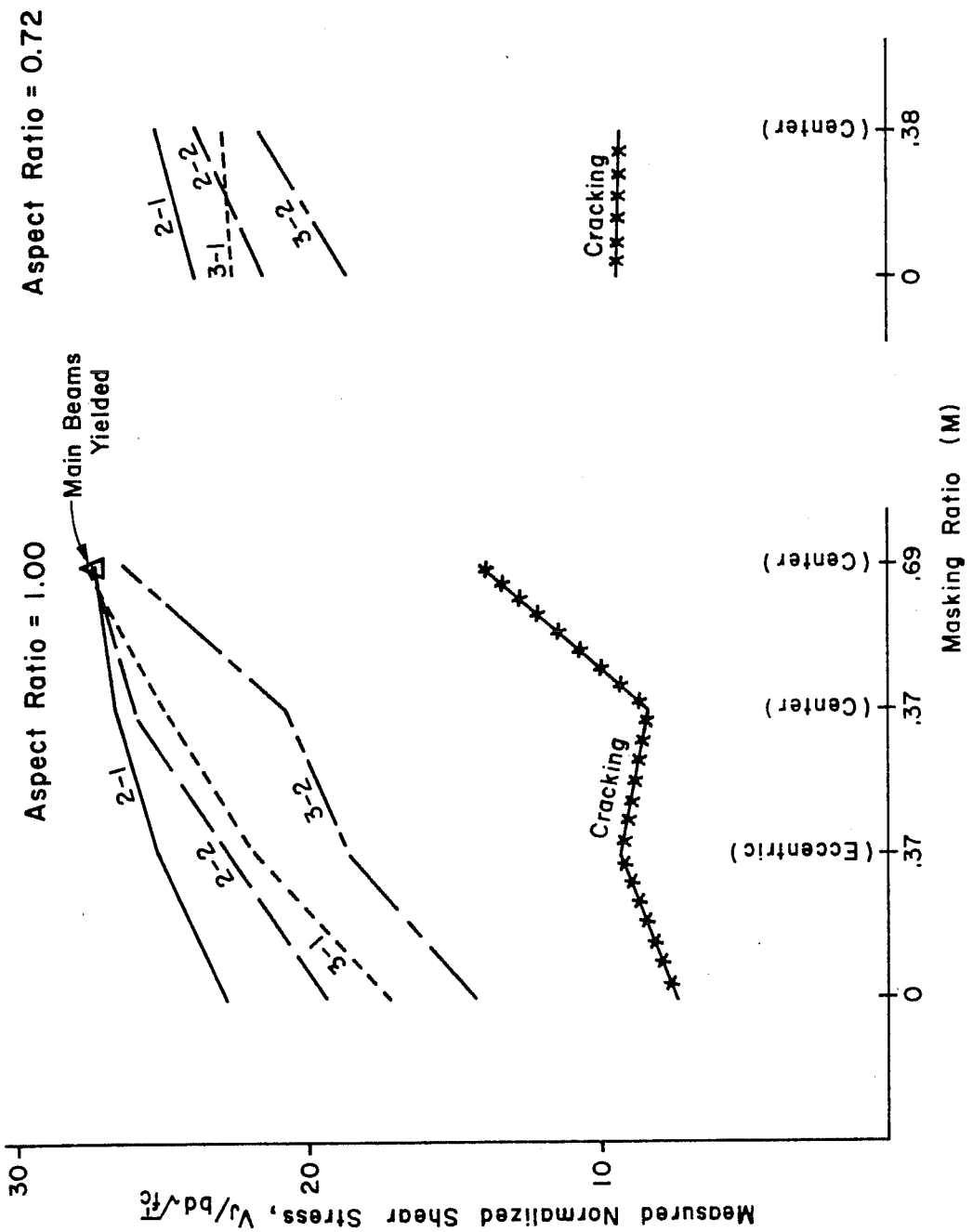

Fig. 4.19 Effect of size and location of lateral beam on joint shear strength

In none of the tests were the lateral beams loaded. Under loadings in two directions it is likely that the results observed here could be altered.

4.7 Effect of Concrete Strength

The final variable to be discussed in this chapter is the effect of concrete compressive strength on the joint shear strength. Two specimens, Specimens II and III, will be considered because of their nearly identical construction. The two specimens are not identical with regard to column longitudinal reinforcement, but they represent a realistic variation in concrete compressive strength. Specimen III had a greater percentage of column reinforcement than Specimen II (6.67 percent versus 4.32 percent). In Section 4.2, it was concluded that column reinforcement had a very nominal effect on joint shear strength because Specimens II and III had essentially the same normalized joint shear strength.

These two specimens will be compared using curves of applied joint shear versus shear strain because all other parameters are identical, except the magnitude of the column reinforcing steel and the concrete compressive strength. Curves representing the joint shear in Cycle 2 are shown in Fig. 4.20. The two curves indicate a significant difference in the joint shear strength as the concrete compressive strength changed. Specimen II, the stronger of the two specimens, had a concrete strength of 6060 psi, whereas Specimen III had a concrete strength of only 3860 psi.

Although the concrete strength of Specimen II was 50 percent more than that of Specimen III, the shear strength of II did not increase in the same proportion. Figures 4.20 and 4.21 point out that the shear strength of the joint is dependent upon the concrete strength and that joint shear strength degradation exists regardless of concrete compressive strength.

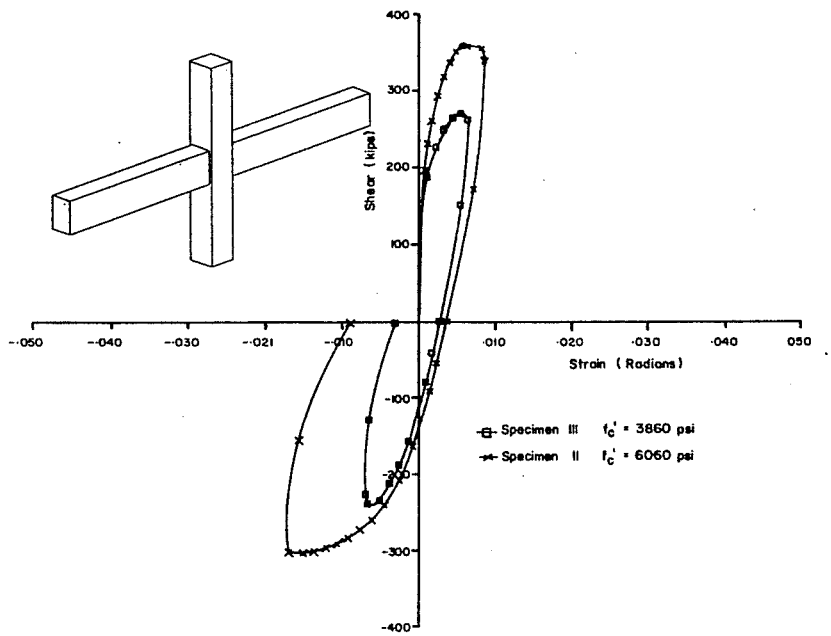

Fig. 4.20 Shear strength comparisons with concrete strength as the variable

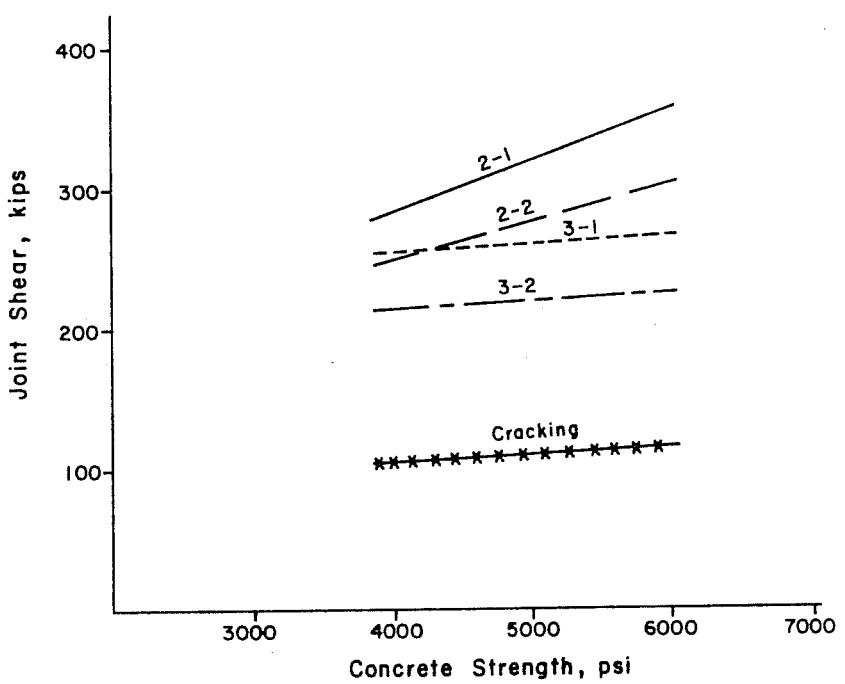

Fig. 4.21 Effect of concrete strength on joint shear strength

4.8 Effect of Reversal and Repeated Load

After the monotonic shear strength was measured in each specimen, Cycle 2-1, the applied loads were reversed to measure the shear strength in the opposite direction. A second cycle, in which large shear deformations were applied to the joint, was used to measure the repeated load capabilities of these specimens.

The measured maximum normalized shear stresses for each half cycle of loading are plotted in Fig. 4.22. The abscissa of Fig. 4.22 is the absolute value of the total deflection experienced by the main beam. Since there are two beams, each experiencing the same general deflection history, the average deflection of both beams is used.

In three tests the joint had sufficient strength to cause yielding moments in the main beams. The three specimens (VI, VIII, and XII) represent tests in which the maximum value of a particular parameter was considered. Those specimens that had a joint strong enough to cause yielding of the main beam are indicated with the symbol "Y" adjacent to the data point. Only one of the 14 specimens, Specimen VIII, developed yield in the main beam during both Cycle 2 and 3. The strength of the other specimens generally showed a decrease as the total deflection increased. The joint performance was better when the deformation normal to the applied shear stress was efficiently confined.

There is a broad band of shear strengths plotted in Fig. 4.22. Those specimens which did not perform well, near the bottom of the range, were in general capable of carrying shear stresses of $15\sqrt{f'_c}$ through an imposed total deflection near 20 times the deflection at yield in the main beam. Regardless of geometry or confinement, all specimens sustained deflections greater than $10\Delta_y$ without the shear stress being less than $15\sqrt{f'_c}$.

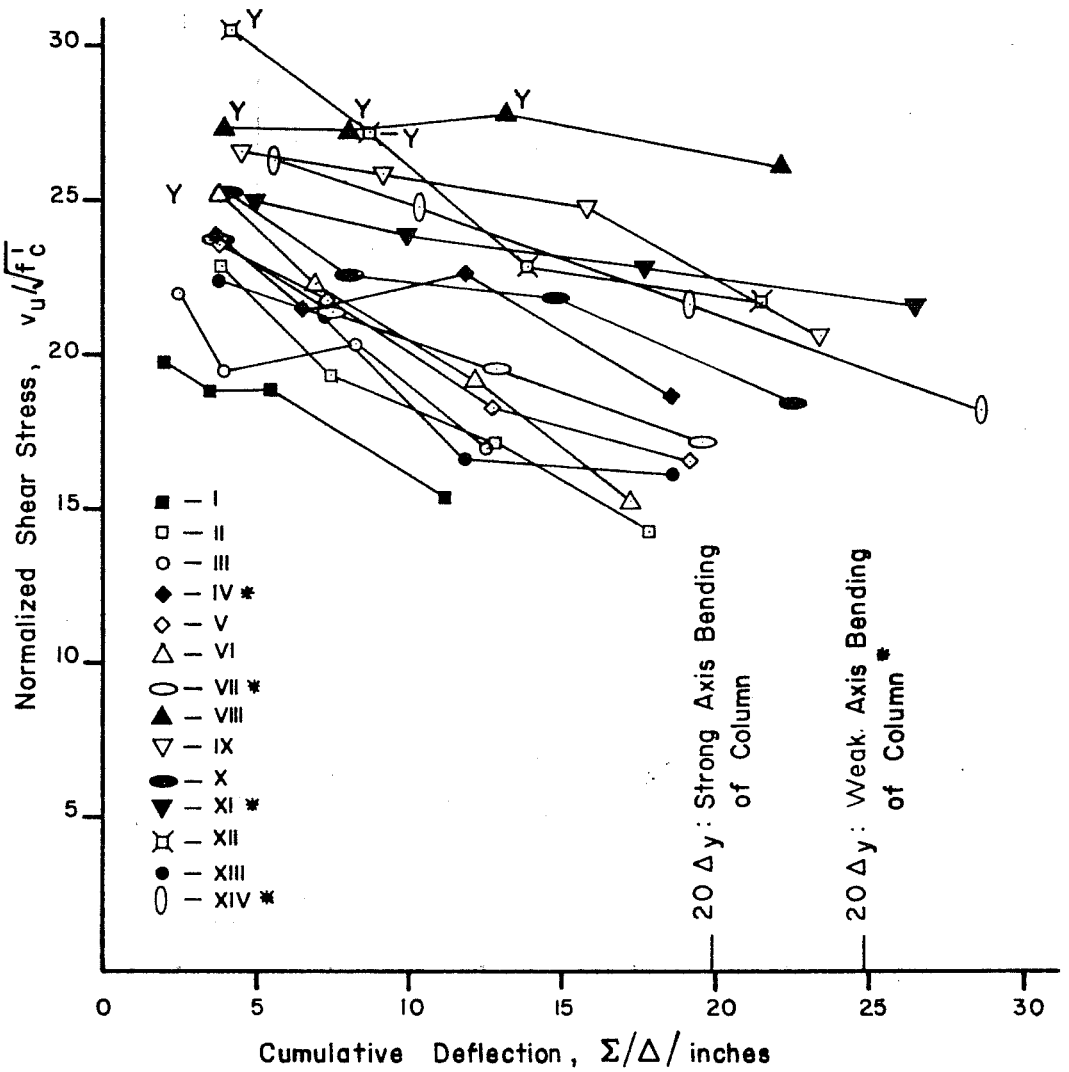

Fig. 4.22 Effect of load reversal on joint strength

It should be remembered that only one specimen, Specimen XII, was designed to have ductility and allow the main beams to yield. All the other specimens were designed to fail in the joint before the main beams yielded and were not required to maintain the joint strength for ductility. These tests represent substantially better behavior than anticipated using the recommended procedure of ACI-ASCE 352.[2,9]

CHAPTER 5

THE CALCULATION OF JOINT SHEAR STRENGTH

5.1 General

The design of the test specimens followed the current state-of-the-art procedure[9] for proportioning a joint subjected to large shearing forces in a reinforced concrete building. The design procedure assumes that the beam-column joint behaves as a reinforced concrete beam having web shear (stirrup) reinforcement. The total shear is separated into a portion which is carried by the concrete alone and the remainder of the total shear is assigned to and carried by the web reinforcement. This additive law for shear design has worked successfully for designing reinforced concrete beams.

Application of the additive approach to beam-column design is subject to question in light of the fact that the shear strength of the concrete was obtained from test data on the shear strength of axially loaded beams.[9] An important assumption made in the beam approach to shear design is that once the concrete cracks in tension, the concrete has little ability to pick up additional shear through friction or aggregate interlock because of the separation at the shear crack. Therefore, the capacity of the concrete in shear is limited to the cracking strength of the concrete.

Using observed test results it will be shown that in a beam-column joint the concrete has a post-cracking load-carrying capacity and that the joint shear strength follows a behavior other than that predicted by the additive law used for reinforced concrete beams.

Using the additive shear strength law with the recommended equations for the concrete and steel contributions,[9] ratios of

ultimate joint shear strength (v_u) to the parameter $\sqrt{f'_c}$ were calculated. The factor $\sqrt{f'_c}$ was used to normalize all the data with respect to concrete strength. The ultimate joint shear strengths (v_u) calculated using measured material properties and the effective joint area in shear (bd) are shown in Column 4 of Table 5.1. Major changes in shear strength were anticipated when the column load changed (Specimens V, VI, and VII, Column 1), when the lateral beam had an area of at least 56 percent of the exposed joint area (Specimen VIII), and when the amount of included hoop reinforcement in the joint was increased (Specimens XII, XIII, and XIV).

Also listed in Table 5.1, Column 5, is the mode of failure expected for each specimen under monotonic loading to failure. Note that only one specimen (XII) was expected to have a joint strength great enough to cause the formation of yield moments in the main beams. All other specimens were specifically underdesigned to fail in joint shear before the main beams reached yielding.

Measured strength results for cracking and each half-cycle of loading are also recorded in Table 5.1, Columns 6 through 10. Again, the data are normalized with the factor $\sqrt{f'_c}$. Test data found in Column 7 represent the maximum shear stress carried by the joint in a test simulating monotonic loading to failure. The monotonic test has been previously referred to as Cycle 2-1 in Chapter 4. Columns 8, 9, and 10 are the maximum shear stresses when the loads on the main beams were sequentially reversed. Of main interest is the magnitude of the shear strength of the joint, Column 7, and the observed mode of failure, Column 11. The mode of failure, Column 11, is that observed during the loading producing the maximum shear stress recorded in Column 7. As anticipated, Specimen XII failed by yielding of the flexural reinforcement in the main beams. Yielding of the main beam flexural reinforcement is a desirable mode of failure. Specimens VI and VIII, specimens which offered confinement to increase the concrete shear strength by the additive law approach,

TABLE 5.1 NORMALIZED SHEAR STRENGTH

Specimen	f'_c	bd	ACI-ASCE 352		Measured Results						
			$v_u/\sqrt{f'_c}$	Failure Mode	$v_{cr}/\sqrt{f'_c}$	$v_{j21}/\sqrt{f'_c}$	$v_{j22}/\sqrt{f'_c}$	$v_{j31}/\sqrt{f'_c}$	$v_{j32}/\sqrt{f'_c}$	Failure Mode	v_{j32}/v_{j21}
(1)	(2)	(3)	(4)	(5)	(6)	(7)	(8)	(9)	(10)	(11)	(12)
I	3800	201	13.69	Shear	7.32	19.75	18.84	18.85	15.36	Joint	0.78
II	6060	201	12.92	Shear	7.41	22.91	19.35	17.15	14.25	Joint	0.62
III	3860	201	13.65	Shear	8.25	22.01	19.46	20.34	17.06	Joint	0.78
IV	5230	189	13.40	Shear	9.40	23.93	21.52	22.68	18.66	Joint	0.78
V	5200	201	9.10	Shear	3.35	23.66	21.75	18.28	16.63	Joint	0.69
VI	5330	201	15.38	Shear	10.84	25.18	22.31	19.15	15.33	Beam Yielding	0.61
VII	5400	189	15.32	Shear	12.96	23.75	21.76	19.59	17.25	Joint	0.73
VIII	4800	201	17.19	Shear	14.18	27.27	27.34	27.79	26.21	Beam Yielding	0.96
IX	4500	201	13.49	Shear	8.23	26.59	25.90	24.92	20.69	Joint	0.78
X	4290	201	13.48	Shear	9.46	25.16	22.61	21.88	18.53	Joint	0.72
XI	3720	189	13.84	Shear	9.28	25.05	23.85	22.90	21.69	Joint	0.87
XII	5100	201	25.30	Yielding	8.57	30.46	27.28	22.85	21.81	Beam Yielding	0.72
XIII	5990	201	18.97	Shear	8.97	22.42	21.34	16.65	16.26	Joint	0.73
XIV	4810	189	20.78	Shear	9.73	26.37	24.78	21.67	18.16	Joint	0.69

$$v_{u_{ACI\ 352}} = v_c + v_s = 3.58\gamma\sqrt{f'_c(1 + 0.002N_u/A_g)} + A_s f_y/bs \qquad \text{[Eqs. (1-4), (1-5), (1-6)]}$$

also were able to yield the main beam flexural reinforcement. Although not reflected in Table 5.1, the maximum shear stresses in Column 7 of all of the other specimens were much closer to formation of yield stress in the main beams than had been originally anticipated.

Trends distinctive of the test results reported in Table 5.1 can be subdivided into three major categories of structural behavior.

Cracking Strength. The magnitude of the column load which was varied for Specimens II, IV, V, VI, and VII was the most influential parameter affecting joint cracking (see Fig. 4.12). Theoretical analysis assuming homogeneous elastic materials would result in this same conclusion (Mohr Circle Analysis). Specimen VIII with large lateral beams also showed a significant improvement in shear cracking strength. This is tentatively attributed to the shear crack also propagating through the unloaded lateral beam.

Static Strength. No one parameter could be established as an effective and efficient means of increasing the shear strength of the beam-column joint. Joint hoop reinforcement did increase the joint strength, but only when it represented about 5 percent of the volume of the joint core. The concrete in the core appeared to be a major source of joint shear strength. The range in concrete strengths of 3800 to 6000 psi did not produce a linear increase in the joint strength. For specimens of different geometry or column loading, but with approximately the same concrete strength, the shear strength of the joint was generally not significantly influenced. An exception is the one cited above for joint hoop reinforcement.

Repeated Load Strength. With the exception of Specimen VIII, all specimens, including the one with a large number of joint hoops (XII), had deteriorating joint strengths with cyclic loading as seen in Fig. 4.22.

The distinctive trends cited above can be used to develop an appropriate approach to predicting the strength of the beam-column joint in shear. Figure 5.1 shows a comparison of the shear strengths predicted by the additive law[9] and those measured in Cycle 2-1, a strength test. Measured results indicate that no matter what is done to the specimen geometrically, internally, or externally, the shear strength remains about the same. Column reinforcement and column orientation did not significantly influence the strength. The only specimens in which the main beam flexural steel yields (VI, VIII, and XII) represent cases where confinement in the form of column load, lateral beams, or joint hoops had maximum values in the test program. This may indicate that a threshold amount of confinement is important before shear strength is improved. An additive design approach, assuming beam action, is not fully compatible with these measured results. The additive approach may overemphasize the joint hoop contribution when applied to beam-column joint design. Finally, cracking of the concrete is not the end of its contribution to the shear-carrying capacity of the joint. It appears feasible that the concrete can carry a substantial shear by friction or other means after cracking has occurred.

5.2 Hypothesis of Strength

There are several possible approaches to predicting the shear strength of the beam-column joint. These theories or combinations of theories would ideally explain the observed behavior and predict strength. Approaches considering confinement, maximum shear stress, shear friction, or empirical relationships will be discussed. In considering any of the possible explanations of behavior, the strength should not be dependent upon elastic constants.

Confinement Approach. When idealizing the beam-column joint as a plane stress or plane strain problem, an increase in one of the applied compressive stresses or one of the compressive principal stresses without changing the other applied or principal stresses

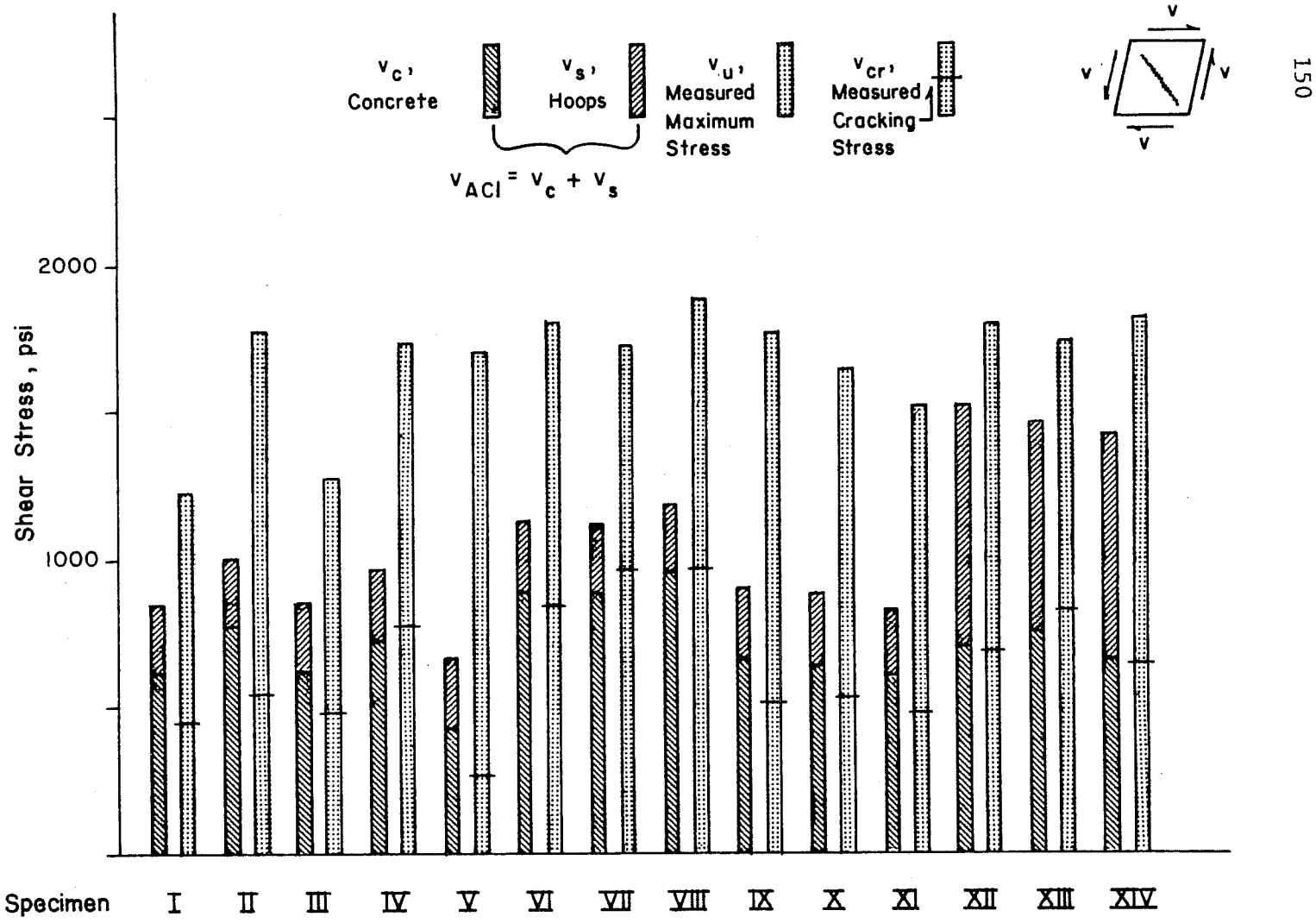

Fig. 5.1 Expected and measured shear stresses on beam-column joints

should be effective in confining the joint. If the joint is idealized in a plane stress state, varying the magnitude of the compressive column load, which would change one of the applied stresses, could alter the confinement on the joint. Recalling the test data, the shear strength was particularly unaffected by the magnitude of the column load.

The plane strain conditions, i.e., $\epsilon_z = 0$, were not satisfied as evidenced by visual observations from these tests as well as comments relative to lateral expansion (bulging) of the joint by other investigators. Third dimension deformations, ϵ_z, were always visible which suggested that restraining this type of deformation might prove useful to joint behavior. To a certain extent, joint hoops and lateral beams did confine the third dimension deformations and improved joint strength.

Compressive confinement in the two-dimensional sense should be discussed in terms of a Mohr-Coulomb theory. However, a Mohr-Coulomb theory, when applied to the test results, produces an inconsistency with the observed behavior.

States of stress within a homogeneous uncracked body are actually neither plane stress nor plane strain. The lateral stresses (σ_z) are probably greater than the plane stress condition of $\sigma_z = 0$, but are not as great as the hydrostatic triaxial ($\sigma_x = \sigma_y$ or $\sigma_y = \sigma_z$) state of stress.

The more realistic stress case in the beam-column joint is one of a true triaxial stress state where $\sigma_x \neq \sigma_y \neq \sigma_z$. Multi-axis failure theories, namely the octahedral shear stress theory, have been used successfully to predict failure for homogeneous metallic materials.[32] The octahedral shear stress theory is used almost exclusively for failure prediction in metallic materials[32] and has been tried on concrete with varying success.[33,34,35,36,37,38,39,40] Soils have also been triaxially tested and compared with the

octahedral shear stress theory.[41] Nevertheless, the major problem with most of the data using the octahedral shear stress theory is that the data have been collected on specimens tested in such a fashion that the results reduce to a biaxial stress state. This is true of Kupfer's[39] tests, but interestingly he has shown a plot of octahedral shear stress versus octahedral shear strain derived from measurements made in all three principal directions. His failure envelope curve of octahedral shear stress versus strain is definitely principal stress or confinement dependent. As the compressive confinement increased, the shear strength and ductility were found to increase.

The use of the octahedral shear stress theory has some definite possibilities as long as the material behaves as a homogeneous uncracked solid whose load-carrying mechanism, although nonlinear, does not change after attaining a particular stress condition. Indeed, it is well-known that cracking, in terms of microcracking, exists at earlier stages of loading than when the first crack is visible. Several studies[42,43] have suggested that cracking initiates failure and that when cracks form, the principal tensile strains are known values. The specific tensile strains are again very dependent upon the state of stress and in particular the magnitude of the compressive confinement stress. Recalling the test data, when the beam-column joint was loaded, load reversed and then reloaded, for example in Cycle 3, cracks existed due to the previous load history, but the existence of cracks did not keep the joint from accepting load.

With due respect for the power of the octahedral shear stress theory adapted to a confinement approach, the test data collected really are not accordant with any of the theories that consider confining compressive stresses as influencing strength. This means, perhaps, that there is no "effective stress" that substantially improves the shear strength of the beam-column joint.

Maximum shear stress approach. In soil mechanics work, if a soil is tested in the undrained condition, making the total stress the variable, the shear strength of the soil is independent of the confining stresses, i.e., shear strength is a constant.

Figure 5.2 is a bar graph of the data tabulated in Table 5.1. Invariably, each specimen shows some degradation of strength with reversal of load. Disregarding degradation and concentrating specifically on the shear strength measured in the strength test, Cycle 2-1, the strength of the joint is, within reason, a constant (concrete has a maximum shear capacity) and is relatively insensitive to the confinement technique (column load, joint hoops, lateral beams) that should have resulted in an increase in the joint shear strength by multi-axis stress theories of failure. Recalling Fig. 5.1, the ultimate shear stress was definitely influenced by the magnitude of concrete strength as seen by a comparison of Specimens I, II, and III. The other measured strengths are about constant and nearly at the level required to cause yielding of the beam flexural reinforcement, as occurred in Specimens VI, VIII, and XII.

Repeated load strengths were shown in Fig. 5.2. When lateral beams covered about 70 percent of the joint area, Specimen VIII, repeated yielding of the main beams was possible with little degradation of strength. In effect, it seems that the lateral beams increase the effective joint shear area allowing the joint of Specimen VIII to deteriorate at a slower rate and consequently show very desirable repeated load characteristics.

The strong indication from the data in Fig. 5.2 is that the joint shear strength depends upon the quality of the concrete and the size of the shear area at the connection.

Specimen XII was successful in allowing the beam flexural reinforcement to yield. However, if confining with joint hoops

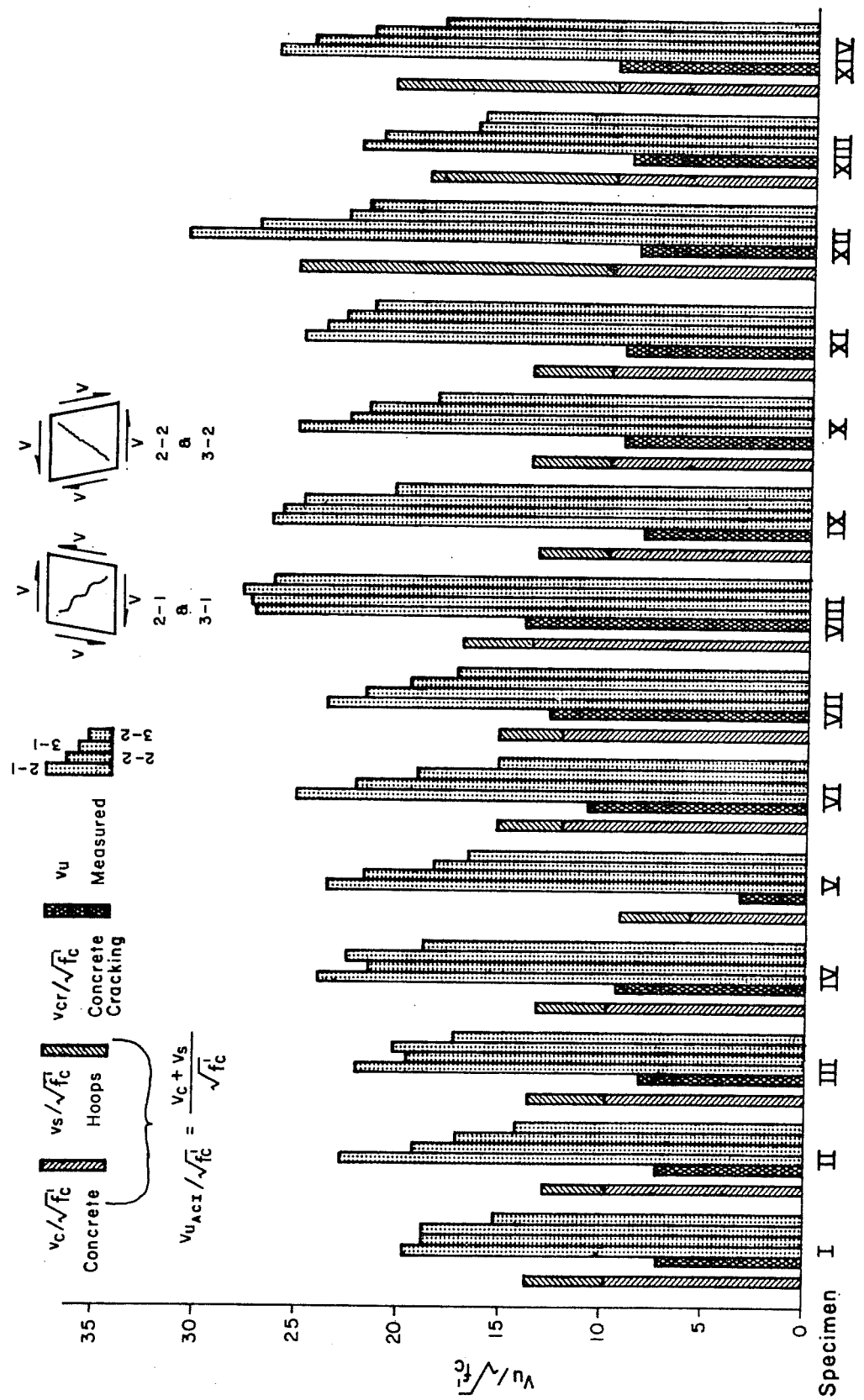

Fig. 5.2 Normalized maximum shear stress for each load direction

improved the shear strength under monotonic loading, that advantage was lost in subsequent load reversals. Confining the joint concrete is not completely unpromising, but it appears that the type of joint hoops investigated here should not be relied upon for their beneficial confining effects to the joint shear strength under load reversals. Beam-column joints appear to be capable of carrying a consistent maximum shear stress which is dependent on the concrete strength and not on other geometric variables.

Shear friction approach. Classical approaches to shear behavior usually make the assumption that the concrete force components parallel to a potential shear crack are present only while the concrete is uncracked. Normally, when shear cracking occurs in beams the cracks tend to separate and forces can be carried only by interlocking of the aggregate as the shear crack widens. More recent studies[44,45] have demonstrated that the aggregate interlock mechanism for beams can carry a significant shear load.

In beam-column connections, the force components parallel to the shear crack are not solely dependent on the cracking strength of the concrete. Components parallel to the shear crack can increase due to friction caused by aggregate interlock as long as there is no significant separation or widening of the shear crack. To transfer force along a crack by friction it is necessary to provide some external restraint to crack separation. Tension forces developed in reinforcing bars crossing the crack, or external compressive forces with a component perpendicular to the crack can keep the crack from separating, allowing the shearing forces to be carried by friction.

In the beam-column joint, normal forces can be developed by the existing joint hoop reinforcement in a fashion similar to the shear friction approach as it is applied to corbel and beam seat design.[46] Additional normal force components are possible to develop in the zones of compression resulting from internal

equilibrium in the beam and column. These zones of compression exist in opposite corners of the interior beam-column joint during a particular loading direction. An idealization of the external force system and the two types of forces along an inclined crack are shown in Figs. 5.3(a) and (b), respectively. It is true that if a compressive force such as C_c shown in Fig. 5.3(b) exists, concrete cracking which is a result of tension should not be present. Of course, this is contrary to the visual observations made of joint cracking in Chapter 3. Unfortunately, no crack width measurements were made on the specimens, but from logs kept of visual observations for each test the crack widths were definitely wider in the center of the diagonal shear cracks than they were closer to the end or corners of the beam-column joint.

Suppose V_{jf} is the shear force parallel to an existing inclined crack that is activated by the normal forces from the reinforcement and the concrete compression zones, both of which interact with the aggregate to cause it to interlock. V_{jf} is the sum of the contributions made by the reinforcement and compression zones. The magnitude and exact distribution of each component to the shear force is unknown.

$$V_{jf} = \eta T_s \tan \chi + \lambda C_c \tan \chi$$

where η and λ are constants

T_s = tensile force in the reinforcing bars

C_c = compression force in the concrete

$\tan \chi$ = equivalent coefficient of friction

If $T_s = A_s f_s = 0$, i.e., no hoops in the joint, this frictional hypothesis helps explain measured joint shear strengths considerably greater than the measured tensile cracking strength of concrete.

Many other investigators[12,13,19,20,21] have made the observation that joint hoops away from the center of the joint are not as

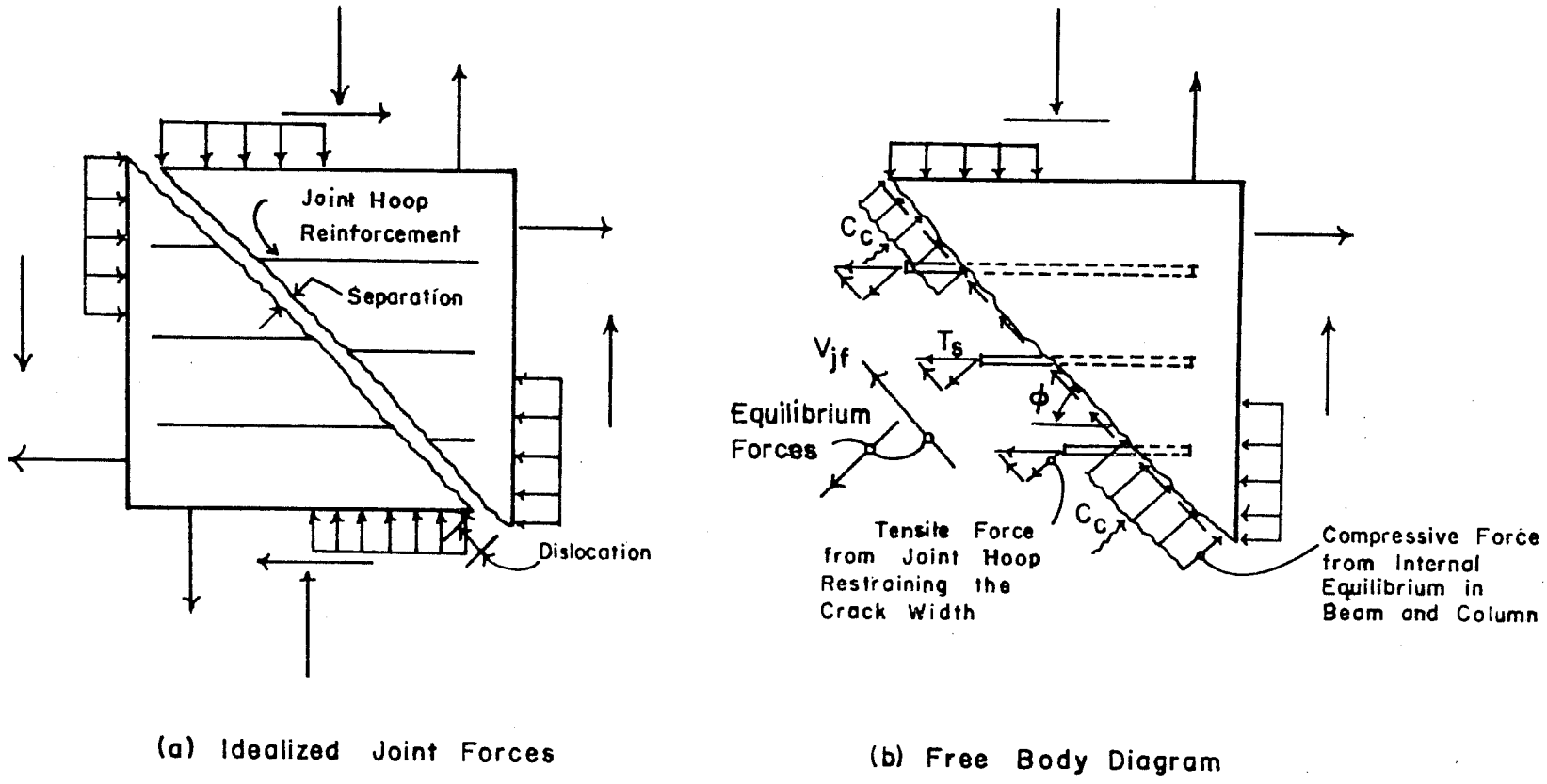

Fig. 5.3 Forces acting on an inclined joint crack

effective as those in the center. Since the compression zones restraining the crack width are concentrated in the corners of the joint, away from the center, only those hoops closest to the center have an opportunity to work as tying elements for shear friction. This approach appears consistent with observed structural behavior.

The equilibrium model for the shear friction approach to shear strength of the beam-column joint is far from a perfect one. Emphasis is placed on the presence of joint hoops as well as the column load possibly contributing to changing the shear strength. Although not a perfect model, it is one which can explain the behavior of the joint. Each of the main beams developed about the same magnitude of compressive force at the face of the column, i.e., almost equal in all specimens to the yield force in the tension reinforcing bars. Therefore, the zones of compression along the shear crack, which are a function of the beam compression force, may have caused the maximum shear stress in monotonic loading to remain about constant. Regardless of the confinement conditions, as long as the shear area is relatively constant and the main beams can develop a compressive force, i.e., the tension bars can be anchored, shear strength could feasibly remain constant.

Empirical approach. Each of the preceding discussions has contributed to an explanation of the shear behavior of a beam-column joint. However, none of the theories provides a solution to the joint shear problem. Parts of each approach can conveniently be used in an empirical approach to joint shear strength.

Six variables were included in the test program: the concrete cylinder strength, f'_c; the percentage of column reinforcement, ρ_g; the volumetric percentage of reinforcement in the joint, ρ_s; the nominal stress on the column, P/A_g; the aspect ratio of the joint, h_{column}/h_{beam}; and the ratio of the width of the lateral beam to the depth of the column, $w_{lateral}/h_{column}$. The yield strength of the

beam flexural reinforcement, column longitudinal reinforcement, and joint hoops remained constant. The lateral beams were all a constant percentage (83 percent) of the depth of the main beam, which was also constant for all specimens. Another geometric parameter used to further define the joint aspect ratio was the ratio of the column width to the beam width, b_c/b_b.

(a) Statistical analysis. Empirical equations with the joint shear strength as the dependent variable were obtained by using a multiple linear regression analysis on the results of the fourteen experimental tests. The statistical approach used to obtain an empirical equation was the method of least squares for estimating the coefficients of the independent variables.

A computer program capable of doing a stepwise multiple regression analysis is available as one of the UCLA Biomedical Series statistical programs.[47] This program, BMD02R, on its first step through the statistical analysis selects the variable considered to be the most significant in determining the dependent variable. At the end of the first step, a regression equation containing only one variable is written along with the correlation parameters indicating how well this equation, with one variable, fits the data. In the next step, the next most significant variable is selected for the regression equation, and new regression coefficients are calculated along with new correlation parameters. Consideration of the second independent variable generally improves the fit of the empirical equation. With each additional step one more variable can either be added or removed from the regression equation as the computer program attempts to better the fit of the regression equation. Variables selected for use in the regression equation are picked by searching the unused independent variables and choosing that variable with the greatest variance ratio when compared to the variance of the dependent variable, known as the F test. Variance is the square of the standard deviation. The stepwise regression procedure is continued until all the independent variables are used

or the improvement in fit of the equation by the introduction of another variable is insignificant. The stepwise regression variables are introduced into the equation regardless of their correlation with the dependent variable. An analysis of the variable correlation with the dependent variable will be discussed after specific empirical equations have been obtained.

(b) Empirical equation forms. Two general forms of a regression equation were considered in the empirical approach to strength prediction. Independent variables were considered to be either linear functions of the linear or nonlinear independent variables or multiplicative combinations of the independent variables. Hence, results will be presented in two forms, either in linear or exponential equation form.

Empirical regression equations both in linear and exponential form providing the best predictions of measured maximum shear stress in Cycle 2-1 (v_{j21}), a representation of the monotonic strength, follow.

A linear equation, following the same general format as the current[9] shear strength equation for the beam-column joint, was obtained by considering the following free independent variables: (a) f'_c or $\sqrt{f'_c}$ or $\sqrt[3]{f'_c}$ or $\sqrt[3]{f'^2_c}$, (b) ρ_g, (c) ρ_s, (d) P/A_g, (e) b_c/b_b, (f) h_c/h_b, and (g) M, the masking ratio of the lateral beams. The concrete strength (f'_c) and nominal column compressive stress (P/A_g) are in psi units and all variables were zero or greater. The empirical linear equation derived by selecting all variables that continuously improve the prediction equation resulted in the following two forms. The correlation coefficient (r) of both forms is about 0.89, indicating that the r^2 of these equations accounts for about 79 percent of the variation in the joint shear strength. If r is ± 1.0, the regression equation is in perfect agreement with the data. If $r = 0$, there is no correlation between the regression equation and the data.

$$v_{j21} = -57.5 + 27.7\sqrt{f'_c} + 9853\rho_s + 503M + 3487\rho_g + 0.034P/A_g + 511b_c/b_b \quad (5\text{-}1)$$

$$v_{j21} = -1029 + 171\sqrt[3]{f'_c} + 9807\rho_s + 501M + 3476\rho_g + 0.034P/Ag + 506b_c/b_b \quad (5\text{-}2)$$

The variables written from left to right appear in the order they were selected to be included into the empirical equation.

It is also possible to force the BMDO2R computer program to have a zero y-intercept value. Regression equations with zero intercepts and about the same level of prediction accuracy are shown below.

$$v_{j21} = 27.6\sqrt{f'_c} + 9857\rho_s + 503M + 3481\rho_g + 0.034P/A_g + 557b_c/b_b \quad (5\text{-}3)$$

$$v_{j21} = 163\sqrt[3]{f'_c} + 9920\rho_s + 498M + 3336\rho_g + 0.024P/A_g + 1253b_c/b_b \quad (5\text{-}4)$$

When performing the exponential regression analysis, all the variables considered for the above linear analysis were transformed to their equivalent natural logarithmic form. The analysis proceeds identically, except that the coefficients of the independent variables are now powers to which the independent variables are raised. Again, considering all variables which continuously improved the prediction equation resulted in the following exponential equation:

$$v_{j21} = 12.041(f'_c)^{0.628}\ (1+\rho_s)^{5.346}\ (1+w_L/h_c)^{0.334}\ (\rho_g)^{0.123}\ (P/A_g)^{-0.004}\ (b_c/b_b)^{-0.602} \quad (5\text{-}5)$$

The exponential regression was found to be slightly more precise in predicting the shear strength of the joint. Equation (5-5) has a

correlation coefficient (r) of 0.91, which indicates it accounts for about 83 percent of the variation in joint shear strength.

(c) Correlation of the variables. As mentioned above, the statistically derived equations include independent variables that may or may not correlate with the dependent variable. In addition, one of the premises of regression analysis is that all the independent variables are truly independent. Computer program BMD02R can produce a table of correlation factors which the user can use to check the correlation between the dependent and independent variables and cross correlations between independent variables. For analyzing the correlation between dependent and independent variables, it is desirable to have correlation factors that are either +1.0 or -1.0, indicating that the independent variable is perfectly correlated to the dependent variable. Conversely, correlation factors of 0.0 indicate that the particular independent variable does not correlate at all with the dependent variable. A check for independence of the independent variables would proceed on just the opposite scheme described above, i.e., the independent variables should have cross correlation factors close to zero.

In the case where the strength equation is a linear combination of terms, the correlation matrix for the variables considered in the analysis is given in Table 5.2. The first row of that triangular matrix is a comparison of how the independent variables correlate with the measured joint shear strength, the first column of that matrix. Note that any one of the functions of the concrete cylinder strength (f'_c) and the joint hoop reinforcement percentage (ρ_s) have reasonably large correlation factors. However, the lateral beam parameter (M), ρ_g, P/A_g, b_c/b_b, and h_c/h_b have very low correlation factors, making them statistically dubious contributors to the joint shear strength.

A similar correlation matrix for the exponential form of the strength equation is found in Table 5.3. Again, the joint shear

TABLE 5.2 CORRELATION MATRIX FOR EMPIRICAL LINEAR EQUATION

	v_{j21}	f'_c	$(f'_c)^{1/2}$	$(f'_c)^{1/3}$	$(f'_c)^{2/3}$	ρ_s	M	ρ_g	P/A_g	b_c/b_b	h_c/h_b
v_{j21}	1.000	0.609	0.629	0.635	0.622	0.571	0.094	0.144	0.111	0.045	0.029
f'_c		1.000	0.999	0.999	1.000	0.267	-0.373	0.013	0.111	0.064	0.064
$(f'_c)^{1/2}$			1.000	1.000	1.000	0.271	-0.364	0.015	0.111	0.060	0.060
$(f'_c)^{1/3}$				1.000	1.000	0.273	-0.361	0.015	0.111	0.059	0.059
$(f'_c)^{2/3}$					1.000	0.270	-0.367	0.014	0.111	0.061	0.061
ρ_s						1.000	-0.294	-0.001	-0.044	0.027	0.027
M							1.000	0.002	-0.063	0.098	0.098
ρ_g								1.000	-0.011	0.038	-0.008
P/A_g									1.000	-0.249	-0.249
b_c/b_b										1.000	1.000
h_c/h_b											1.000

TABLE 5.3 CORRELATION MATRIX FOR EXPONENTIAL EQUATION

	$\ell n\ v_{j21}$	$\ell n\ f'_c$	$\ell n(1+\rho_s)$	$\ell n(1+w_L/h_c)$	$\ell n\ \rho_g$	$\ell n(P/A_g)$	$\ell n(b_c/b_b)$	$\ell n(h_c/h_b)$
$\ell n\ v_{j21}$	1.000	0.671	0.517	0.088	0.381	0.042	-0.005	-0.005
$\ell n\ f'_c$		1.000	0.277	-0.380	0.168	-0.035	0.057	0.057
$\ell n(1+\rho_s)$			1.000	-0.301	0.050	0.064	0.026	0.026
$\ell n(1+w_L/h_c)$				1.000	0.064	0.074	0.088	0.088
$\ell n\ \rho_g$					1.000	-0.019	-0.031	-0.031
$\ell n(P/A_g)$						1.000	-0.223	-0.223
$\ell n(b_c/b_b)$							1.000	1.000
$\ell n(h_c/h_b)$								1.000

strength correlates better with (f'_c) and ($1 + \rho_s$) than any of the other variables. (See the first row of Table 5.3.)

Based on this output, joint shear strength should be based on two variables, f'_c and ρ_s. Nevertheless, when one considers the test data, the presence of lateral beams did have a measurable effect on strength, whereas column reinforcement had a negligible influence. Consequently, it was decided to take the empirical equations of strength as functions of the concrete strength (f'_c), joint hoop reinforcement (ρ_s), and lateral beams (w_L/h_c or M).

It is desirable to check the cross correlation factors between the independent variables selected for further consideration to make sure the variables are independent. For the variables to be independent, the cross correlation coefficient should be near zero. For the linear form of the strength equation, the correlation between the various functions of f'_c are high, as shown in Table 5.2. However, if only one such function of f'_c is used, the regression equation will remain composed of independent variables. The other cross correlations are not ideally zero, but neither can they be considered highly interdependent. The largest cross correlation factors occur with the parameter M, which is the variable with the least correlation of those variables considered significant in determining the dependent variable, shear strength.

Surveying the cross correlation factors for the exponential equation (see Table 5.3) results in the same conclusions as above. The parameter showing the most interdependence with the other independent variables was again the parameter representing the existence of lateral beams ($1 + w_L/h_c$).

Sifted regression equations can now be written with more legitimacy considering the results found in the correlative matrices of Tables 5.2 and 5.3. The fit of these new equations will not be as good as the previous equations, but the equations have the

advantage of being easier to calculate and include only those parameters which are significant in determining strength.

Only three equations will be presented, two in linear form and one exponential.

Linear Equations

$$v_{j21} = -460 + 28\sqrt{f'_c} + 9670\rho_s + 490M \quad (5\text{-}6)$$

$$v_{j21} = 21.4\sqrt{f'_c} + 9856\rho_s + 430M \quad (5\text{-}7)$$

Exponential Equation

$$v_{j21} = 5.492(f'_c)^{0.660}\ (1 + \rho_s)^{5.371}\ (1 + w_L/h_c)^{0.346} \quad (5\text{-}8)$$

The correlation coefficients (r^2) of all three equations are in the same range accounting for 76 to 78 percent of the variation in the measured shear strengths. Although the lateral beam parameter did not correlate well with the dependent variable (v_{j21}), including it in the regression equation increases the equation's correlation coefficient while continuing to decrease the error in the estimate of the dependent variable. An analysis of variance, as measured by the F-ratio statistic, also showed that the Eqs. (5-6) through (5-8) have confidence limits no smaller than the 97.5 percent level, and in most cases would also satisfy the 99 percent level.

(d) Comparisons of equations. A comparison of the empirical equations and the current design procedure[9] is given in Table 5.4. For convenience, the ratio of the measured shear strength to the calculated shear strength is shown for each specimen for the three empirical relationships derived from these tests (Columns 5, 7, and 9) and the current design equation (Column 3). Table 5.4 clearly shows that the current procedure, Columns 3 and 4, consistently underestimates the shear strength by a considerable margin. Each of the empirical relationships represent a significant improvement in estimating the joint shear strength. Although Eq. (5-7),

TABLE 5.4 COMPARISON OF PREDICTED JOINT SHEAR STRENGTHS

Specimen (1)	Measured Joint Strength (2)	$v^*_{ACI\ 352}$ psi (3)	Test(2)/Calc(3) (4)	v_{j21} psi (Eq 5-6) (5)	Test(2)/Calc(5) (6)	v_{j21} psi (Eq 5-7) (7)	Test(2)/Calc(7) (8)	v_{j21} psi (Eq 5-8) (9)	Test(2)/Calc(9) (10)
I	1200	845	1.42	1365	0.88	1430	0.84	1345	0.89
II	1780	1005	1.77	1820	0.98	1775	1.00	1830	0.97
III	1375	850	1.62	1380	1.00	1440	0.95	1360	1.01
IV	1720	970	1.77	1665	1.03	1655	1.04	1665	1.03
V	1705	655	2.60	1660	1.03	1655	1.03	1655	1.03
VI	1835+	1125	1.63	1685	1.09	1670	1.10	1685	1.09
VII	1735	1125	1.54	1695	1.02	1680	1.03	1700	1.02
VIII	1890+	1190	1.59	1920	0.98	1890	1.00	1940	0.97
IX	1780	905	1.97	1700	1.05	1705	1.04	1710	1.04
X	1650	885	1.86	1655	1.00	1670	0.99	1655	1.00
XI	1520	845	1.80	1535	0.99	1580	0.96	1515	1.00
XII	2175+	1805	1.20	2030	1.07	2040	1.07	2020	1.08
XIII	1735	1470	1.18	2020	0.86	1985	0.87	2045	0.85
XIV	1820	1440	1.26	1795	1.01	1815	1.00	1770	1.03
Average Test/Calc			1.66		1.00		0.99		1.00
Standard Deviation			0.37		0.06		0.07		0.07

*$v_{ACI\ 352} = v_c + v_s = 3.5\beta\gamma\sqrt{f'_c(1 + 0.002N_u/A_g)} + A_s f_y/sb$

+Main beam flexural reinforcement yields.

Column 7, is not quite as good as Eq. (5-6), Column 5, it has the advantage that there is one less term to manipulate in calculating the shear strength. Equation (5-8), the exponential form, gives a slightly more accurate prediction of the shear strength because of a larger correlation coefficient than Eqs. (5-6) or (5-7).

The computational effort, slide rule or hand calculator, with either of the two empirical forms, would not be subject to large roundoff errors because the operations involve terms of the same order of magnitude. From the practical viewpoint, the exponential equation is a better choice except for the odd exponential powers. However, this disadvantage can be overcome by factoring out specific influences and considering them as multiplying constants to a basic joint strength equation. Discussion of possible design simplification will be presented in Section 5.4. Perhaps more importantly, the exponential equation has a greater advantage than the linear form because it presents the strength of the joint as a unit and not one that becomes meaningless if the concrete strength is low. In light of the observations stated by other investigators about joint hoops being less effective as the distance from the center of the joint increases, the exponential relationship, because of its multiplicative nature, gives a better representation of observed joint behavior. Therefore, in subsequent analyses of strength the exponential equation, Eq. (5-8), will be used.

5.3 The Cracking Strength of Concrete in the Beam-Column Joint

Concrete shear cracking, as observed in the fourteen tests reported herein, did not cause any immediate change in joint stiffness as is observed in flexural cracking in a beam. Cracking, in general, did not signal major distress unless the joint was severely cracked. Severe cracking is indicated by numerous parallel diagonal cracks and possibly some crushing of the concrete perpendicular to these diagonal cracks. Cracking of the concrete in the joint is

not an indication of joint failure. When the joint reaches ultimate in shear, the joint will be extensively fractured.

In the Sugano and Koreishi approach to joint design,[10,16,48] the cracking strength of the concrete (tensile strength) is calculated but not used to assess the concrete contribution to joint shear strength. The Japanese suggest that the concrete shear strength has a larger magnitude than the current ACI-ASCE 352[9] procedure, Eq. (1-4), and that when the concrete contribution to joint strength is exceeded, the stiffness of the joint changes.

Cracking shear stresses were measured in this investigation and are tabulated in Column 2 of Table 5.5. Again, a statistical regression analysis was performed on the fourteen test specimens using the cracking strengths as the dependent variable. Both exponential and linear equations were attempted and good prediction equations resulted. Each equation was able to account for at least 80 percent of the variation in cracking strength. The best equation of fit was again an exponential form which is shown below.

$$v_{cr} = 0.0124(f'_c)^{0.85} (P/A_g)^{0.485} (1 + w_L/h_c)^{0.57} \qquad (5\text{-}9)$$

Particular note is made of the variables included in Eq. (5-9). Other than concrete compressive strength, the magnitude of the column stress was the single most significant influencing factor. The confinement that results when the column load is increased follows directly from the theoretical analysis made with Mohr's circle on a homogeneous solid. The current ACI equation, Eq. (1-4), for concrete shear strength, Column 9 of Table 5.5, is reasonable for predicting the concrete shear cracking stress, especially when the column load magnitude is large or lateral beams are present.

Cracking is also influenced by unloaded lateral beams. The lateral beam effectively increases the joint shear area. An increase

TABLE 5.5 CRACKING SHEAR STRENGTHS

Specimen	$v_{cr_{meas}}$	v^*_{cr} Exponential	Test/Calc	v^{**}_{cr} Linear	Test/Calc	v^{***}_{cr}	Test/Calc	$v_{cr_{ACI}}$	Test/Calc
(1)	(2)	(3)	(4)	(5)	(6)	(7)	(8)	(9)	(10)
I	451	475	0.95	557	0.81	542	0.83	608	0.74
II	577	709	0.81	609	0.95	643	0.90	770	0.75
III	513	481	1.07	558	0.92	545	0.94	612	0.84
IV	680	628	1.08	596	1.14	613	1.11	718	0.95
V	242	235	1.03	269	0.90	243	1.00	420	0.58
VI	791	816	0.97	846	0.93	778	1.02	887	0.89
VII	952	822	1.16	842	1.13	778	1.22	890	1.07
VIII	982	817	1.20	799	1.23	764	1.29	955	1.03
IX	552	686	0.80	701	0.79	684	0.81	669	0.83
X	620	652	0.95	689	0.90	665	0.93	647	0.96
XI	566	579	0.98	676	0.84	633	0.89	608	0.93
XII	610	615	0.99	593	1.03	607	1.00	709	0.86
XIII	692	696	0.99	601	1.15	635	1.09	760	0.91
XIV	674	585	1.15	587	1.15	595	1.13	688	0.98
Average			1.010		0.990		1.012		0.88
Standard Deviation			0.117		0.146		0.142		0.128

$v^*_{cr} = 0.0124 f'^{0.85}_c (P/A_g)^{0.485}(1 + w_L/h_c)^{0.57}$ $R^2 = 0.88$

$v^{**}_{cr} = 3.04\sqrt{f'_c} + 0.242\ P/A_g + 318\ \text{Mask}$ $R^2 \cong 0.80$

$v^{***}_{cr} = f'^{0.36}_c (P/A_g)^{0.40}(1 + w_L/h_c)^{0.43}$ $R^2 \simeq 0.85$

$v_{cr_{ACI}} = 3.5\beta\gamma\sqrt{f'_c(1 + 0.002N_u/A_g)}$ $\beta = 1.0$ unless lateral beams are present. $\gamma = 1.4$.

in cracking shear can be expected as the lateral beam gets larger; however, the increase is not as dramatic as the change in column load. The multiplying factor from the statistical analysis for lateral beams which meet the minimum dimension requirements of ACI-ASCE 352[9] (covering 56 percent of the joint area) is 1.38. ACI-ASCE 352 currently recommends an increase in the concrete shear strength of 1.4 if lateral beams of minimum dimensions are present at the beam-column joint.

Two other empirical equations are also shown in Table 5.5, Columns 5 and 7. Equations have zero intercepts are given because of the slightly more convenient form. The ratios of test to calculated cracking shear strengths using each of the three empirically derived equations are tabulated in Columns 4, 6, and 8. All have average test/calculated ratios very close to 1.0. Equations represented by Columns 5 and 7 do, however, have a larger scatter as measured by standard deviation. The concrete shear strengths of the beam-column joint using ACI 318-71,[2] Eq. (1-4), are tabulated in Column 9. Test-to-calculated ratios are shown in Column 10, with an average ratio of 0.88. This means that Eq. (1-4) tended to overestimate the cracking strength of the concrete. The consequence of overestimating the concrete contribution to joint shear strength using the recommended[9] design approach is inconsequential, since that approach tended to underestimate the shear strength of the entire joint. This fact was brought out previously in Section 5.3.

In summary, the cracking shear strength of the concrete in the beam-column joint is not an important factor in determining joint strength. Cracking does occur, but does not signify failure or distress unless the joint is severely fractured.

5.4 Application of Strength Equation to Other Test Results

Numerous other research investigations have been conducted on beam-column joint assemblies.[12,13,14,19,20,21,22,49,50,51] Several different types of beam-column joint specimens have been tested. Because of a large volume of information necessary to describe the specimen geometry, reinforcements, and type of failure, a table has been included in Appendix D. For each test, the maximum shear stress on the joint in an "early" stage of loading was calculated and is shown in Column 25 of Table D1. The empirical shear strength equation, Eq. (5-8), was then used to predict the stress at which the joint should fail by shear. Predicted shear strengths using Eq. (5-8) are shown in Column 27 of Table D1. A comparison of these two columns shows that the maximum joint shear stress at an "early" stage in the loading history was always less than the predicted shear strength, indicating that there were no joint shear failures determining the maximum load in the "early" stages of loading. Other information pertinent to the previous statement may be found in Appendix D. The data in Appendix D will have more utility when analyzing applications of Eq. (5-8), or its simplification, to predict the cyclic joint shear strength.

5.5 Simplifications to the Shear Strength Equation for Design

Strength Equation. The empirical equation as derived from the fourteen tests conducted in this investigation [Eq. (5-8)] is satisfactory for research purposes. However, a structural engineer proportioning a beam-column joint for particular design loads would find Eq. (5-8) awkward to apply and simplifications are needed.

Two parameters representing transverse joint hoop reinforcement and lateral beams were separated from Eq. (5-8) and plotted using ρ_s and w_L/h_c as the independent variables and $(1 + \rho_s)^{5.371}$ and $(1 + w_L/h_c)^{0.346}$ as the dependent variables. Figures 5.4(a) and (b)

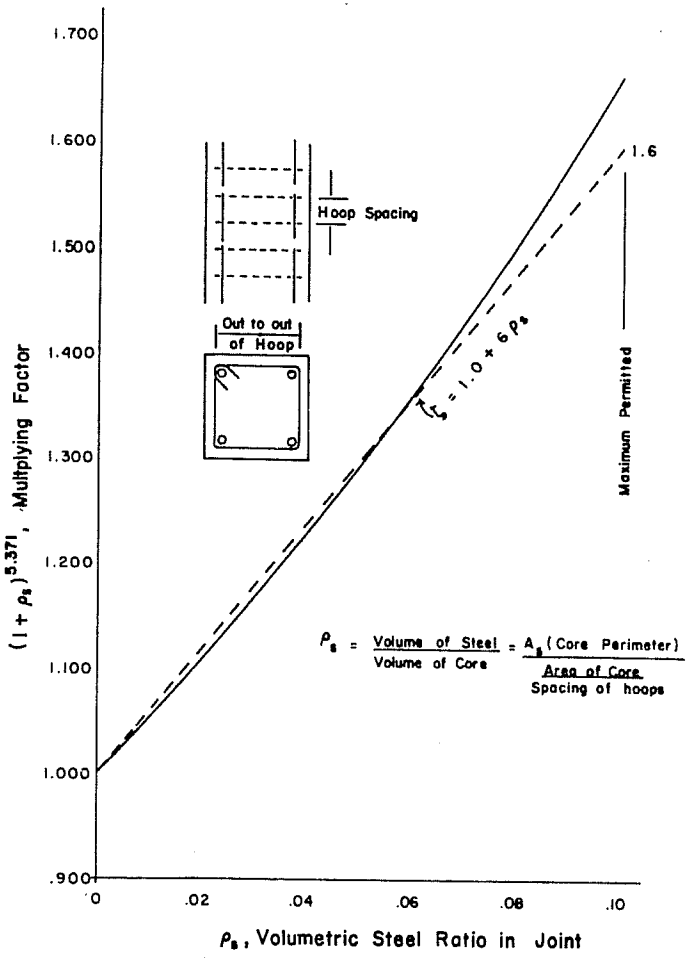

(a) Multiplying factor for joint hoop reinforcement

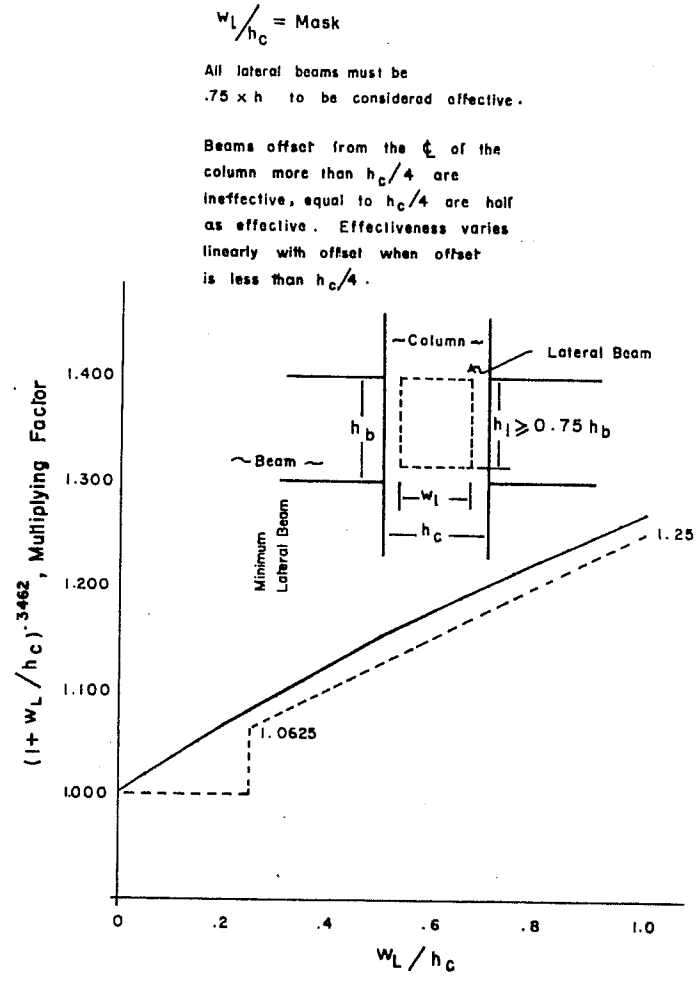

(b) Multiplying factor for lateral beams

Fig. 5.4 Multiplying factors of joint shear strength

are plots of the multiplying factors for joint hoop reinforcement and lateral beams. Note that the multiplying factors of Figs. 5.4(a) and (b) are linear in the range the variables ρ_s and w_L/h_c would likely fall. Convenient round number linear approximations for the exponential form were made and shown in terms of ζ and β, representing joint hoop reinforcement and lateral beams, respectively.

Since the variables of hoop reinforcement and lateral beams can be represented as above, a convenient and much simpler equation for the shear strength of the beam-column joint can be written as follows:

$$v_u = 5.1\beta\zeta(f'_c)^{2/3} \qquad (5\text{-}10)$$

where f'_c = concrete compressive strength, psi

$\beta = 1 + 0.25w_L/h_c$ (influence of lateral beams)

w_L = width of the lateral beam perpendicular to the applied joint shear, in.

h_c = width of the column into which the lateral beam frames, in.

$\zeta = 1 + 6\rho_s \leq 1.6$ (influence of joint hoop reinforcement)

ρ_s = the volumetric percentage of transverse joint hoop reinforcement

$$= \frac{A_h(2b^* + 2h^*)}{s_h b^* h^*}$$

A_h = area of the joint hoop bar (one bar area), $in.^2$

b^* = joint core dimension to outside of hoop, in.

h^* = joint core dimension to outside of hoop, in.

s_h = spacing of joint hoops, in.

Limits are suggested for β and ζ, as indicated in Fig. 5.5, and are discussed below.

Lateral beams at the joint, to be considered effective, should be not less than three-fourths as deep as the beams perpendicular to the lateral beams in question. In addition, lateral beams must be present on both sides of the joint. The width of the

lateral beam in all cases should be greater than $0.25h_c$ if it is to be effective; and, if the centerline of the lateral beam is displaced such that the offset distance between the centerline of the column and centerline of the lateral beam is more than $h_c/4$, the lateral beam should be ignored in calculations. When the offset distance is equal to $h_c/4$, the width of the lateral beam should be taken as one-half the actual beam width. For offset distances less than $h_c/4$, the lateral beam width should vary linearly with offset.

The only limit placed on the factor ζ is that it should not exceed 1.6. Zeta equals 1.6 when $\rho_s = 0.10$, which is a very large volumetric steel ratio. It is quite improbable, although not impossible, that this much steel could be placed in the joint. Other problems such as congestion, clearance, or fabrication would keep the volumetric steel ratio smaller. Typical manageable values of ρ_s are in the 0.03 to 0.04 range.

Table 5.6 is a comparison of the measured joint strengths to the predicted joint strengths using Eq. (5-8) and its simplified form, Eq. (5-10). Note that the test/calculated ratios for Eq. (5-10) are generally greater than 1.0, indicating a slight underestimation of the joint shear strength under monotonic loading conditions.

Comparisons of the proposed strength equation [Eq. (5-10)] to the recommended shear strength equations of ACI-ASCE 352, Eq. (1-4), Eq. (1-5), and Eq. (1-6), have been made in tabular form in Table 5.4. These comparisons are specific applications of the design equations. It is more illustrative to make comparisons in graphical form (Fig. 5.5), where a range of the parameters can be studied.

Most influential in the current design method is the amount of joint hoop reinforcement. Figure 5.5(a) compares the dependence of joint shear strength on joint hoop reinforcement. As seen by the slope of the ACI-ASCE 352 curves [Eq. (1-4) through (1-6)], joint

TABLE 5.6 COMPARISON OF SIMPLIFIED JOINT SHEAR STRENGTH EQUATION WITH MEASURED DATA

Specimen (1)	Measured Joint Strength (2)	v_{j21} psi (Eq 5-8) (3)	Test(2)/Calc(3) (4)	v_{j21} psi (Eq 5-10) (5)	Test(2)/Calc(5) (6)
I	1200	1345	0.89	1325	0.91
II	1780	1830	0.97	1805	0.99
III	1375	1360	1.01	1340	1.03
IV	1720	1665	1.03	1640	1.05
V	1705	1655	1.03	1635	1.04
VI	1835+	1685	1.09	1660	1.11
VII	1735	1700	1.02	1675	1.04
VIII	1890+	1940	0.97	1870	1.01
IX	1780	1710	1.04	1645	1.08
X	1650	1655	1.00	1525x	1.08
XI	1520	1515	1.00	1455	1.04
XII	2175+	2020	1.08	1980	1.10
XIII	1735	2045	0.85	2020	0.86
XIV	1820	1770	1.03	1745	1.04
	Average		1.00		1.03
	Standard Deviation		0.07		0.07

+Main beam flexural reinforcement yielded.

xLateral beam considered half as effective.

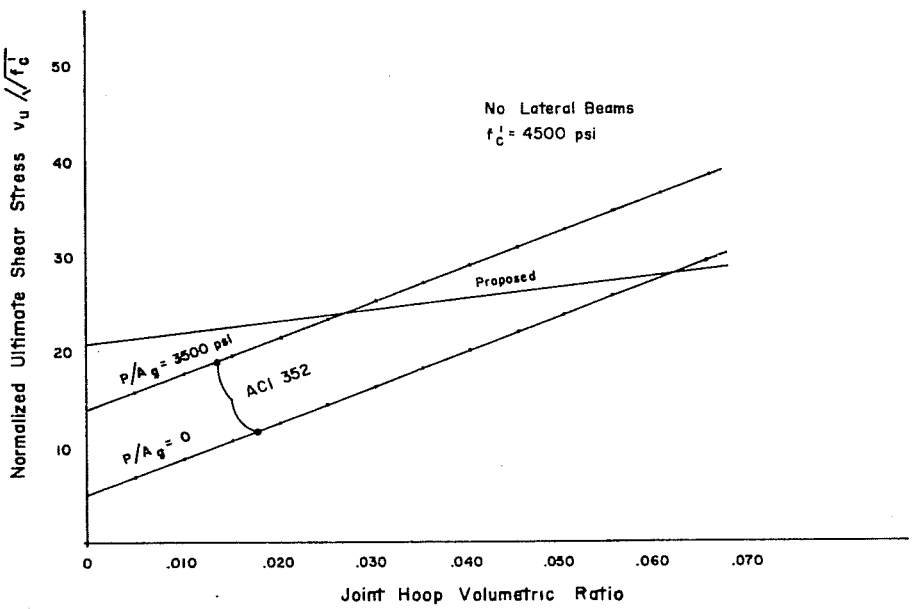

(a) Effect of joint hoop reinforcement

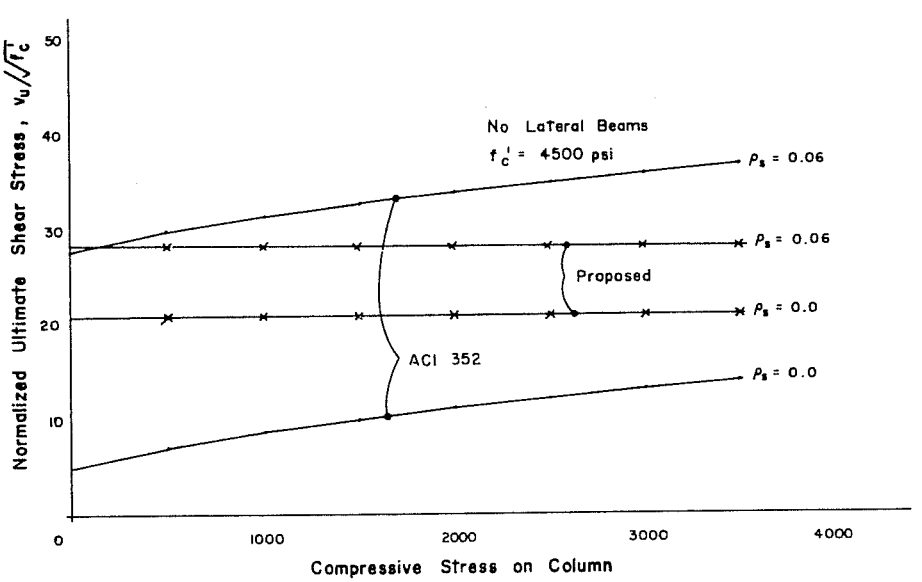

(b) Effect of column load

Fig. 5.5 Comparison of ACI 352 recommendations and proposed joint shear strength equations

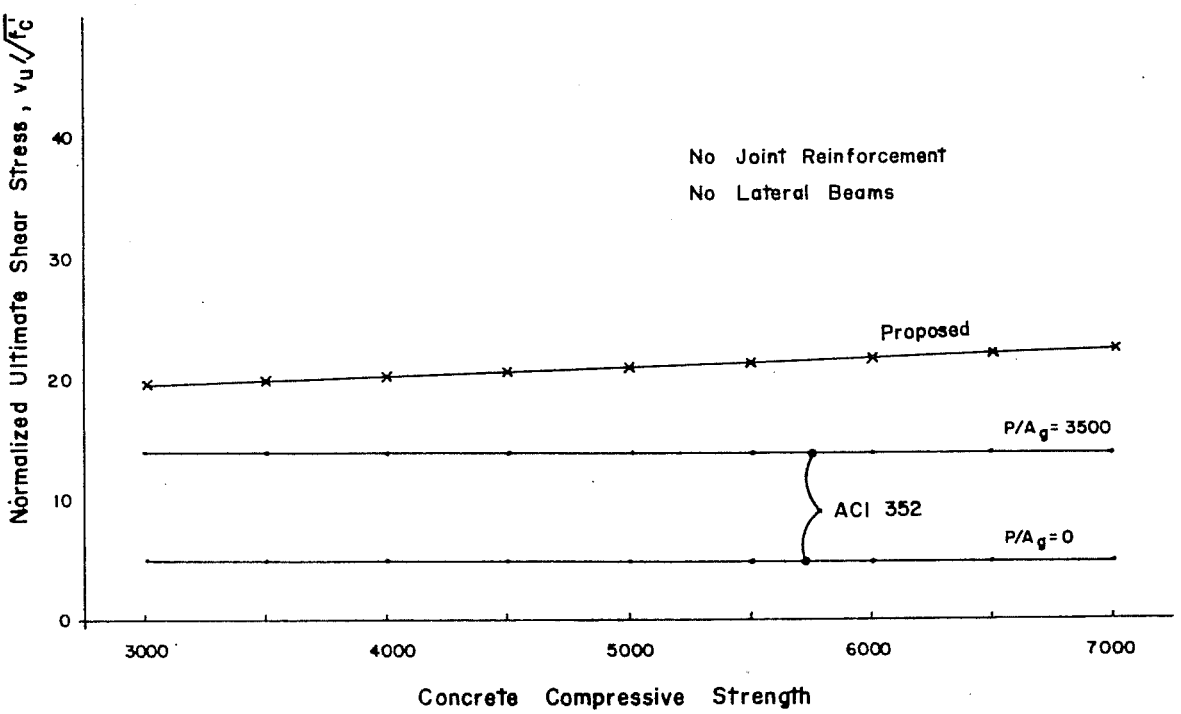

(c) Effect of concrete strength

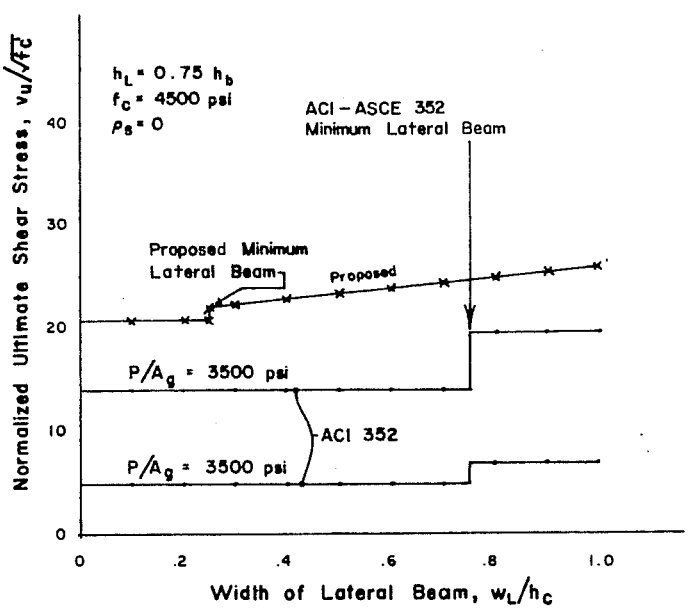

(d) Effect of lateral beams

Fig. 5.5 (Continued)

strength can rapidly increase by including hoops. The proposed strength equation would place less emphasis on hoop reinforcement.

The ultimate shear stress can also be changed by changing the column compressive stress according to ACI-ASCE 352 as seen in both Figs. 5.5(a) and (b). Note in Fig. 5.5(b) that joint strength would be overestimated when the column load and the amount of joint hoop reinforcement are high.

Concrete strength was observed to be an important variable for the test specimens. Figure 5.5(c) shows the variation of shear strength with concrete compressive strength. The relative importance of f'_c is not readily apparent because of the ordinate chosen which normalizes this plot. It is, however, apparent that concrete strength does have more influence in the proposed equation than the ACI-ASCE 352 equations. The curves of Fig. 5.5(c), since they are plotted for conditions of no joint reinforcement and lateral beams, show the concrete contribution to shear strength. ACI-ASCE 352 considerably underestimates the ability of concrete to carry shear.

Lateral beams appear to increase shear strength by primarily increasing the shear area of the joint. Figure 5.5(d) shows the effects of lateral beams on shear strength. Due to an underestimation of concrete contribution in ACI-ASCE 352 recommendations, the proposed equation shows a higher shear strength than the ACI-ASCE 352 curve.

Cyclic Strength Equation. Equation (5-10) predicts the strength under monotonic loading conditions. Previously, in Section 4.8 it was observed that the test specimens were able to experience total deflections of about $20\Delta_y$ without the shear strength falling below $15\sqrt{f'_c}$. It is well-recognized that the shear strength of the concrete will deteriorate with cycling. To account for cycling, an additional factor can be applied to Eq. (5-10). This factor would reduce the shear strength so that the joint design strength would be higher in earlier cycles of loading, but eventually

deteriorate to a cyclic strength level necessary to maintain yielding of the main member through several large deformation cycles.

For the fourteen specimens tested, the ratio of shear strength in the third cycle to peak shear strength (v_{j32}/v_{j21}) is 0.75, with a standard deviation of 0.09 (see Table 5.1, Column 12). Using these data, a cyclic strength level was chosen as 0.6 of the monotonic shear strength. A lower limit on the data shown in Fig. 4.22 indicates that the cyclic strength is about $12\sqrt{f'_c}$. The 0.6 cyclic strength factor was applied to the predicted joint shear strengths of Table D1 to check its applicability. The results for those tests which actually failed in shear due to load cycling are given in Table 5.7. Many of the specimens required four to six complete reversals of load before the maximum joint shear stress dropped below the predicted cyclic strength. The results indicate that the proposed cyclic shear strength factor is a reasonable estimate of the behavior under load reversals. Note that many of the specimens in Table D1 are of the corner type (see description in Appendix D), having bars anchored in the joint. The corner specimen often exhibits anchorage deterioration not present in an interior joint, and is the reason many of the specimens in Table D1 are not included in Table 5.7. It is possible that in the corner specimen a greater reduction in joint strength could be used to account for the anchorage problems.

A proposed design equation for beam-column joint shear strength for either a strength design or a strength and ductility design is as follows:

$$v_u = 5.1\beta\gamma\zeta(f'_c)^{2/3} \qquad (5\text{-}11)$$

where f'_c = compressive strength of concrete, psi

$\beta = 1 + 0.25w_L/h_c$, with $w_L/h_c \geq 0.25$

TABLE 5.7 PREDICTED CYCLIC STRENGTHS FROM OTHER INVESTIGATIONS

Reference and Specimen	Maximum Applied Joint Shear Stress	Predicted Joint Shear Strength (Eq. 5-8)	Predicted Cycle Strength (Eq. 5-11)	Type of Joint (see Appendix D)	Cycles before Measured Shear Stress Less than Eq. 5-11	Ratio of Maximum Deflection in each Cycle/Deflection at First Yielding
Hanson-Conner[12]						
I	931	1265	759	Corner	5	1.8, 2.2, 3.7, 4.4, 5.3
IA	877	1157	694	Corner	3	1.8, 2.6, 4.0
II	880	1308	785	Corner	8+	1.8, 2.3, 4.2, 4.7, 5.4, 6.4, 8.0, 9.6
III	1077	1199	719	Corner	4	1.0, 2.6, 3.6,
V	926	1130	678	Corner	2	1.0, 1.9
Hanson[13]						
1	1330	1925	1155	Interior	5+	2.0, 3.1, 4.5, 5.9, 8.0
2	1353	1417	850	Interior	5+	1.6, 2.2, 2.8, 3.8, 4.5
3	968	1682	1009	Corner	5+	1.8, 2.3, 3.5, 4.3, 5.4
Hanson-Conner[14]						
7	853	1626	976	Corner	4	1.6, 2.4, 4.0, 4.8
8	1162	1696	1018	Interior	4+	1.3, 1.8, 3.4, 5.3
9	1142	1429	858	Interior	5+	1.6, 2.5, 3.4, 5.4, 7.8
10	1432	1918	1151	Interior	6+	1.9, 2.5, 3.0, 3.4, 3.9, 7.9
Park-Thompson[51]						
T3	1400	2119	1271	Interior	2	0.8, 2.8
Higashi-Ohwada[43]						
SD35Aa-5	942	1444	867	Interior	2	1.8, 3.7
SD35Aa-6	1065	1532	919	Interior	2	2.5, 4.6
SD24Aa-4	985	1454	872	Interior	2	2.6
Uzumeri[22]						
SP4	880	1573	944	Corner	5+	1.6, 3.1, 6.3, 11.7
SP8	1005	1531	919	Corner	3	2.4, 3.2, 5.1

γ = 1.0, joint designed for strength only, or
0.6, joint designed for load reversals producing inelastic deformations

$\zeta = 1 + 6\rho_s < 1.6$

For joints designed for load reversals producing inelastic deformations, some minimum transverse steel should be provided to confine the core. Until additional research becomes available, the recommendations of ACI-ASCE Committee 352 should be utilized. It should also be noted that the values of β are based on tests in which the lateral beams were not loaded. Where beams in both directions are overloaded simultaneously, the value of β should be reduced. For biaxial loading on the joint, additional research will be required to define β and to evaluate the applicability of Eq. (5-11) to cases where shear forces are imposed on the joint from beams in both directions.

CHAPTER 6

CONCLUSIONS

6.1 Summary of Test Program

Fourteen interior joints of a frame structure were tested to assess the basic shear strength of the beam-column joint. The joint designs followed the recommendations of ACI-ASCE Committee 352, Joints and Connections in Monolithic Concrete Structures, and ACI 318-71, Building Code Requirements for Reinforced Concrete. The variables investigated were: (1) the magnitude of the column load, (2) the percentage of column reinforcement passing through the joint, (3) the amount of transverse reinforcement in the joint (joint hoops), (4) the shear span or aspect ratio of the joint, (5) intersecting lateral beams normal to the applied forces, and (6) the quality of the concrete.

Each specimen had a 13 in. by 18 in. rectangular column. The column was rotated so bending moments could be applied about either the strong or weak bending axis. By rotating the column the aspect ratio of the joint could be changed. The depth of the main beam was a constant 18 in. for all specimens. The width of the main beam was always 2 in. less than the width of the column into which the beam framed. All reinforcement, beam flexural, beam stirrup, column vertical, column tie, and joint transverse, was ASTM A615 Grade 60. All the deformed reinforcing bars used as main reinforcement in the beam and column were continuous through the joint. Use of continuous main reinforcement eliminated bar anchorage failures as one of the possible modes of failure.

Loads were applied at the ends of both main beams. Main beam loads were applied in opposite directions, causing an overturning moment at the beam-column joint. The column load was concentric with the centroidal axis of the column cross section and the column was restrained from deflecting at the supported ends The support ends were at midheight of the column, an assumed point of inflection. Each specimen was tested by applying loads to the main beam as required to cause both beams to deflect equal amounts in opposite directions. The forces on the joint were reversed by changing the direction of the load on the main beam. Three complete deflection controlled cycles were applied to the main beams of each test specimen.

Deflection increments were applied to determine (1) the cracking shear strength of the concrete in the joint, (2) the shear strength of the beam-column joint under monotonic loading, and (3) the shear strength of the joint under load reversal and cyclic loading.

6.2 Summary of Observed Behavior

Joint Shear Cracking. Cracking shear strength was found to be influenced by the magnitude of the compressive column load and the presence of a lateral beam. The increase in the cracking shear strength as a result of compressive column loads follows directly from a Mohr Circle analysis on a homogeneous elastic body. With lateral beams, the joint shear cracks were observed to propagate through the lateral beam.

The concrete shear strength of the beam-column joint is not represented by joint shear cracking. The joint concrete was observed to have a post-cracking strength. Post-cracking joint shear can be carried by a combination of aggregate interlock (friction) and confinement (joint hoops). The test program clearly showed that the

behavior of the beam-column joint in shear is not the same as the shear behavior of a reinforced concrete beam.

Ultimate Joint Shear Strength. The ultimate joint shear strength was found to be approximately twice the cracking shear strength of the joint. Variables which significantly influenced the ultimate shear strength were as follows. Increases in the percentage of transverse joint hoops increased the shear strength, but the increase was not proportional to the force the hoop could carry. Lateral beams perpendicular to the applied joint shear stress and present on both sides of the joint increased the ultimate shear strength. The shear strength increased with the size of the lateral beam for those beams centered on the column centerline. Lateral beams located eccentric to the column centerline also increased the ultimate joint shear strength, but not as significantly as the centered beams. The strength of the concrete placed in the joint was also a very significant parameter in determining the ultimate joint shear strength. The increase in joint shear strength was, however, again not linearly related to increases in the concrete compressive strength.

Cyclic Shear Strength. The same variables that determined the ultimate joint shear strength were also found to be significant in improving the cyclic shear strength. The joint of the specimen with the largest lateral beam, covering 69 percent of the joint area, best maintained its integrity through cyclic loading. Maximum load through one and one-half cycles of deflection was controlled by flexural yielding of the main beam at the joint rather than by shear failure of the joint. Flexural failures in the members away from the beam-column joint are a desirable mode of failure. Improvement in cyclic behavior was also seen as the percentage of transverse joint hoop reinforcement increased. However, with load reversal and cyclic loading, the concrete was always seen to deteriorate and the

joint hoops used in these tests could not maintain the shear strength of the joint at a level high enough to cause member hinging.

6.3 Design Recommendations

An empirical design equation for the ultimate joint shear strength was obtained by statistically analyzing the monotonic strength of the fourteen experimental tests. The three most significant variables--transverse joint hoop reinforcement, lateral beams, and concrete strength--were considered in a least squares analysis to estimate the regression coefficients. A simplified conservative form of the rigorous regression equation follows. The original regression equation had a confidence limit level of 97 percent.

The shear stresses used in the regression analysis were nominal shear stresses in the joint on a horizontal plane. Nominal shear stresses were computed by dividing the maximum shear forces in the joint by an effective cross-sectional area. The effective cross-sectional area was taken as the width of the column at the joint times the effective depth (to the centroid of the longitudinal reinforcement in the column) in the direction of the shear force considered.

A permissible shear stress carried by an interior beam-column joint with main reinforcing bars in both the beam and column continuous through the joint should not exceed:

$$v_j \leq 5.1 \beta \gamma \zeta (f'_c)^{2/3}$$

where v_j = the nominal shear stress in the joint on a horizontal plane, psi

f'_c = compressive strength of the joint concrete, psi

β = factor reflecting influence of lateral beams

γ = factor reflecting type of loading

ζ = factor reflecting effect of transverse reinforcement

To be considered effective, lateral beams should be not less than three-fourths of the depth of the deepest main beam framing into the joint. Simple adjustments are made for a varying lateral beam width or when the lateral beam is displaced from the column centerline. It should be noted that the confinement provided by the lateral beam may be reduced if beams in both directions are subjected to overloads simultaneously.

From the tests it was apparent that under load reversal and cyclic loading the concrete shear strength deteriorates. The strength equation was made applicable to cyclic loadings by including a factor γ which accounts for the type of loading conditions on the joint. For joints in which the primary design criterion is strength and when no significant inelastic deformations are expected, the factor γ is taken as 1.0. When the primary design criterion is sustained strength under load reversals in the inelastic range, γ should be taken as 0.6. Predicted cyclic strengths using the above equation were compared to cyclic behavior of existing test data where the joint eventually failed due to shear in the beam-column joint.

The only limitation placed on the factor ζ, the factor representing transverse joint hoop reinforcement, is one of practicality. The suggested limit on ζ is that it should not exceed 1.6, which occurs when the volumetric steel ratio is 0.10. Large volumetric steel ratios will probably be accompanied by congestion and/or fabrication difficulties before the suggested limit is reached. For joints designed using $\gamma = 0.6$, some minimum amount of transverse reinforcement may be required to ensure joint integrity. Current minimum requirements for transverse reinforcement to provide confinement as recommended by ACI-ASCE Committee 352 should be used until additional research results become available to clarify this aspect of behavior.

The design equation presented above does not follow the current ACI-ASCE Committee 352 recommendation. Committee 352 recommends an additive equation to account for contributions of the concrete and steel separately. The proposed multiplicative form is suitable for design purposes and, based on the tests conducted in this investigation, gives a better representation of the structural behavior of the beam-column joint than do current design procedures.

A P P E N D I X A

REINFORCING BAR DETAILS

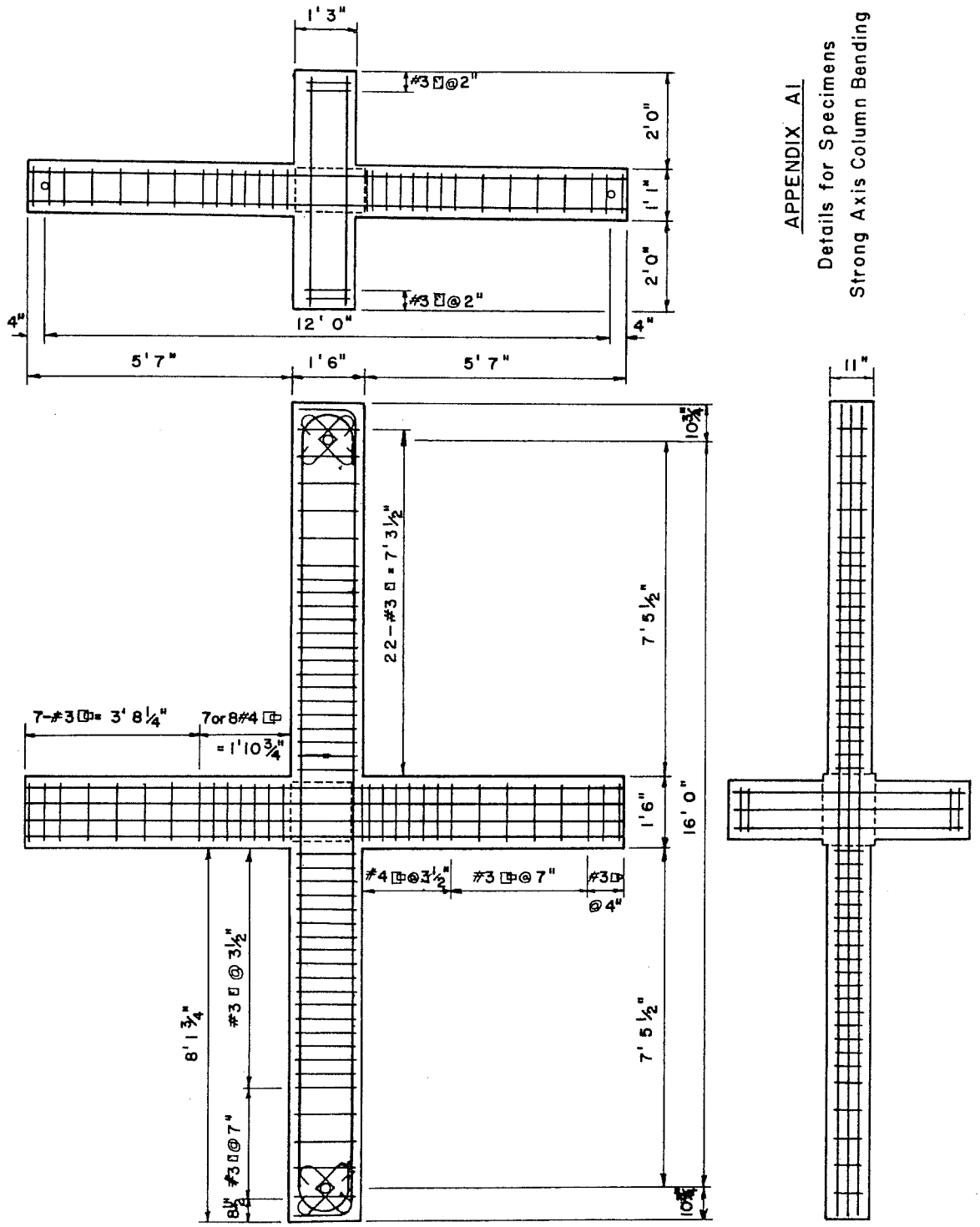

APPENDIX A1

Details for Specimens

Strong Axis Column Bending $P_u > .4P_{bal}$

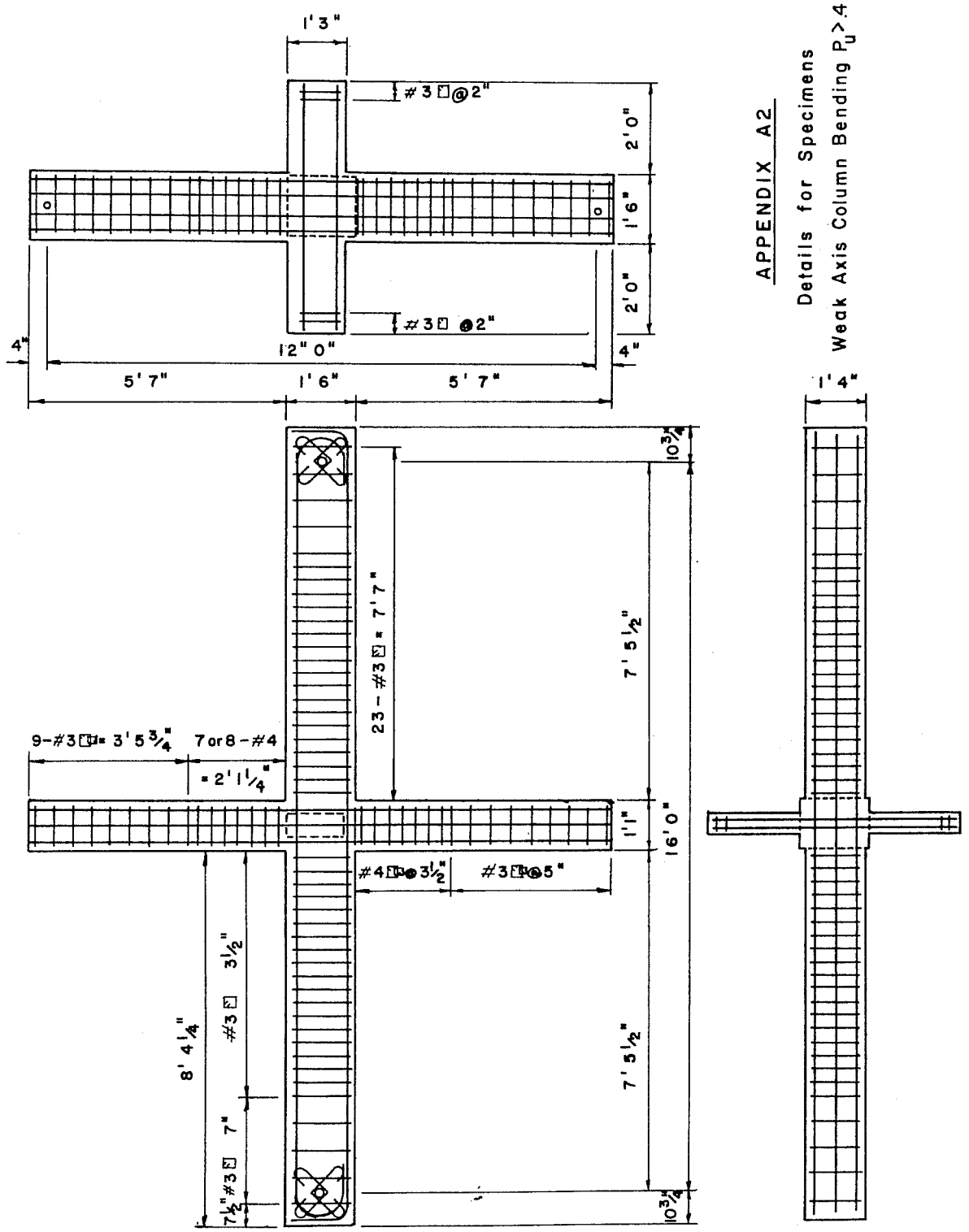

APPENDIX A2

Details for Specimens

Weak Axis Column Bending $P_u > .4P_{bal}$

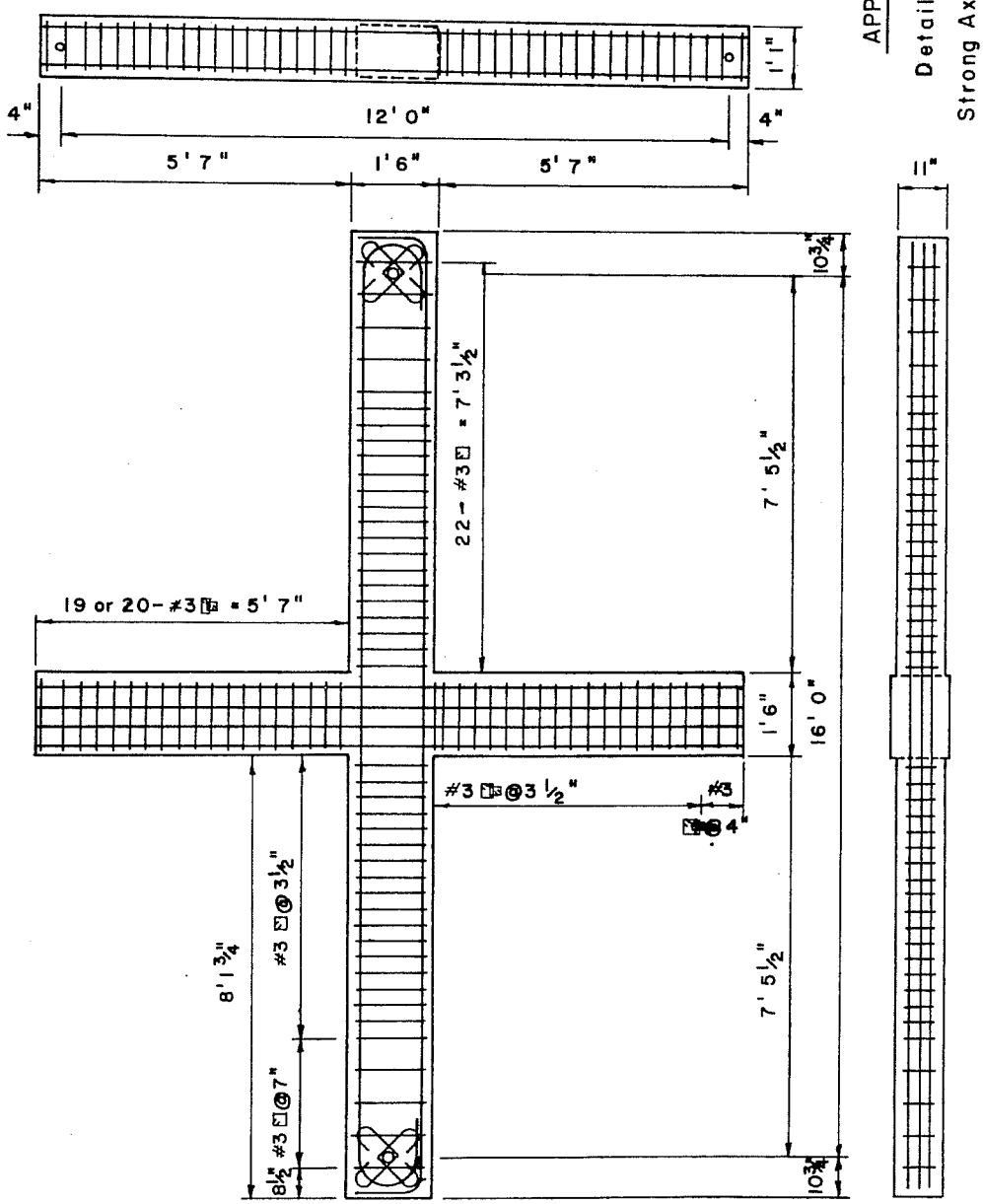

APPENDIX A3

Details for Specimens

Strong Axis Column Bending

$P_u < .4 P_{bal}$

A P P E N D I X B

SPECIMEN FORCE DEFORMATION RELATIONSHIPS

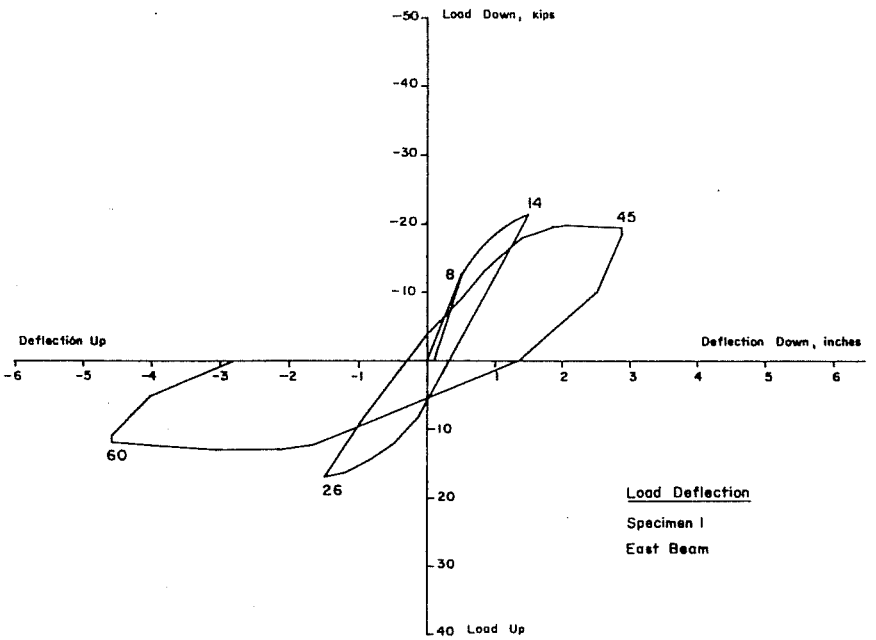
Load Down, kips
-50
-40
-30
-20
-10
Deflection Up
Deflection Down, inches
-6 -5 -4 -3 -2 -1 1 2 3 4 5 6
10
20
30
40 Load Up
14
45
8
60
26
Load Deflection
Specimen I
East Beam

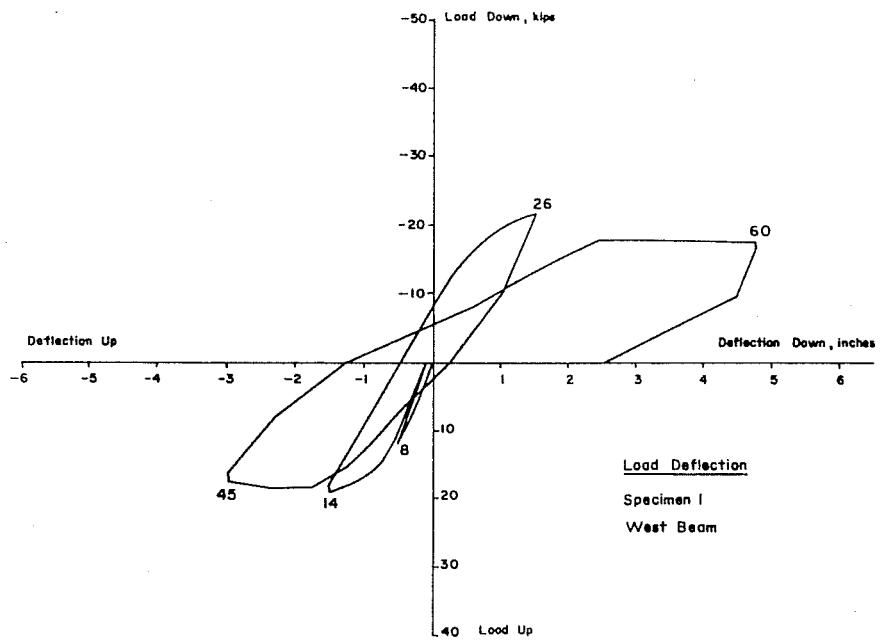
Load Down, kips
-50
-40
-30
-20
-10
Deflection Up
Deflection Down, inches
-6 -5 -4 -3 -2 -1 1 2 3 4 5 6
10
20
30
40 Load Up
26
60
8
45
14
Load Deflection
Specimen I
West Beam

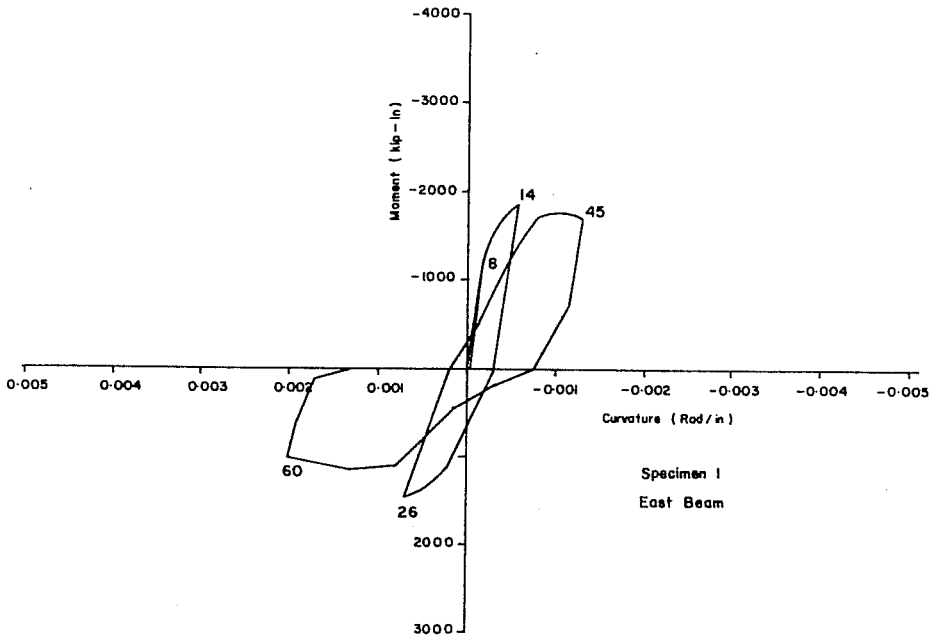
-4000
-3000
-2000
-1000
Moment (kip-in)
14
45
8
0·005
0·004
0·003
0·002
0·001
-0·001
-0·002
-0·003
-0·004
-0·005
Curvature (Rad / in)
60
26
2000
3000
Specimen I
East Beam

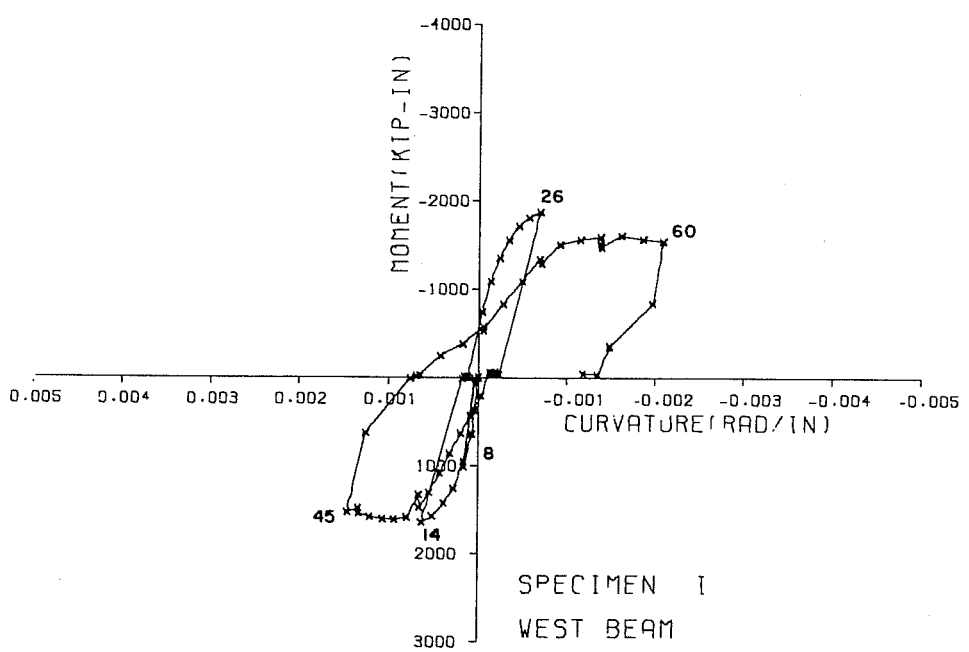
-4000
-3000
-2000
-1000
MOMENT(KIP-IN)
26
60
0.005
0.004
0.003
0.002
0.001
-0.001
-0.002
-0.003
-0.004
-0.005
CURVATURE(RAD/IN)
8
1000
45
14
2000
3000
SPECIMEN I
WEST BEAM

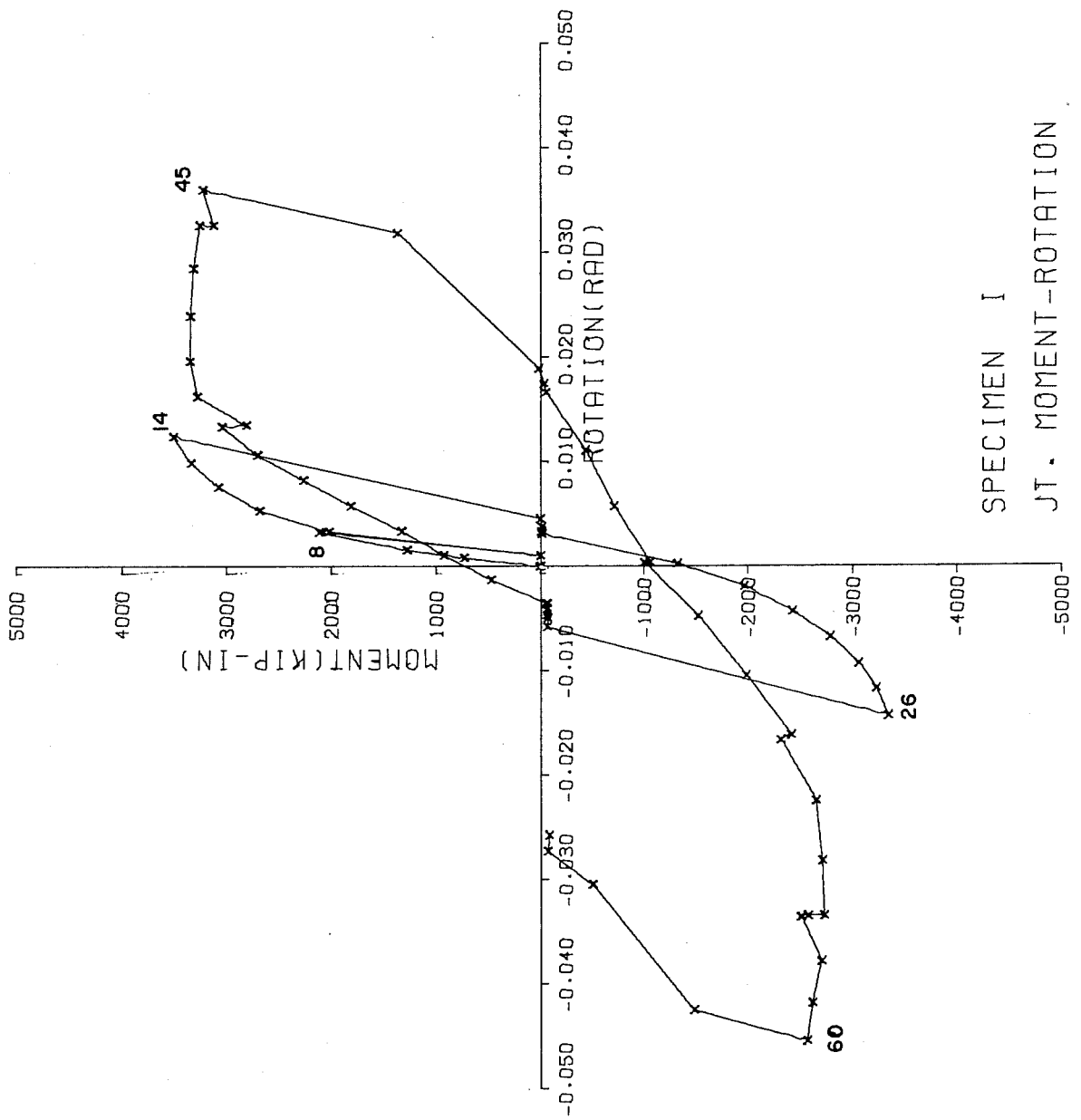
SPECIMEN I
JT. MOMENT-ROTATION
MOMENT(KIP-IN)
ROTATION(RAD)
5000
4000
3000
2000
1000
-1000
-2000
-3000
-4000
-5000
0.050
0.040
0.030
0.020
0.010
-0.010
-0.020
-0.030
-0.040
-0.050
45
14
8
26
60

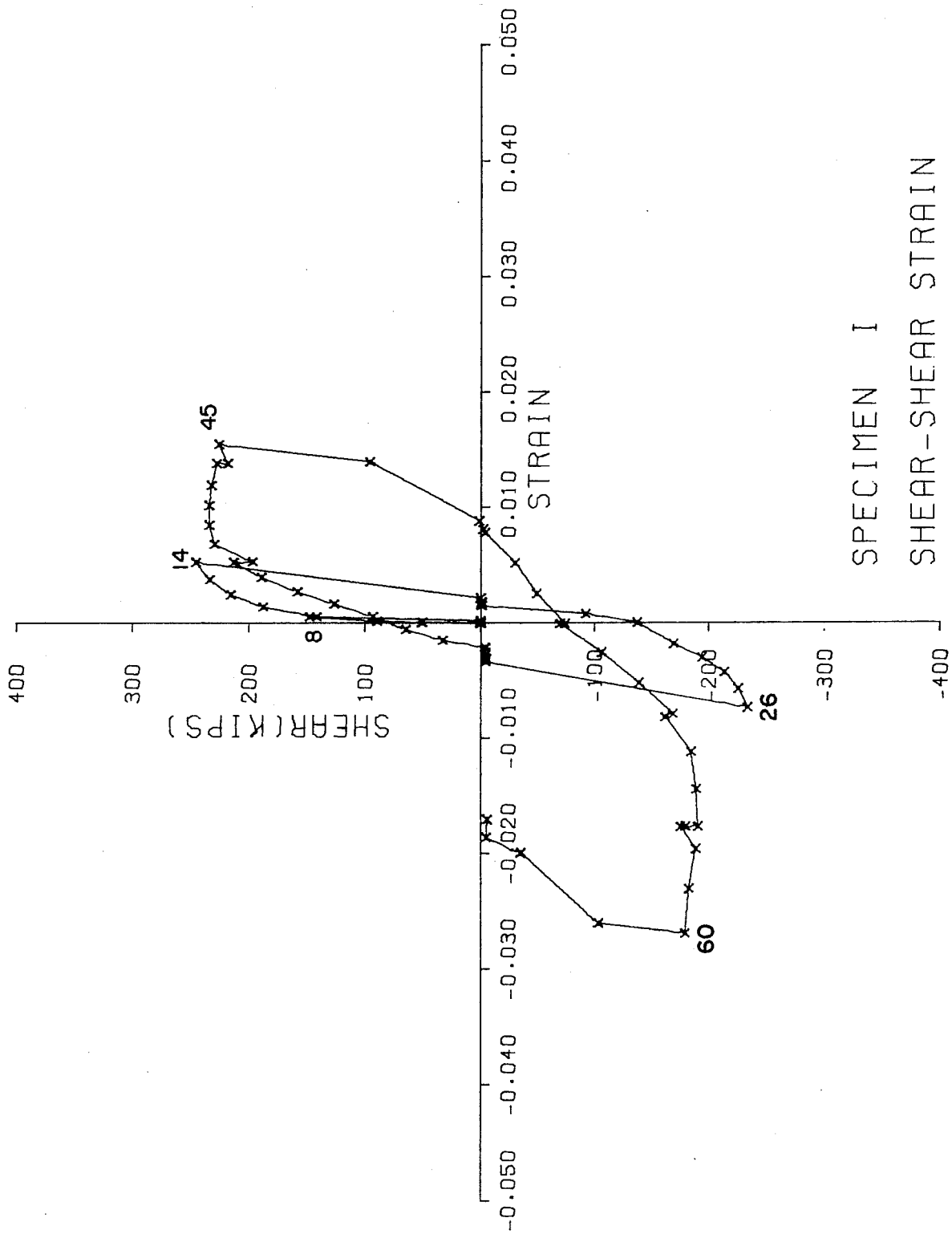
SPECIMEN I
SHEAR-SHEAR STRAIN
SHEAR(KIPS)
STRAIN
400
300
200
100
-100
-200
-300
-400
0.050
0.040
0.030
0.020
0.010
-0.010
-0.020
-0.030
-0.040
-0.050
45
14
8
26
60

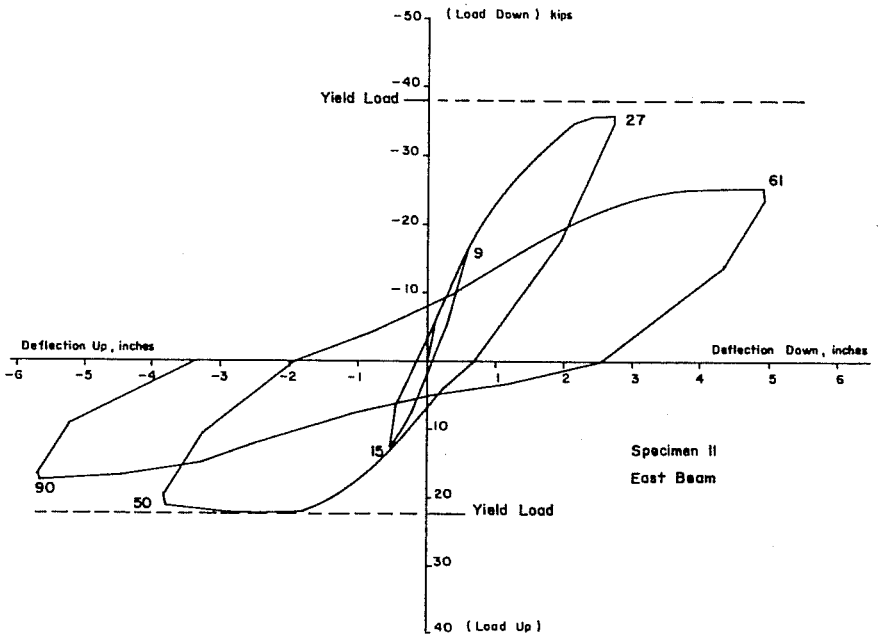
(Load Down) kips
Yield Load
27
61
9
Deflection Up, inches
Deflection Down, inches
15
90
50
Yield Load
Specimen II
East Beam
(Load Up)

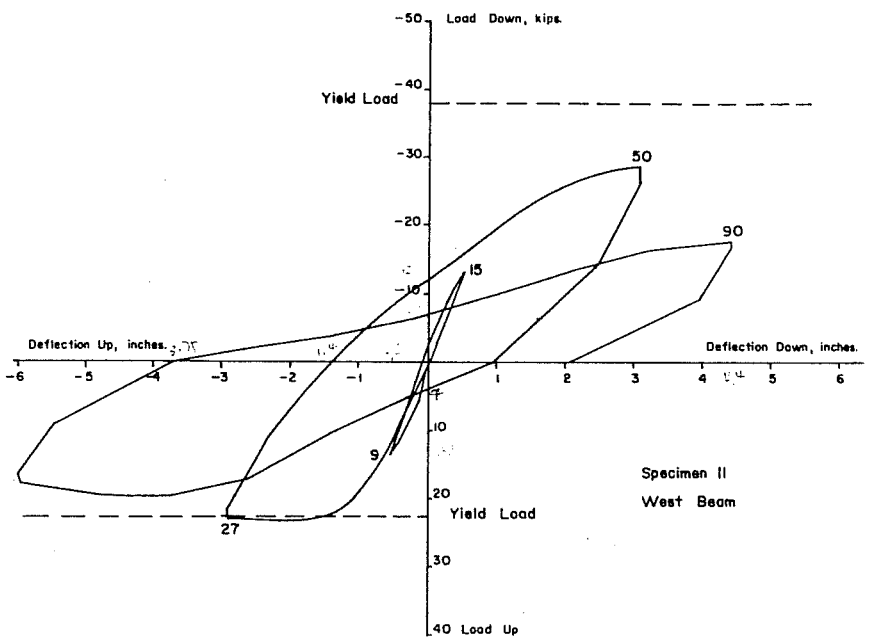
Load Down, kips.
Yield Load
50
90
15
Deflection Up, inches.
Deflection Down, inches.
9
Specimen II
West Beam
27
Yield Load
Load Up

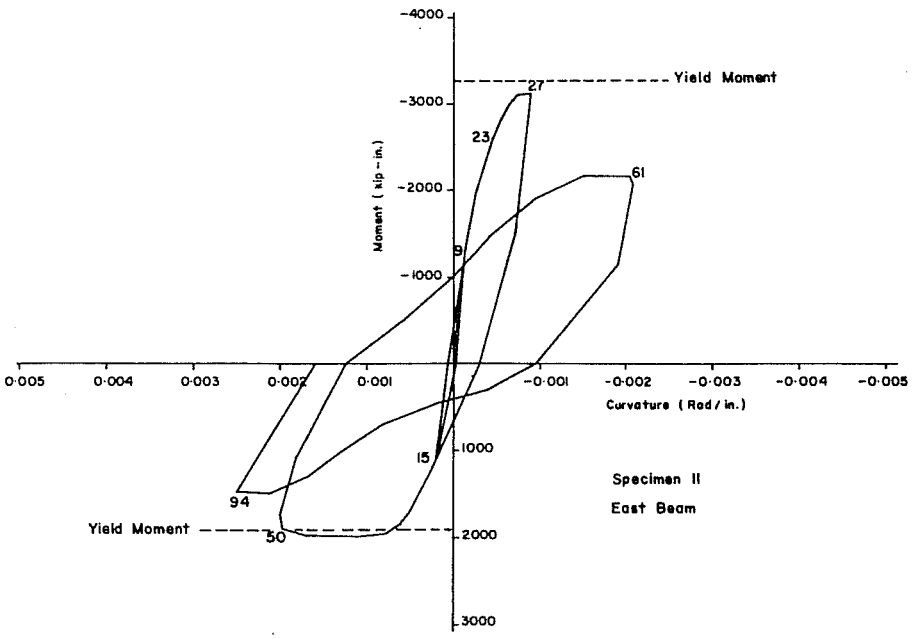
-4000
-3000
-2000
-1000
1000
2000
3000
Yield Moment
27
23
61
9
15
94
50
Yield Moment
Moment (kip - in.)
0·005
0·004
0·003
0·002
0·001
-0·001
-0·002
-0·003
-0·004
-0·005
Curvature (Rad / in.)
Specimen II
East Beam

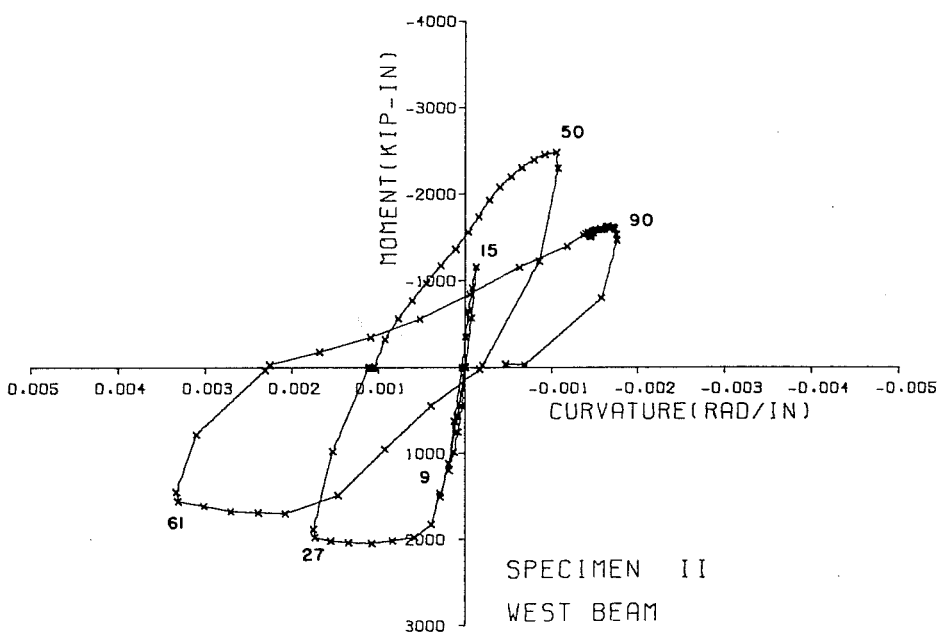
-4000
-3000
-2000
-1000
1000
2000
3000
MOMENT(KIP-IN)
50
90
15
9
61
27
0.005
0.004
0.003
0.002
0.001
-0.001
-0.002
-0.003
-0.004
-0.005
CURVATURE(RAD/IN)
SPECIMEN II
WEST BEAM

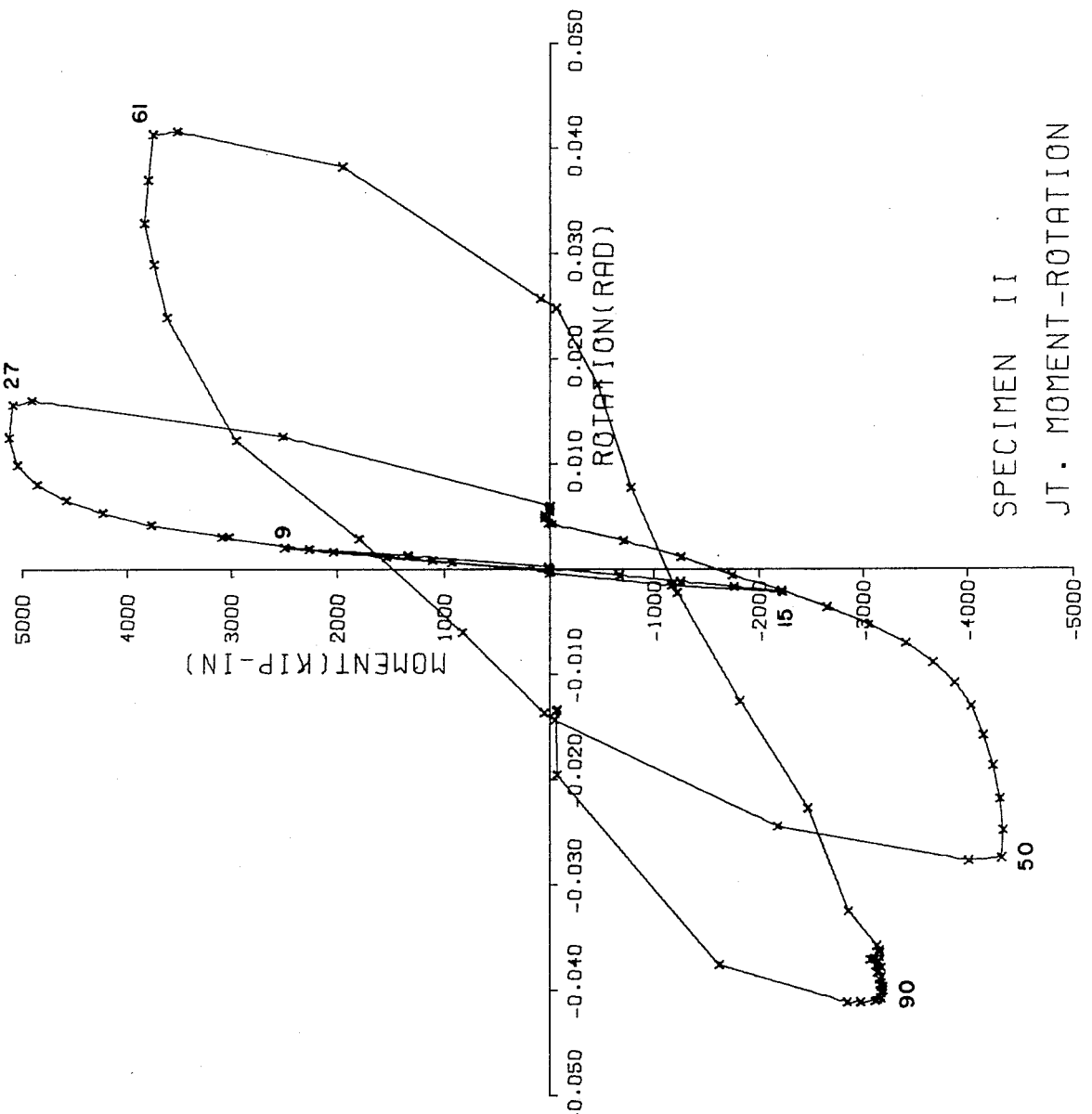
SPECIMEN II
JT. MOMENT-ROTATION
MOMENT(KIP-IN)
ROTATION(RAD)
5000
4000
3000
2000
1000
-1000
-2000
-3000
-4000
-5000
0.050
0.040
0.030
0.020
0.010
-0.010
-0.020
-0.030
-0.040
-0.050
61
27
9
15
50
90

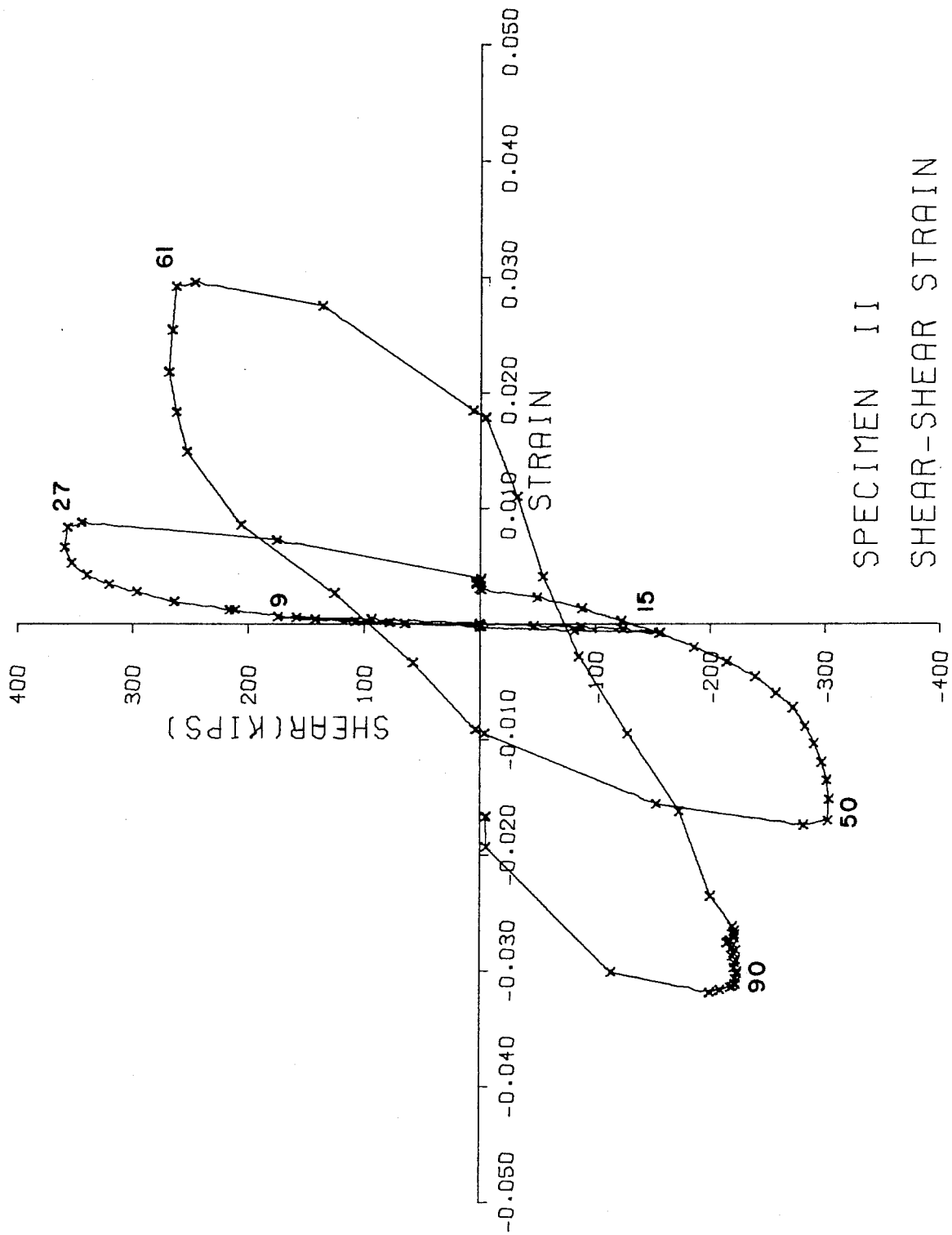
SHEAR-SHEAR STRAIN
SPECIMEN II
SHEAR(KIPS)
STRAIN
400
300
200
100
-100
-200
-300
-400
0.050
0.040
0.030
0.020
0.010
-0.010
-0.020
-0.030
-0.040
-0.050
61
27
9
15
50
90

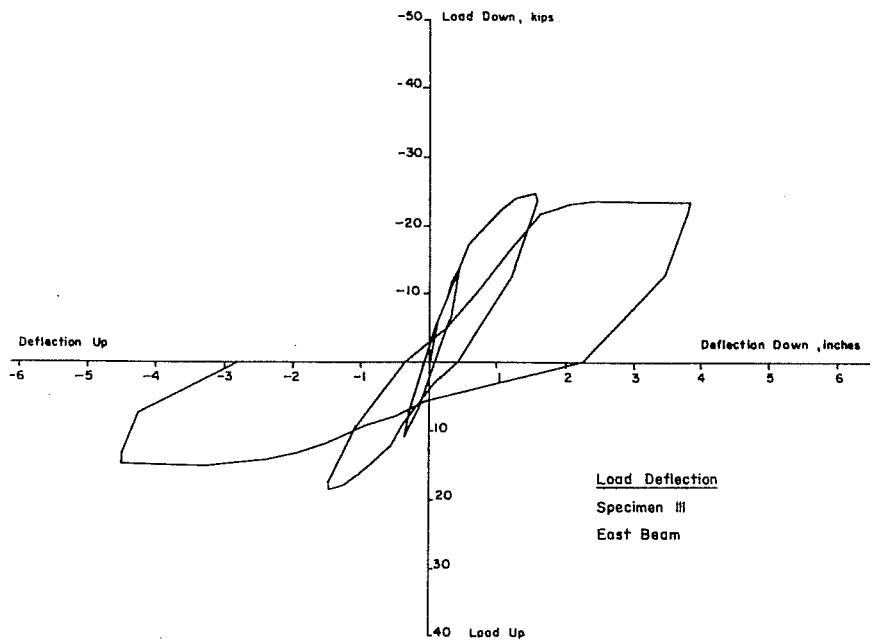
Load Down, kips
-50
-40
-30
-20
-10
Deflection Up
Deflection Down, inches
-6 -5 -4 -3 -2 -1 1 2 3 4 5 6
10
20
30
40 Load Up
Load Deflection
Specimen III
East Beam

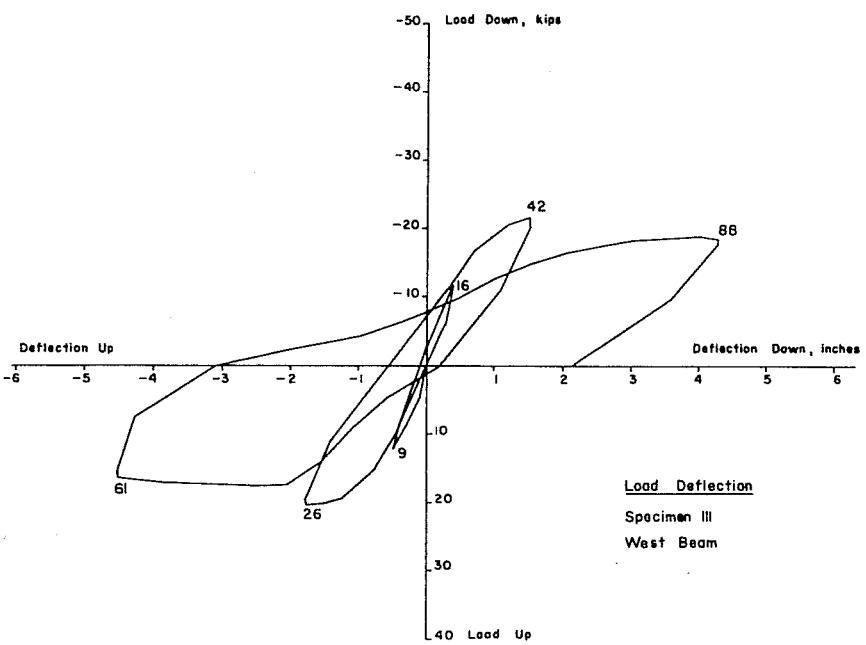
Load Down, kips
-50
-40
-30
-20
-10
42
86
16
9
61
26
Deflection Up
Deflection Down, inches
-6 -5 -4 -3 -2 -1 1 2 3 4 5 6
10
20
30
40 Load Up
Load Deflection
Specimen III
West Beam

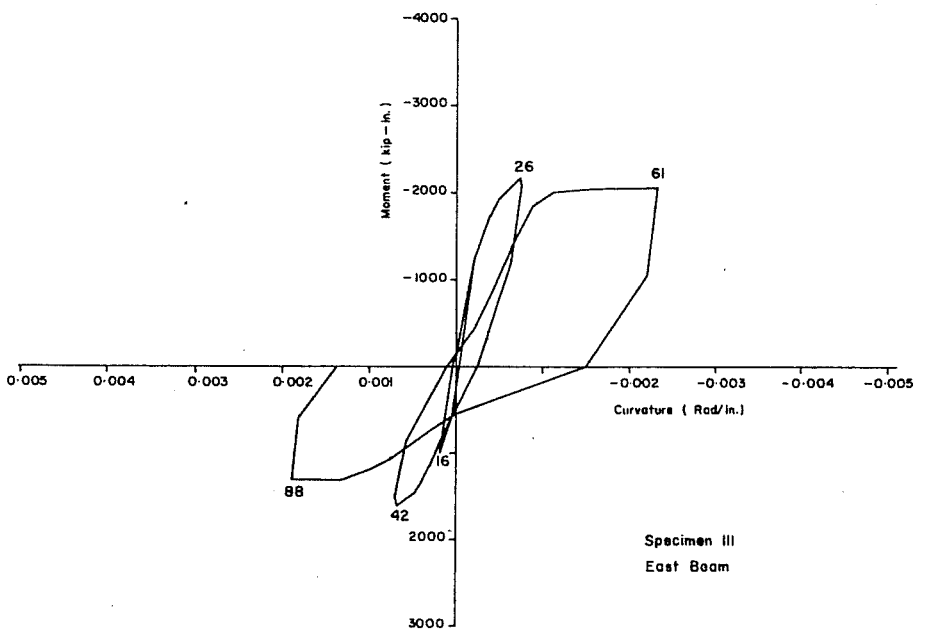
-4000
-3000
-2000
-1000
Moment (kip – in.)
26
61
0·005
0·004
0·003
0·002
0·001
-0·002
-0·003
-0·004
-0·005
Curvature (Rad/in.)
16
88
42
2000
3000
Specimen III
East Beam

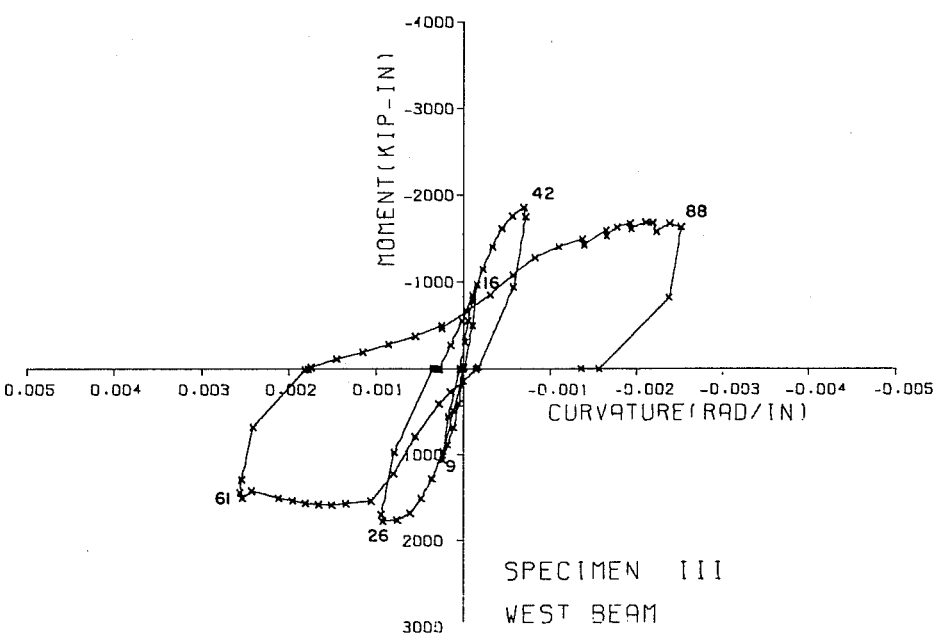
-4000
-3000
-2000
-1000
MOMENT(KIP-IN)
42
88
16
0.005
0.004
0.003
0.002
0.001
-0.001
-0.002
-0.003
-0.004
-0.005
CURVATURE(RAD/IN)
9
61
26
2000
3000
SPECIMEN III
WEST BEAM

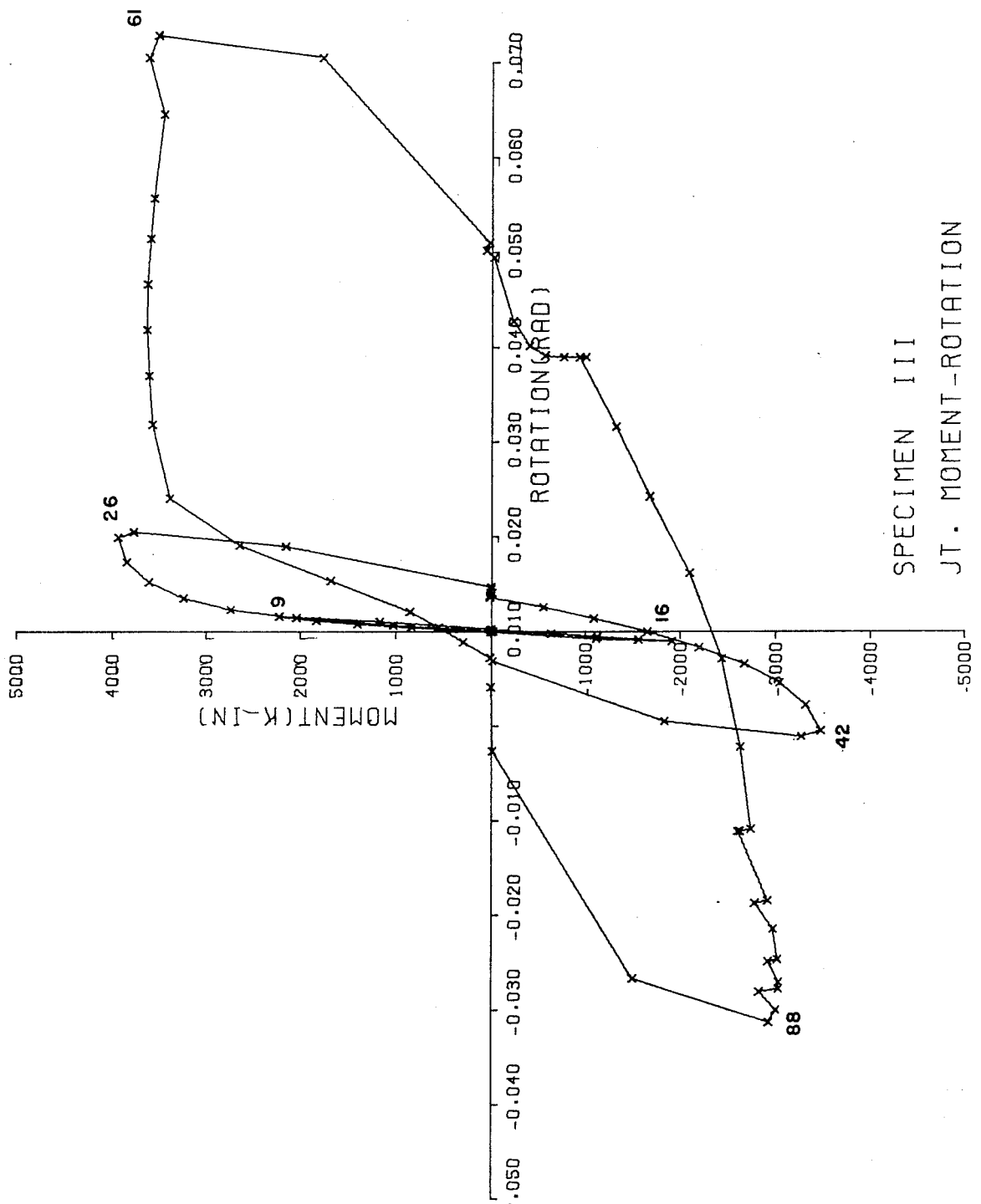
SPECIMEN III
JT. MOMENT-ROTATION
MOMENT(K-IN)
ROTATION(RAD)
5000
4000
3000
2000
1000
-1000
-2000
-3000
-4000
-5000
0.070
0.060
0.050
0.040
0.030
0.020
0.010
-0.010
-0.020
-0.030
-0.040
-0.050
61
26
9
16
42
88

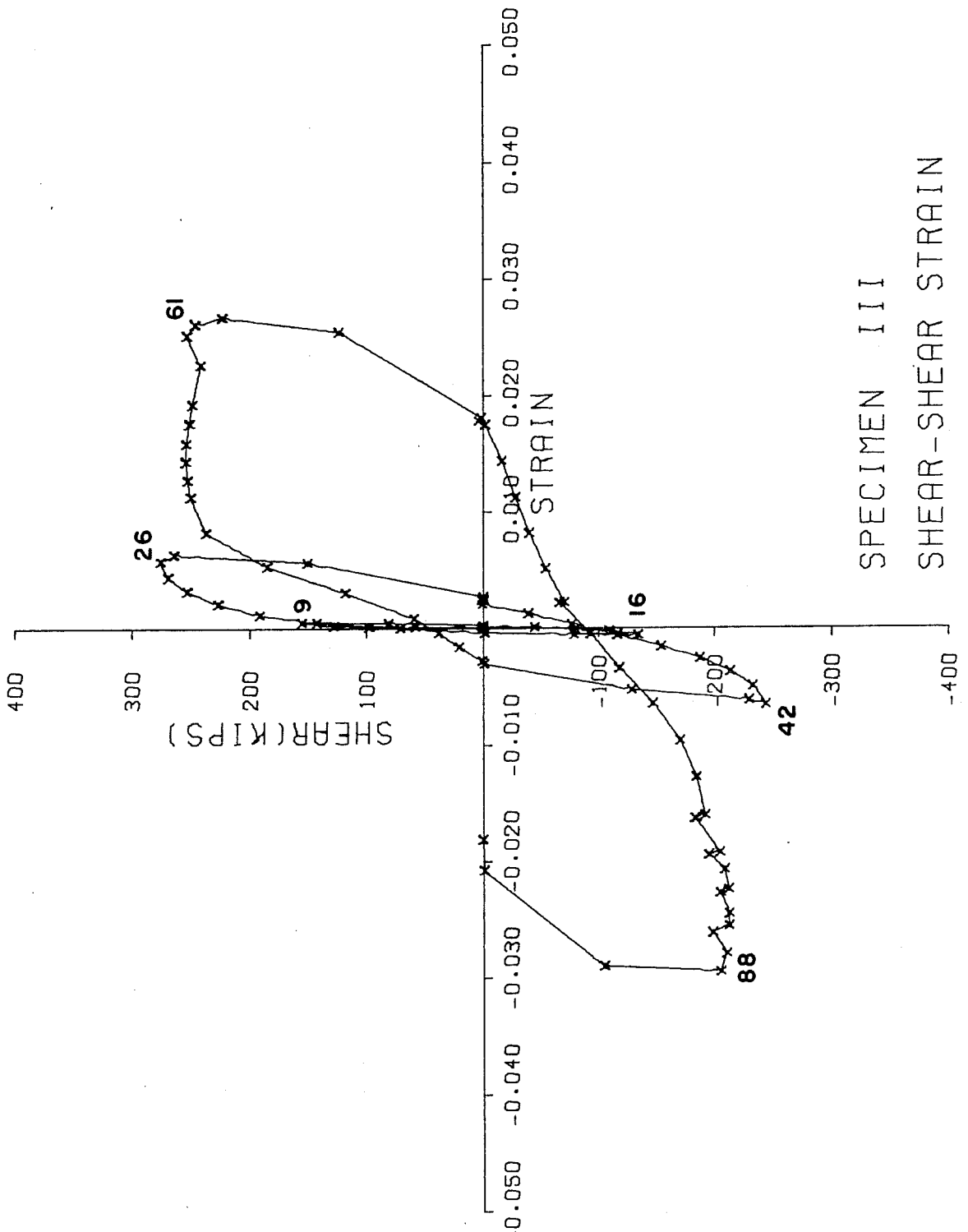
SPECIMEN III
SHEAR-SHEAR STRAIN
SHEAR(KIPS)
STRAIN
400
300
200
100
-100
-200
-300
-400
0.050
0.040
0.030
0.020
0.010
-0.010
-0.020
-0.030
-0.040
-0.050
61
26
9
16
42
88

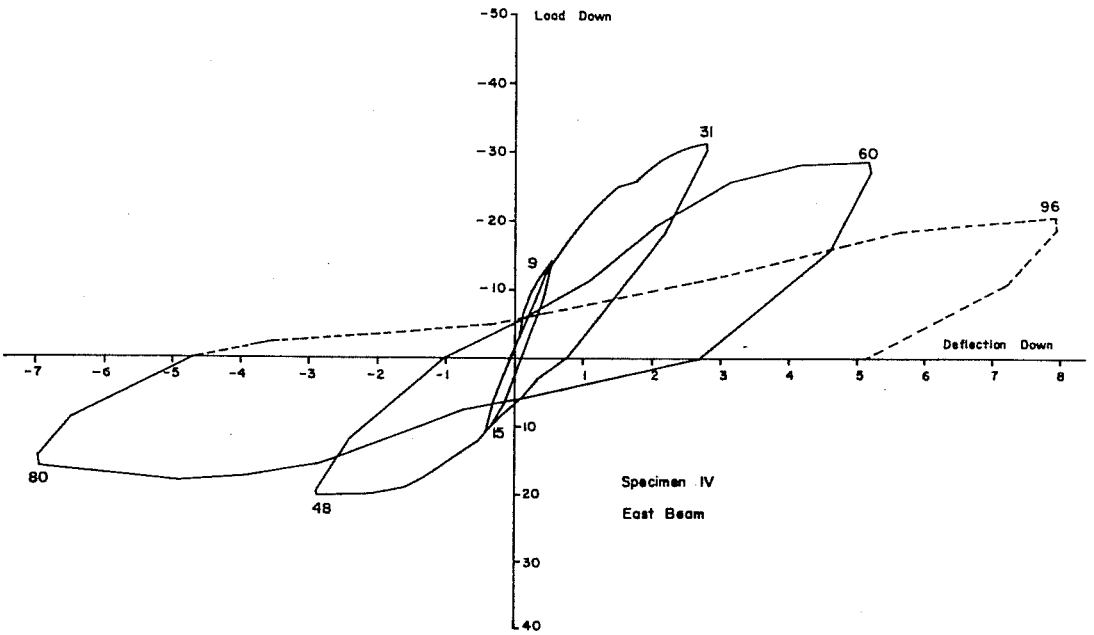
Load Down
Deflection Down
31
60
96
9
15
80
48
Specimen IV
East Beam

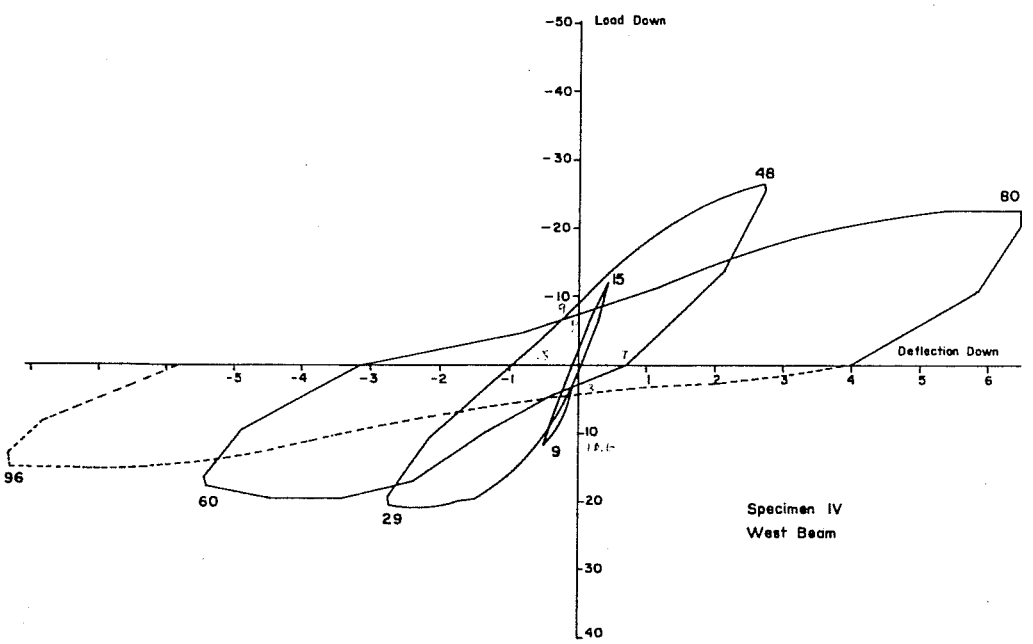
Load Down
Deflection Down
48
80
15
9
96
60
29
Specimen IV
West Beam

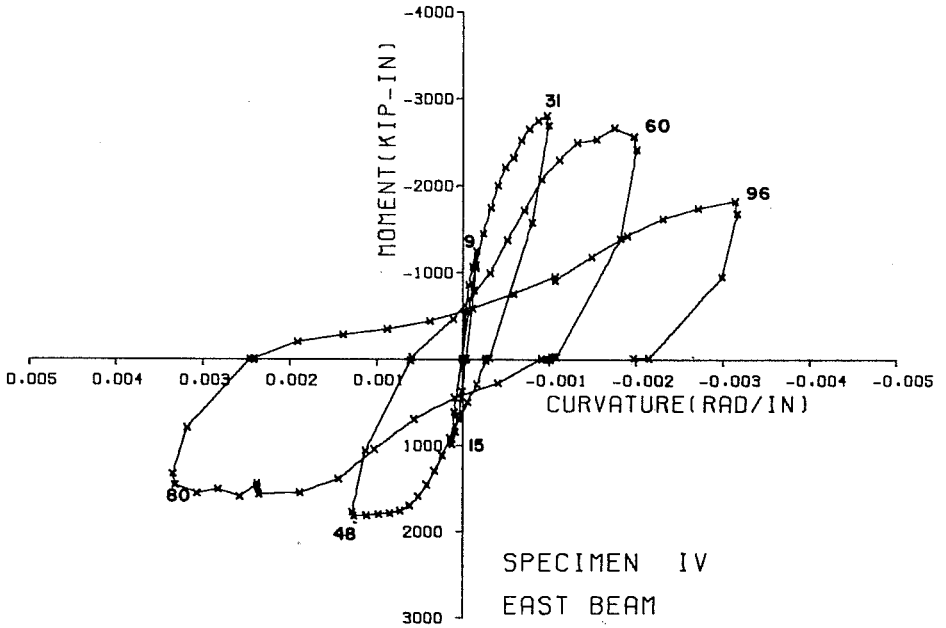
-4000
-3000
-2000
-1000
1000
2000
3000
MOMENT(KIP-IN)
0.005
0.004
0.003
0.002
0.001
-0.001
-0.002
-0.003
-0.004
-0.005
CURVATURE(RAD/IN)
31
60
96
9
15
80
48
SPECIMEN IV
EAST BEAM

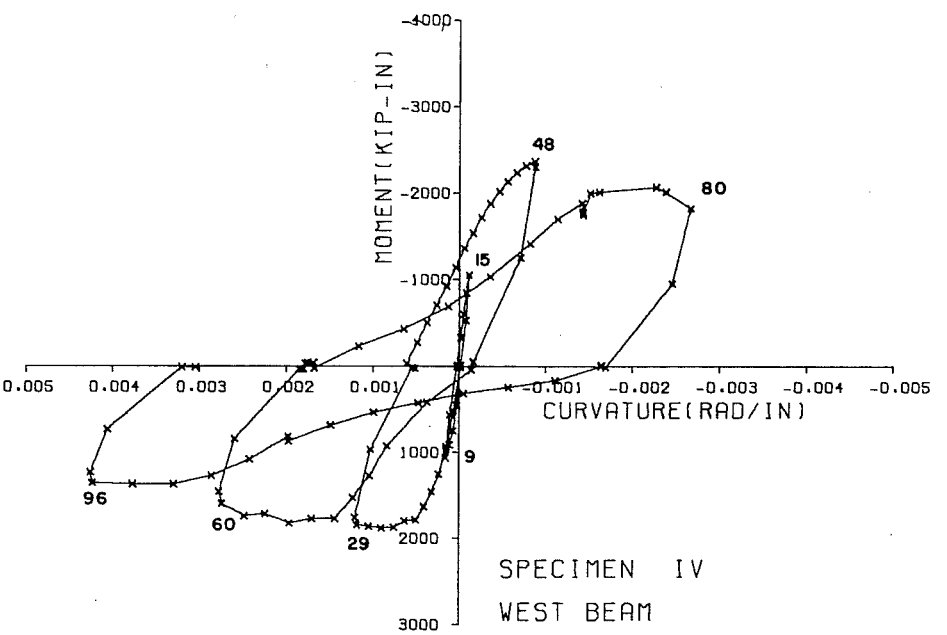
-4000
-3000
-2000
-1000
1000
2000
3000
MOMENT(KIP-IN)
0.005
0.004
0.003
0.002
0.001
-0.001
-0.002
-0.003
-0.004
-0.005
CURVATURE(RAD/IN)
48
80
15
9
96
60
29
SPECIMEN IV
WEST BEAM

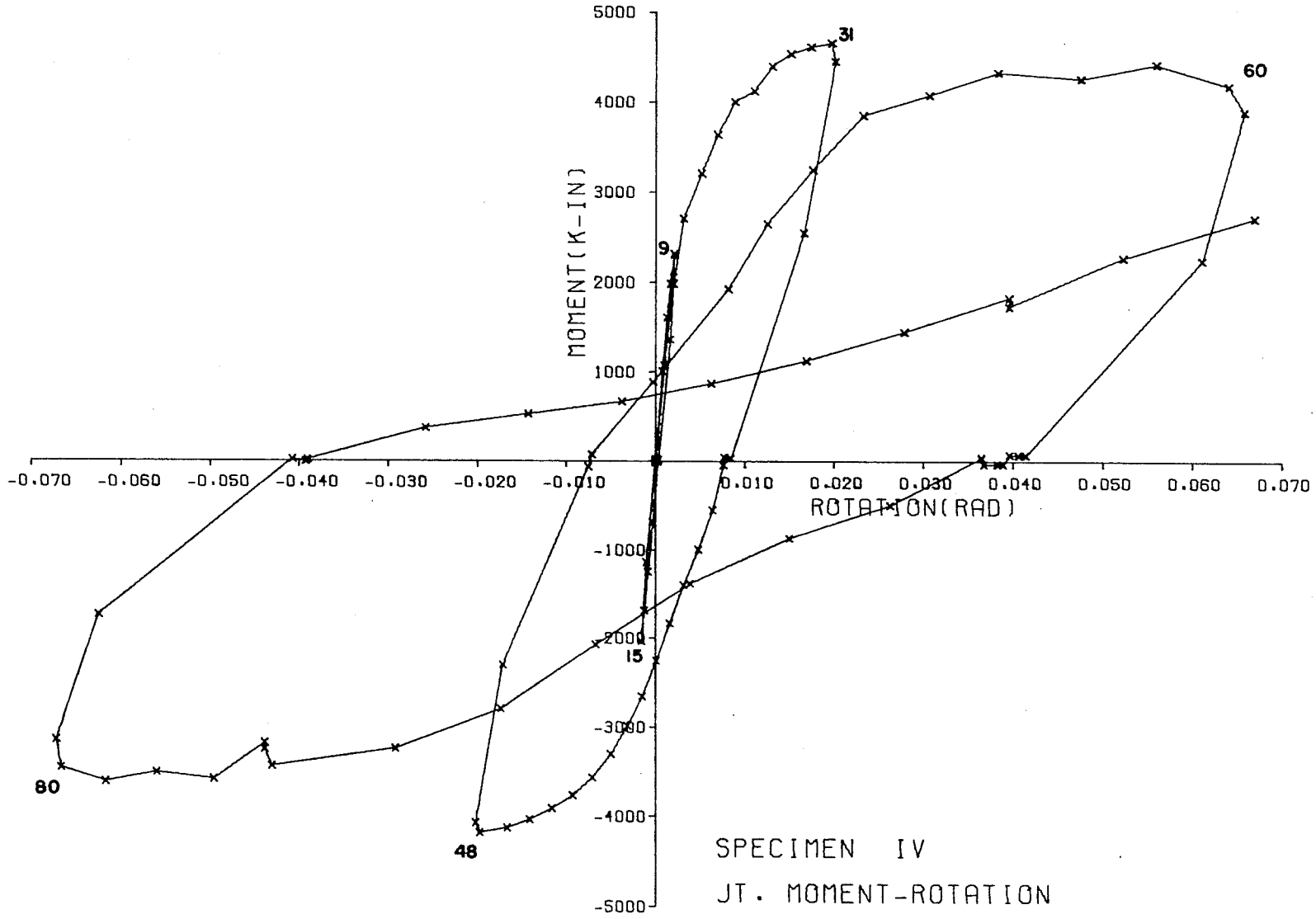
5000
4000
3000
2000
1000
-1000
-2000
-3000
-4000
-5000
MOMENT(K-IN)
-0.070
-0.060
-0.050
-0.040
-0.030
-0.020
-0.010
0.010
0.020
0.030
0.040
0.050
0.060
0.070
ROTATION(RAD)
31
60
9
15
80
48
SPECIMEN IV
JT. MOMENT-ROTATION

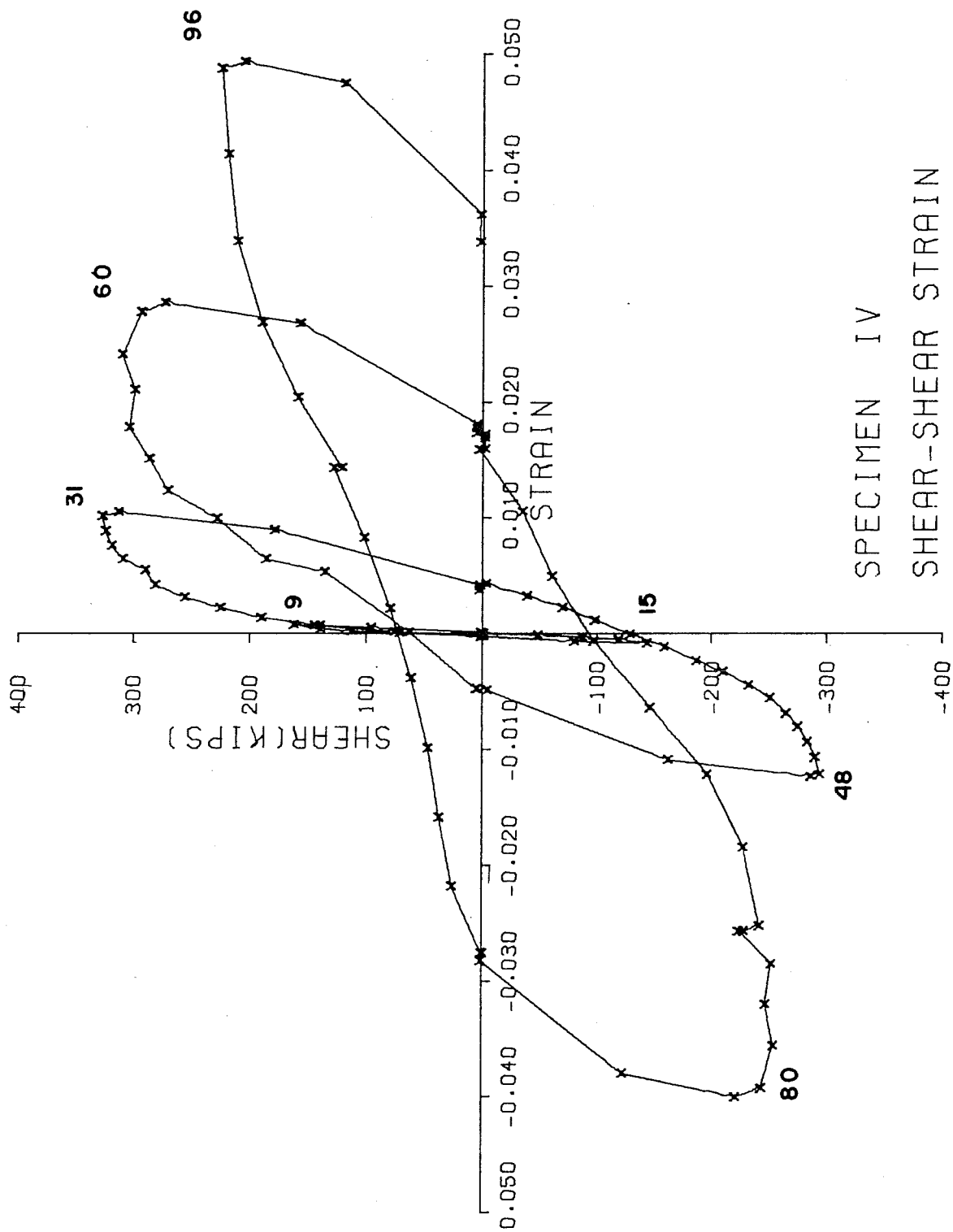
SPECIMEN IV
SHEAR-SHEAR STRAIN
SHEAR(KIPS)
STRAIN
400
300
200
100
-100
-200
-300
-400
0.050
0.040
0.030
0.020
0.010
-0.010
-0.020
-0.030
-0.040
-0.050
96
60
31
9
15
48
80

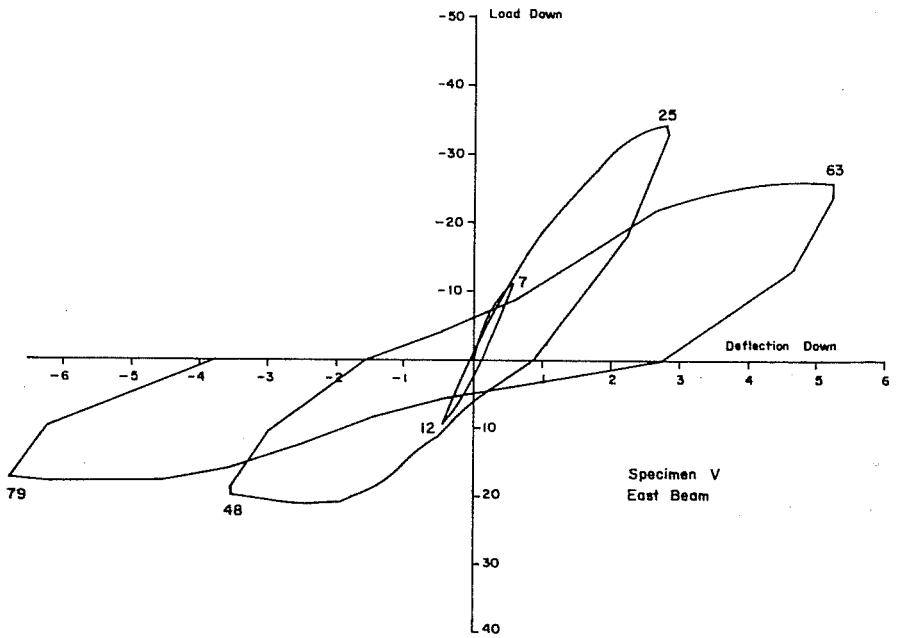
Load Down
-50
-40
-30
-20
-10
25
63
7
Deflection Down
-6 -5 -4 -3 -2 -1 1 2 3 4 5 6
12
10
20
30
40
79
48
Specimen V
East Beam

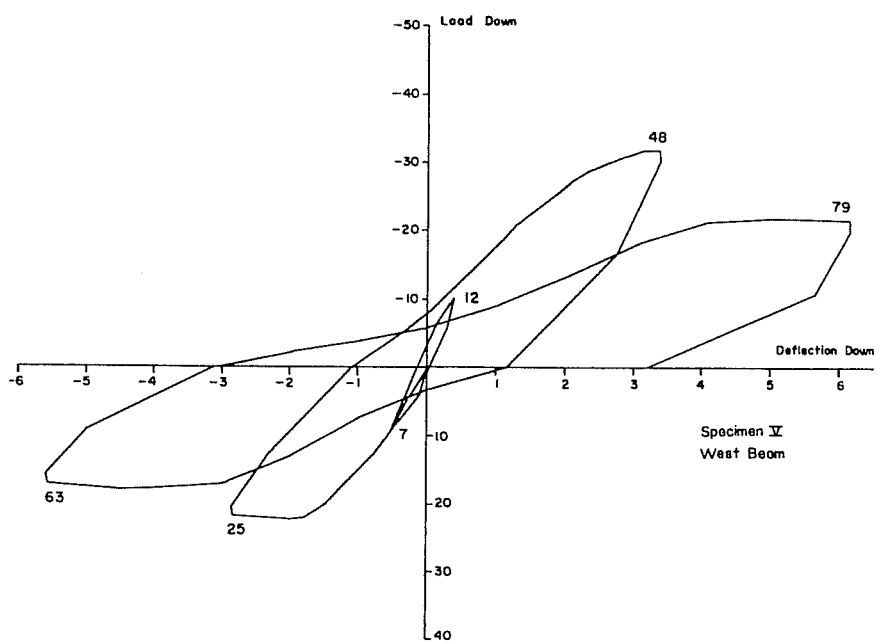
Load Down
-50
-40
-30
-20
-10
48
79
12
Deflection Down
-6 -5 -4 -3 -2 -1 1 2 3 4 5 6
7
10
20
30
40
63
25
Specimen V
West Beam

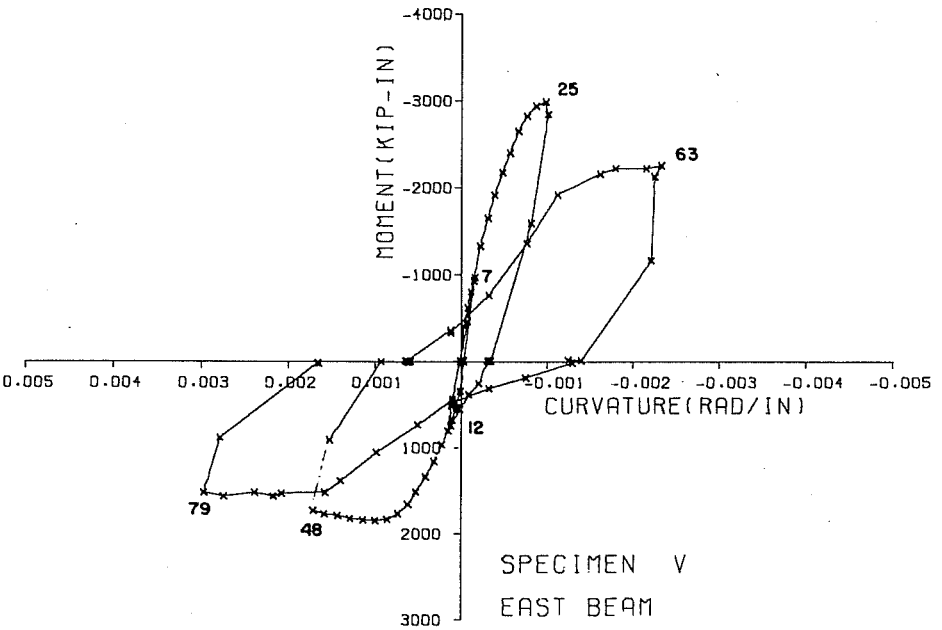
-4000
-3000
-2000
-1000
MOMENT(KIP-IN)
25
63
7
12
79
48
1000
2000
3000
0.005
0.004
0.003
0.002
0.001
-0.001
-0.002
-0.003
-0.004
-0.005
CURVATURE(RAD/IN)
SPECIMEN V
EAST BEAM

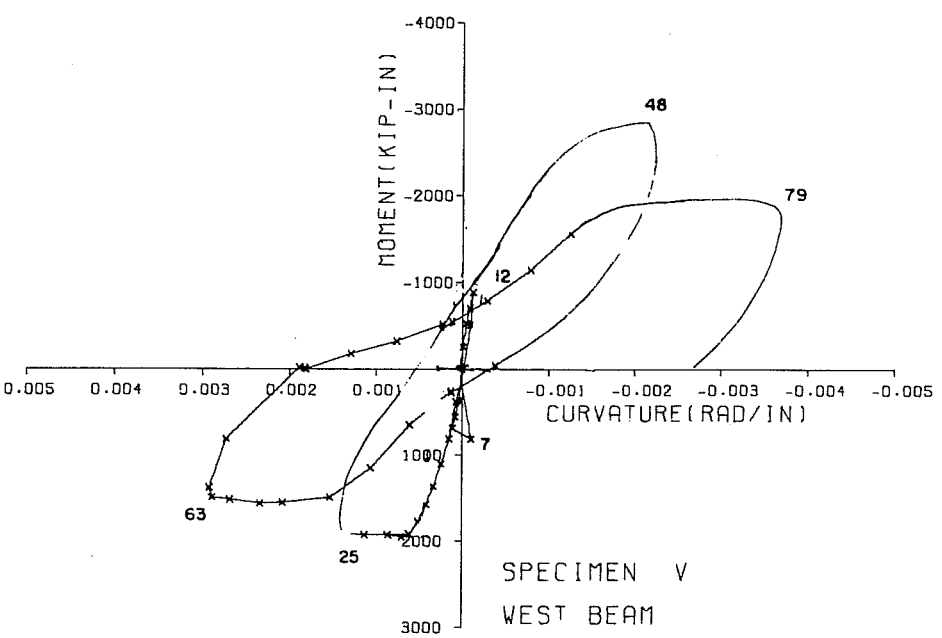
-4000
-3000
-2000
-1000
MOMENT(KIP-IN)
48
79
12
7
63
25
1000
2000
3000
0.005
0.004
0.003
0.002
0.001
-0.001
-0.002
-0.003
-0.004
-0.005
CURVATURE(RAD/IN)
SPECIMEN V
WEST BEAM

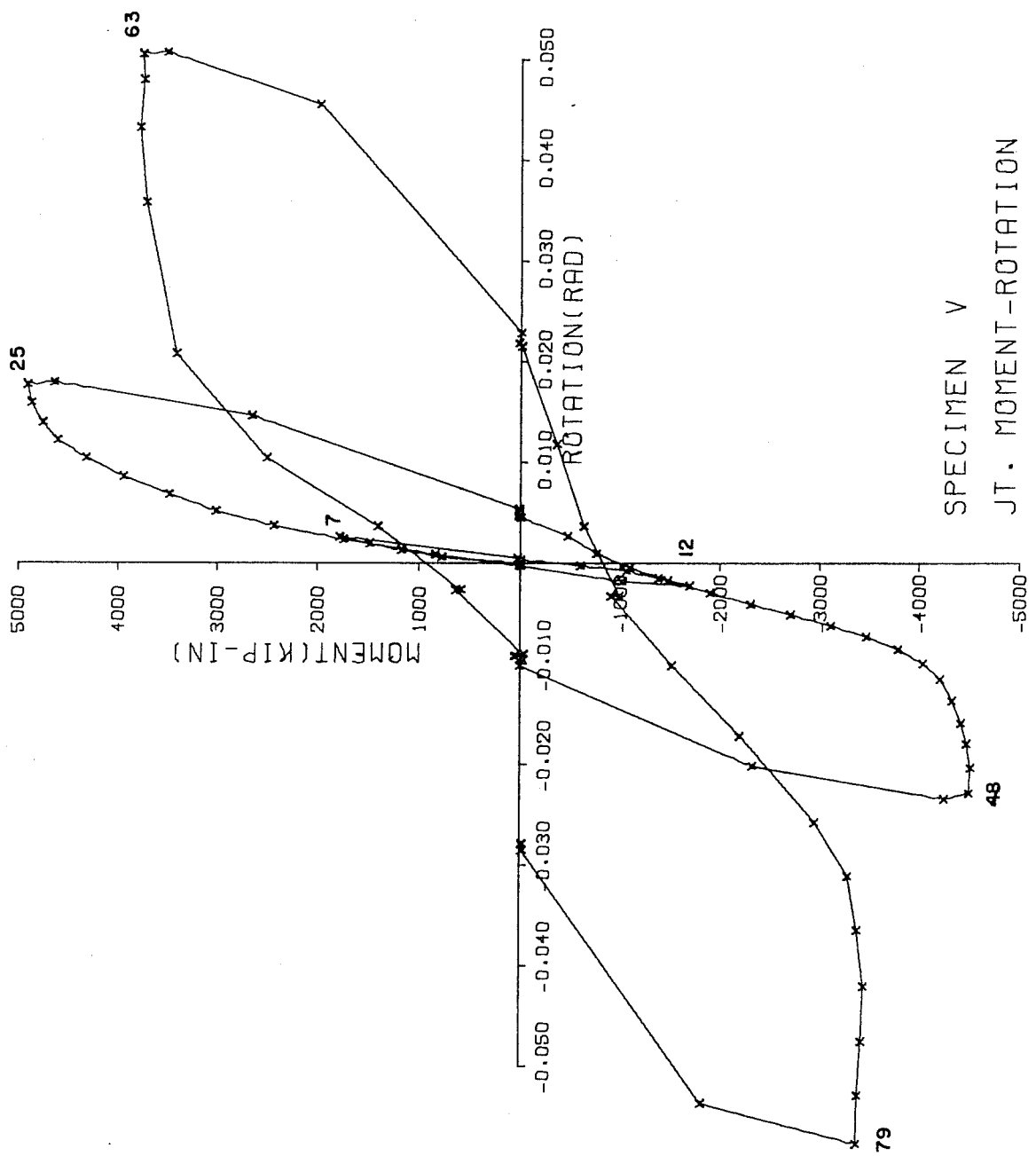
SPECIMEN V
JT. MOMENT-ROTATION
MOMENT(KIP-IN)
ROTATION(RAD)
5000
4000
3000
2000
1000
-1000
-2000
-3000
-4000
-5000
0.050
0.040
0.030
0.020
0.010
-0.010
-0.020
-0.030
-0.040
-0.050
63
25
7
12
48
79

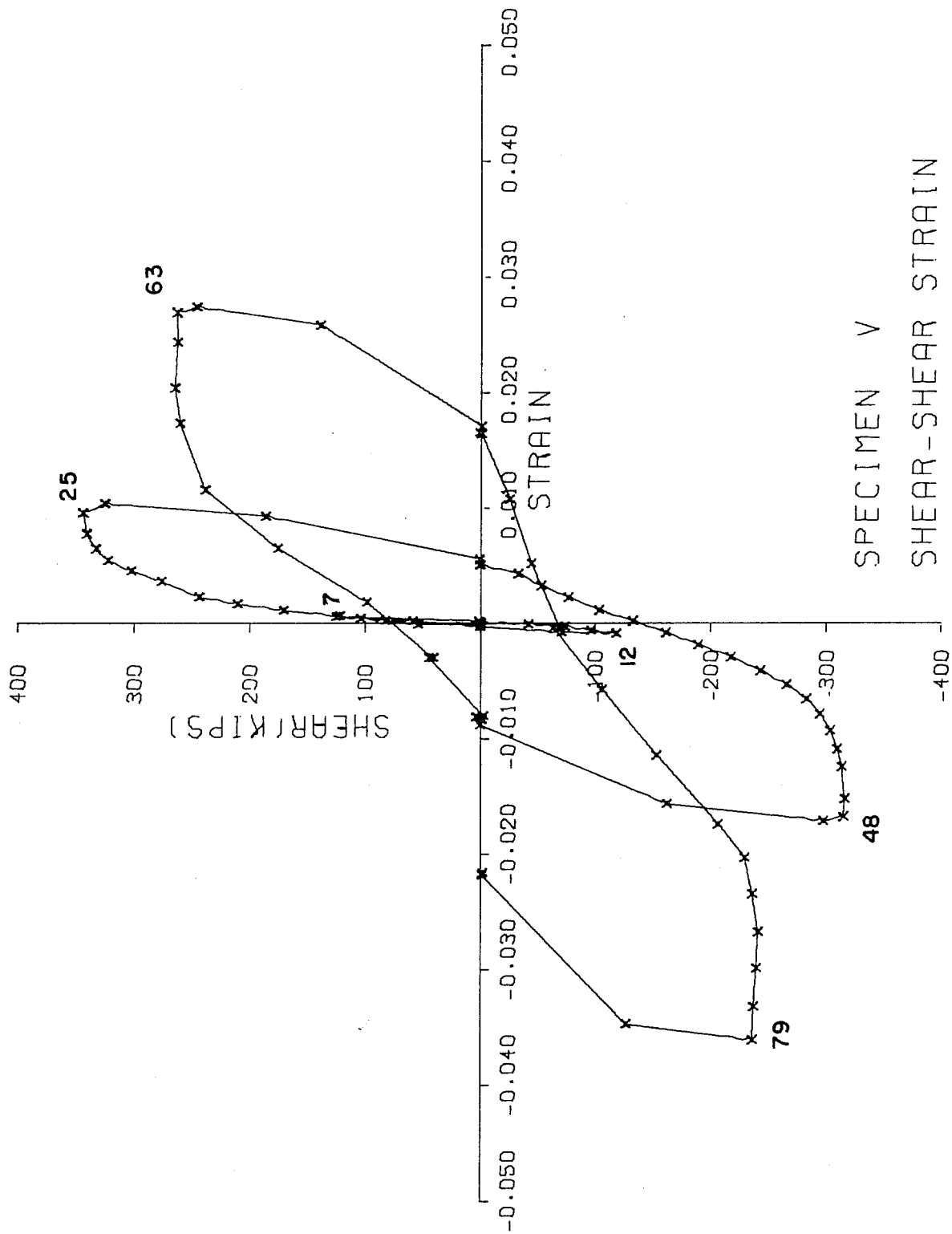
SPECIMEN V
SHEAR-SHEAR STRAIN
STRAIN
SHEAR(KIPS)
0.050
0.040
0.030
0.020
0.010
-0.010
-0.020
-0.030
-0.040
-0.050
400
300
200
100
-100
-200
-300
-400
63
25
7
12
48
79

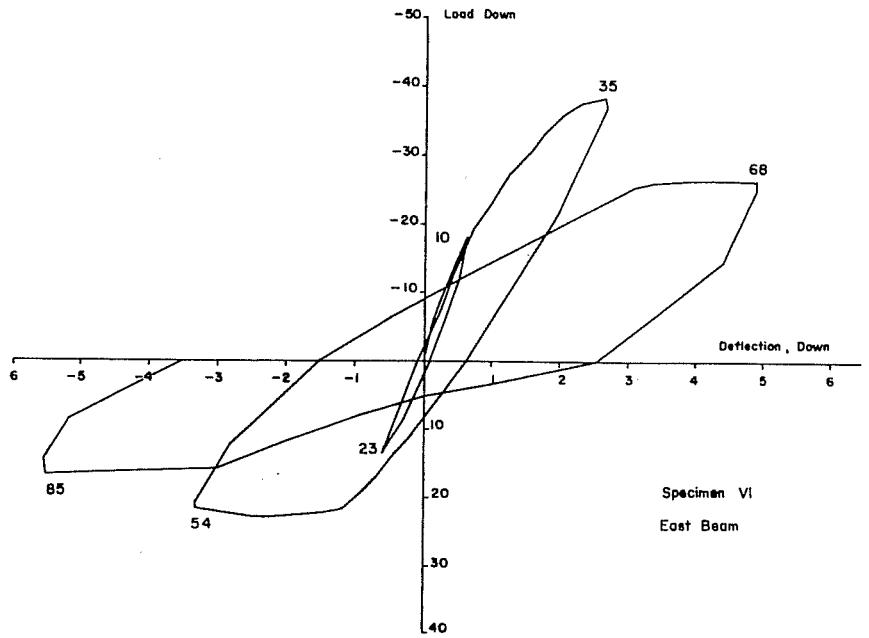
Load Down
-50
-40
-30
-20
-10
Deflection, Down
6
-5
-4
-3
-2
-1
1
2
3
4
5
6
10
20
30
40
35
68
10
23
85
54
Specimen VI
East Beam

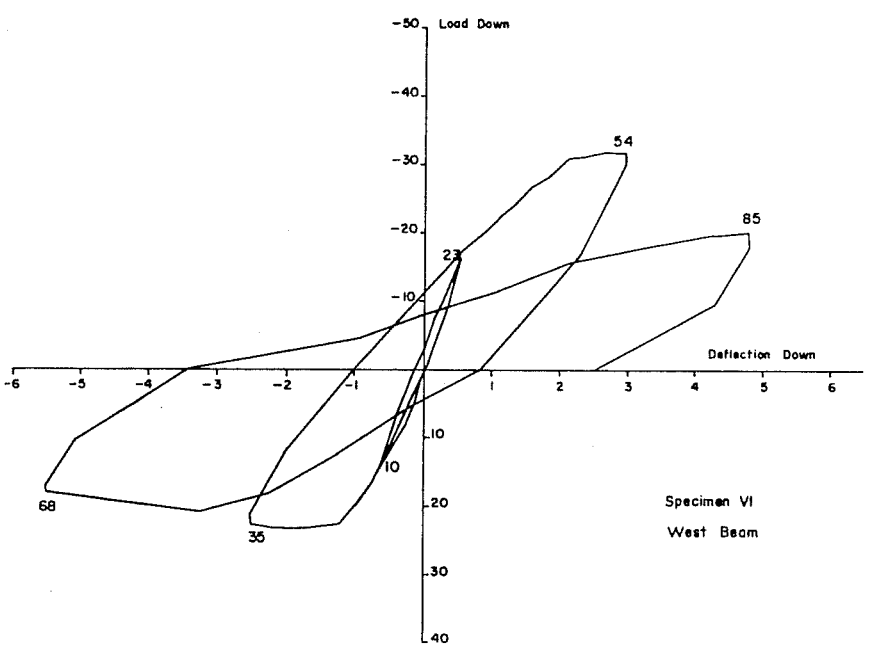
Load Down
-50
-40
-30
-20
-10
Deflection Down
-6
-5
-4
-3
-2
-1
1
2
3
4
5
6
10
20
30
40
54
85
23
10
68
35
Specimen VI
West Beam

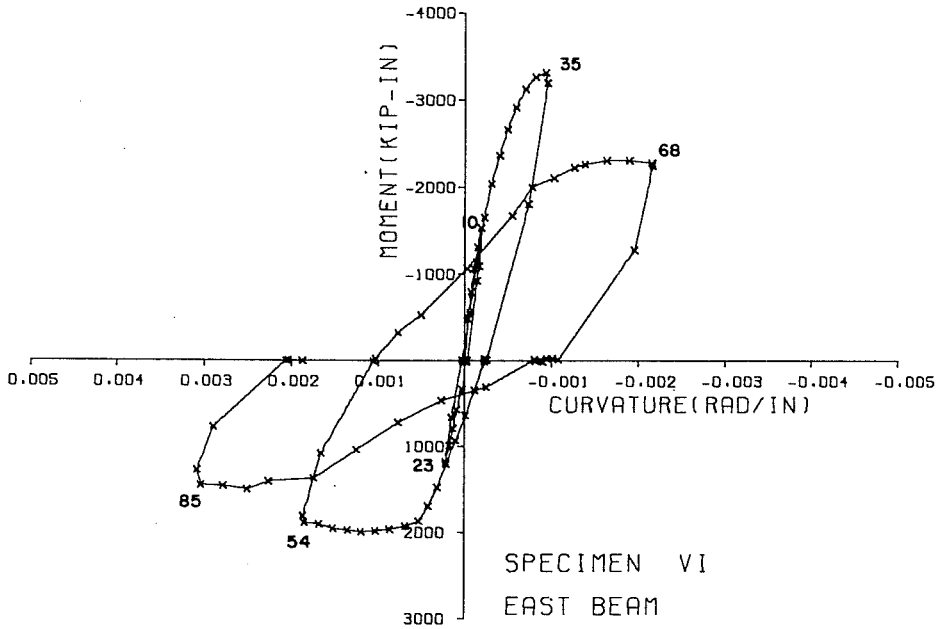
-4000
-3000
-2000
-1000
1000
2000
3000
MOMENT(KIP-IN)
0.005
0.004
0.003
0.002
0.001
-0.001
-0.002
-0.003
-0.004
-0.005
CURVATURE(RAD/IN)
35
68
0
23
85
54
SPECIMEN VI
EAST BEAM

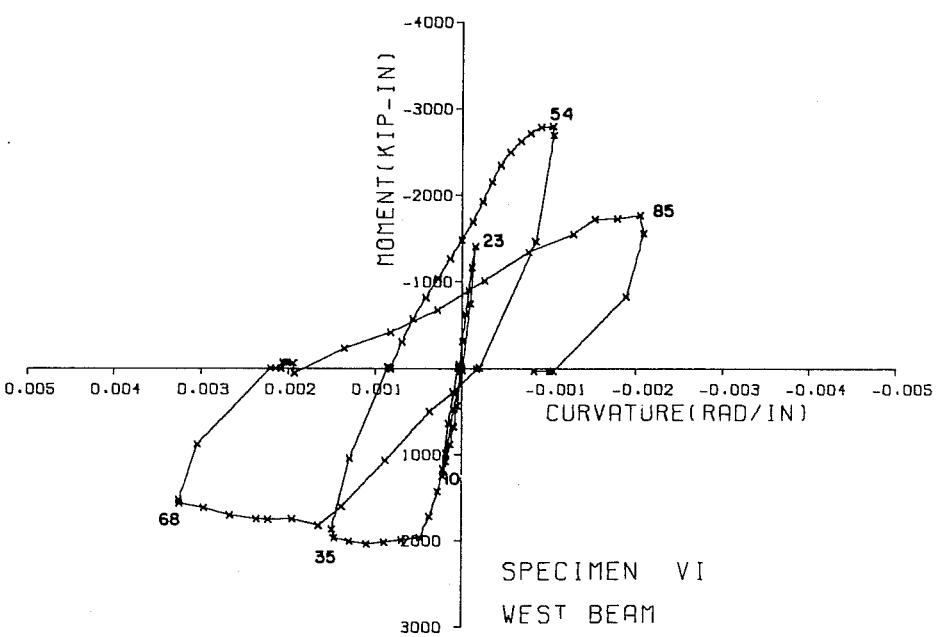
-4000
-3000
-2000
-1000
1000
2000
3000
MOMENT(KIP-IN)
0.005
0.004
0.003
0.002
0.001
-0.001
-0.002
-0.003
-0.004
-0.005
CURVATURE(RAD/IN)
54
85
23
68
0
35
SPECIMEN VI
WEST BEAM

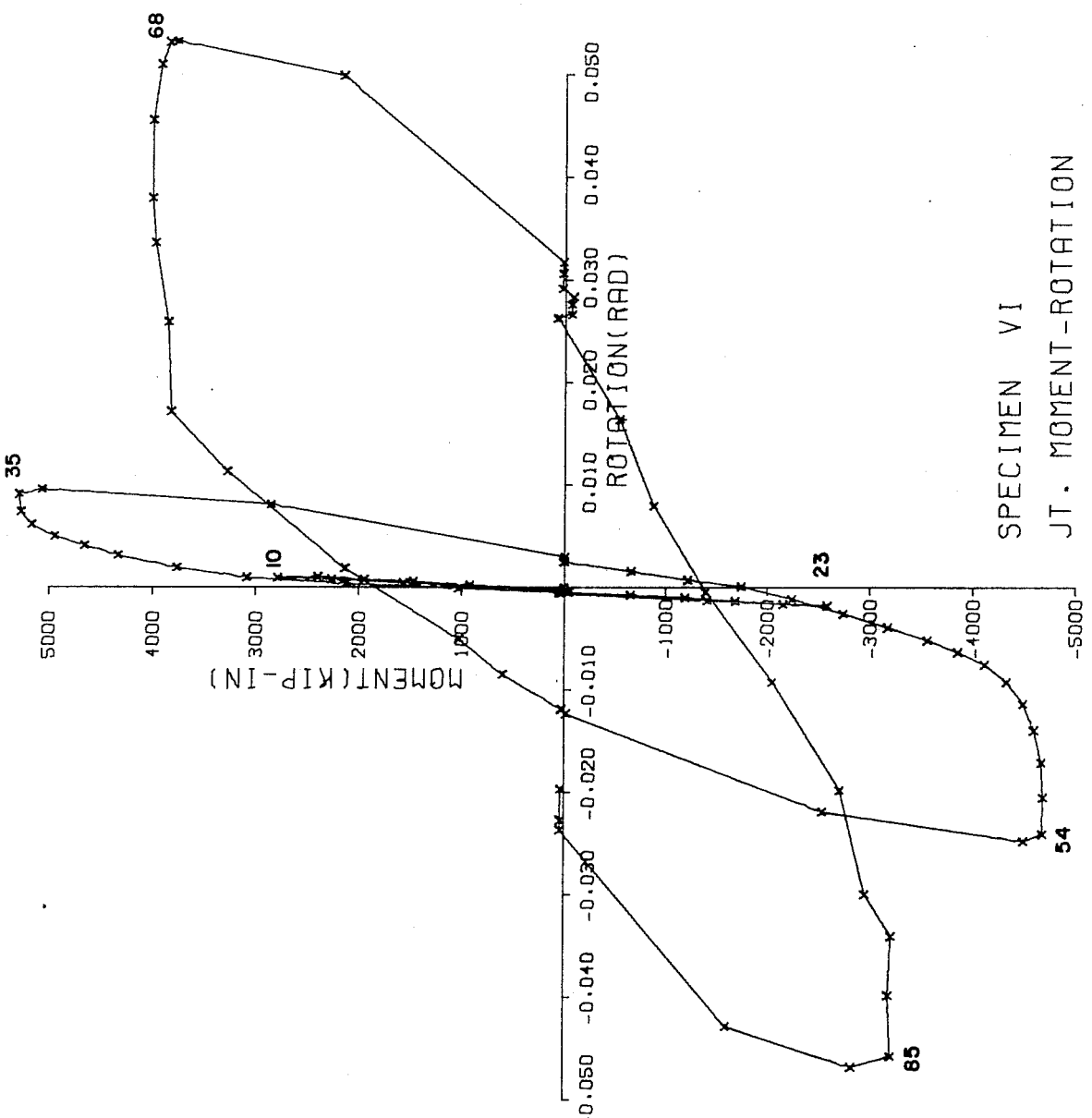
SPECIMEN VI
JT. MOMENT-ROTATION
MOMENT(KIP-IN)
ROTATION(RAD)
5000
4000
3000
2000
1000
-1000
-2000
-3000
-4000
-5000
0.050
0.040
0.030
0.020
0.010
-0.010
-0.020
-0.030
-0.040
-0.050
68
35
10
23
54
85

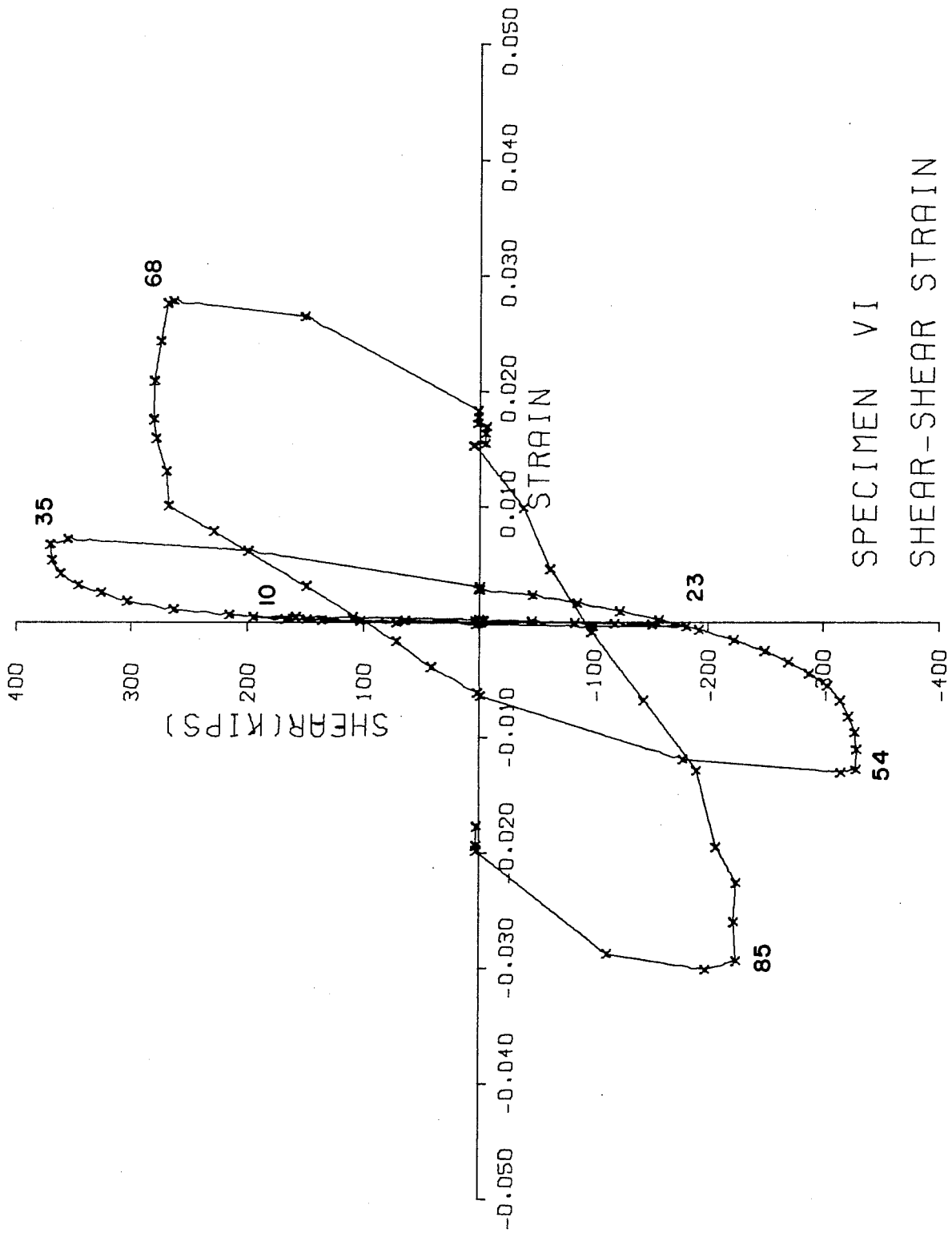
SPECIMEN VI
SHEAR-SHEAR STRAIN
SHEAR(KIPS)
STRAIN
400
300
200
100
-100
-200
-300
-400
0.050
0.040
0.030
0.020
0.010
-0.010
-0.020
-0.030
-0.040
-0.050
68
35
10
23
54
85

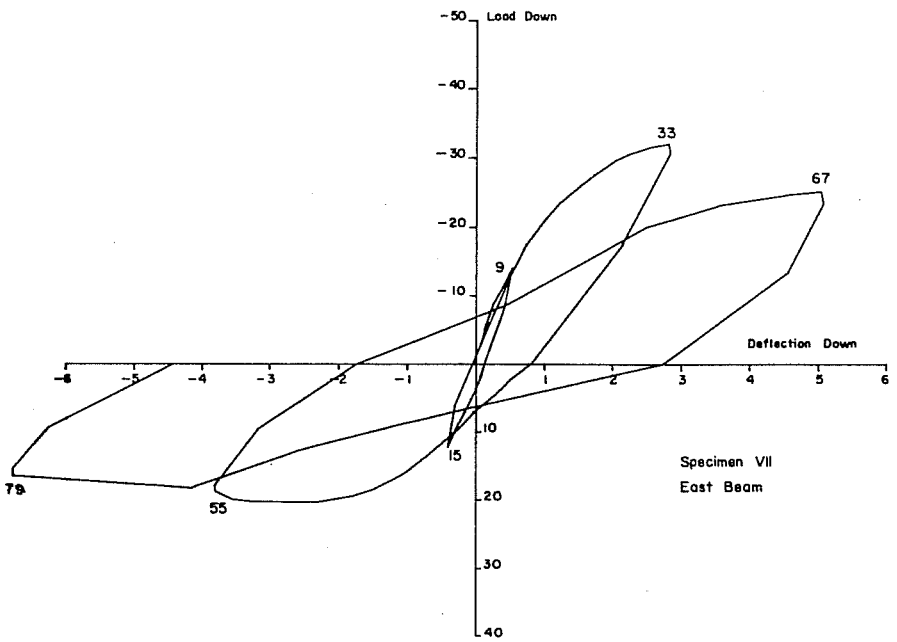
Load Down
Deflection Down
33
67
9
15
79
55
Specimen VII
East Beam

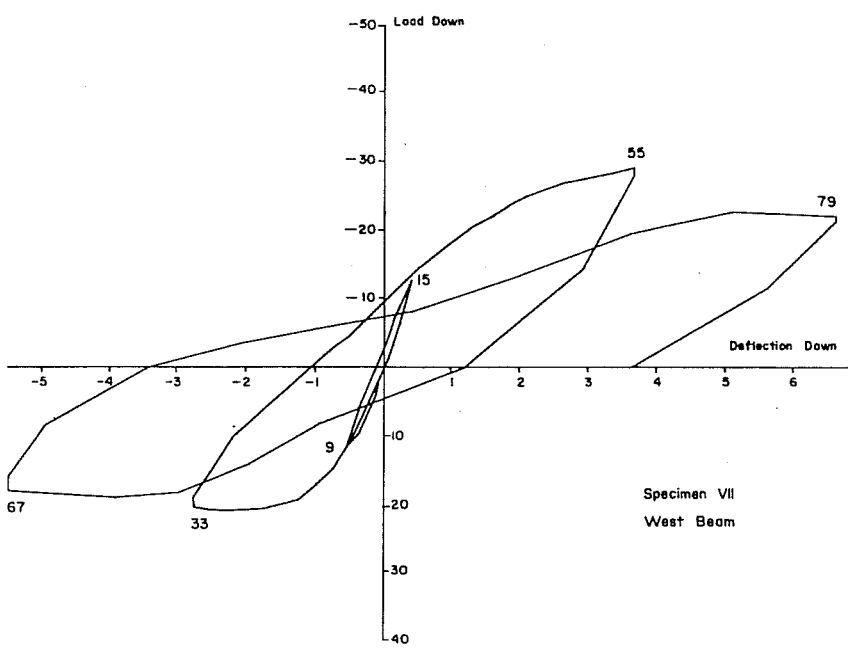
Load Down
Deflection Down
55
79
15
9
67
33
Specimen VII
West Beam

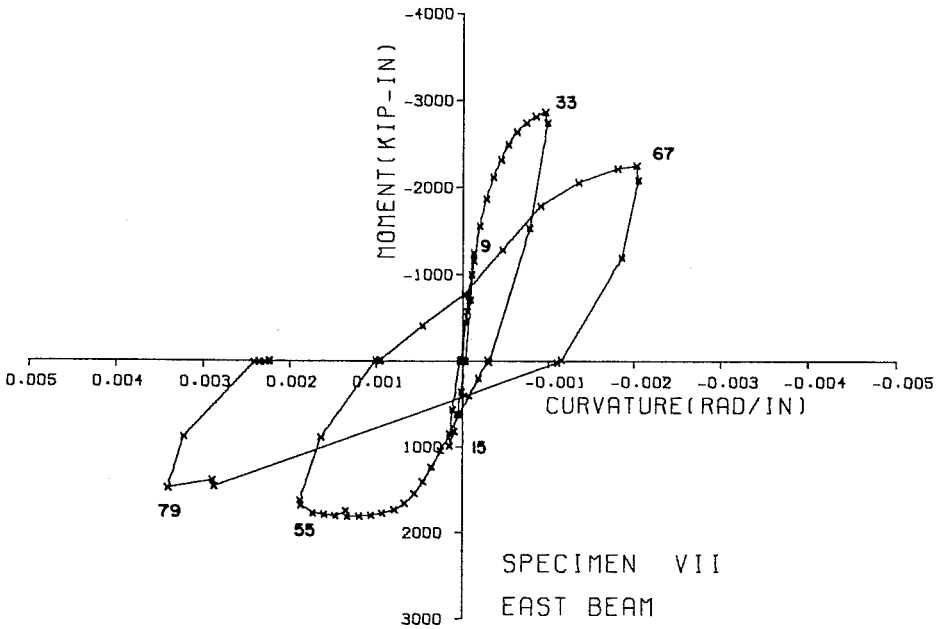
-4000
-3000
-2000
-1000
1000
2000
3000
MOMENT(KIP-IN)
0.005
0.004
0.003
0.002
0.001
-0.001
-0.002
-0.003
-0.004
-0.005
CURVATURE(RAD/IN)
33
67
9
15
79
55
SPECIMEN VII
EAST BEAM

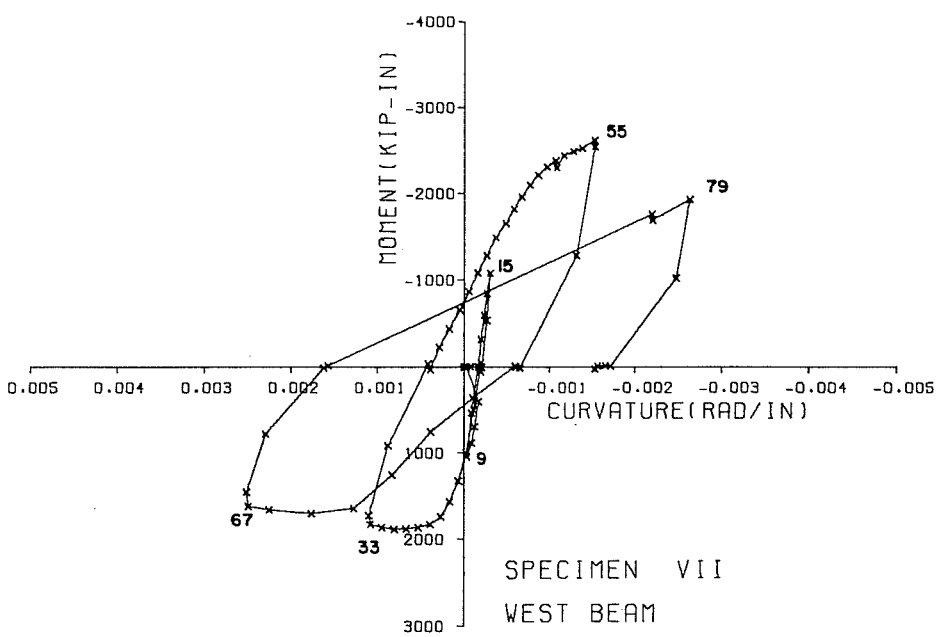
-4000
-3000
-2000
-1000
1000
2000
3000
MOMENT(KIP-IN)
0.005
0.004
0.003
0.002
0.001
-0.001
-0.002
-0.003
-0.004
-0.005
CURVATURE(RAD/IN)
55
79
15
9
67
33
SPECIMEN VII
WEST BEAM

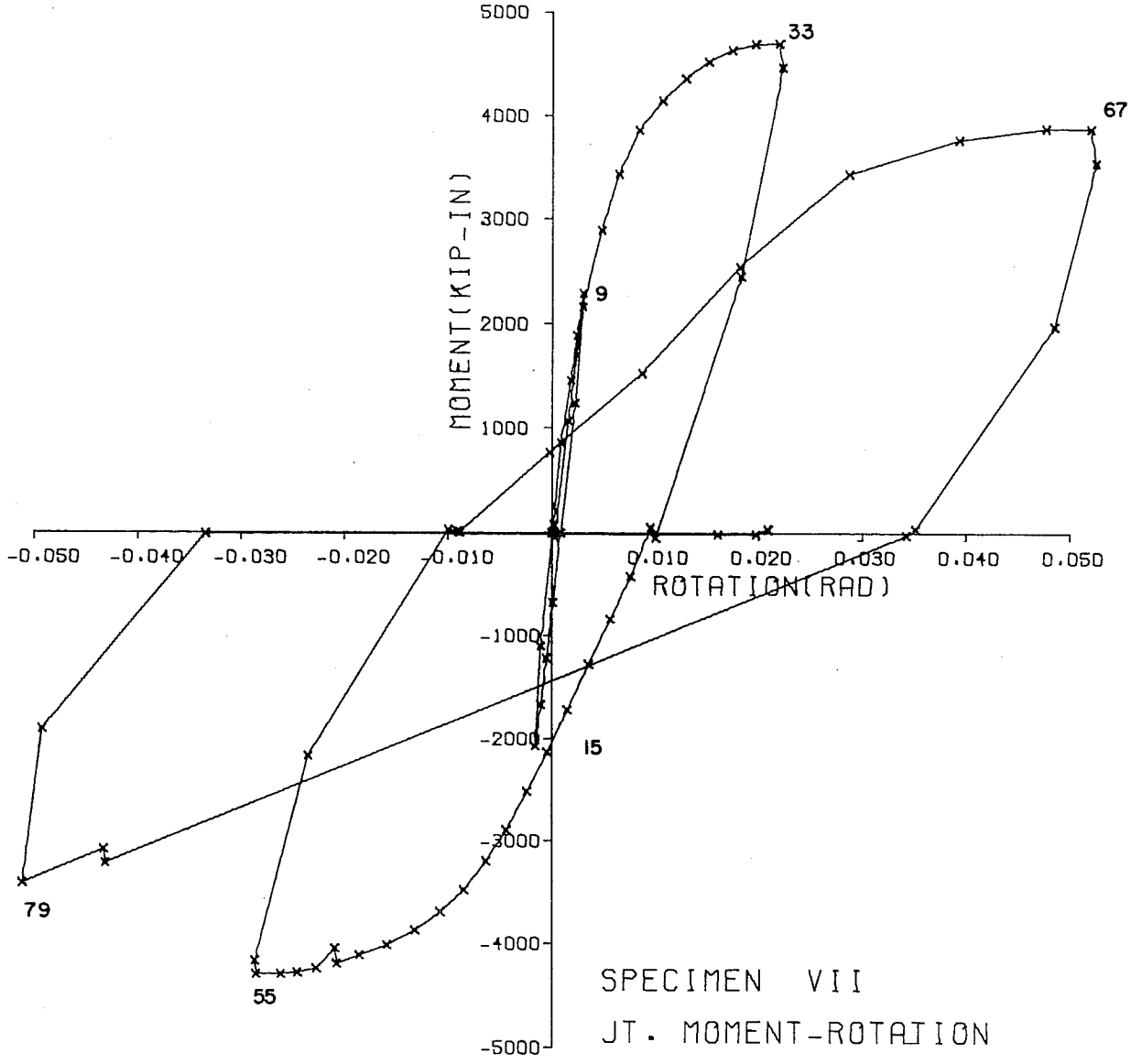
5000
4000
3000
2000
1000
-1000
-2000
-3000
-4000
-5000
MOMENT(KIP-IN)
-0.050
-0.040
-0.030
-0.020
-0.010
0.010
0.020
0.030
0.040
0.050
ROTATION(RAD)
33
67
9
15
79
55
SPECIMEN VII
JT. MOMENT-ROTATION

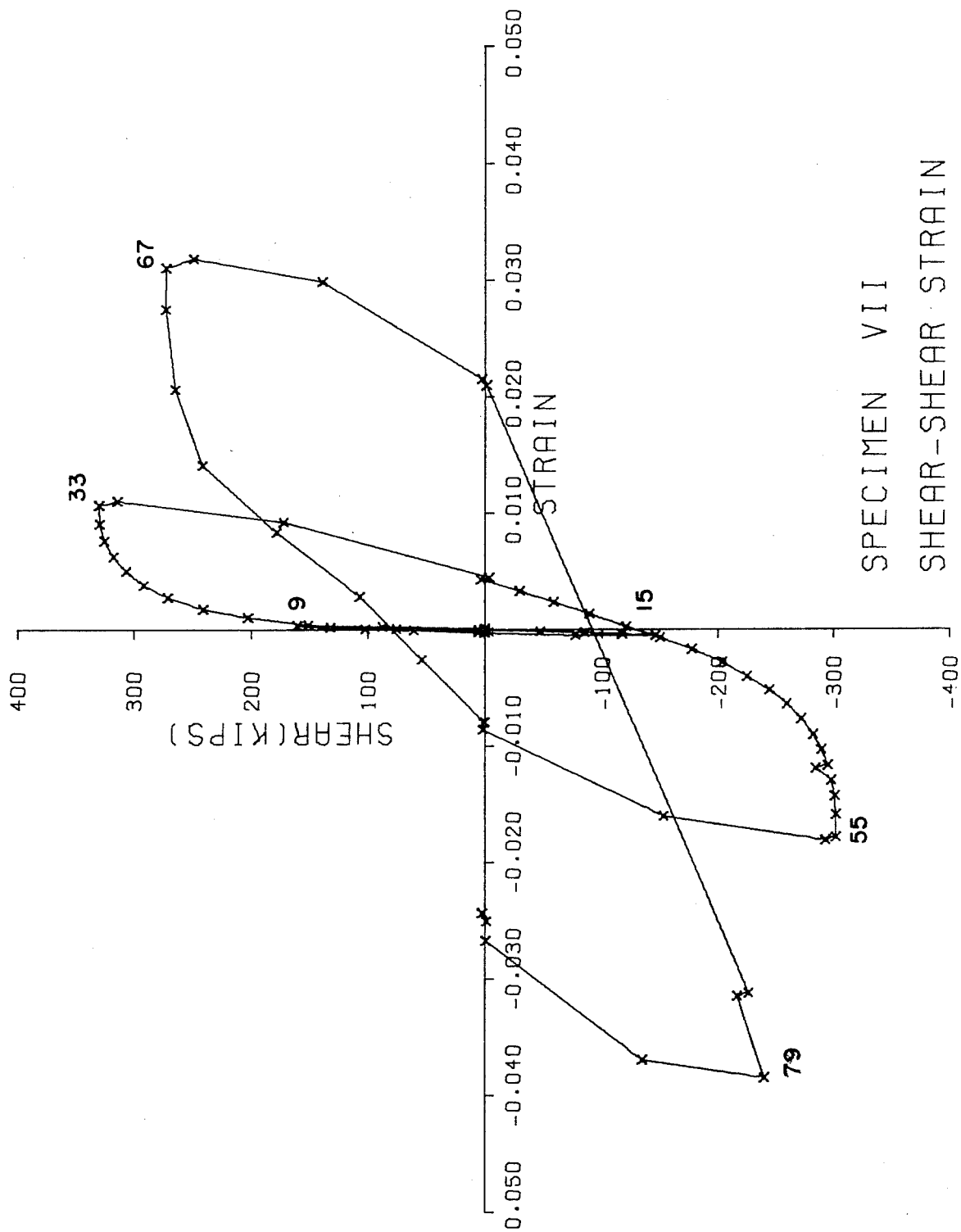
SPECIMEN VII
SHEAR-SHEAR STRAIN
SHEAR(KIPS)
STRAIN
400
300
200
100
-100
-200
-300
-400
0.050
0.040
0.030
0.020
0.010
-0.010
-0.020
-0.030
-0.040
-0.050
67
33
9
15
55
79

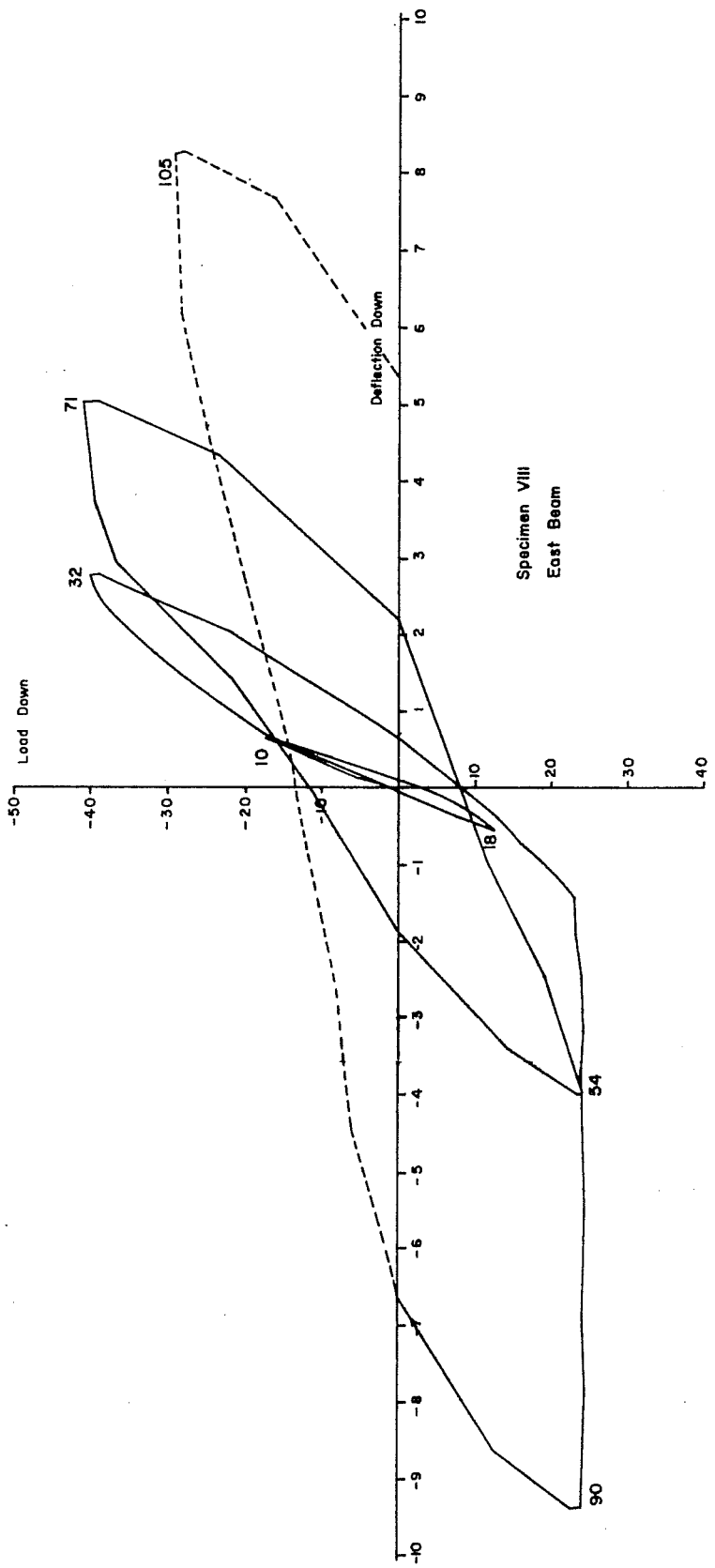
Specimen VIII
East Beam
Load Down
Deflection Down
105
71
32
10
18
54
90

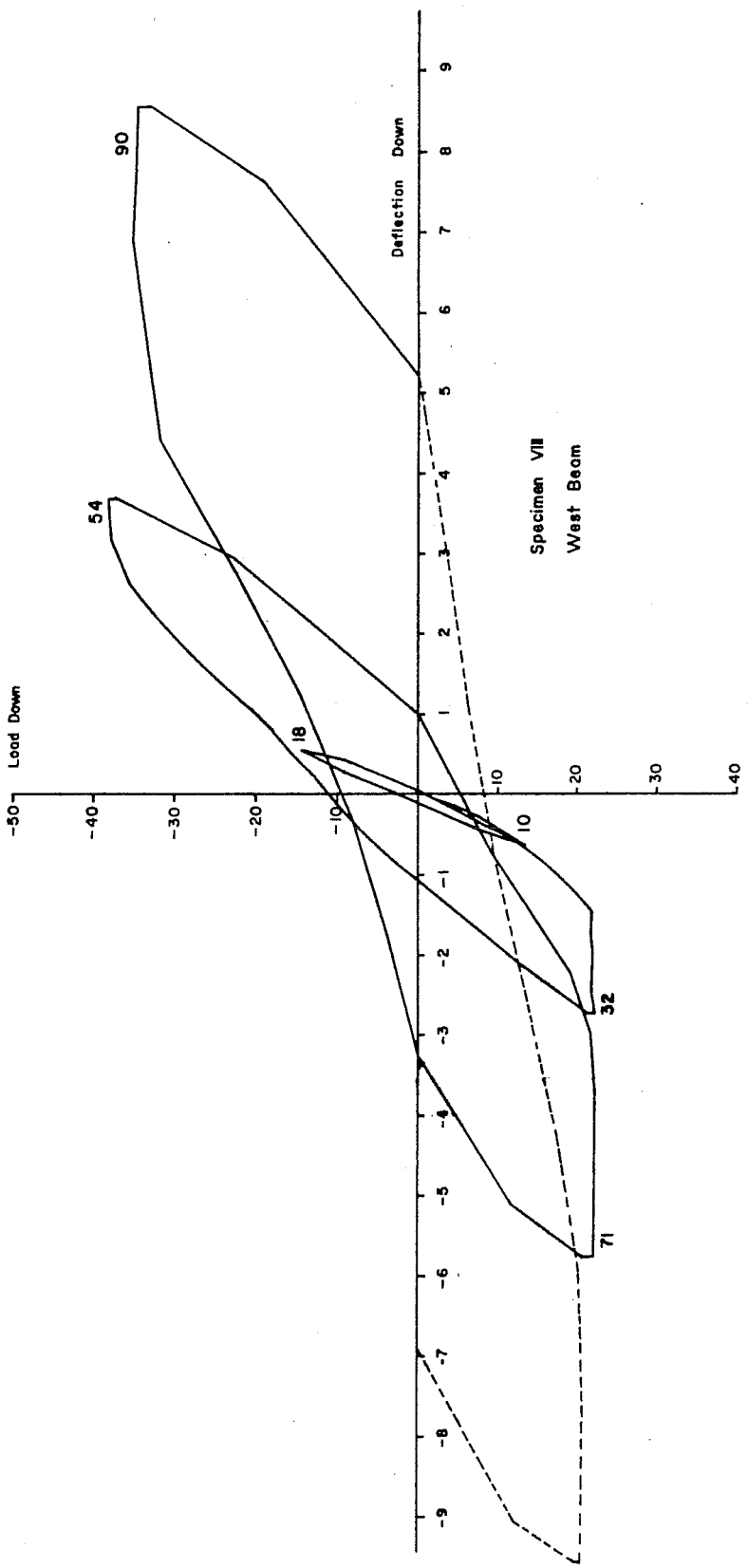
Load Down
Deflection Down
Specimen VII
West Beam
90
54
18
10
32
71
-50
-40
-30
-20
-10
10
20
30
40
-9
-8
-7
-6
-5
-4
-3
-2
-1
1
2
3
4
5
6
7
8
9

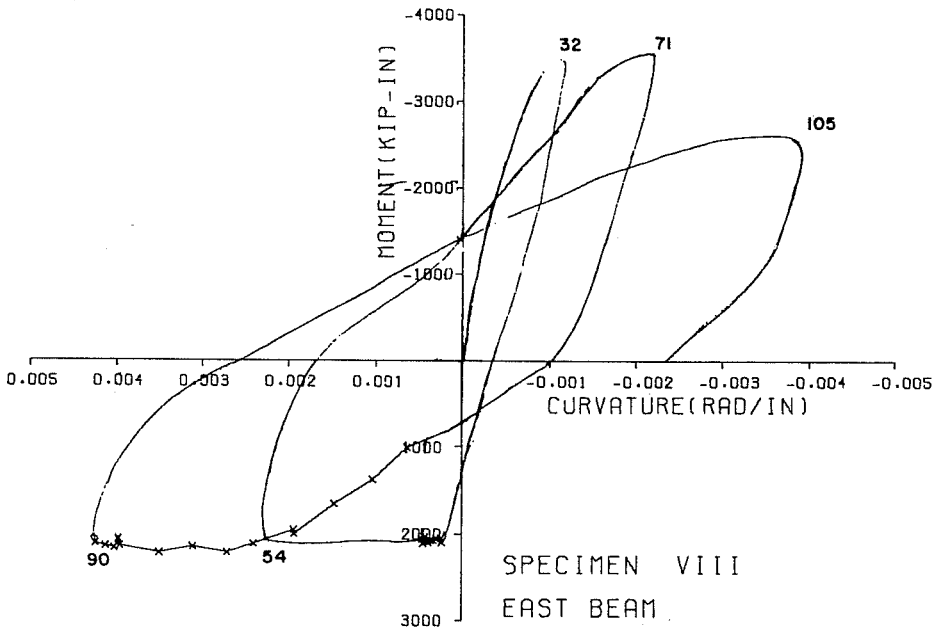
-4000
-3000
-2000
-1000
1000
2000
3000
MOMENT(KIP-IN)
0.005
0.004
0.003
0.002
0.001
-0.001
-0.002
-0.003
-0.004
-0.005
CURVATURE(RAD/IN)
32
71
105
90
54
SPECIMEN VIII
EAST BEAM

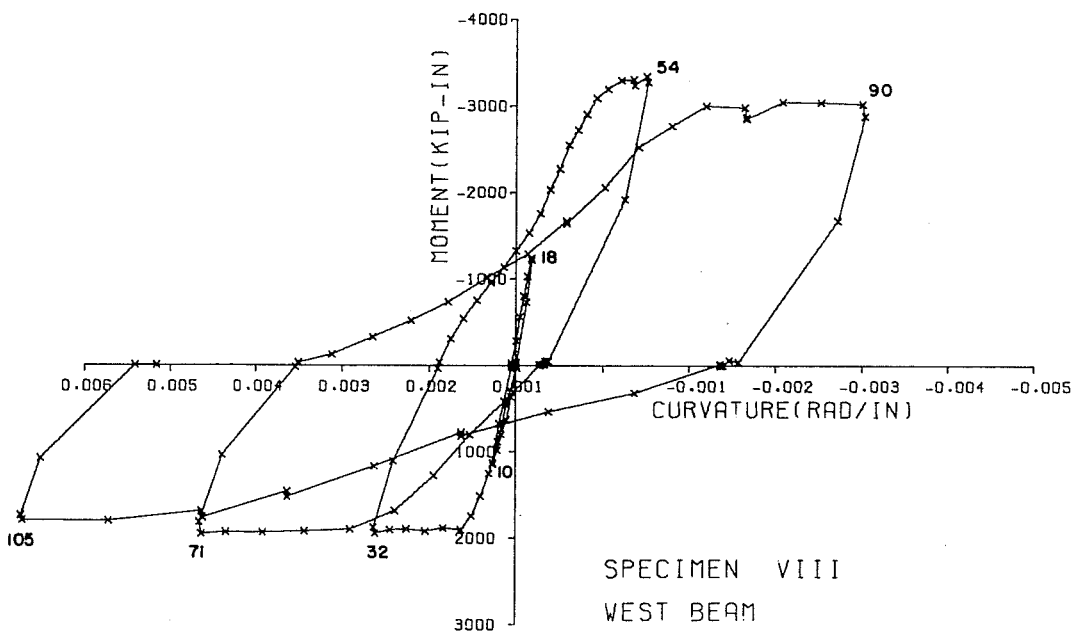
-4000
-3000
-2000
-1000
1000
2000
3000
MOMENT(KIP-IN)
0.006
0.005
0.004
0.003
0.002
0.001
-0.001
-0.002
-0.003
-0.004
-0.005
CURVATURE(RAD/IN)
54
90
18
10
105
71
32
SPECIMEN VIII
WEST BEAM

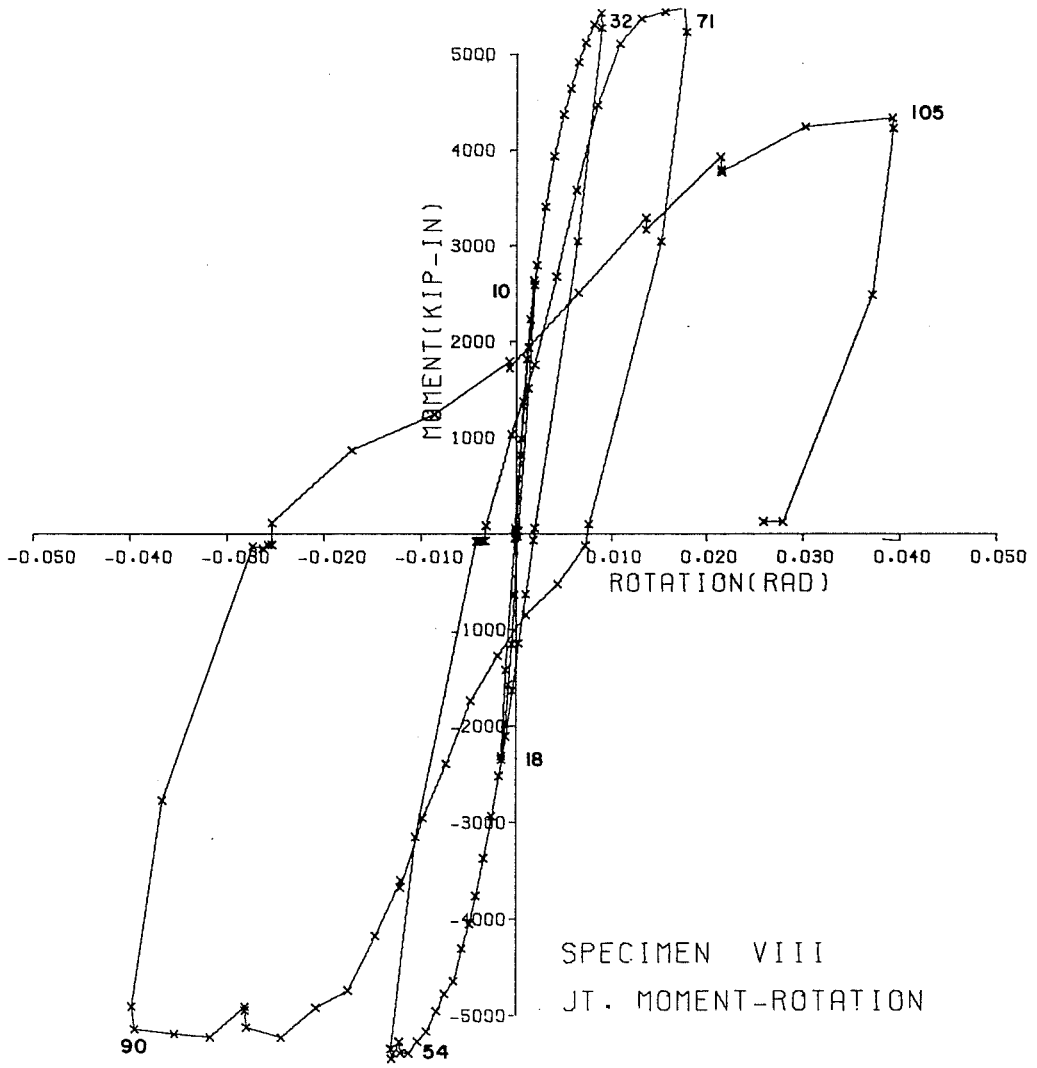
MOMENT(KIP-IN)
ROTATION(RAD)
5000
4000
3000
2000
1000
-1000
-2000
-3000
-4000
-5000
-0.050
-0.040
-0.030
-0.020
-0.010
0.010
0.020
0.030
0.040
0.050
32
71
105
10
18
90
54
SPECIMEN VIII
JT. MOMENT-ROTATION

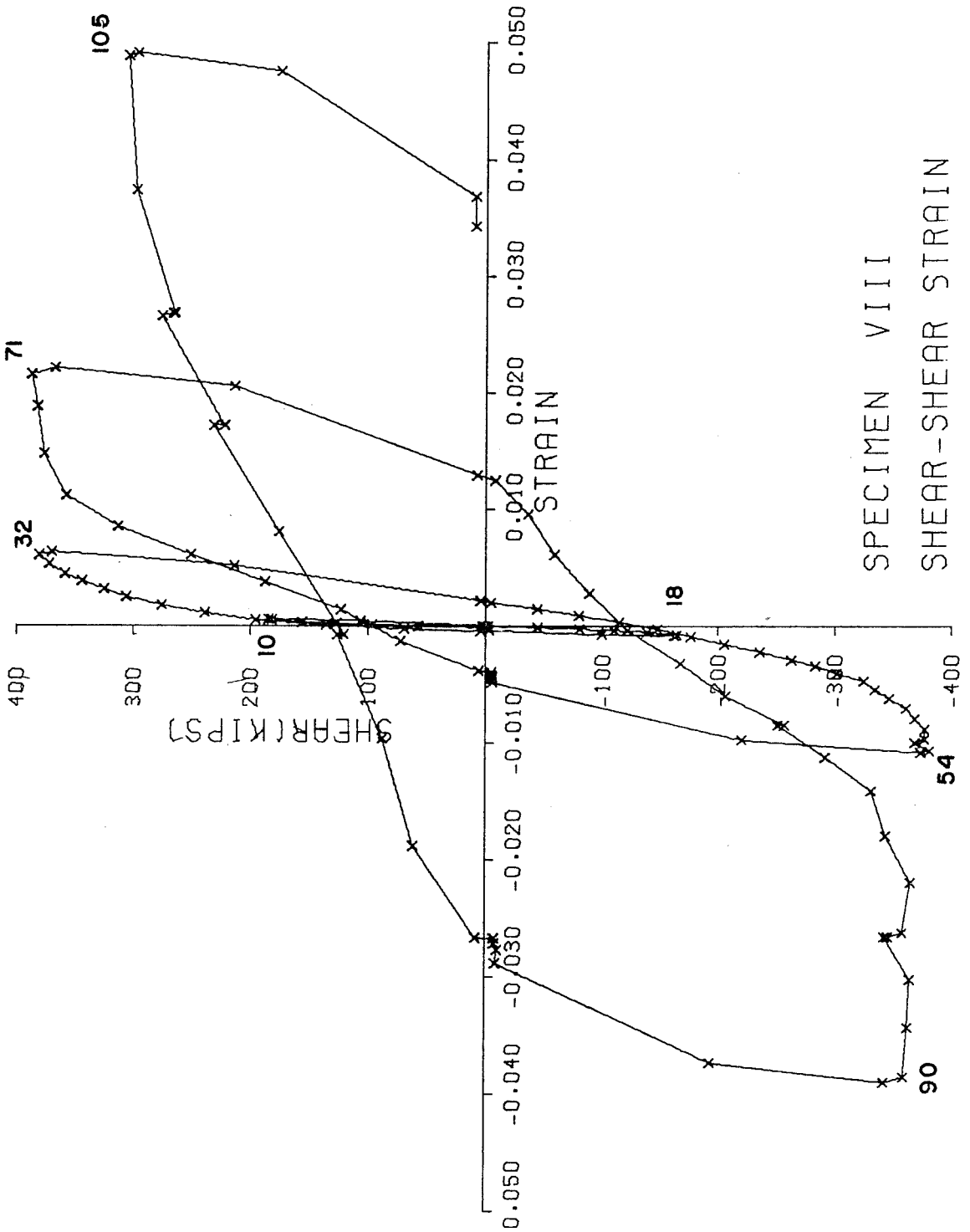
SPECIMEN VIII
SHEAR-SHEAR STRAIN
STRAIN
SHEAR(KIPS)
0.050
0.040
0.030
0.020
0.010
-0.010
-0.020
-0.030
-0.040
-0.050
400
300
200
100
-100
-200
-300
-400
105
71
32
10
18
54
90

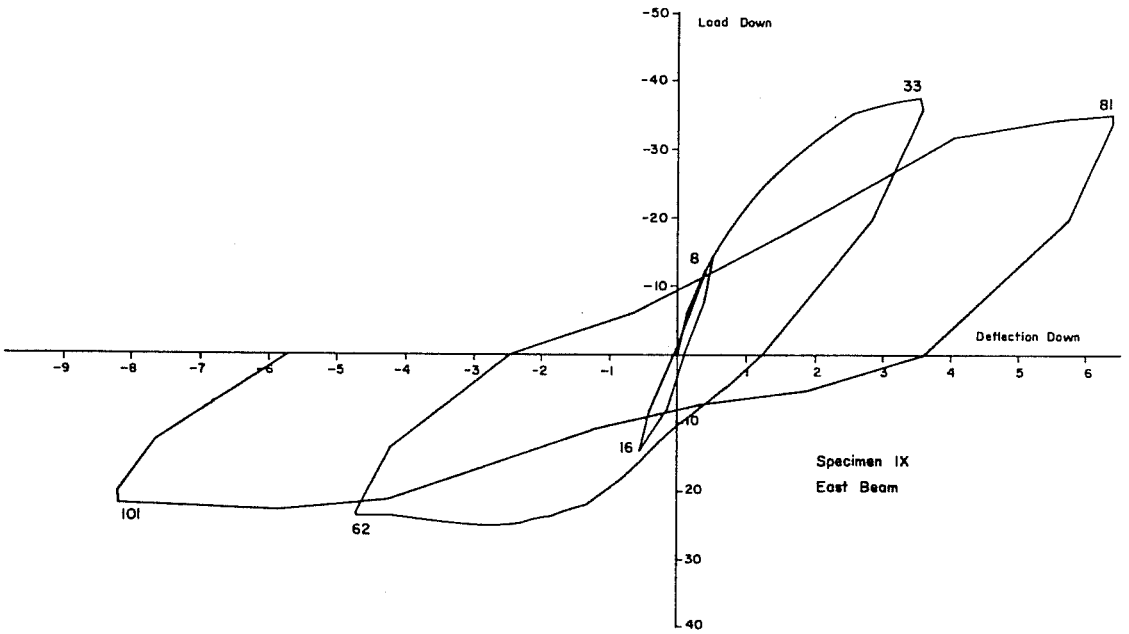
Load Down
Deflection Down
33
81
8
16
101
62
Specimen IX
East Beam

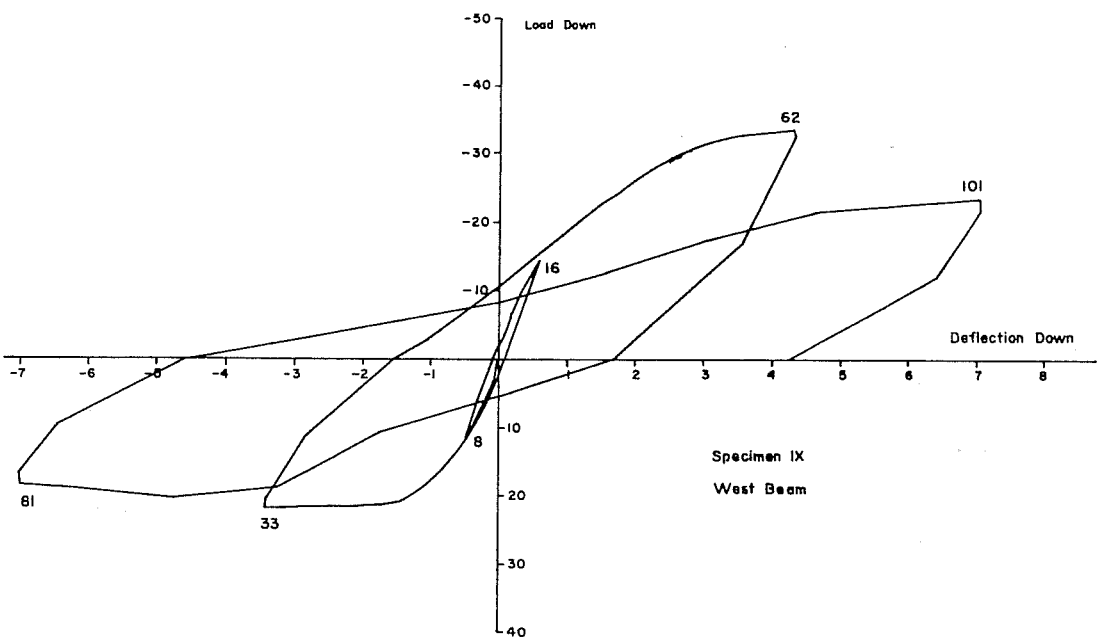
Load Down
Deflection Down
62
101
16
8
81
33
Specimen IX
West Beam

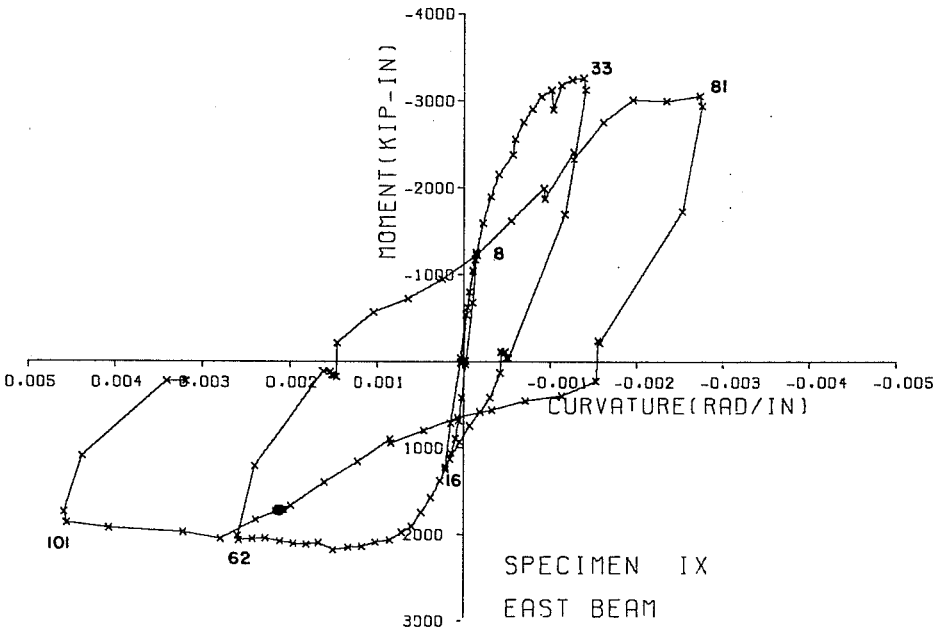
-4000
-3000
-2000
-1000
1000
2000
3000
MOMENT(KIP-IN)
0.005
0.004
0.003
0.002
0.001
-0.001
-0.002
-0.003
-0.004
-0.005
CURVATURE(RAD/IN)
33
81
8
16
101
62
SPECIMEN IX
EAST BEAM

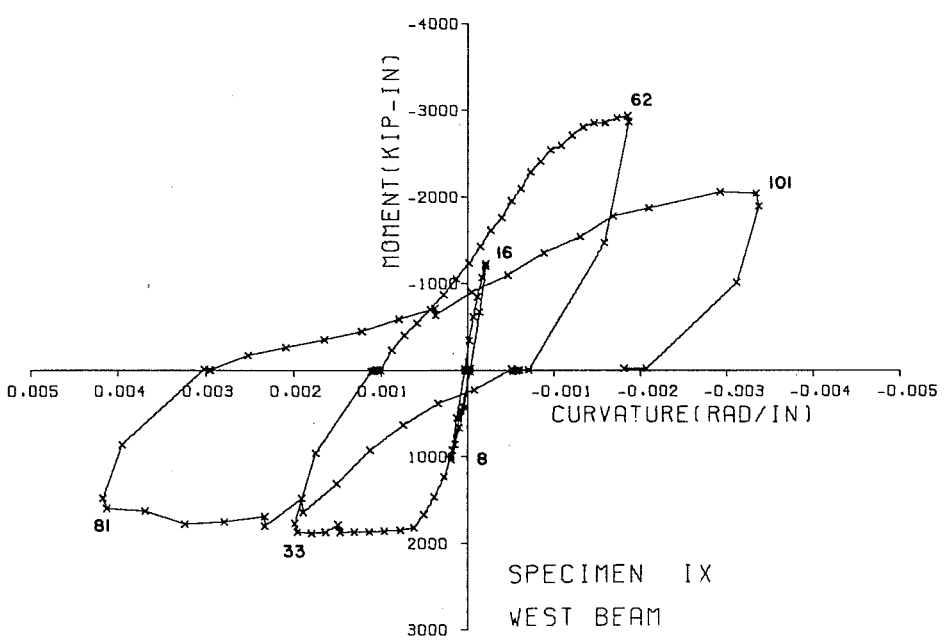
-4000
-3000
-2000
-1000
1000
2000
3000
MOMENT(KIP-IN)
0.005
0.004
0.003
0.002
0.001
-0.001
-0.002
-0.003
-0.004
-0.005
CURVATURE(RAD/IN)
62
101
16
8
81
33
SPECIMEN IX
WEST BEAM

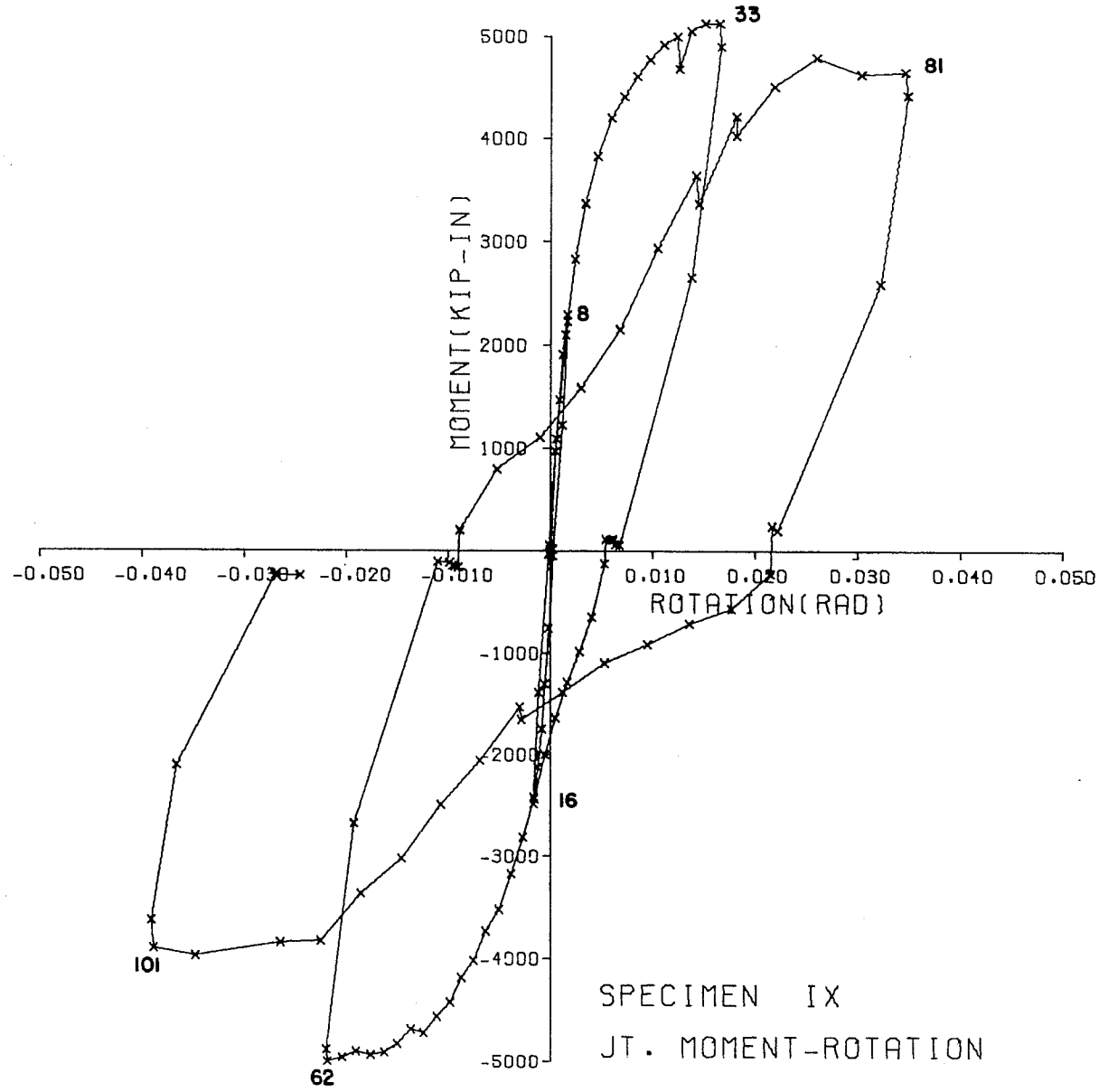
33
81
8
16
101
62
5000
4000
3000
2000
1000
-1000
-2000
-3000
-4000
-5000
MOMENT(KIP-IN)
-0.050
-0.040
-0.030
-0.020
-0.010
0.010
0.020
0.030
0.040
0.050
ROTATION(RAD)
SPECIMEN IX
JT. MOMENT-ROTATION

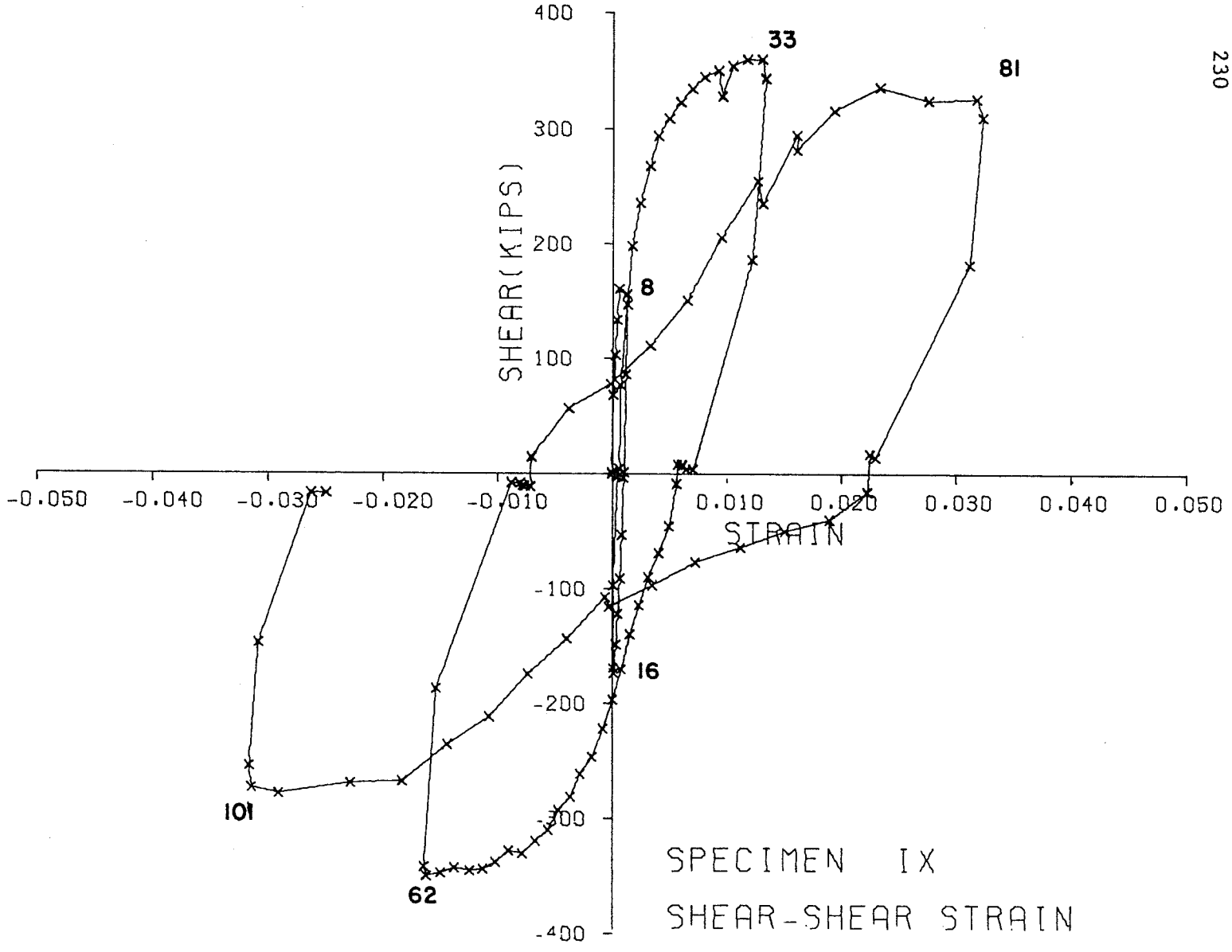
400
300
200
100
-100
-200
-300
-400
SHEAR(KIPS)
-0.050
-0.040
-0.030
-0.020
-0.010
0.010
0.020
0.030
0.040
0.050
STRAIN
33
81
8
16
101
62
SPECIMEN IX
SHEAR-SHEAR STRAIN

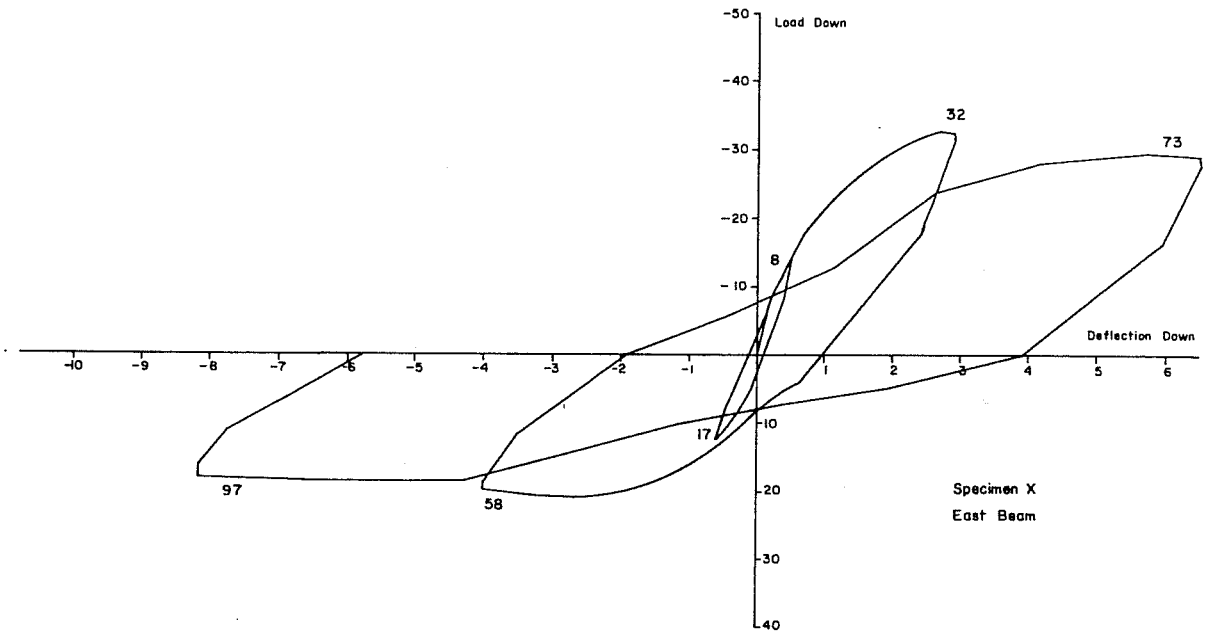
Load Down
Deflection Down
32
73
8
17
97
58
Specimen X
East Beam

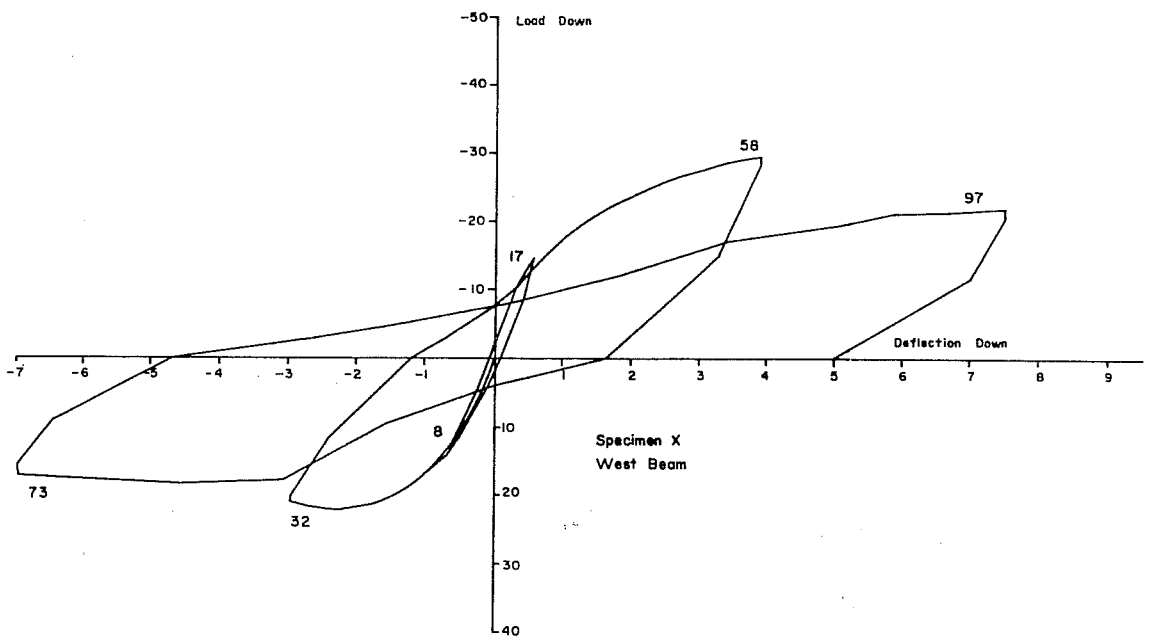
Load Down
Deflection Down
58
97
17
8
73
32
Specimen X
West Beam

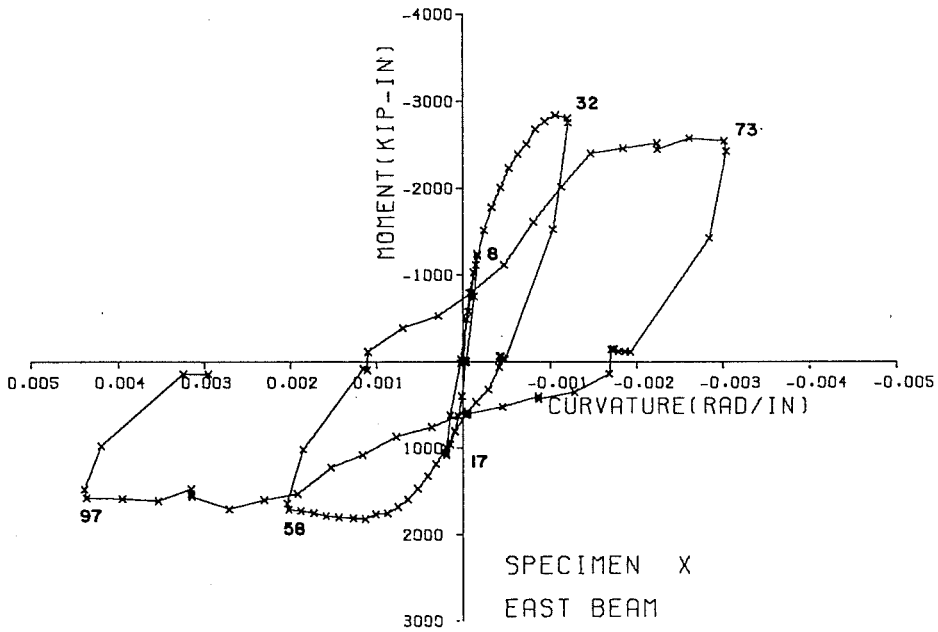
-4000
-3000
-2000
-1000
1000
2000
3000
MOMENT(KIP-IN)
0.005
0.004
0.003
0.002
0.001
-0.001
-0.002
-0.003
-0.004
-0.005
CURVATURE(RAD/IN)
32
73
8
17
97
58
SPECIMEN X
EAST BEAM

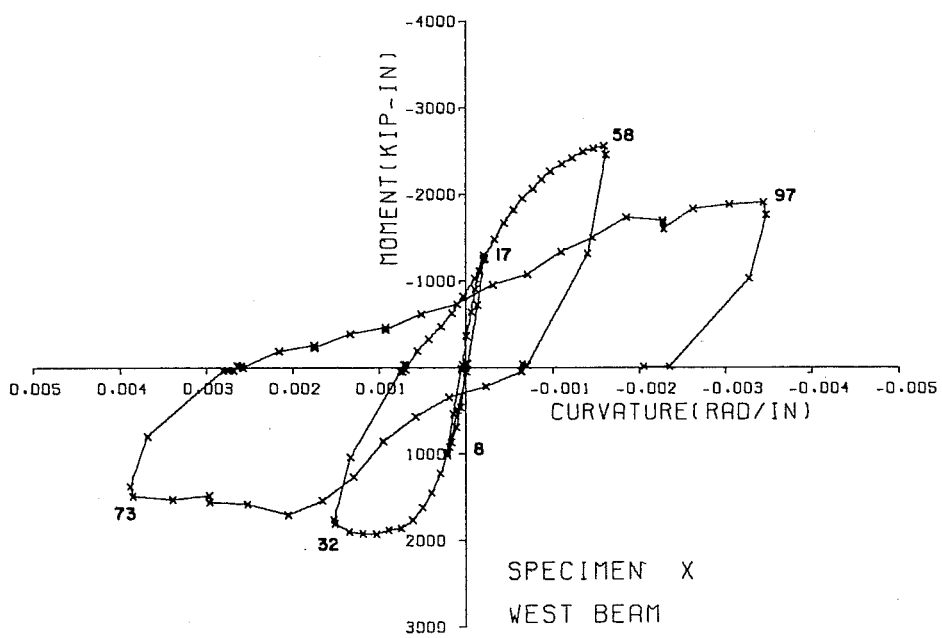
-4000
-3000
-2000
-1000
1000
2000
3000
MOMENT(KIP-IN)
0.005
0.004
0.003
0.002
0.001
-0.001
-0.002
-0.003
-0.004
-0.005
CURVATURE(RAD/IN)
58
97
17
8
73
32
SPECIMEN X
WEST BEAM

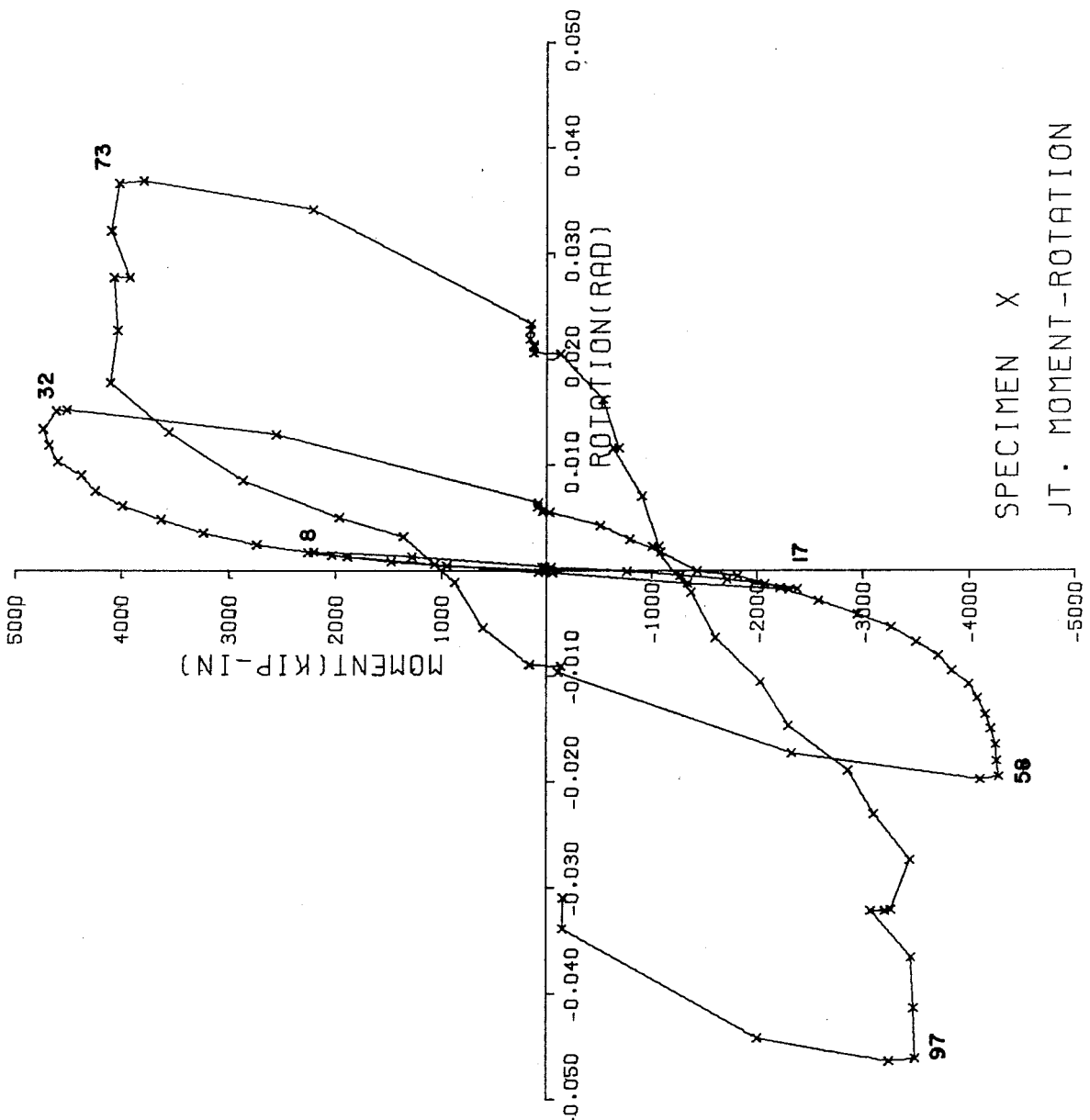
SPECIMEN X
JT. MOMENT-ROTATION
MOMENT(KIP-IN)
ROTATION(RAD)
5000
4000
3000
2000
1000
-1000
-2000
-3000
-4000
-5000
0.050
0.040
0.030
0.020
0.010
-0.010
-0.020
-0.030
-0.040
-0.050
73
32
8
17
58
97

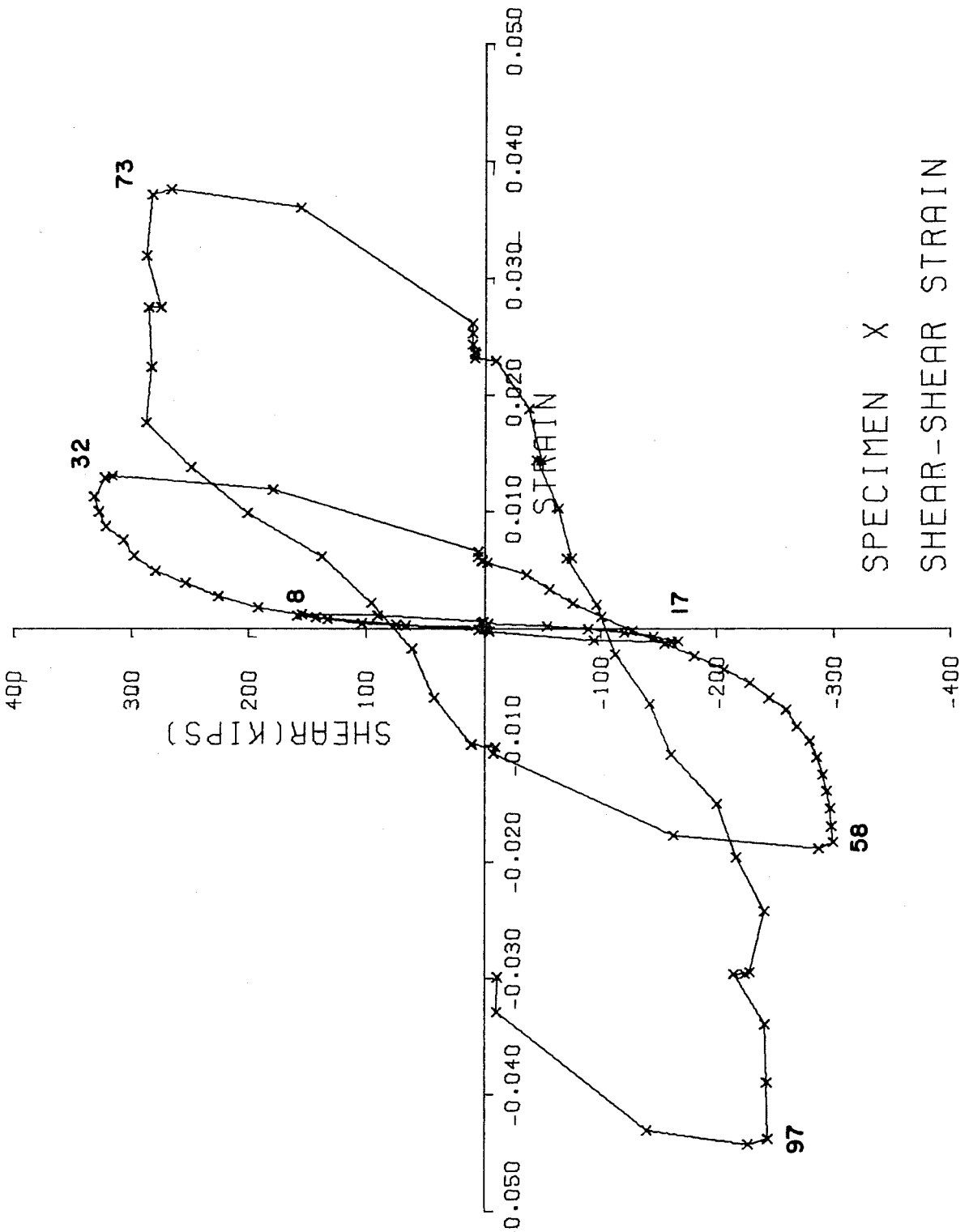
SPECIMEN X
SHEAR-SHEAR STRAIN
SHEAR(KIPS)
STRAIN
400
300
200
100
-100
-200
-300
-400
0.050
0.040
0.030
0.020
0.010
-0.010
-0.020
-0.030
-0.040
-0.050
73
32
8
17
58
97

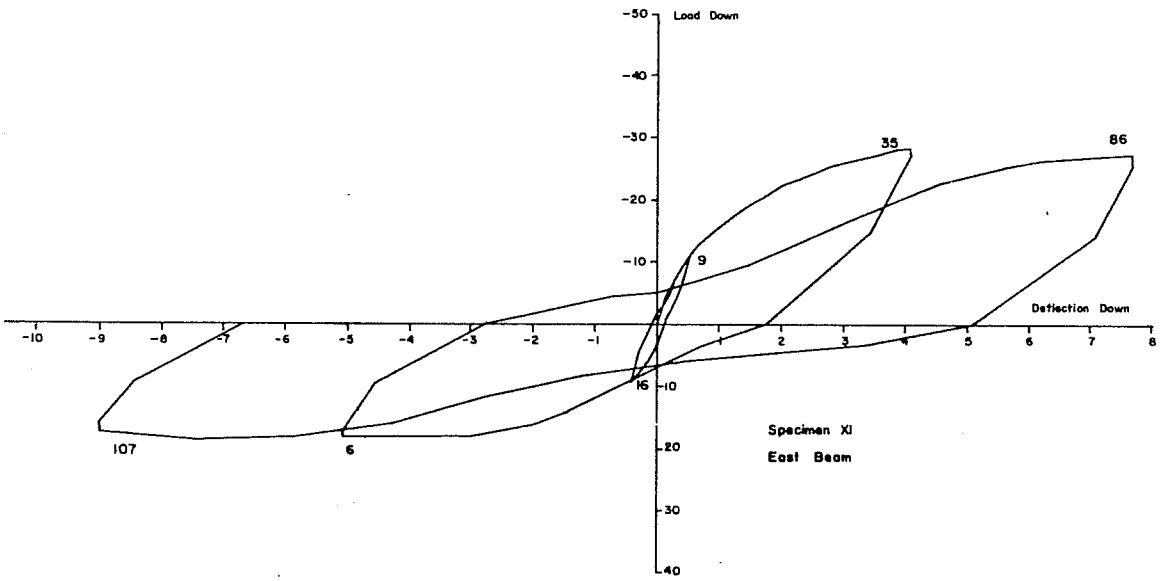
Load Down
Deflection Down
35
86
9
16
107
6
Specimen XI
East Beam

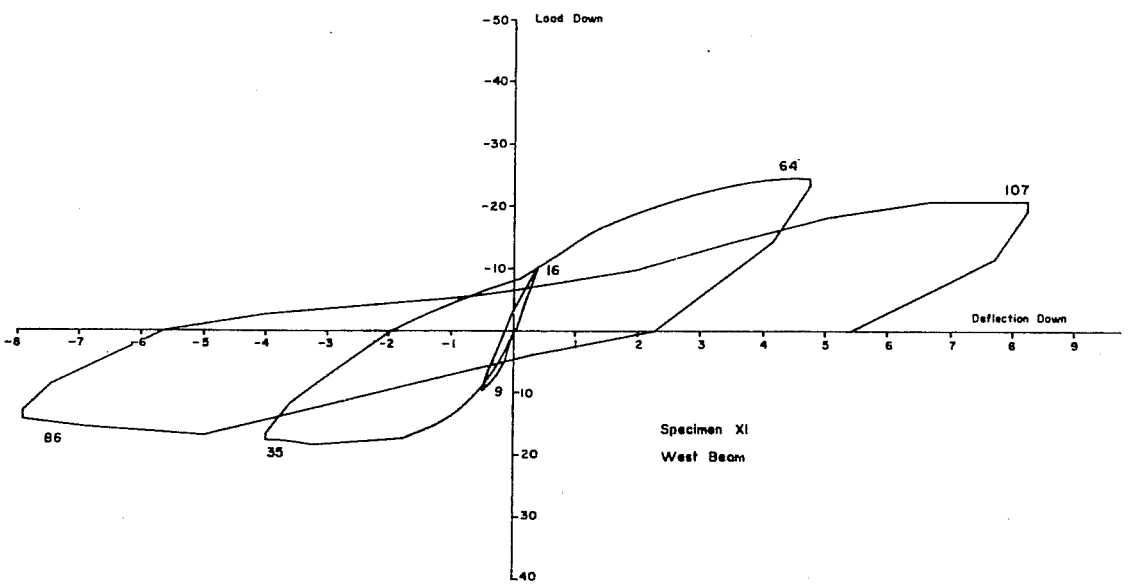
Load Down
Deflection Down
64
107
16
9
86
35
Specimen XI
West Beam

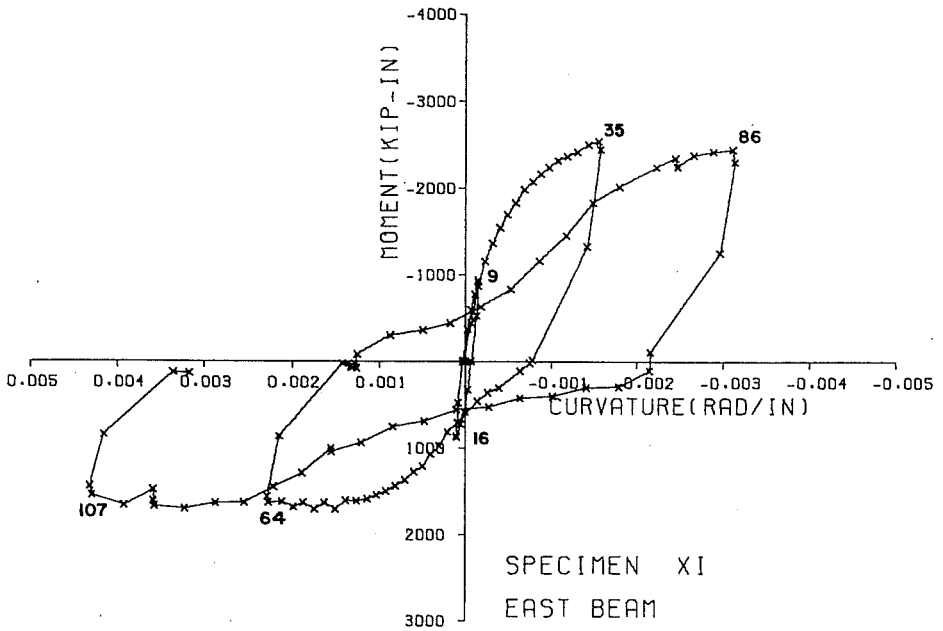
-4000
-3000
-2000
-1000
1000
2000
3000
MOMENT(KIP-IN)
0.005
0.004
0.003
0.002
0.001
-0.001
-0.002
-0.003
-0.004
-0.005
CURVATURE(RAD/IN)
35
86
9
16
107
64
SPECIMEN XI
EAST BEAM

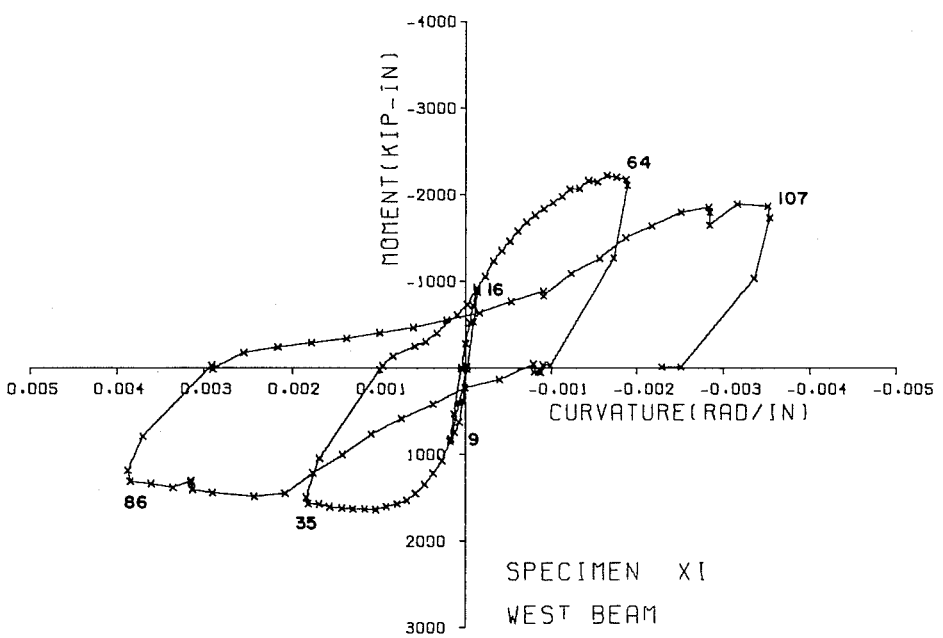
-4000
-3000
-2000
-1000
1000
2000
3000
MOMENT(KIP-IN)
0.005
0.004
0.003
0.002
0.001
-0.001
-0.002
-0.003
-0.004
-0.005
CURVATURE(RAD/IN)
64
107
16
9
86
35
SPECIMEN XI
WEST BEAM

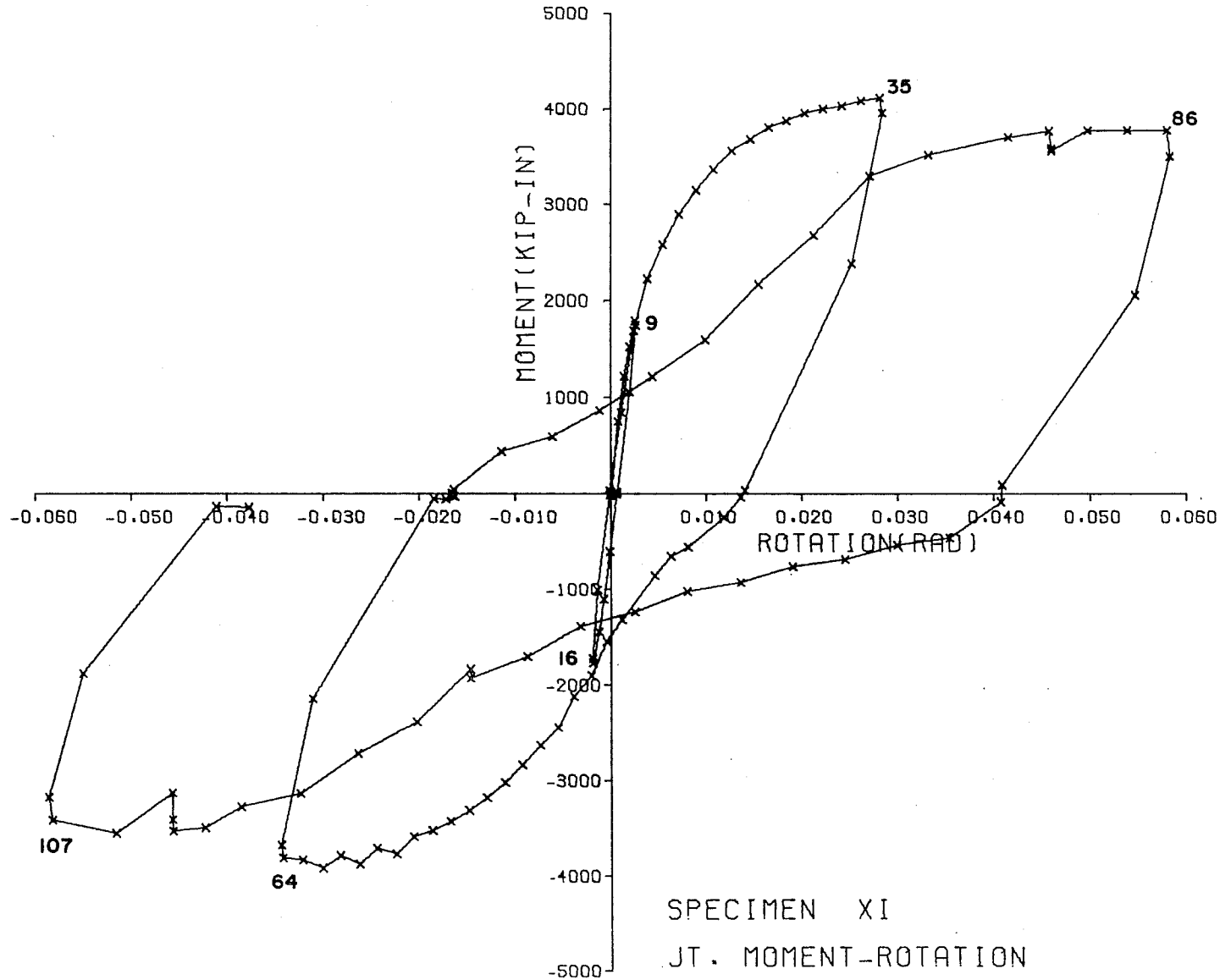
5000
4000
3000
2000
1000
-1000
-2000
-3000
-4000
-5000
MOMENT(KIP-IN)
-0.060
-0.050
-0.040
-0.030
-0.020
-0.010
0.010
0.020
0.030
0.040
0.050
0.060
ROTATION(RAD)
35
86
9
16
107
64
SPECIMEN XI
JT. MOMENT-ROTATION

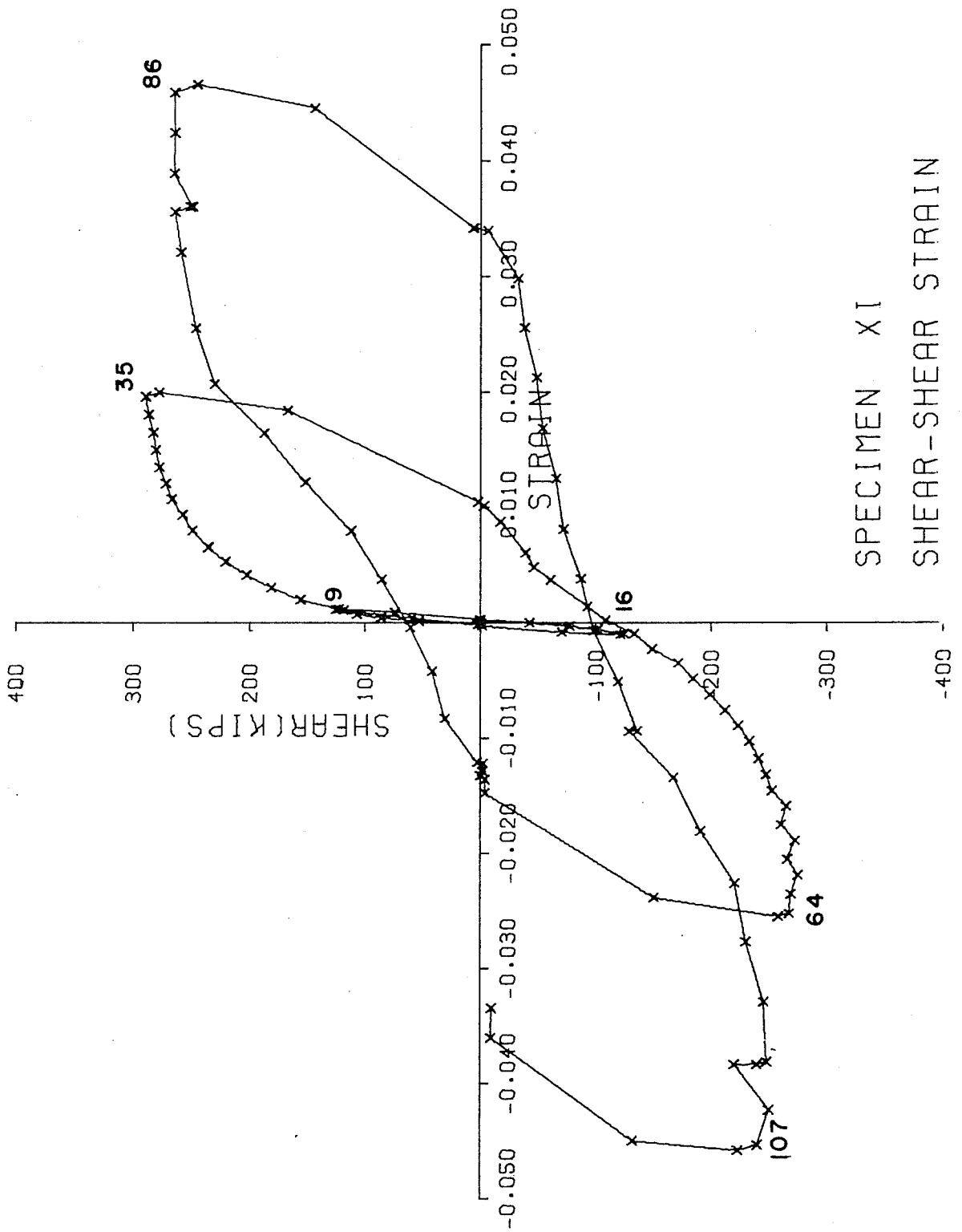
SPECIMEN XI
SHEAR-SHEAR STRAIN
SHEAR(KIPS)
STRAIN
400
300
200
100
-100
-200
-300
-400
0.050
0.040
0.030
0.020
0.010
-0.010
-0.020
-0.030
-0.040
-0.050
86
35
9
16
64
107

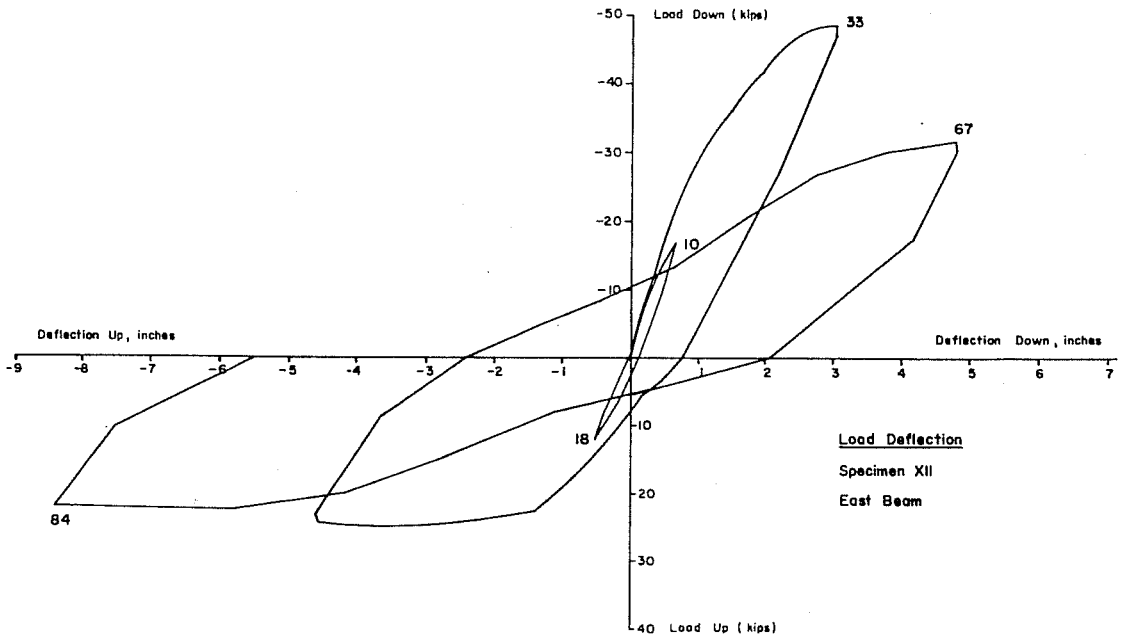
Load Down (kips)
-50
-40
-30
-20
-10
33
67
10
18
84
Deflection Up, inches
Deflection Down, inches
-9 -8 -7 -6 -5 -4 -3 -2 -1 1 2 3 4 5 6 7
10
20
30
40 Load Up (kips)
Load Deflection
Specimen XII
East Beam

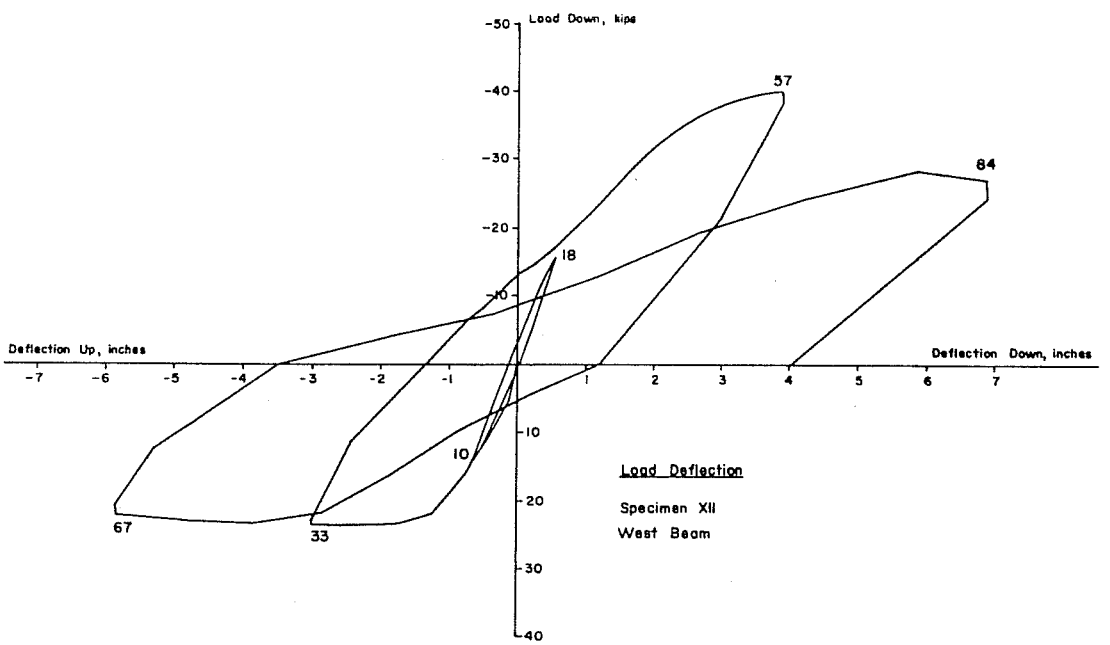
Load Down, kips
-50
-40
-30
-20
-10
57
84
18
10
67
33
Deflection Up, inches
Deflection Down, inches
-7 -6 -5 -4 -3 -2 -1 1 2 3 4 5 6 7
10
20
30
40
Load Deflection
Specimen XII
West Beam

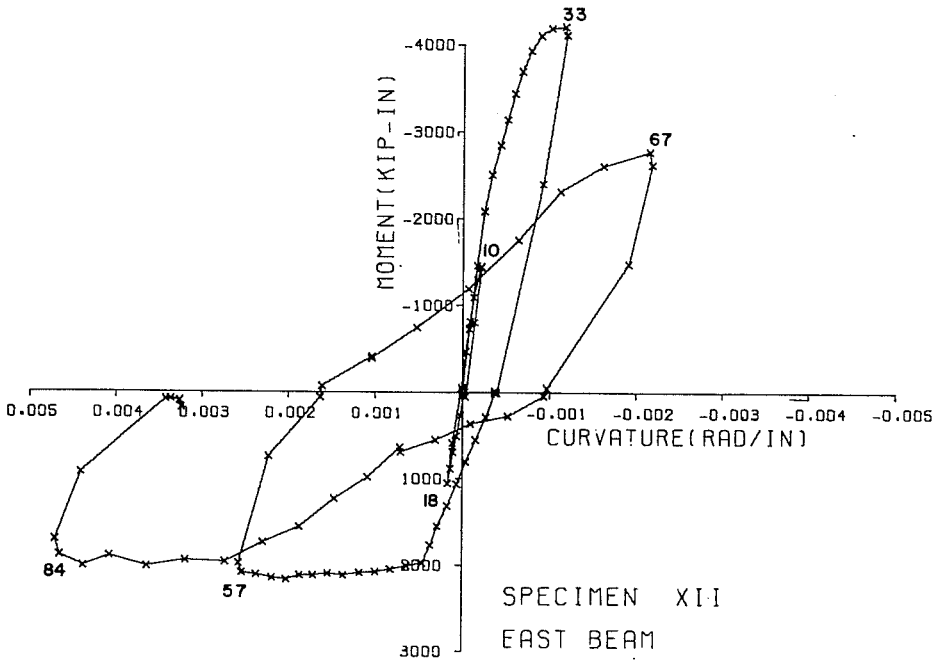
33
67
10
18
84
57
MOMENT(KIP-IN)
-4000
-3000
-2000
-1000
1000
2000
3000
0.005
0.004
0.003
0.002
0.001
-0.001
-0.002
-0.003
-0.004
-0.005
CURVATURE(RAD/IN)
SPECIMEN XII
EAST BEAM

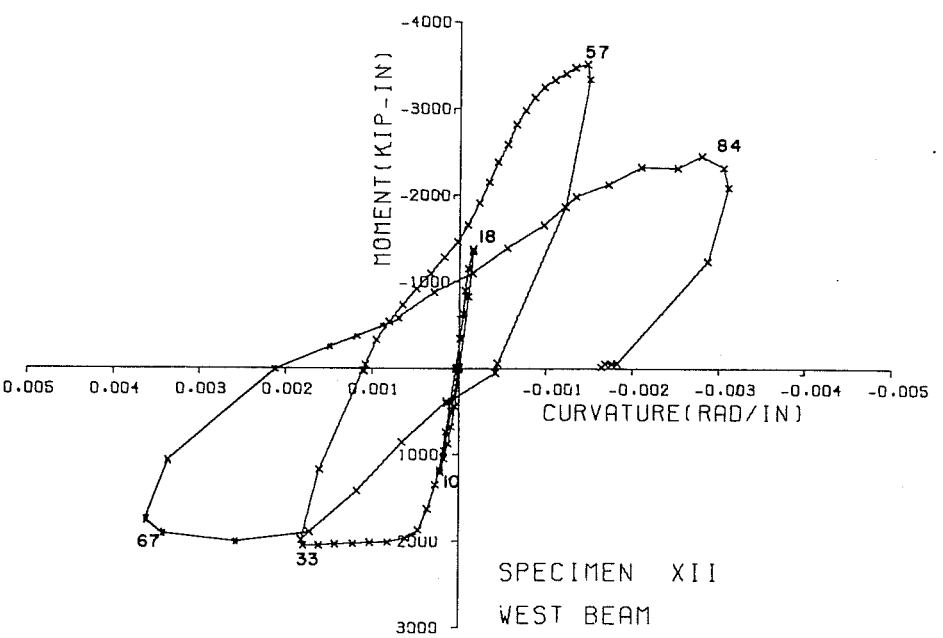
57
84
18
10
67
33
MOMENT(KIP-IN)
-4000
-3000
-2000
-1000
1000
2000
3000
0.005
0.004
0.003
0.002
0.001
-0.001
-0.002
-0.003
-0.004
-0.005
CURVATURE(RAD/IN)
SPECIMEN XII
WEST BEAM

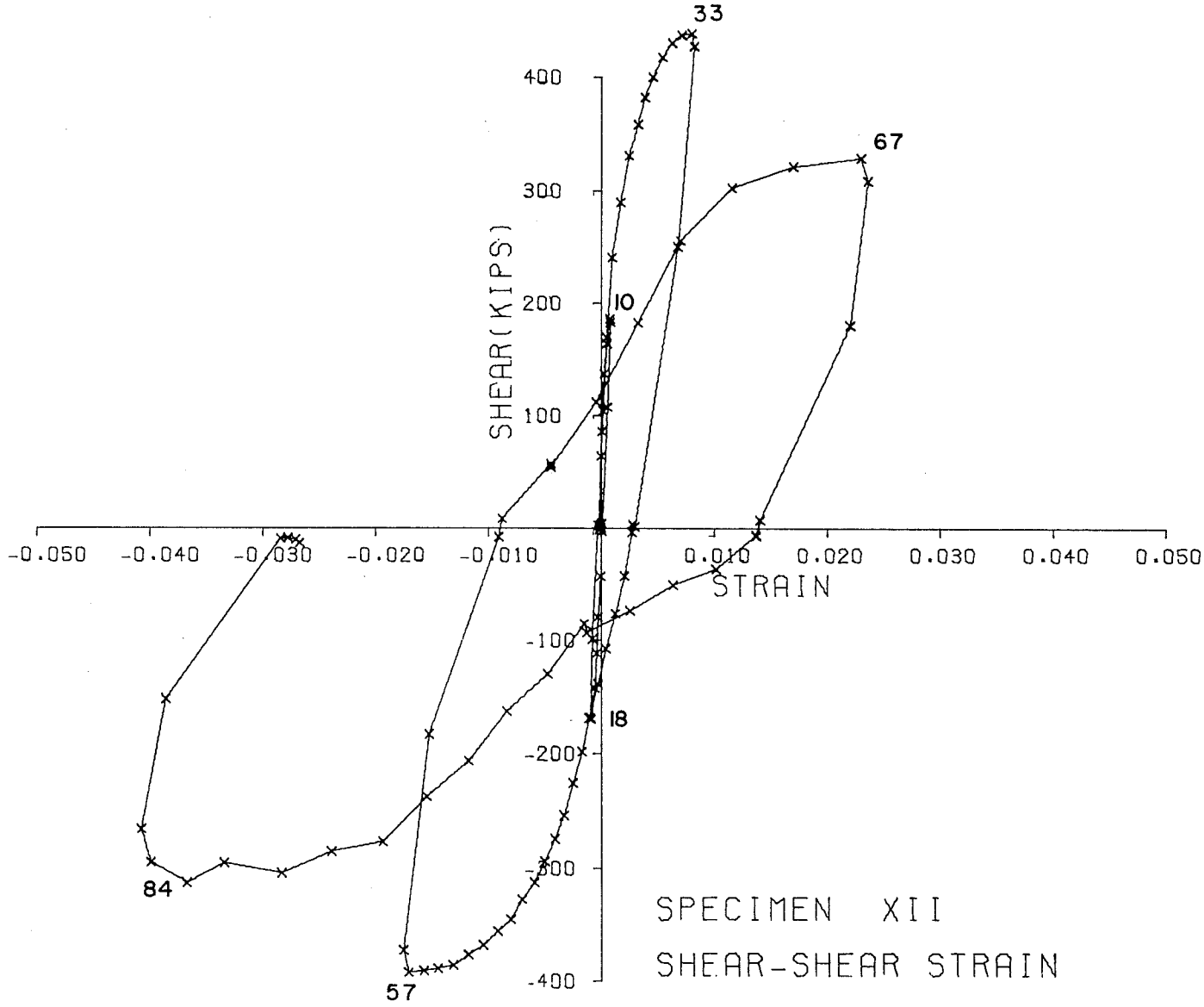
33
67
10
18
84
57
400
300
200
100
-100
-200
-300
-400
SHEAR(KIPS)
-0.050
-0.040
-0.030
-0.020
-0.010
0.010
0.020
0.030
0.040
0.050
STRAIN
SPECIMEN XII
SHEAR-SHEAR STRAIN

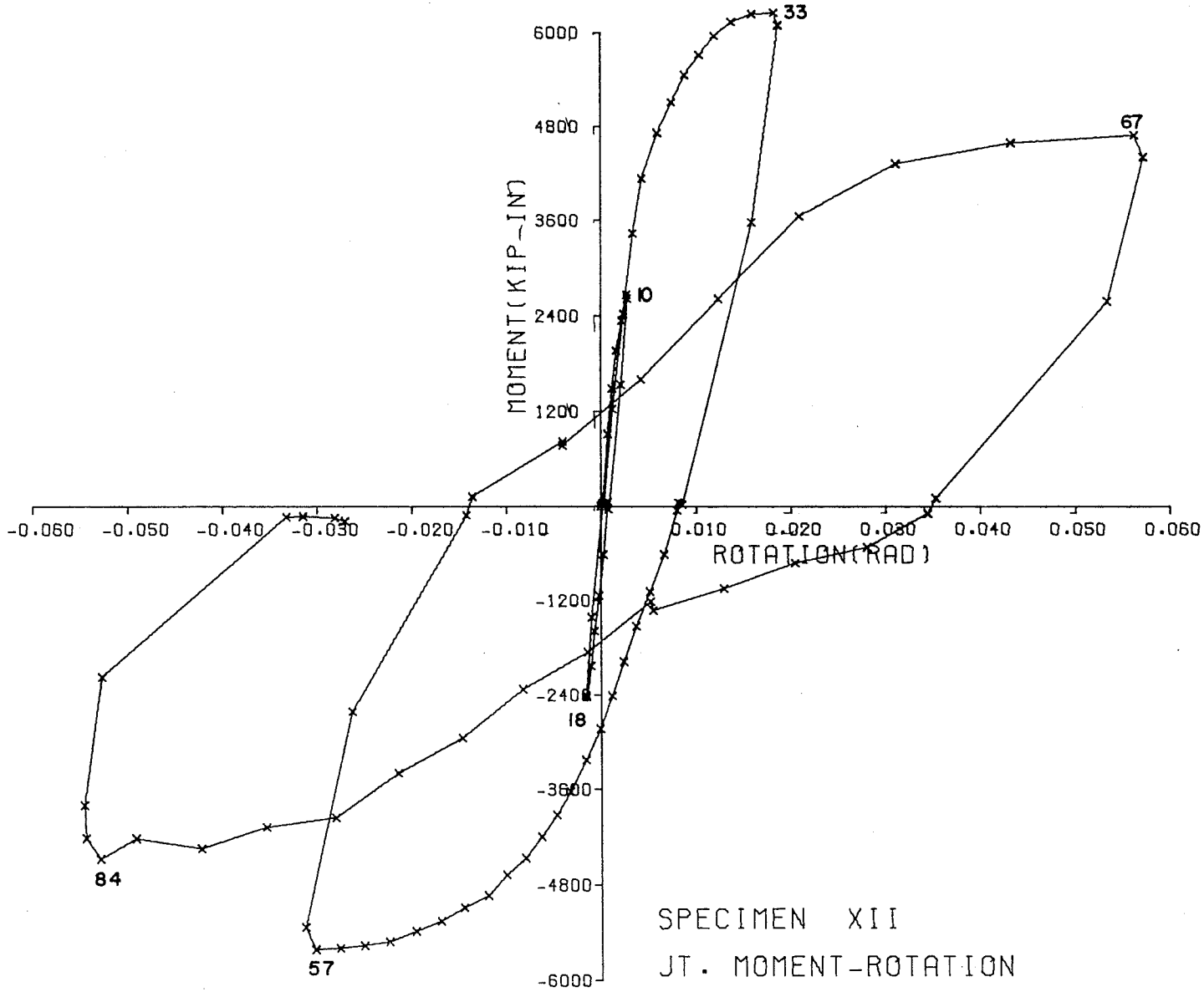
MOMENT(KIP-IN)
ROTATION(RAD)
6000
4800
3600
2400
1200
-1200
-2400
-3600
-4800
-6000
-0.060
-0.050
-0.040
-0.030
-0.020
-0.010
0.010
0.020
0.030
0.040
0.050
0.060
33
67
10
18
84
57
SPECIMEN XII
JT. MOMENT-ROTATION

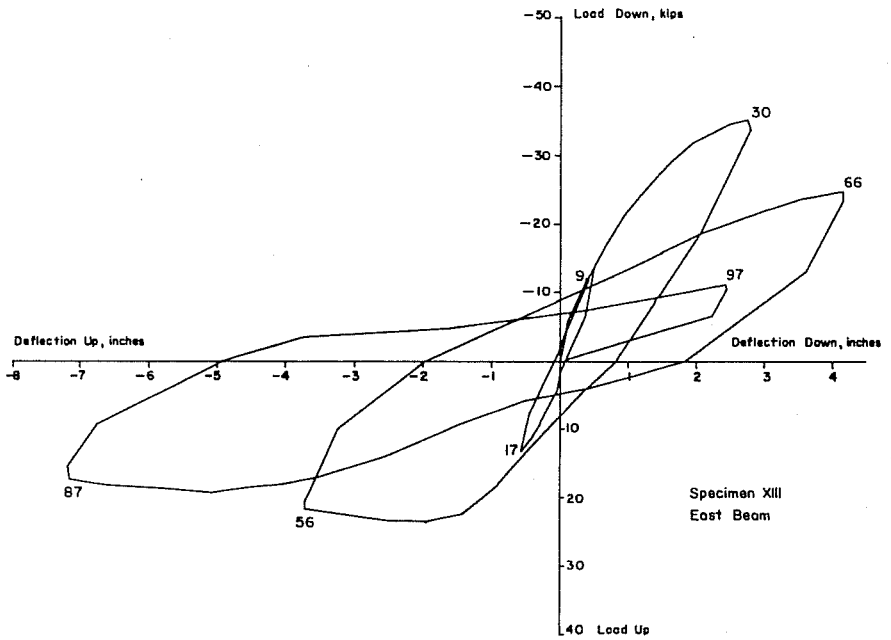
Load Down, kips
-50
-40
-30
-20
-10
Deflection Up, inches
-8 -7 -6 -5 -4 -3 -2 -1
Deflection Down, inches
1 2 3 4
10
20
30
40 Load Up
30
66
9
97
17
87
56
Specimen XIII
East Beam

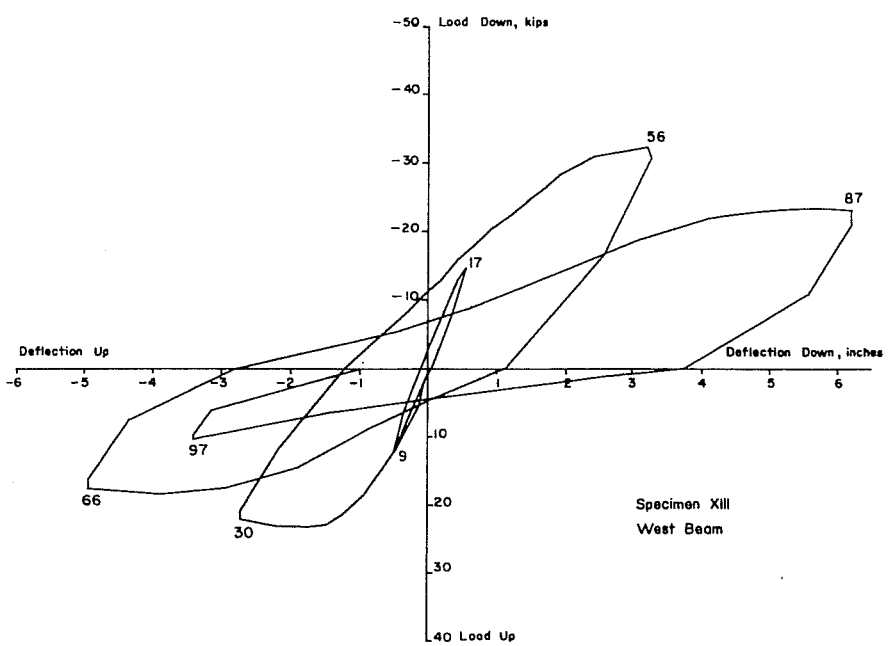
Load Down, kips
-50
-40
-30
-20
-10
Deflection Up
-6 -5 -4 -3 -2 -1
Deflection Down, inches
1 2 3 4 5 6
10
20
30
40 Load Up
56
87
17
97
9
66
30
Specimen XIII
West Beam

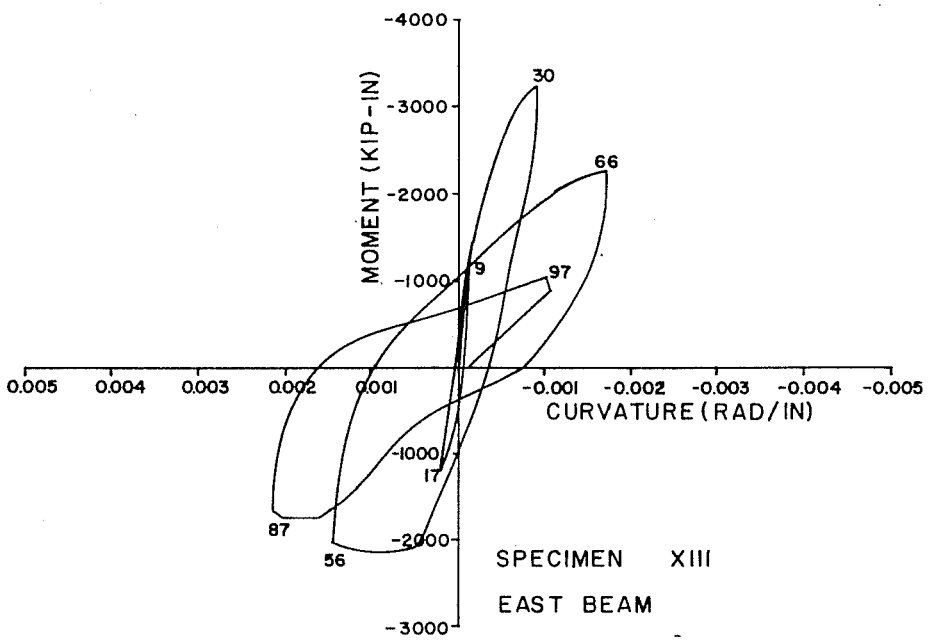
-4000
-3000
-2000
-1000
MOMENT (KIP-IN)
30
66
9
97
17
87
56
0.005
0.004
0.003
0.002
0.001
-0.001
-0.002
-0.003
-0.004
-0.005
CURVATURE (RAD/IN)
SPECIMEN XIII
EAST BEAM

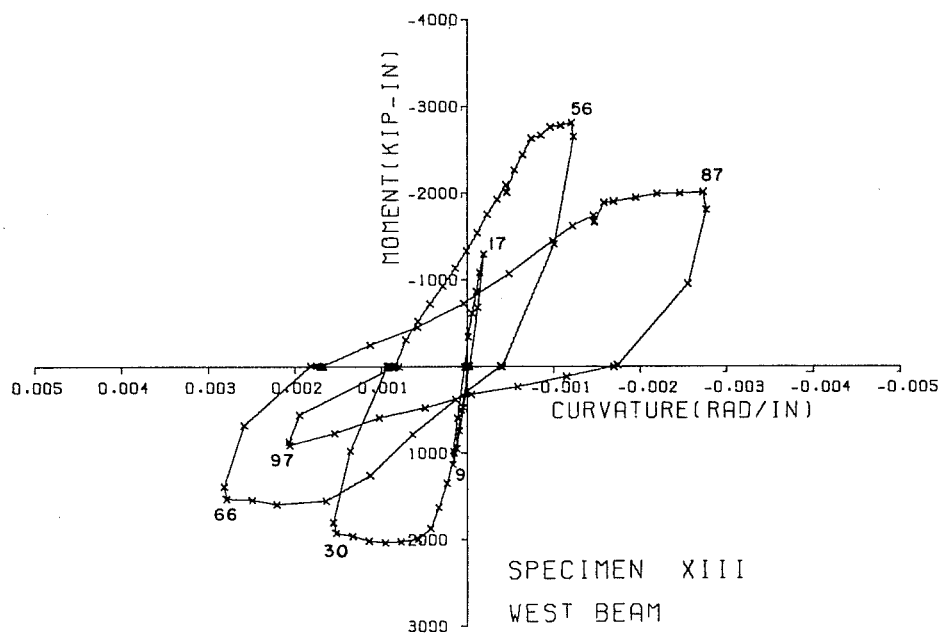
-4000
-3000
-2000
-1000
MOMENT(KIP-IN)
56
87
17
97
9
66
30
1000
2000
3000
0.005
0.004
0.003
0.002
0.001
-0.001
-0.002
-0.003
-0.004
-0.005
CURVATURE(RAD/IN)
SPECIMEN XIII
WEST BEAM

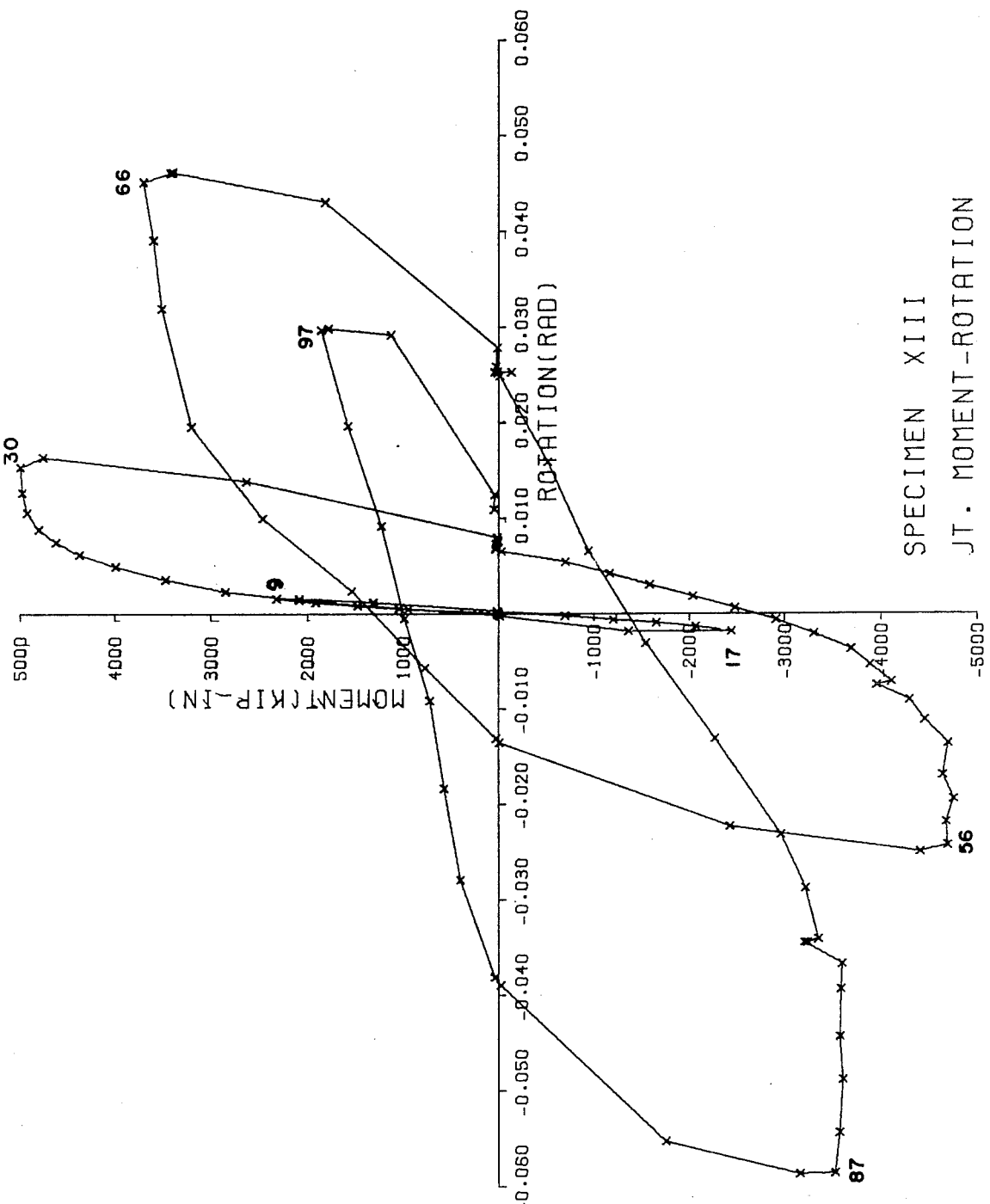
SPECIMEN XIII
JT. MOMENT-ROTATION
MOMENT(KIP-IN)
ROTATION(RAD)
5000
4000
3000
2000
1000
-1000
-2000
-3000
-4000
-5000
0.060
0.050
0.040
0.030
0.020
0.010
-0.010
-0.020
-0.030
-0.040
-0.050
-0.060
66
97
30
9
17
56
87

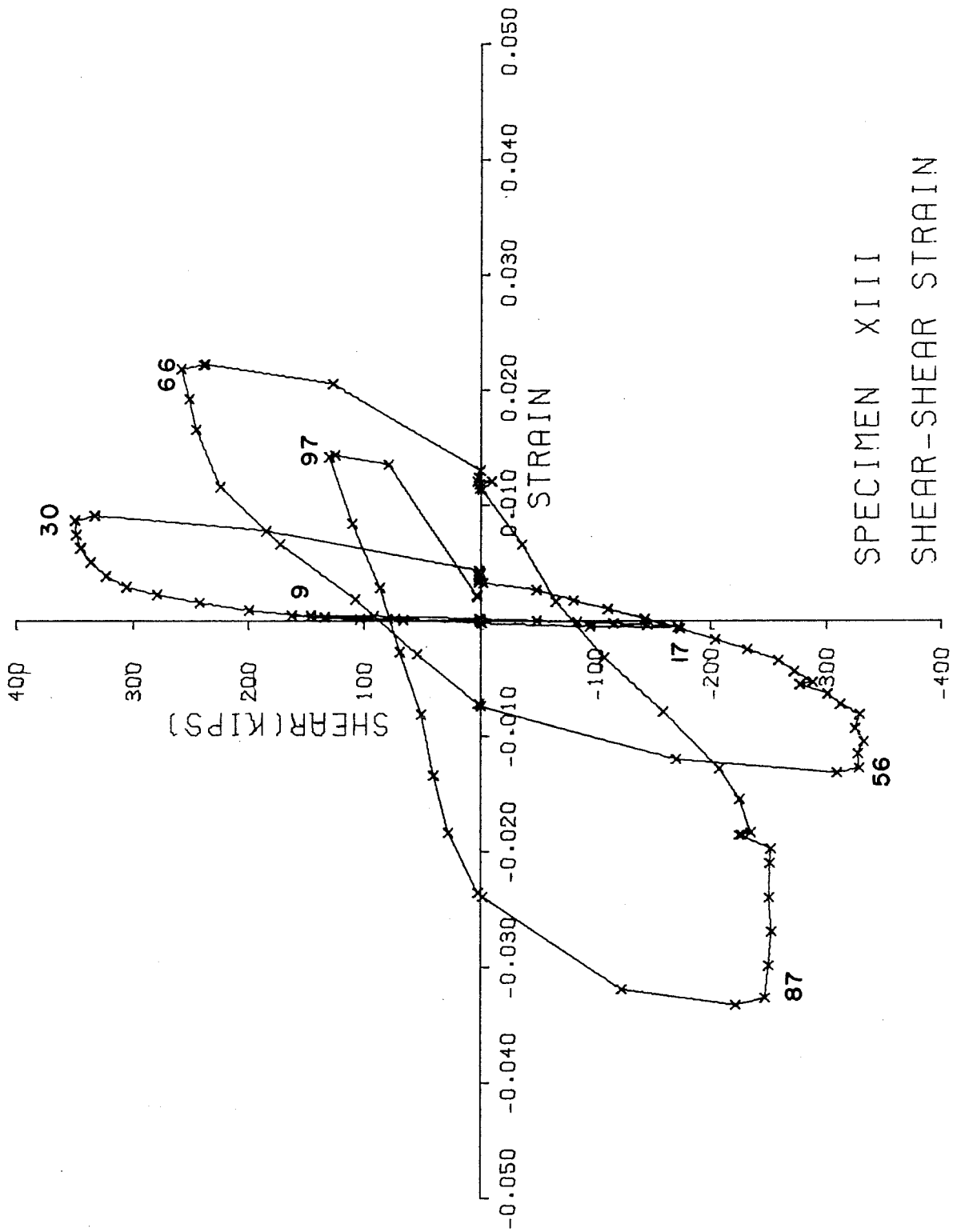
SPECIMEN XIII
SHEAR-SHEAR STRAIN
SHEAR(KIPS)
STRAIN
400
300
200
100
-100
-200
-300
-400
0.050
0.040
0.030
0.020
0.010
-0.010
-0.020
-0.030
-0.040
-0.050
66
97
30
9
17
56
87

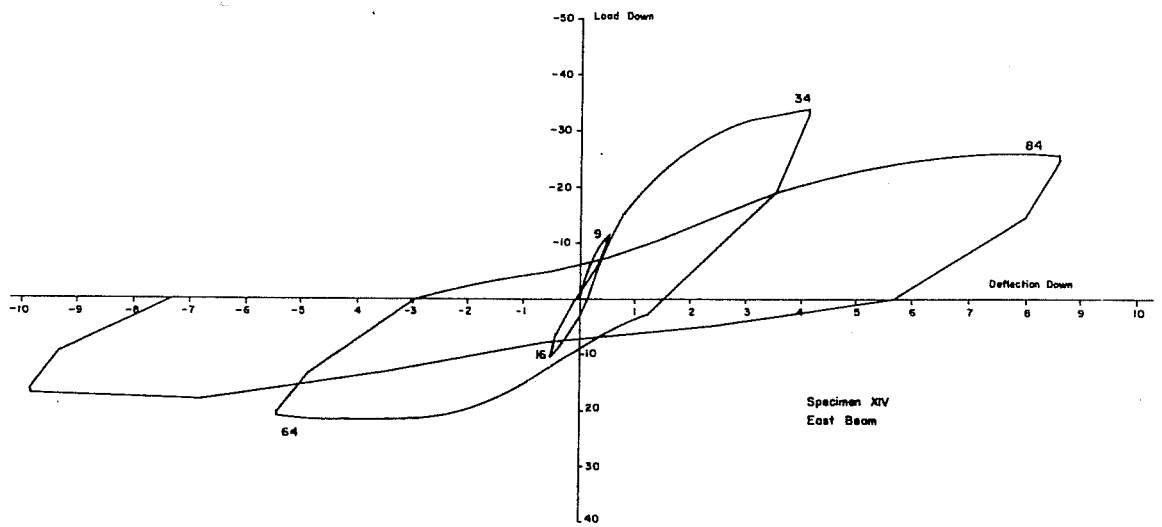
Load Down
Deflection Down
34
84
9
16
64
Specimen XIV
East Beam

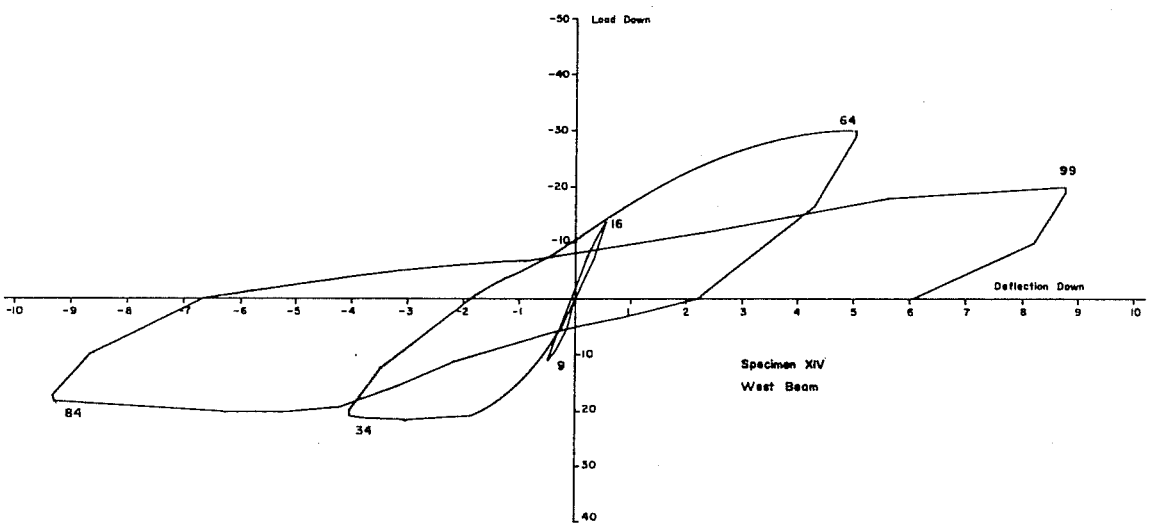
Load Down
Deflection Down
64
99
16
9
84
34
Specimen XIV
West Beam

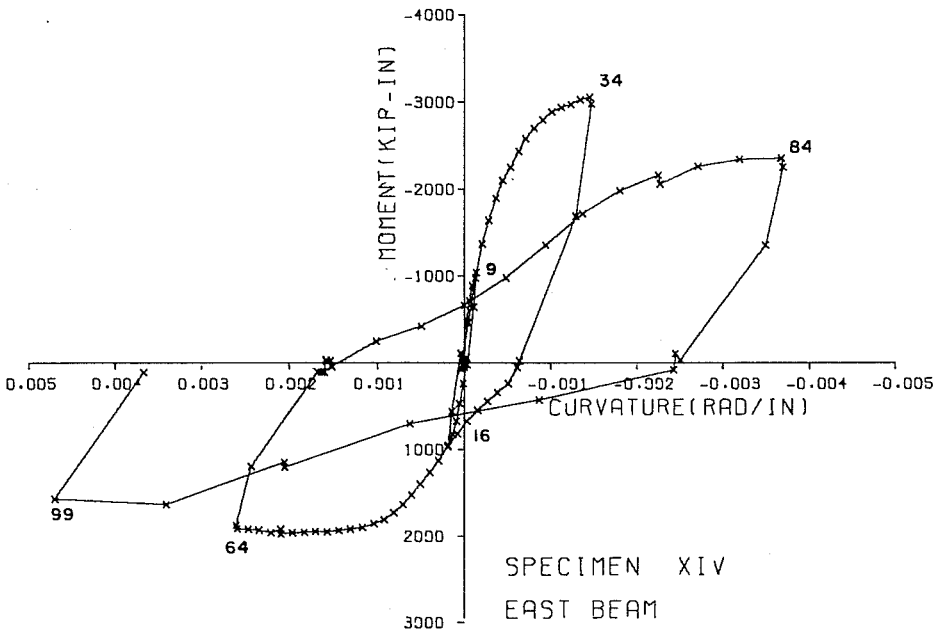
-4000
-3000
-2000
-1000
1000
2000
3000
MOMENT(KIP-IN)
0.005
0.004
0.003
0.002
0.001
-0.001
-0.002
-0.003
-0.004
-0.005
CURVATURE(RAD/IN)
34
84
9
16
99
64
SPECIMEN XIV
EAST BEAM

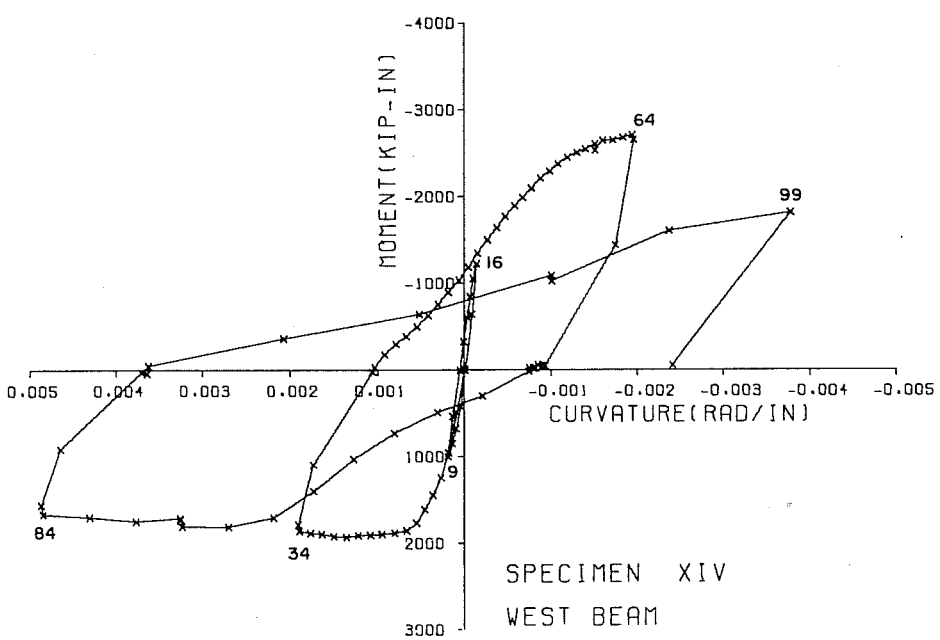
-4000
-3000
-2000
-1000
1000
2000
3000
MOMENT(KIP-IN)
0.005
0.004
0.003
0.002
0.001
-0.001
-0.002
-0.003
-0.004
-0.005
CURVATURE(RAD/IN)
64
99
16
9
84
34
SPECIMEN XIV
WEST BEAM

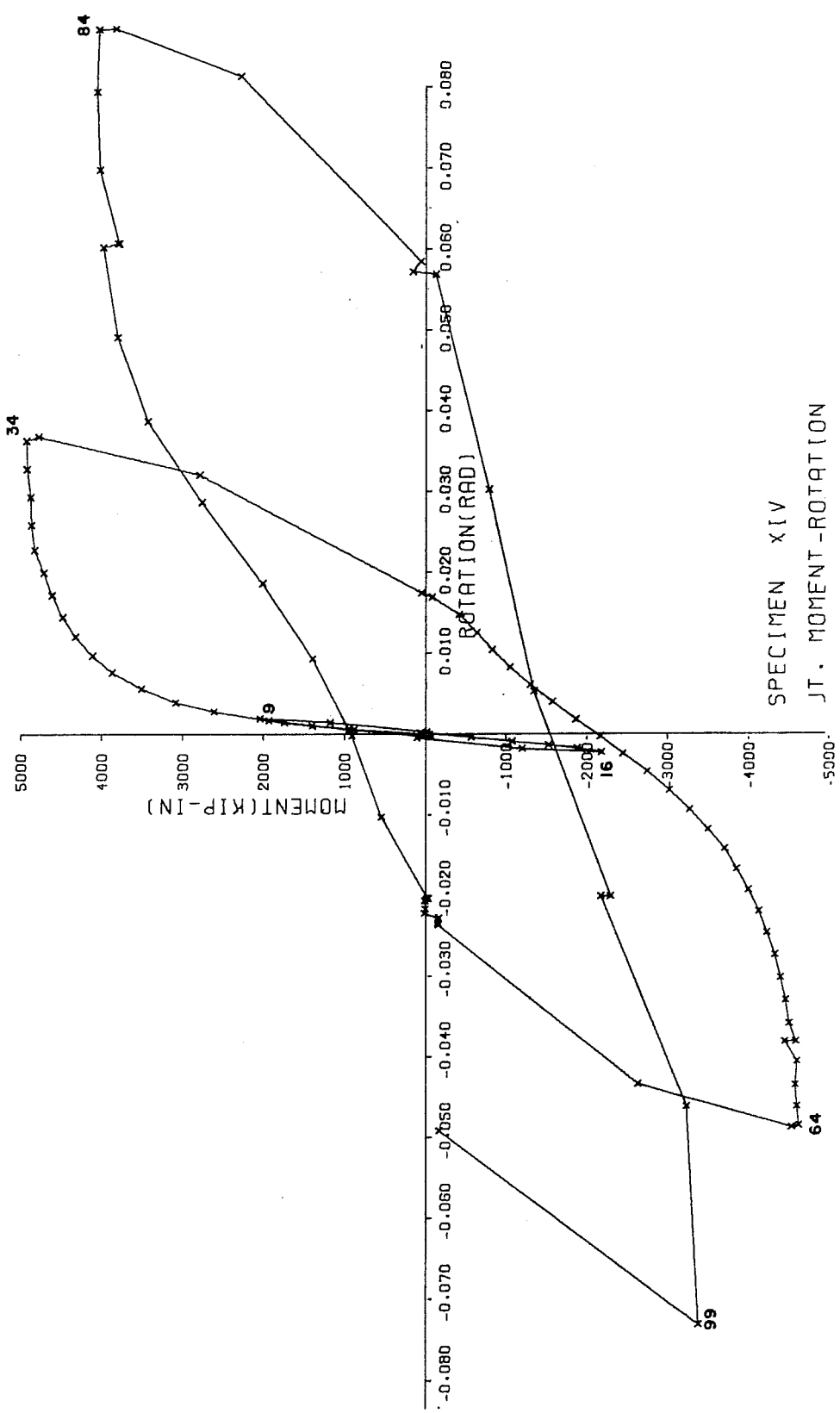
SPECIMEN XIV
JT. MOMENT-ROTATION
MOMENT(KIP-IN)
ROTATION(RAD)
5000
4000
3000
2000
1000
-1000
-2000
-3000
-4000
-5000
0.080
0.070
0.060
0.050
0.040
0.030
0.020
0.010
-0.010
-0.020
-0.030
-0.040
-0.050
-0.060
-0.070
-0.080
84
34
9
16
64
99

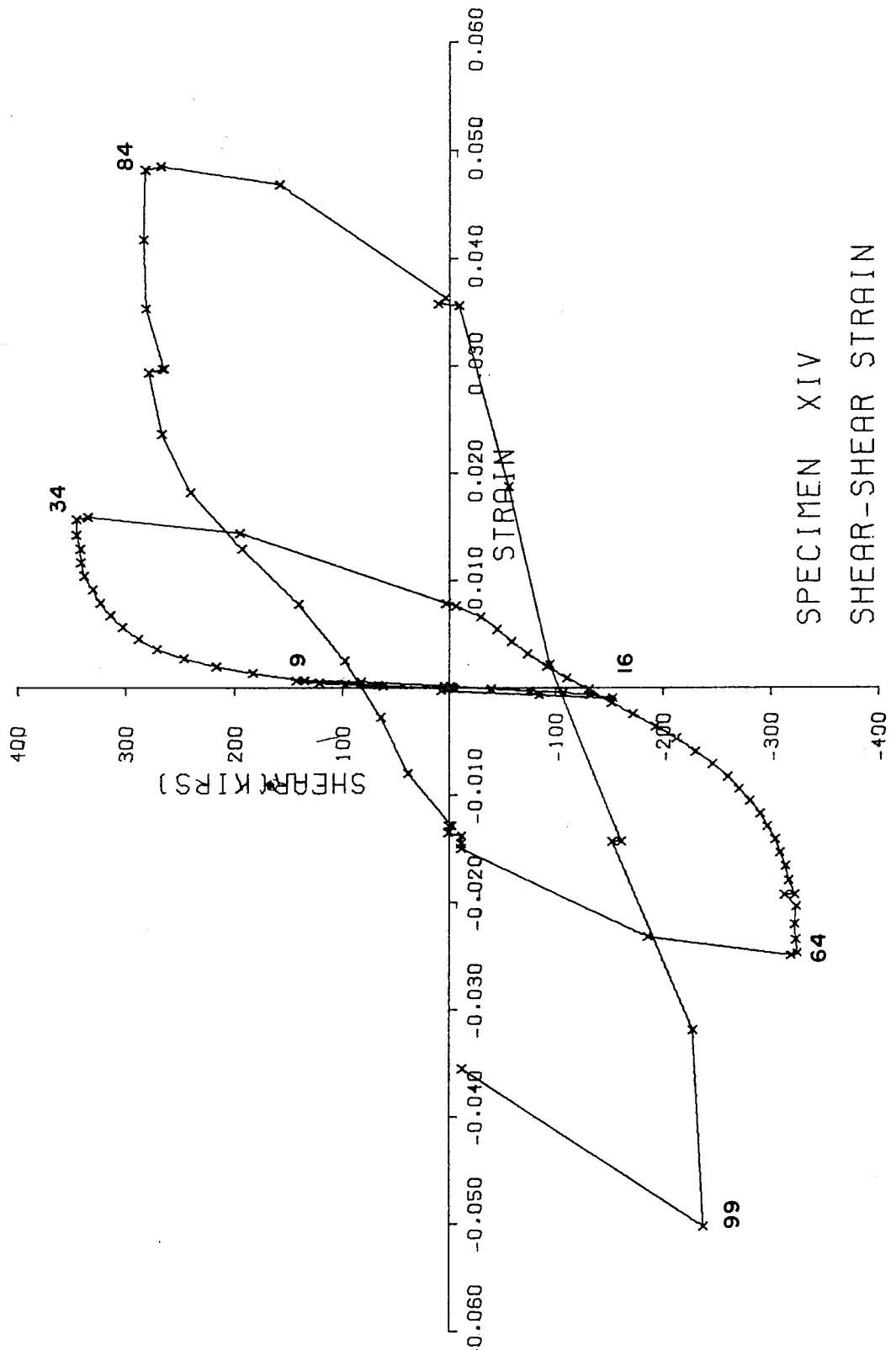
SPECIMEN XIV
SHEAR-SHEAR STRAIN
SHEAR (KIPS)
STRAIN
400
300
200
100
-100
-200
-300
-400
0.060
0.050
0.040
0.030
0.020
0.010
-0.010
-0.020
-0.030
-0.040
-0.050
-0.060
84
34
9
16
64
99

A P P E N D I X C

CRACKING PATTERNS OF LATERAL BEAMS

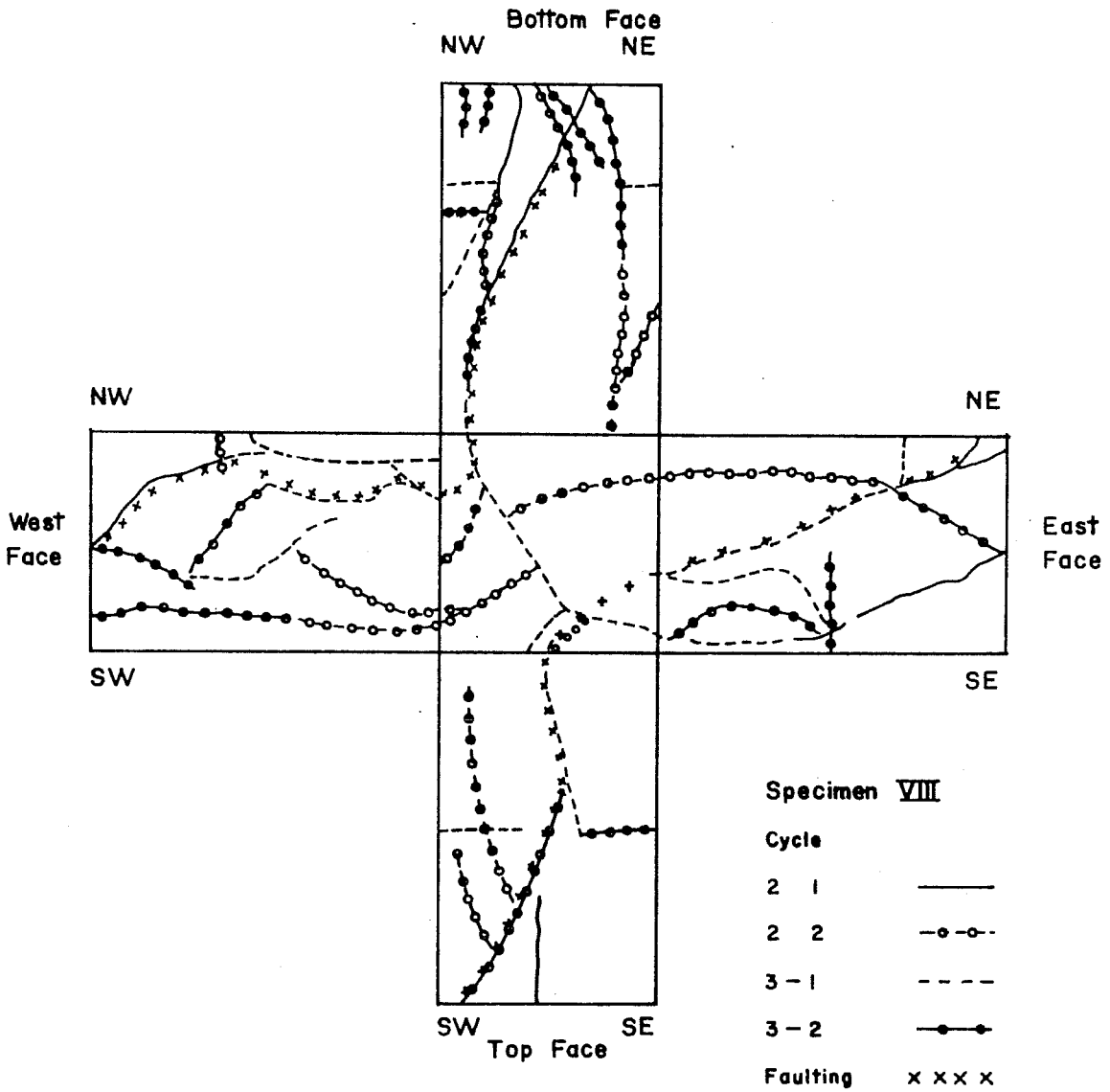

C1 Cracking pattern of lateral beam--Specimen VIII

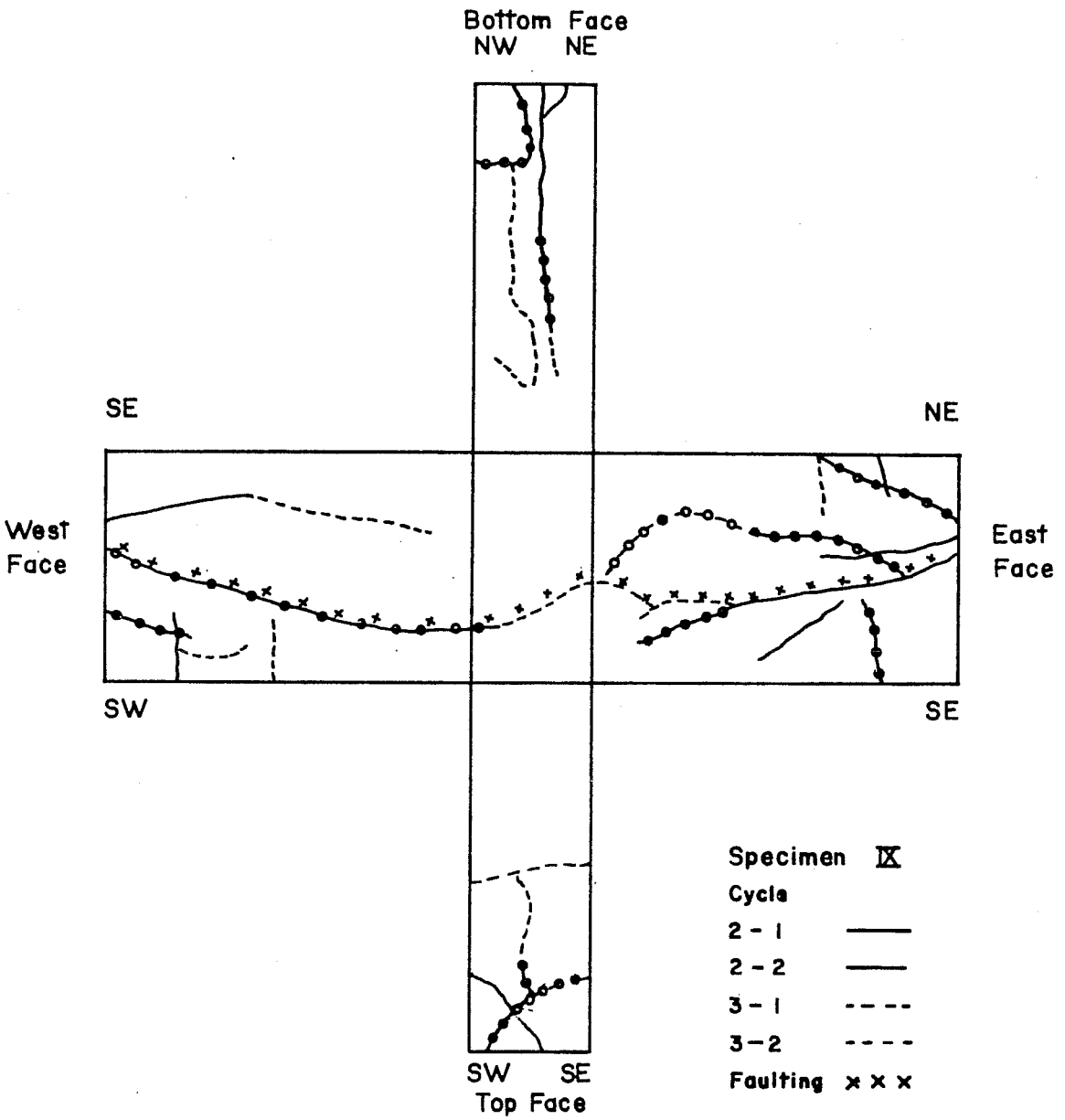

C2 Cracking pattern of lateral beam--Specimen IX

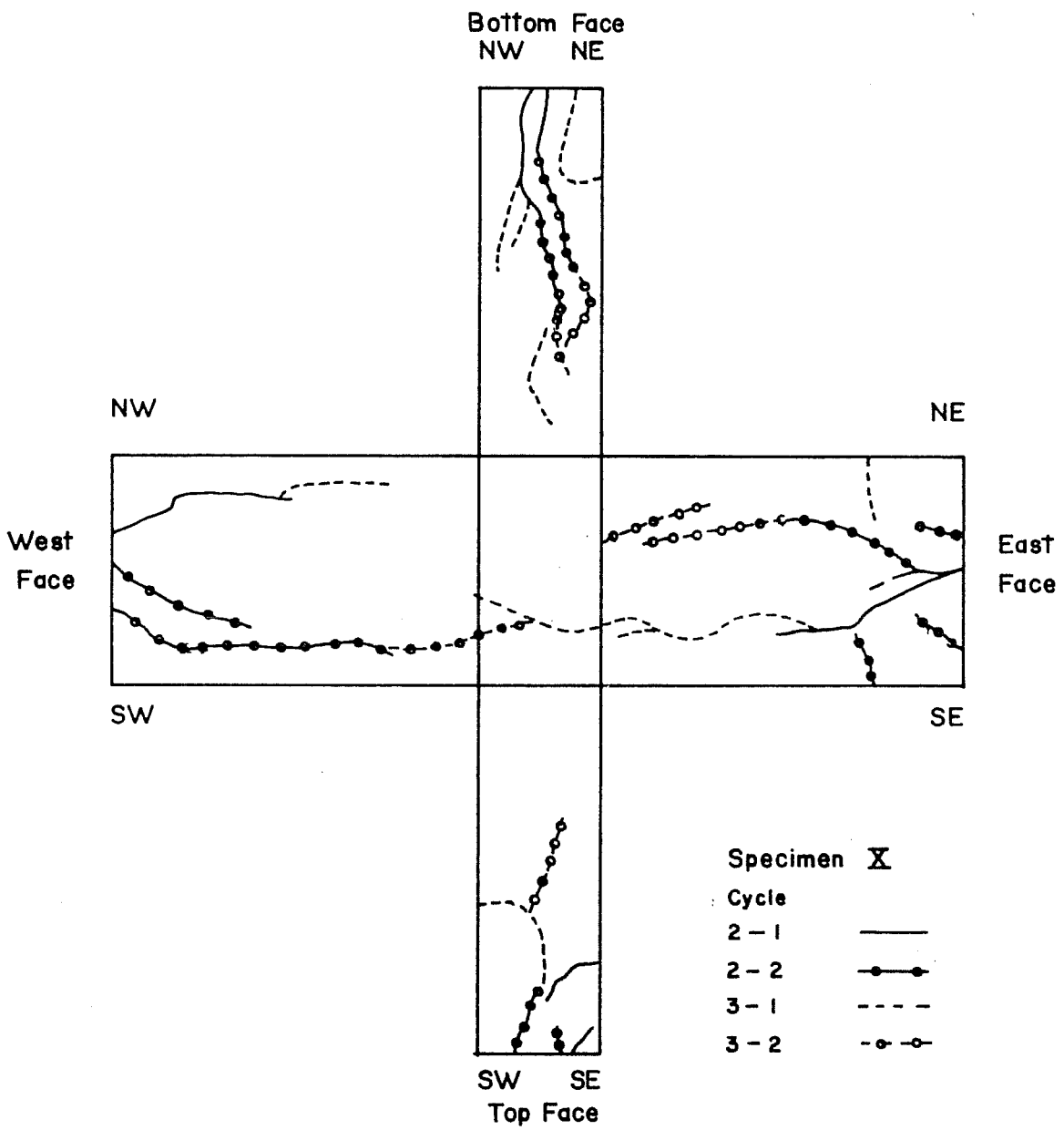

C3 Cracking pattern of lateral beam--Specimen X

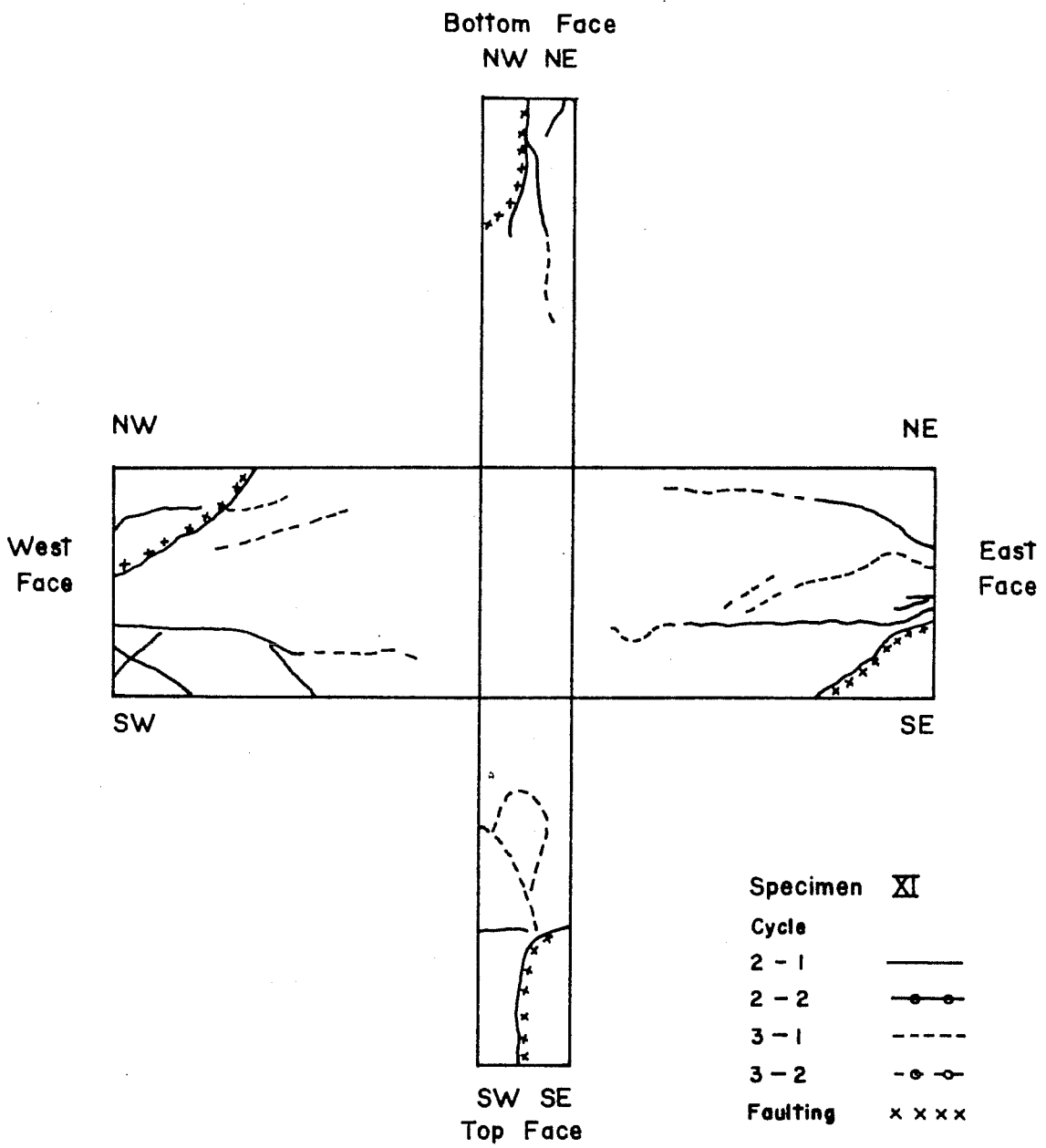

C4 Cracking pattern of lateral beam--Specimen XI

A P P E N D I X D

ANALYSIS OF OTHER TEST RESULTS

Data to be considered subsequently will be restricted to tests on reinforced concrete beam-column specimens. Data on reinforced concrete corner joints having only one column and beam at the joint are excluded. Several types of beam-column joint specimens different from those reported here have been tested. They are the corner, isolated, edge, edge modified, and interior elements shown in Fig. D1. Specifically, the empirical equations have been developed using the edge modified and interior type of specimen.

Because of the many different geometric configurations in specimen types and because researchers have found that specimens having lateral beams must have two lateral beams to be truly effective, two broad classes of specimen types will be designated. The first classification will consist of specimens of the corner and isolated type and will be called corner type, as shown in Fig. D1. The other classification relates to the beam being continuous at the joint; therefore, the edge, edge modified, and interior will henceforth all be called interior type. Specimens having lateral beams will be so indicated.

However, all data will be considered regardless of the specific type of joint, joint geometry, or failure mode. The only requirement is that the specimen has columns above and below the joint, as shown in Fig. D1.

Beam-column joint specimen failure can be classified in three distinct failure modes. They are:

(1) Joint shear failures--where the joint fails in shear before the framing beams can reach their yield moments.

(2) Beam or column yielding--a desirable failure mode where the flexural reinforcement yields in tension and starts the formation of a plastic hinge away from the joint.

(3) Bar anchorage failure--where the reinforcing bars lose their ability to transfer the tensile or compressive bar

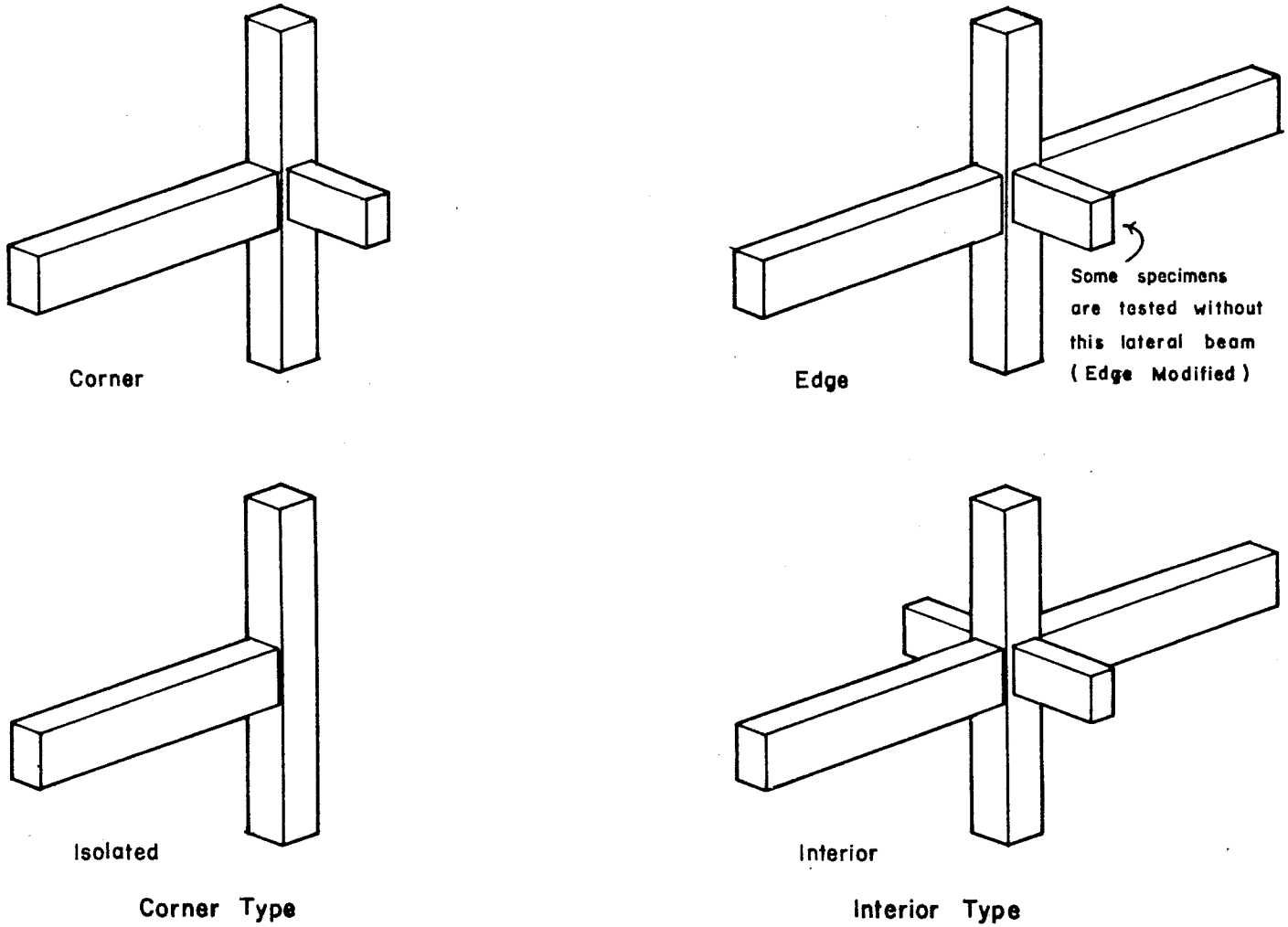

Fig. D1 Type of beam-column joint specimens

forces to the concrete by bond and proceed to pull out of the concrete due to insufficient anchorage length. Specimens in which the bars are either continuous through the joint or where they terminate in the joint are both considered.

Not all test specimens in the literature have been tested in an identical manner. Therefore, the maximum "peak" load on the beam registered in the "early" stages of loading will be used to analyze the joint shear strength. In describing the stages of loading, the term "early" is intended to signify the first cycle or the first cycle causing a major deformation, rotation, or strain to the members framing into the joint or causing major deformations in the joint proper.

Data from other test programs will be presented in tabular form. A brief description of each individual program is also presented.

(A) Hanson-Conner[12]: (1967) The earliest published data on the behavior of beam-column assemblies in the U.S. The authors tested seven specimens of the corner type, having the flexural beam reinforcement hooked and anchored in the joint. Variables included column load, joint reinforcing, column yielding or beam yielding, and lateral beams.

(B) Hanson[13]: (1971) Part of the continuing series of tests conducted by the Portland Cement Association Laboratories. These five specimens were of either the corner or interior types using a higher strength reinforcement than used for specimens in Ref. (A) above. Variables investigated were joint reinforcement, column load, and lateral beams.

(C) Hanson-Conner[14]: (1972) Part of the continuing series of tests conducted at PCA. Four specimens of the corner and interior types were tested using reinforcement yield strengths comparable to Ref. (A). The presence of lateral beams or joint reinforcement was the main variable.

(D) Megget[19,49]: (1971) These are the first tests in an extensive investigation into beam-column joint behavior at The University of Canterbury. The three specimens reported were of the corner variety with the major variable being the anchorage detail of the beam flexural reinforcement.

(E) Smith[20]: (1972) Megget's tests [Ref. (D)] showed a need to improve the strength of the beam-column joint. These three tests varied the internal joint reinforcement while keeping other parameters constant.

(F) Patton[50]: (1972) Previous tests showed anchorage of beam flexural bars in the joint core of a corner type joint to be a major problem in connection detailing. These three tests showed that anchoring the bars outside of the corner joint had very beneficial effects. The main objective of Patton's tests was to reinforce the beam-column joint so that it could repeatedly develop a flexural mode of failure in the bending members.

(G) Renton[21]: (1972) These are the last reported tests on corner type connections tested at The University of Canterbury. Four tests were conducted investigating different anchorage details of the beam flexural reinforcement and different beam-column joint reinforcing.

(H) Park-Thompson[51]: (1974) Seven tests were conducted at The University of Canterbury on interior type joints with the beam flexural reinforcing bars and/or prestressed reinforcement continuous through the beam-column joint area. The beams of the assemblies were either prestressed, partially prestressed, or of reinforced concrete. All the specimens had the same joint reinforcement. The main variable was the method of reinforcing the beams, i.e., prestressing.

(I) Higashi-Ohwada[48]: (1969) The Tokyo Metropolitan University conducted several test programs on both normal weight and lightweight aggregate concrete beam-column joints and on connections where the

beams were either rectangular, tee, or haunched. All the tests were on interior type joints. Other variables, in addition to those mentioned above, were column load, method of anchoring the beam reinforcement at or in the joint, and lateral beams. Specimens of particular interest for this analysis are those with constant section rectangular beams made of normal weight concrete.

(J) Uzumeri[22]: (1976) Eight tests on reinforced concrete beam-column joints are presented. Variables were the amount and size of joint reinforcement, steel yield strength, and column size. All of these specimens were of the corner joint type with beam flexural bars anchored in accordance with ACI 318-71.[2]

Test data related to the maximum shear carried by the beam-column joint are tabulated in Table D1 for each of the above research programs. For completeness, geometric dimensions for each test are also given. Maximum shear stress on the joint for each specimen was taken either from that reported in the reference or calculated using a load-deflection curve, when available. In cases where the load-deflection curves were used to calculate joint shear, the column shear and beam moments were calculated from the reported lengths of the specimen members and by applying static equilibrium. The predicted joint shear stresses from Eq. (5-8) were computed using the actual specimen material properties.

For each test in Table D1, the predicted joint shear strength is greater than the shear stress applied during the "early" stages of loading. This means that all the specimens should have yielded the flexural reinforcement before the joint shear strength was exceeded. From each of the investigators' own observations, this was exactly the case, except when the flexural bars terminating in the joint did not have adequate anchorage, see test series (C). This is a good indication that for those tests reported in Table D1 in which the flexural reinforcement was adequately anchored, the joint did not determine the maximum load in the first cycle of loading.

TABLE D1 TEST RESULTS FROM OTHER INVESTIGATIONS

Specimen	Column Size and Details					Beam Size and Details								Joint Details		
	h_c (in.)	b_c (in.)	d_c (in.)	ρ_g	f_y (ksi)	h_b (in.)	b_b (in.)	d_b (in.)	Top	ρ_{top}	Bottom	ρ_{bot}	f_y (ksi)	Hoops	ρ_s	f_y (ksi)
(1)	(2)	(3)	(4)	(5)	(6)	(7)	(8)	(9)	(10)	(11)	(12)	(13)	(14)	(15)	(16)	(17)
Hanson-Conner: (A)																
I	15	15	12.8	0.0555	67.0	20	12	17.94	4-#9	0.0186	2-#9	0.0093	51.6	5-#4@4.5"	0.0137	46.7
IA	"	"	"	"	69.8	"	"	"	"	"	"	"	47.8	5-#3@4.5"	0.0075	52.8
II	"	"	"	"	70.3	"	"	"	"	"	"	"	48.3	5-#4@4.5"	0.0137	54.8
III	12	"	10	0.0175	47.3	"	"	"	"	"	"	"	48.2	"	"	49.2
IV	"	"	"	"	46.9	"	"	"	"	"	"	"	49.9	"	"	50.5
V	15	"	12.8	0.0555	64.8	"	"	"	"	"	"	"	51.0	None	---	---
VA	"	"	"	"	70.2	"	"	"	"	"	"	"	49.8	None	---	---
Hanson: (B)																
1	15	15	12.8	0.0555	60.6	20	12	17.94	4-#8	0.0147	2-#8	0.0073	63.1	6-#4@3.5"	0.0352	66.8
2	"	"	"	"	59.8	"	"	"	"	"	"	"	65.0	5-#4@4.1"	0.0300	67.0
3	"	"	"	"	60.2	"	"	"	"	"	"	"	64.1	5-#3@4.1"	0.0165	73.5
4	"	"	"	"	60.8	"	"	"	"	"	"	"	63.4	4-#3@6"	0.0113	"
5	"	"	"	"	62.0	"	"	"	"	"	"	"	65.0	6-#3@3.5"	0.0193	"
Hanson-Conner: (C)																
7	15	15	12.8	0.0555	81.8	20	12	17.94	4-#9	0.0186	2-#8	0.0093	50.7	None	---	---
8	"	"	"	"	"	"	"	"	"	"	"	"	44.4	None	---	---
9	"	"	"	"	62.4	"	"	"	"	"	"	"	"	None	---	---
10	"	"	"	"	64.8	"	"	"	"	"	"	"	44.0	5-#4@4.1"	0.0300	45.0
Megget: (D)																
M1	15	13	12.56	0.0123	44.2	18	10	15.44	2-#9	0.0130	2-#9	0.0130	41.5	3-#4@5"	0.0147	46.0
M2	"	"	"	"	"	"	"	"	"	"	"	"	42.0	"	"	"
M3	"	"	"	"	"	"	"	"	"	"	"	"	41.5	4-#4@3.6"	0.0204	36.2
Smith: (E)																
S4	15	13	12.56	0.0123	39.8	18	10	15.44	2-#9	0.0130	2-#9	0.0130	42.9	5-#4@2-3/4"	0.0267	45.1
S5	"	"	"	"	"	"	"	"	"	"	"	"	43.6	4-#3@3-3/4" plus 1% spiral	0.0232	45.1 48.4
S6	"	"	"	"	43.1	"	"	"	1-#8 2-#7	0.0129	2-#7 2-#6	0.0135	40.4top 43.4bot	5-#4@3" plus rect. cage	0.0329	45.4 48.4
Patton: (F)																
P1	15	15	12.94	0.0178	42.1	25	12	22.86	4-#10	0.0185	4-#10	0.0185	41.4	9-#5 14-#2	0.0387	46.2 46.5
P2	"	"	"	"	"	"	"	"	"	"	"	"	"	9-#5 5-#5	0.0416	46.2
P3	"	"	"	"	"	"	"	"	"	"	"	"	"	5-#5@4.5"	0.0208	"
Renton: (G)																
R1	15	15	12.94	0.0178	44.7	25	12	22.86	4-#10	0.0185	4-#10	0.0185	43.1	5-#5@4"	0.0234	45.1
R2	"	"	"	"	45.3	"	"	"	"	"	"	"	42.2	7-#5@2-3/4"	0.0340	46.7
R3	"	"	"	"	45.2	"	"	"	"	"	"	"	41.9	9-#5@2-1/4"	0.0416	45.4
R4	"	"	"	"	45.4	"	"	"	"	"	"	"	43.7	9-#5@2-1/4"	"	"
Park & Thompson: (H)																
T1	16	12	13.69	0.0125	58.8	18	9	(4-#3 + 3-12W/.2 Prestress)					41.1	7-#5@2"	0.0583	43.5
T2	"	"	"	"	59.2	"	"	(4-#9 + 1-12W/.2 Prestress)					41.4	"	"	"
T3	"	"	"	"	60.2	"	"	15.56	2-#9 1-#8	0.0199	2-#9 1-#8	0.0199	40.4 46.0	"	"	"
T4	"	"	"	"	57.6	"	"	(4-#3 + 3-12W/.2 Prestress)					47.1	"	"	"
T5	"	"	"	"	58.5	"	"	(4-#3 + 2-10W/.276 Prestress)					47.2	"	"	"
T6	"	"	"	"	59.0	"	"	(8-#6 + 2-#4 + 1-12W/.2 Prestress)					42.8	"	"	"
T7	"	"	"	"	58.7	"	"	(4-#6 + 3-4W/.276 Prestress)					42.1 41.5	"	"	"
Higashi & Ohwada: (I)																
1SD35Aa-4	7.87	7.87	6.69	0.0158	60.7	11.81	5.91	11.02	3-#D10	0.0056	3-#D10	0.0056	60.7	6-#4.1w@1.57"	0.0078	39.8
2SD35Aa-5	"	"	"	0.0118	"	"	"	10.75	5-#D10	0.0096	5-#D10	0.0096	"	"	"	"
3SD35Aa-6	"	"	"	"	"	"	"	"	"	"	"	"	"	"	"	"
4SD35Aa-7	"	"	"	0.0158	58.0	"	"	11.02	3-#D10	0.0056	3-#D10	0.0056	58.0	"	"	"
5SD35Aa-8	"	"	"	"	"	"	"	"	"	"	"	"	"	"	"	"
6SR24Aa-4	"	"	"	0.0127	45.5	"	"	10.75	7-#9$_{cp}$	0.0109	7-#9$_{cp}$	0.0109	45.5	"	"	"
7SR24Aa-5	"	"	"	0.0127	"	"	"	"	"	"	"	"	"	"	"	"
8SD35Ba-2	"	"	"	0.0158	60.7	"	"	11.02	3-#D10	0.0056	3-#D10	0.0056	60.7	"	"	"
9SD35Ba-3	"	"	"	"	"	"	"	"	"	"	"	"	"	"	"	"
10LSD35Aa-1 LW	"	"	"	"	58.0	"	"	"	"	"	"	"	58.0	"	"	"
11LSD35Aa-2 LW	"	"	"	"	"	"	"	"	"	"	"	"	"	"	"	"
12LSD35Ab-1 LW	"	"	"	"	"	"	"	"	"	"	"	"	"	"	"	"
13LSD35Ab-2 LW	"	"	"	"	"	"	"	"	"	"	"	"	"	"	"	"
14LSR24Aa-1 LW	"	"	"	0.0159	43.8	"	"	11.04	4-#9$_{cp}$	0.0060	4-#9$_{cp}$	0.0060	43.8	"	"	"
15LSR24Ab-1 LW	"	"	"	"	"	"	"	"	"	"	"	"	"	"	"	"
16LSD35Ba-1 LW	"	"	"	0.0158	58.0	"	"	11.02	3-#D10	0.0056	3-#D10	0.0056	58.0	"	"	"
17LSD35Ba-2 LW	"	"	"	"	"	"	"	"	"	"	"	"	"	"	"	"
Higashi & Ohwada: (I) (Much of this information is assumed.)																
No. 1	7.87	7.87	6.69	0.0318		11.81	5.91	10.97	4-#D13	0.0122	4-#D13	0.0122		None	---	---
No. 2	"	"	"	"		"	"	"	"	"	"	"		6-#4.1c@1.57"	0.0078	
No. 3	"	"	"	"		"	"	"	"	"	"	"		12-#4.1c@0.79"	0.0156	
Uzumeri: (J)																
SP1	15	15	12.5	0.0281	48.1	20	12	17.6	3-#9	0.0142	2-#9	0.0095	50.3	None	---	---
SP2	"	"	"	"	48.6	"	"	"	"	"	"	"	50.6	None	---	---
SP3	"	"	"	"	48.8	"	"	"	"	"	"	"	50.8	4-#3@3"	0.0122	62.0
SP4	"	"	"	"	48.2	"	"	"	"	"	"	"	50.6	4-#4@3"	0.0222	55.0
SP5	"	"	"	"	48.7	"	15	"	"	0.0114	"	0.0076	50.4	None	---	---
SP6	"	"	"	"	49.3	"	"	"	"	"	"	"	51.1	8-#4@1-3/4"	0.0381	51.8
SP7	"	"	"	"	"	"	"	"	"	"	"	"	"	4-#4@3"	0.0222	53.0
SP8	"	"	"	"	56.5	"	"	"	4-#9	0.0152	3-#9	0.0114	"	8-#4@1-3/4"	0.0381	"

Lateral Beam(s) w_L (in.) (18)	Lateral Beam(s) h_L (in.) (19)	Lateral Beam(s) Mask (1) One Side (2) Two Sides (20)	Aspect Ratio h_c/h_b (21)	Column Stress (psi) (22)	Concrete Strength in Joint (psi) (23)	Type of Joint (24)	Maximum Applied Joint Shear (psi) (25)	Failure Mode 1st Cycle (26)	Predicted Eq. (5-8) Ultimate Joint Shear (psi) (27)	Eq. (5-11) Predicted Cyclic Strength (28)	Cycles before Maximum Shear Stress < (28) (29)	Remarks (30)
	None		0.75	2862	3470	Corner	931	Flex-Beam	1280	759	5	
	None		"	2875	3200	"	877	" "	1175	694	3	
	None		"	1262	3650	"	880	" "	1325	785	8+	
	None		0.60	1861	3200	"	1077	Flex-Column	1230	719	4	
	None		"	167	3475	"	563	" "	1295	760		Max. stress always < (28)
	None		0.75	2826	3300	"	926	Shear-Joint ?	1135	678	2	
12	20	0.80(2)	"	2884	5420	Corner w/Lat. Beams	905	Flex-Beam	1960	1186		Max. stress always < (28)
12	20	0.80(1)	0.75	2884	5500	Interior	1330	Flex-Beam	1945	1155	5	Max. stress never < (28)
"	"	0.80(2)	"	"	2930	Interior w/Lat. Beams	1353	" "	1530	850	5	" " " "
"	"	0.80(1)	"	"	5200	Corner	968	" "	1700	1009	5	" " " "
	None		"	"	5380	"	936	" "	1690	1003		Max. stress always < (28)
	None		"	1422	5230	"	956	" "	1730	1029		" " " "
12	20	0.80(1)	0.75	2884	5695	Corner	853	Flex-Beam	1655	976	4	
"	"	"	"	"	6065	Interior	1162	" "	1725	1018	4+	Max. stress never < (28)
"	"	0.80(2)	"	"	3805	Interior w/Lat. Beams	1142	" "	1555	858	5+	" " " "
"	"	0.80(1)	"	"	5690	Interior	1432	" "	1935	1151	6+	" " " "
	None		0.833	0	4110	Corner	440	Flex-Beam	1440	854		Max. stress always < (28)
	None		"	"	3905	"	415	Anchorage-U Bars	1395	826		" " " "
	None		"	"	5190	"	425	Flex-Beam	1735	1030		" " " "
	None		0.833	0	2970	Corner	448	Flex-Beam	1240	734		Max. stress always < (28)
	None		"	"	2920	"	455	" "	1205	712		" " " "
	None		"	"	2570	"	469	" "	1164	687		" " " "
	None		0.60	658	4820	Corner w/Anchor Stub	895	Flex-Column ?	1815	1076		Max. stress always < (28)
	None		"	"	3830	Corner	903	" "	1585	936		" " " "
	None		"	"	4510	"	903	" "	1585	940		" " " "
	None		0.60	658	3730	Corner	674	Anchorage Bars	1415	839		Max. stress always < (28)
	None		"	"	5570	"	698	" "	1950	1158		" " " "
	None		"	"	3440	"	668	" "	1475	871		" " " "
	None		"	"	4220	"	859	" "	1690	999		" " " "
	None		0.89	1042	4630	Interior	1385+	Flex-Beam				
	None		"	"	5510	"	1345+	" "				
	None		"	"	5400	"	1400	" "	2164	1271	2	
	None		"	"	5050	"	1563+	" "				
	None		"	"	5240	"	1624+	" "				
	None		"	"	5360	"	1421+	" "				
	None		"	"	5330	"	1264+	" "				
							+Estimated from design data					
	None		0.66	284	4410	Interior-Hook	695		1461	861		Max. stress always < (28)
	None		"	"	4450	" "	942		1469	867	2	
	None		"	569	4860	" "	1065		1558	919	2	
	None		"	284	5520	" "						
	None		"	569	5520	" "						
	None		"	"	4495	" "	985		1474	872	1	
	None		"	284	4510	" "	777		1501	874		Max. stress always < (28)
3.94	11.81	0.50(2)	"	"	4350	Interior w/Lat. Beam-Hook	722		1629	960		" " " "
7.87	11.81	1.0 (2)	"	"	4610	" " " "	698		1880	1109		" " " "
	None		"	"	5960	Interior-Hook	827					
	None		"	569	"	" "						
	None		"	284	"	Interior-Pass Through	654					
	None		"	569	"	" " "						
	None		"	284	"	Interior-Hook						
	None		"	"	"	Interior-Pass Through	616					
3.94	11.81	0.50(2)	"	"	"	Interior w/Lat. Beam-Hook	663					
7.87	11.81	1.0 (2)	"	"	"	" " " "						
	None		0.66			Interior-Pass Through	1109					
	None		"			" " "	1007					
	None		"			" " "	896					
12	20	0.80(1)	0.75	2311	4460	Corner w/Lat. Beam	751	Flex-Beam	1405	829		Max. stress always < (28)
	None		"	"	4510	Corner	750	" "	1415	835		" " " "
12	20	0.80(1)	"	"	3920	Corner w/Lat. Beam	777	" "	1380	816		" " " "
12	20	0.80(1)	"	"	4490	" " "	880	" "	1590	944	5	Max. stress never < (28)
15	20	1.0 (1)	"	"	4630	" " "	729	" "	1440	963		Max. stress always < (28)
	None		"	"	5250	Corner	873	" "	1915	1136		" " " "
	None		"	"	4460	"	838	" "	1585	940		" " " "
	None		"	"	3820	"	1005	" "	1555	919	5	Max. stress never < (28)

Unfortunately, applying the empirical shear strength equation, Eq. (5-8), to other data did not adequately test its utility in determining the shear strength of the beam-column joint. The data found in Table D1 were primarily from investigations testing the cyclic strength of the beam-column joint. Under many cycles of load reversal, the tests in Table D1 have shown that joint reinforcement and lateral beams are a significant factor in determining the shear strength, because the concrete tends to lose its ability to carry a repeated high shear stress. The reduction is due to degradation of aggregate interlock because of the movement (dislocation) occurring parallel to the cracked surfaces. The dislocation is an inevitable consequence of large deformations and load reversals on the beam-column joint.

R E F E R E N C E S

1. Schmidt, W., and Hoffman, E. S., "9000 psi Concrete--Why? Why Not?," Civil Engineering--ASCE, May 1975, pp. 52-55.

2. ACI Committee 318, Building Code Requirements for Reinforced Concrete (ACI 318-71), American Concrete Institute, Detroit, 1971, 78 pp.

3. Fintel, M., "Resistance of Earthquake--Philosophy, Ductility and Details," Response of Multistory Concrete Structures to Lateral Forces, American Concrete Institute, SP-36, Detroit, 1973, pp. 76-95.

4. Kunze, W. W., Sbarounis, J. A., and Amrhein, J. E., "The March 27 Alaskan Earthquake--Effects on Structures in Anchorage," Journal of the American Concrete Institute, Proc. V. 62, No. 6, June 1963, pp. 635-649.

5. Sozen, M. A., Jennings, P. C., Matthiesen, R. B., Hansen, G. W., and Newmark, N. M., Engineering Report on the Caracas Earthquake of 29 July 1967, National Academy of Sciences, 1968.

6. Fintel, M., "Behavior of Structures in the Caracas Earthquake," Civil Engineering--ASCE, February 1968, pp. 42-46.

7. Nielsen, N. N., "The Tokachi-Oki Earthquake, Japan, May 16, 1968--A Preliminary Report on Damage to Structures," International Institute of Seismology and Earthquake Engineering, Tokyo, Japan, June 1968.

8. Lew, H. S., Leyendecker, E. V., and Dikkers, R. D., Engineering Aspects of the 1971 San Fernando Earthquake, National Bureau of Standards, Building Science Series 40, December 1971.

9. ACI-ASCE Joint Committee 352, "Recommendations for Design of Beam-Column Joints in Monolithic Reinforced Concrete Structures," Journal of the American Concrete Institute, Proc. V. 73, No. 7, July 1976.

10. Sugano, S., and Koreishi, I., "An Empirical Evaluation of Inelastic Behavior of Structural Elements in Reinforced Concrete Frames Subjected to Lateral Forces," Fifth World Conference on Earthquake Engineering, Paper 99, Session 2D: Dynamic Behavior of Structural Elements, Rome, 1973.

Park & Paulay 5WCEE

11. Park, R., and Paulay, T., Reinforced Concrete Structures, John Wiley and Sons, New York, 1975.

12. Hanson, N. W., and Conner, H. W., "Seismic Resistance of Reinforced Concrete Beam-Column Joints," Journal of the Structural Division, ASCE, Vol. 93, ST5, October 1967, pp. 533-560.

13. Hanson, N. W., "Seismic Resistance of Concrete Frames with Grade 60 Reinforcement," Journal of the Structural Division, ASCE, Vol. 97, ST6, June 1971, pp. 1685-1700.

14. Hanson, N. W., and Conner, H. W., "Tests of Reinforced Concrete Beam-Column Joints under Simulated Seismic Loading" (RD012.01D), Portland Cement Association, 1972.

15. Uzumeri, S. M., "Strength and Ductility of Cast-in-Place Beam-Column Joints," American Concrete Institute Special Publication on Earthquake Resistance, to be published.

16. Higashi, Y., and Ohwada, Y., "Reinforced Concrete Beam-Column Joints," Invited Discussion, Technical Committee 21, ASCE-IABSE International Conference on Tall Buildings, August 1972.

17. ACI-ASCE Committee 326, "Shear and Diagonal Tension," Journal of the American Concrete Institute, Proc. V. 59, No. 1, January 1962, pp. 1-30; No. 2, February 1962, pp. 277-334; and No. 3, March 1962, pp. 352-396.

18. Richart, F. E., Brandtzaeg, A., and Brown, R. L., A Study of the Failure of Concrete under Combined Compressive Stress, University of Illinois Engineering Experiment Station, Bulletin No. 185, 1928.

19. Megget, L. M., and Park, R., "Reinforced Concrete Exterior Beam-Column Joints under Seismic Loading," New Zealand Engineering, 15 November 1971, pp. 341-353.

20. Smith, B. J., "Exterior Reinforced Concrete Joints with Low Axial Load under Seismic Loading," Report to the University of Canterbury, Christchurch, New Zealand, in partial fulfillment of the requirements for the degree of Master of Engineering, 1972, 103 pp.

21. Renton, G. W., "The Behavior of Reinforced Concrete Beam-Column Joints under Cyclic Loading," Thesis submitted to the University of Canterbury, Christchurch, New Zealand, in partial fulfillment of the requirements for the degree of Master of Engineering in Civil Engineering, 1972.

22. Uzumeri, S. M., and Seckin, M., "Behavior of Reinforced Concrete Beam Column Joints Subjected to Slow Load Reversals," Publication 74-05, Department of Civil Engineering, University of Toronto, March 1974.

23. ASTM Designation: C143-74, "Standard Method of Test for Slump of Portland Cement Concrete," ASTM Standards, Part 14, Philadelphia, 1975.

24. ASTM Designation: A615-72, "Standard Specifications for Deformed and Plain Billet-Steel Bars for Concrete Reinforcement," ASTM Standards, Part 4, Philadelphia, 1974.

25. ASTM Designation: C192-69, "Standard Method of Making and Curing Concrete Specimens in the Laboratory," ASTM Standards, Part 14, Philadelphia, 1975.

26. ASTM Designation: C39-72, "Standard Method of Test for Compressive Strength of Cylindrical Concrete Specimens," ASTM Standards, Part 14, Philadelphia, 1975.

27. ASTM Designation: C496-71, "Standard Method of Test of Splitting Tensile Strength of Cylindrical Concrete Specimens," ASTM Standards, Part 14, Philadelphia, 1975.

28. Thompson, M. A., Jirsa, J. O., Breen, J. E., and Meinheit, D. F., "The Behavior of Multiple Lap Splices in Wide Sections," Research Report 154-1, Center for Highway Research, The University of Texas at Austin, January 1975.

29. Ferguson, P. M., and Thompson, J. N., "Development Length of High Strength Reinforcing Bars in Bond," Journal of the American Concrete Institute, Proc. V. 59, No. 7, July 1962, p. 887.

30. de Aleman, M. A., "Influence of Lateral Beams on the Behavior of Beam-Column Joints," thesis to be submitted to The University of Texas at Austin, in partial fulfillment of the requirements for the degree of Master of Science in Engineering.

31. MacGregor, James G., Chmn., "The Shear Strength of Reinforced Concrete Members, by the Task Committee on Masonry and Reinforced Concrete of the Structural Division," Journal of the Structural Division, ASCE, Vol. 99, No. ST6, June 1973, pp. 1091-1187.

32. Marin, J., Mechanical Behavior of Engineering Materials, Prentice-Hall, Inc., Englewood Cliffs, N. J., 1962.

33. Balmer, G. A., "Shearing Strength of Concrete under High Triaxial Stress--Computation of Mohr's Envelope as a Curve," Structural Research Laboratory Report No. SP-23, U. S. Department of Interior, Bureau of Reclamation, October 1949.

34. Bresler, B., and Pister, K. S., "Failure of Plain Concrete under Combined Stresses," Transactions, ASCE, Vol. 122, 1957, pp. 1049-1059.

35. Bresler, B., and Pister, K. S., "Strength of Concrete under Combined Stresses," Journal of the American Concrete Institute, Proc. V. 55, No. 3, September 1958, pp. 321-346.

36. McHenry, D., and Karni, J., "Strength of Concrete under Combined Tensile and Compressive Stress," Journal of the American Concrete Institute, Proc. V. 54, No. 4, April 1958, pp. 829-840.

37. Chinn, J., and Zimmerman, R. M., "Behavior of Plain Concrete under Various High Triaxial Compression Loading Conditions," Air Force Weapons Laboratory Report, WL TR 64-163, August 1967.

38. Kupfer, H., Hilsdorf, H. K., and Rusch, H., "Behavior of Concrete under Biaxial Stresses," Journal of the American Concrete Institute, Proc. V. 66, No. 8, August 1969, pp. 656-666.

39. Kupfer, H. B., and Gerstle, K. H., "Behavior of Concrete Under Biaxial Stresses," Journal of the Engineering Mechanics Division, ASCE, Vol. 99, No. EM4, August 1973, pp. 853-866.

40. Palaniswamy, R., and Shah, S. P., "Fracture and Stress-Strain Relationships of Concrete under Triaxial Compression," Journal of the Structural Division, ASCE, Vol. 100, No. ST5, May 1974, pp. 901-916.

41. Lomize, G. M., and Kryzhanvoskii, A. L., "Soil Strength," Hydrotechnical Construction, No. 3, March 1967, pp. 255-261.

42. Rosenthal, I., and Glucklich, J., "Strength of Plain Concrete under Biaxial Stress," Journal of the American Concrete Institute, Proc. V. 67, No. 11, November 1970, pp. 903-914.

43. Carino, N. J., and Slate, F. O., "Limiting Tensile Strain Criterion for Failure of Concrete," Journal of the American Concrete Institute, Proc. V. 73, No. 3, March 1976, pp. 160-165.

44. Fenwick, R. C., and Paulay, T., "Mechanisms of Shear Resistance of Concrete Beams," Journal of the Structural Division, ASCE, Vol. 94, No. ST10, October 1968, pp. 2325-2350.

45. Taylor, H. P. J., Investigation of the Forces Carried Across Cracks in Reinforced Concrete Beams by Interlock of Aggregate, Cement and Concrete Association, London, TRA 42 447, 1970, 22 pp.

46. Mast, R. F., "Auxiliary Reinforcement in Concrete Connections," Journal of the Structural Division, ASCE, Vol. 94, No. ST6, June 1968, pp. 1485-1504.

47. Dixon, W. J. (Ed.), BMD-Biomedical Computer Programs, Health Sciences Computing Facility, Department of Biomathematics, School of Medicine, University of California, Los Angeles, University of California Press, January 1973.

48. Higashi, Y., and Ohwada, Y., "Failing Behaviors of Reinforced Concrete Beam-Column Connections Subjected to Lateral Loads," No. 19, Memoirs of Faculty of Technology, Tokyo Metropolitan University, 1969.

49. Megget, L. M., "Anchorage of Beam Reinforcement in Seismic Resistant Reinforced Concrete Frames," Master of Engineering Report, University of Canterbury, Christchurch, New Zealand, 1971, 85 pp.

50. Patton, R. N., "Behavior under Seismic Loading of Reinforced Concrete Beam-Column Joints with Anchor Blocks," Master of Engineering Report, University of Canterbury, Christchurch, New Zealand, 1972, 103 pp.

51. Park, R., and Thompson, K. J., "Behavior of Prestressed Partially Prestressed and Reinforced Concrete Interior Beam-Column Assemblies under Cyclic Loading: Test Results of Units 1 to 7," Research Report 74-9, Department of Civil Engineering, University of Canterbury, Christchurch, New Zealand, 1974, 42 pp.